The Palaeoptera Problem and the Evolution of Head Structures of Dicondylia (Insecta)

DISSERTATION

zur Erlangung des Doktorgrades (Dr. rer. nat.)
der Mathematisch-Naturwissenschaftlichen Fakultät
der Rheinischen Friedrich-Wilhelms-Universität Bonn
vorgelegt von

Alexander Blanke
aus Bonn

Bonn – Februar 2013

The Palaeoptera Problem and the Evolution of Head Structures of Dicondylia (Insecta)

DISSERTATION

zur
Erlangung des Doktorgrades (Dr. rer. nat.)
der
Mathematisch-Naturwissenschaftlichen Fakultät
der
Rheinischen Friedrich-Wilhelms-Universität Bonn
vorgelegt von

Alexander Blanke
aus
Bonn

Bonn, Februar 2013

Angefertigt mit Genehmigung der Mathematisch-Naturwissenschaftlichen Fakultät
der Rheinischen Friedrich-Wilhelms-Universität Bonn.

Diese Dissertation wurden am Zoologischen Forschungsmuseum Alexander Koenig in Bonn durchgeführt.

Gutachter:

1. Prof. Dr. Bernhard Misof,
   Rheinische Friedrich-Wilhelms-Universität Bonn & Zoologisches Forschungsmuseum Alexander Koenig (ZFMK), Zentrum für molekulare Biodiversität (ZMB)
2. Prof. Dr. Rolf G. Beutel,
   Friedrich-Schiller-Universität Jena, Institut für Spezielle Zoologie und Evolutionsbiologie mit Phyletischem Museum

Tag der Promotion:
Erscheinungsjahr:

In der Dissertation eingebunden:
- Zusammenfassung
- Lebenslauf

Der kleine Prinz war jetzt ganz blaß vor Zorn.

»Es sind nun Millionen Jahre, daß die Blumen Dornen hervorbringen. Es sind Millionen Jahre, daß die Schafe trotzdem die Blumen fressen. Und du findest es unwichtig, wenn man wissen möchte, warum sie sich so viel Mühe geben, Dornen hervorzubringen, die zu nichts Zweck haben? Dieser Kampf der Schafe mit den Blumen soll unwichtig sein? Weniger ernsthaft als die Additionen eines dicken, roten Mannes? Und wenn ich eine Blume kenne, die es in der ganzen Welt nur ein einziges Mal gibt, nirgends anders als auf meinem kleinen Planeten, und wenn ein kleines Schaf, ohne zu wissen, was es tut, diese Blume eines Morgens so mit einem einzigen Biß auslöschen kann, - das soll nicht wichtig sein?!«

Er wurde rot vor Erregung und fuhr fort:

»Wenn einer eine Blume liebt, die es nur ein einziges Mal gibt auf allen Millionen und Millionen Sternen, dann genügt es ihm völlig, daß er zu ihnen hinaufschaut, um glücklich zu sein. Er sagt sich: Meine Blume ist da oben, irgendwo... Wenn aber das Schaf die Blume frißt, so ist es für ihn, als wären plötzlich alle Sterne ausgelöscht! Und das soll nicht wichtig sein?«

Meinen Eltern

...Aber jene eine hatte eines Tages Wurzel geschlagen, aus einem Samen, weiß Gott woher, und der kleine Prinz hatte diesen Sproß, der den andern Sprößlingen nicht glich, sehr genau überwacht. Das konnte eine neue Art Affenbrotbaum sein. Aber der Strauch hörte bald auf zu wachsen und begann, eine Blüte anzusetzen. Der kleine Prinz, der der Entwicklung einer riesigen Knospe beiwohnte, fühlte wohl, es müsse eine wunderbare Erscheinung aus ihr hervorgehen, aber die Blume wurde nicht fertig damit, sich in ihrer grünen Kammer auf ihre Schönheit vorzubereiten. Sie wählte ihre Farben mit Sorgfalt, sie zog sich langsam an, sie ordnete ihre Blütenblätter eins nach dem andern. Sie wollte nicht wie die Mohnblüten ganz zerknittert herauskommen. Sie wollte nicht früher erscheinen als im vollen Ornat ihrer Schönheit. Nun ja! sie wollte gefallen...

und Heike

Cover images:

Left: Lepisma saccharina (Zygentoma) by curtesy of Miroslav Deml

Middle: Ephemerella_aurivillii (Ephemeroptera) by curtesy of Jason Neuswanger

Right: Erpetogomphus lampropeltis (Odonata) by curtesy of Dr. Oliver Niehuis

Content

Content

Danksagung

An erster Stelle möchte ich mich bei meinem Doktorvater und Betreuer Bernhard Misof für seine großartige Unterstützung und seinen schier unerschöpflichen Optimismus bedanken. Die vielen konstruktiven und ideenreichen Diskussionen haben entscheidend zu dem Gelingen dieses Projektes beigetragen. Ich danke ihm für sein großes Vertrauen und freue mich schon sehr auf eine weitere Zusammenarbeit.

Ein großer Dank geht ebenfalls an meinen Zweitgutachter Prof. Dr. Rolf G. Beutel für zahlreiche konstruktive Diskussionen rund um das Thema Palaeoptera und Kopfmorphologie generell. Ohne seine Unterstützung hätte diese Arbeit nicht das Niveau erreichen können welches sie nun hat. Dr. Benjamin Wipfler aus der AG Beutel hat ebenfalls entscheidend zum Gelingen dieser Arbeit beigetragen. Vielen Dank für deine zahlreichen Besuche hier in Bonn und die enge Kooperation! Es hat Spass gemacht mit dir zusammen zu arbeiten und ich freue mich auf die zukünftigen Projekte.

Herrn Prof. Dr. Weigend und Herrn PD Dr. Torsten Wappler danke ich für ihre Gutachtertätigkeit und Teilnahme an der Prüfungskommission. Ich möchte meinen zahlreichen Kollegen am ZFMK danken, die teilweise als Mitautoren, teilweise als Kooperationspartner oder auch einfach dadurch dass sie da waren diese Doktorarbeit indirekt mit gestaltet haben. Im Besonderen sind dies: Dr. Karen Meusemann, Dr. Björn von Reumont (mittlerweile Natural History Museum London), Manuela Thelen, Carola Greve und Sandra Meid. Danke an dich, Susanne Duengelhoef, für all die angenehmen Jahre im gemeinsamen Büro und auch außerhalb. Gut, dass immer dann gelüftet wurde, wenn der andere auch frische Luft wollte! Das ist wohl nicht ganz selbstverständlich für so eine lange Zeit...

Ich danke ebenfalls meinen externen Kooperationspartnern: PhD Dr. Karl Kjer, Dr. Markus Koch, Dr. Frank Friedrich, Prof. Dr. Ryuchiro Machida, PhD Dr. Barbara Holland sowie dem gesamten 1KITE Team. Ein herzlicher Dank geht an Herrn Prof. Dr. J.-W. Wägele für die Ermöglichung dieser Arbeit am Zoologischen Forschungsmuseum Alexander Koenig.

Der Alexander Koenig Gesellschaft, der Alexander Koenig Stiftung sowie der Europäischen Union danke ich für die Finanzierung wichtiger Teilprojekte dieser Arbeit. Ebenfalls danken möchte ich dem Deutschen Elektronen Synchrotron (DESY) und dem Paul-Scherrer Institut (PSI) für die Ermöglichung der microCT Forschung an deren Anlagen. Felix Beckmann, Fabian Wilde (beide GKSS an DESY) sowie Marco Stampanoni, Rajmund Mokso und Peter Modregger (alle PSI) leisteten eine exzellente Betreuung vor, während und nach den Messungen, teilweise auch in Nachtschichten.

Ein Dank geht an Karen Ulmen, Hamideh Fard und Claudia Etzbauer. Ich danke ihnen für ihre Unterstützung im Labor, am REM und in zahlreichen organisatorischen Dingen. Ebenfalls danke ich Herrn Rainer Keller für Unterstützung, Zuspruch und Rat als ich noch in der Sammlung beheimatet war, wo alles anfing...

Ein großer Dank gilt natürlich auch meinen engen Freunden, die schon lange vor dieser Doktorarbeit begonnen haben mich auf meinem Weg zu begleiten und die immer ein guter Ratgeber sind. Neben vielen anderen möchte ich vor allem hervorheben: Volker Dahmen, Johannes Dambach, Moritz Rommerskirchen, Silke Göldner, Jörg Scharfhausen und Frederike Schampera. Danke Heike Schenk für wundervolle 3 1/2 Jahre! Du hast mir sehr geholfen.

Von ganzem Herzen danke ich meiner Familie, vor allem meinen Eltern, Iris und Franz Blanke. Sie haben mich immer in meinen Entscheidungen unterstützt, mir stets Mut zugesprochen und mich in meiner Arbeit bestärkt.

Schlussendlich möchte ich mich bei meiner Kooperationspartnerin Sina David bedanken für ihre großartige Unterstützung, Geduld und die unendliche Kraft, die sie mir gibt. Ich denke wir sollten in Zukunft noch enger zusammenarbeiten...

Summary

Summary

The phylogenetic relationships of dragonflies (Odonata), mayflies (Ephemeroptera), and all other winged insects (Neoptera) is one of the major problems in systematic entomology. Three hypotheses are discussed: the Chiastomyaria hypothesis (Ephemeroptera + Neoptera), the Metapterygota hypothesis (Odonata + Neoptera), and the Palaeoptera hypothesis (Odonata + Ephemeroptera). The outgroup to all winged insects (Pterygota) are the wingless silverfish (Zygentoma), thus rendering a formal morphologic-phylogenetical analysis of wing characters impossible since these characters cannot be homologized. Genitalic structures are equally of no use due to to homologisation problems and missing data.

In contrast, the character system „head“ is not affected by these difficulties. Outer as well as inner anatomy can be homologised between wingless and winged insects. This thesis tries to infer the phylogenetic relationships of the main winged insect groups using the cephalic morphology. Basic studies were necessary in advance: despite their peculiar position, the cephalic morphology of of dragonflies is understudied. Knowledge about the morphology of Zygentoma is equally insufficient.

Thus, one aim of the present thesis is the decription of the anatomy of selected dragonfly (chapters 4,7 & 8), mayfly (chapter 4), and silverfish taxa (chapter 9) focused on the inner anatomy (muscles and endoskeletal elements). Several muscles previously unknown for dragonflies were described, sutures and ridges of the head capsule were homologized with the corresponding structures in other taxa. A cladistic analysis of a cephalic character matrix supports the Palaeoptera hypothesis. Former analyses of cephalic characters supported Metapterygota.

The investigation of the inner anatomy of dragonflies also resulted in differences at the family level. More detailled studies with a broader taxon sampling allowed a phylogenetic analysis of dragonfly families using characters of all tagmata and adding new cephalic characters (chapter 8). Clubtails (Gomphidae) are the sistergroup to all remaining dragonflies according to this dataset.

For the description and analysis of the inner anatomy synchrotron radiation micro computer tomography (SR-microCT) and microCT were used. Latest developments in the field of SR-microCT allowing better resolution and thus the study of even smaller animals are the treated in chapter 2.

One problem of phylogenetic analyses is convergence and its detection. In case of concerted convergence – the parallel change of several characters due to a selective pressure – support values for artificial clades can be high. The present thesis modifies an approach to detect concerted convergence and applies it to the Palaeoptera problem and the phylogenetic relationships of dragonflies. Several groups of characters are indentified with a supposedly high degree of concerted convergence (chapter 5 & 8). Tree reconstructions excluding these character groups result in a corroboration of the palaeoptera hypothesis and a corroboration of gomphids as the sistergroup to all remaining dragonflies.

Zusammenfassung

Zusammenfassung

Die Verwandtschaftsbeziehungen der Insektenlinien Libellen (Odonata), Eintagsfliegen (Ephemeroptera) und aller übrigen geflügelten Insekten (Neoptera) ist eines der großen Probleme in der entomologischen Systematik. Hauptsächlich drei Hypothesen zu den Schwestergruppenbeziehungen werden diskutiert: Die Chiastomyaria Hypothese (Ephemeroptera + Neoptera), die Metapterygota Hypothese (Odonata + Neoptera) und die Palaeoptera Hypothese (Odonata + Ephemeroptera). Fischchen (Zygentoma) als nächstverwandte Außengruppe zu den geflügelten Insekten (Pterygota) sind ungeflügelt, was eine formale morphologisch-phylogenetische Analyse der entsprechenden Flügelmerkmale unmöglich macht, da die Flügelmerkmale nicht polarisiert werden können. Auch die Merkmale des Genitalapparates konnten bis jetzt nicht zufriedenstellend homologisiert werden, um in formal kladistischen Analysen genutzt zu werden.

Im Gegensatz dazu ist der Merkmalskomplex „Kopf“ nicht von diesen Schwierigkeiten betroffen. Sowohl äußere als auch innere Anatomie lassen sich zweifelsfrei zwischen den ungeflügelten und geflügelten Insekten homologisieren. Die vorliegende Dissertation versucht deshalb die Verwandtschaftsbeziehungen der Großgruppen der geflügelten Insektenlinien anhand der Kopfmorphologie aufzuklären. Hierzu mussten zuerst grundlegende Studien durchgeführt werden: Die Kopfmorphologie der Libellen ist trotz ihrer vieldiskutierten Stellung bis jetzt nur unzureichend erforscht. Ein ähnliches Bild ergibt sich für die Zygentoma.

Ein Fokus dieser Dissertation ist folglich die morphologische Beschreibung und Analyse ausgewählter Arten von Libellen (Kapitel 4, 7 & 8), Eintagsfliegen (Kapitel 4) und Fischchen (Kapitel 9) vor allem in Hinblick auf die innere Anatomie (Muskeln und endoskelettalen Elemente). Dabei konnten für Libellen bisher nicht beschriebene Muskeln nachgewiesen werden, Nähte und Verstärkungsleisten der Kopfkapsel wurden den entsprechenden homologen Strukturen bei verwandten Gruppen zugeordnet. Eine darauf folgende kladistische Analyse einer cephalen Merkmalsmatrix resultierte in der Unterstützung der Palaeoptera Hypothese. Frühere Analysen von Kopfmerkmalen unterstützten hingegen die Metapterygota Hypothese.

Die Untersuchung der inneren Kopfanatomie der Libellen ergab auch Unterschiede innerhalb einzelner Familien. Detailliertere Studien mit einer breiter angelegten Artenauswahl führten zu einer phylogenetischen Analyse der Großlibellenfamilien unter Einbeziehung aller Körperteile und der Addition neuer Kopfmerkmale (Kapitel 8). Die Flussjungfern (Gomphidae) sind demnach die Schwestergruppe aller übrigen Großlibellen.

Zur Beschreibung und Analyse der inneren Anatomie wurde vor allem die Methode der synchrotron basierten micro Computer Tomographie (SR-microCT) und auch die microCT über Laborgeräte verwendet. Neueste Entwicklungen auf dem Gebiet der SR-microCT, die feinere Auflösungen und damit die Erforschung noch kleinerer Arten ermöglichen werden, sind Gegenstand von Kapitel 2.

Ein Problem phylogenetischer Analysen ist Konvergenz und deren Erkennung. Im Fall von konzertierter Konvergenz – der gleichzeitigen Änderung mehrerer Merkmale aufgrund einer selektierenden Bedingung – können die Unterstützungswerte für artifizielle Schwestergruppenbeziehungen hoch sein. In der vorliegenden Dissertation wurde ein Ansatz zur Detektion von konzertierter Konvergenz modifiziert und auf die Palaeoptera Problematik sowie auf die Verwandtschaftsanalyse der Großlibellen angewandt. Es konnten mehrere Gruppen von Merkmalen identifiziert werden, deren Merkmalsausprägungen vermutlich einen hohen Grad von konzertierter Konvergenz aufweisen. Baumberechnungen unter Ausschluss dieser Merkmalsgruppen resultieren in einer erhöhten Unterstützung der Palaeoptera Hypothese sowie in einer Bestätigung der Flussjungfern als Schwestergruppe zu allen übrigen Großlibellen.

1 General Introduction

Wenn sie nur kann, wird die Natur dich dreist belügen. (Charles Darwin, 1809 – 1892)

Insects are the most successful group of organisms on this planet if success is measured in terms of species richness (Grimaldi and Engel, 2005). If one wants to understand how this success was realised, one has to understand, apart from ecology, earth history and many other factors, the morphological evolution. One of the most momentous morphological transformations was the acquistion of wings (Hasenfuss, 2002; Hasenfuss, 2008; Klass, 2009), which occurred at an early stage of insect evolution, in the late Devonian or early Carboniferous (e.g., Engel & Grimaldi 2004). The capacity to fly allowed pterygote insects to conquer new habitats, greatly improved dispersal ability, and provided an efficient escape mechanism .

The acquisition of wings is obviously a major morphological change of the body organisation. However, it is likely that transformation of head structures, especially the appendages, also played an important role in the evolution of insects. Important functions concentrated in the head are food uptake and sensory recognition (Westheide and Rieger, 2004).

A systematic and formal investigation of the evolution of cephalic structures of some insect lineages is still at an early stage (Staniczek, 2001; Wipfler, 2012), even though it is apparent that transformations of the head and its organs and appendages are very important in a systematic and evolutionary context (Boudreaux, 1979; Hennig, 1969; Matsuda, 1965). Changes of structures related to the mandibles, for instance, have been considered as key characters to estimate the evolution of the first insect linages (e.g., Hennig 1969). Together with Pterygota (all winged insects) the wingless Zygentoma (silverfish) form the Dicondylia which are characterized by a an additional anterior articulation of the mandible with the head capsule (Hennig, 1953; Snodgrass, 1935). In the evolution of Pterygota not only many variations of the mandible have evolved, but also multiple modifications of the other cephalic appendages and other head structures (Grimaldi and Engel, 2005; Snodgrass, 1935).

The mandible articulation of Dicondylia

Generally, a dicondylous mandibular articulation implies reduced degrees of freedom (Snodgrass, 1935). Depending on the rigidity of the connection the two articulations form a virtual axis of rotation preventing the movement in other axes. At the same time, biting force in the remaining direction of movement is supposedly increased (Staniczek, 2000). This allowed to explore more solid food resources. The mandible articulation of Dicondylia is characterised by a trend towards a more rigid connection to the head.

The posterior (primary) mandibular articulation of Zygentoma is a rounded mandibular condyle that lies in a groove formed by a part of the head capsule and a cephalic condyle ((Chaudonneret, 1950; Staniczek, 2000) see chapter 9 for details). The anterior articulation is formed of a mandibular depression and a caliper-like cephalic structure (in lateral view) on the posterolateral clypeal area and the anterior tentorial arms. The caliper is „wrapped“ around the depression and the mandibular edge thus limiting the movement of the mandible to the transversal plane (Figure 1 & 2).

The posterior articulation in nymphs of Ephemeroptera (mayflies) is composed of a roller-like mandibular condyle. The central part of the roller runs within a postgenal socket (Staniczek, 2001). The anterior articulation is composed of an anterolateral and a posteromedial part (together forming an articulation complex). The anterolateral articulation is formed of an elongated mandibular notch into which the inner margin of the inflected cranium projects (Staniczek, 2001). The posteromedial articulation is formed of a small saddle like socket on the mandible and a cranial processus paratentorialis.

In Odonata (dragonflies) and Neoptera (all remaining winged insects) the posterior articulation is a distinct knob forming a ball-and-socket joint together with the head (Snodgrass, 1935). The anterior articulation is also a ball-and-socket joint but with a cephalic knob and a mandibular socket.

The different formations of dicondylic articulations result in different mandibular movements. The mandible of Zygentoma moves only in the transverse plane, whereas the mandible of ephemeropteran nymphs performs a rotation combined with a transverse movement (Staniczek, 2001). The mandibular movement of Odonata and Neoptera is a strict rotation around the virtual axis formed by the anterior and posterior ball-and-socket joints .

Studying dicondylian head morphology avoids formal phylogenetic problems

Wings are a complex autapomorphy of Pterygota (all winged insects) and arguably the most important single novelty in the hexapod evolution. However, wings as a character system are of limited use for the reconstruction of the basal splitting events in winged insects (Beutel and Gorb, 2006). Since the outgroup – Zygentoma - is wingless, homology assessments of thoracic skeletal elements and muscles related to flight are problematic and character polarisation of features related to flight is not possible between the three major pterygote lineages (Ephmeroptera, Odonata, Neopptera). Also, the mode of flight changed dramatically among the first winged lineages. Odonata are characterized by the exclusive use of direct flight muscles, i.e. muscles inserting directly at the wing base. In contrast, Ephemeroptera and Neoptera have evolved an indirect system. The muscles for the upstroke insert at the tergum (the dorsal part of the thorax) which is moveably connected to the wings and therefore acts as a lever. The downstroke is realized by muscles that are not connected to the wings but run longitudinally through the thorax parallel to the tergum (dorsolongitudinal muscles). Thus, wing motion is realized by a rhythmic deformation of the entire pterothoracic segments. Aside from the indirect muscles, however, direct muscles are also involved in flight (Nachtigall, 2003).

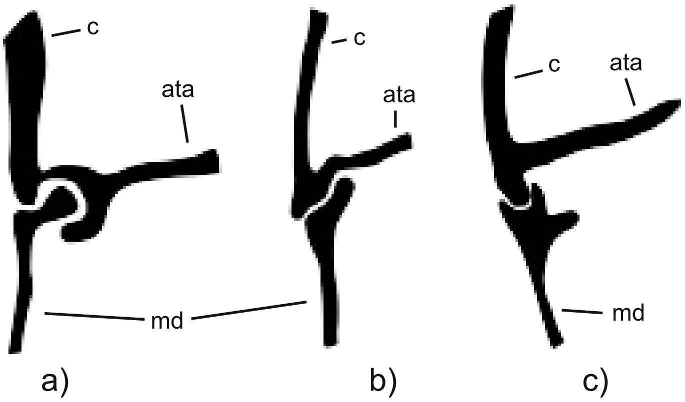

Figure 1 Schematic illustrations of the anterior mandibular articulation of a) Zygentoma; b) Ephemeroptera; c) Odonata + Neoptera. Lateral views. Abbreviations: ata, anterior tentorial arm; c, cranium; md, mandible.

The outgroup problem and the fundamental morphologic changes in the first three lineages of winged insects also apply to sperm transfer / the genital system, which changed from an indirect external mode (Zygentoma) to a direct transfer via an postabdominal intromittent organ in Ephemeroptera and Neoptera. Odonata evolved a secondary copulatory apparatus at the abdominal segments II and III and exhibit a unique form of "indirect" sperm transfer completely different from the condition in all other pterygote lineages. Again, robust homology hypotheses and character polarisations covering winged and wingless groups are difficult (Witte and Doring, 1999), even though more data became available in recent years (Dallai et al., 2011; Klass, 2008; Matushkina, 2008a; Matushkina, 2008b). In contrast to the character complexes wing and sperm transfer head characters can be homologised between Zygentoma and Pterygota. Mouthparts, muscles, endoskeleton, as well as sutures and ridges i.e. the principle head structures are present and can therefore be compared. Although, research on the evolution of head structures has a long history (for a review on earlier literature see Matsuda 1965, Klass 2009), a formal cladistic approach focused on the Palaeoptera has not been undertaken, yet. The data basis for taxa such as Odonata and Ephemeroptera was too fragmentary resulting in high amounts of missing data in former analyses (Wipfler et al., 2011).

The origin of winged insects is still in question

For reasons outlined above the relationships of the three major winged lineages (Odonata, Ephemeroptera and Neoptera) is one of the major unsolved problems in entomology (Klass, 2007; Kristensen, 1991). Issues concerning the relationships between the three clades have often been addressed as the “Palaeoptera problem” (Hovmöller et al., 2002; Ogden and Whiting, 2003; Whitfield and Kjer, 2008), which refers to a possible but insufficiently supported monophylum Ephemeroptera + Odonata. Three solutions have been proposed and are still under discussion. A sistergroup relationship between Ephemeroptera and Odonata (Palaeoptera hypothesis) has been suggested based on characters of the antenna, aquatic immature stages, the wing venation and articulation, and the maxillary configuration (Hennig, 1969; Bechly et al., 2001; Brauckmann and Zessin, 1989; Haas and Kukalová-Peck, 2001; Hennig, 1969; Hovmöller et al., 2002; Kukalová-Peck, 1997; Kukalová-Peck, 2008; Soldán, 2003; Wheeler et al., 2001; Willkommen and Hörnschemeyer, 2007).

A sistergroup relationship between Ephemeroptera and Neoptera (Chiastomyaria hypothesis) is suggested by the mode of direct sperm transfer, the indirect flight musculature, and analyses of molecular data (Boudreaux, 1979; Kjer, 2004; Mallatt and Giribet, 2006; Matsuda, 1970; Simon et al., 2009).

A sistergroup relationship between Odonata and Neoptera (Metapterygota hypothesis) is mainly supported by features of the mandibles and the tracheal system, and also by molecular data (Beutel and Gorb, 2006; Kristensen, 1991; Ogden and Whiting, 2003; Pass et al., 2006; Staniczek, 2000; Staniczek, 2001; Terry and Whiting, 2005; Wheeler et al., 2001). Metapterygota is currently the only hypothesis supported by mandibular characters with unambiguous homology (Staniczek, 2001).

Long branch attraction and concerted convergence hamper phylogenetic reconstruction

The appearance of Ephemeroptera, Odonata and the neopteran orders in a geologically short time span - probably shortly after the Devonian (Engel and Grimaldi, 2004; Gaunt and Miles, 2002; Grimaldi and Engel, 2005) - has been followed by a very long period, in which these lineages evolved separately. This specific evolutionary pattern, previously described as an “ancient rapid radiation”, has been assumed to impede phylogenetic reconstruction (Kjer et al., 2006; Rokas and Carroll,

Figure 2 Schematic illustrations of the mandible movement before (above) and after biting (below) of a) Zygentoma; b) Ephemeroptera; c) Odonata + Neoptera. Arrows indicate the principal movement of the mandibles. 3D reconstructions from SR-microCT data. For further explanations see text. Abbreviations: 0md1, M. craniomandibularis internus; md, mandible.

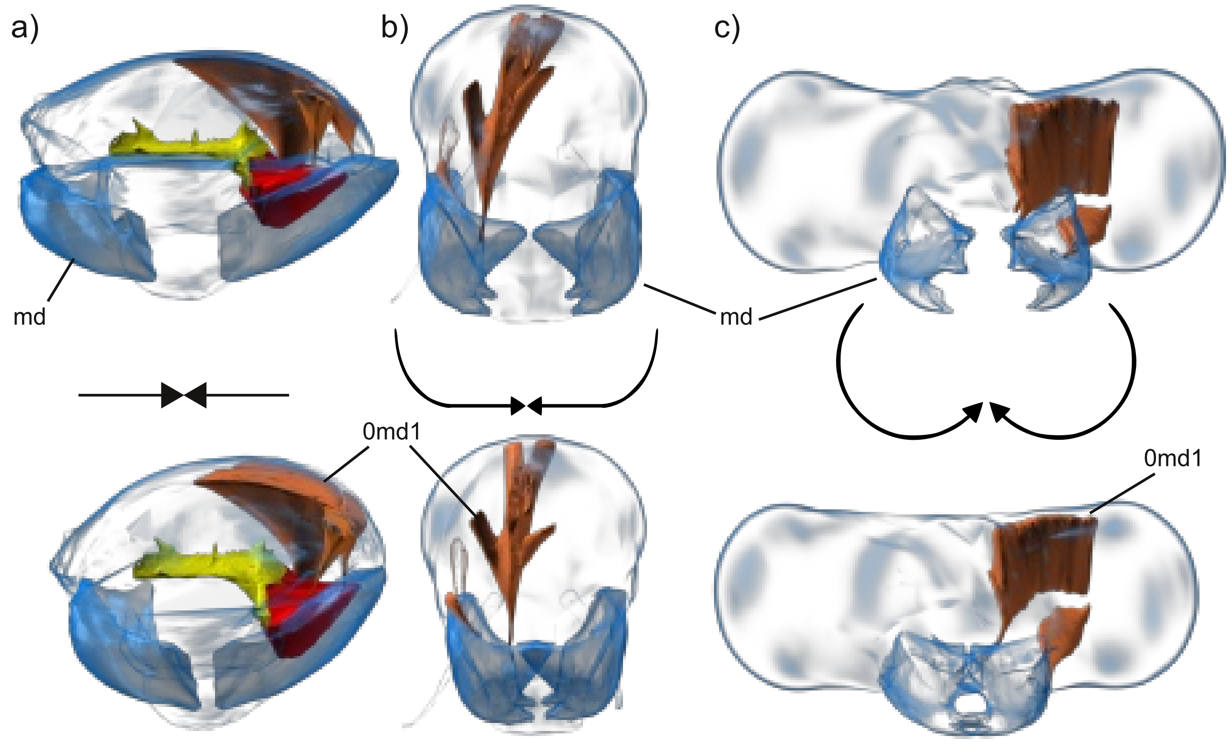

2006; Whitfield and Kjer, 2008; Whitfield and Lockhart, 2007) as all evolutionary changes useful to display the branching patterns of Ephemeroptera, Odonata and Neoptera must have been accumulated in the short branches linking these lineages, whereas subsequent changes occurring in the branches leading to the terminal groups do not provide information about their relationships. Consequently, characters evolving convergently on these branches leading to the terminals might be erroneously interpreted as synapomorphies in parsimony based methods (the "long-branch attraction" phenomenon discussed by Felsenstein (1978)).

Morphological convergence among lineages can be even more extensive due to a phenomenon called concerted convergence (Patterson and Givnish, 2002). This describes a process in which several traits are exposed to the same shared set of environmental conditions or functional requirements, like for instance the character complexes "wings", "mouthparts" or "genitalia". In each of these cases a given selective pressure is assumed to influence the whole character system so that the evolution of sets of single characters occurs in a "concerted" manner. In phylogenetic analyses this can result in artificially increased numbers of presumptive independent apomorphies, and consequently in artificial clades with unjustified support (Holland et al., 2010).

The head of Odonata and Ephemeroptera is understudied

The anatomy of the ephemeropteran head was treated in a considerable number of studies [Siphlonuridae: Schonmann (1981); Heptageniidae: Strenger (1954); Palingeniidae: Strenger (1970); Ephemeridae: Strenger (1975); Euthyplociidae: Strenger (1977)] and also selected substructures (Hudson, 1951). Staniczek (2000, 2001) reviewed and homologised head structures of Ephemeroptera and reconstructed the groundplan based on an investigation of Oniscigaster wakefieldi McLachlan, 1873. Staniczek (2000, 2001) had to rely on the larval morphology, as the mouthparts of adult mayflies are strongly reduced (Edmunds, 1988; Simm, 1914). I generally followed this approach here. The comparison of characters of different life stages is problematic and a potential source of phylogenetic misinterpretations. However, the alternative, i.e. the use of adult head structures, would have been more problematic, as many characters would have been inapplicable for mayflies which would have resulted in an increased amount of missing data.

In terms of available morphological data dragonflies are an unusual case. Whereas the thoracic (Pfau, 1986; Pfau, 1991; Willkommen, 2009; Willkommen and Hörnschemeyer, 2007) and abdominal structures (Klass, 2008; Matushkina, 2008a; Matushkina, 2008b; Pfau, 2002; Pfau, 2005; Whedon, 1918) have been intensively studied, the head has been largely neglected. The last treatments of dragonfly cephalic anatomy (Asahina, 1954; Hakim, 1964; Mathur, 1962; Mathur and Mathur, 1961; Short, 1955; Strenger, 1952) were insufficient for a clarification of the systematic position of the order (Wipfler et al., 2011).

Consequently, an important part of this thesis is the investigation of the external and internal morphology of the odonatan head under a phylogenetic aspect. Current morphological treatments aiming at the reconstruction of the phylogeny of Odonata largely depend on wing characters. Vein branching patterns and sclerite configuration of insect wings have been routinely used in insect phylogenetics and are an important tool to assess affinities of fossils with recent groups of insects (Trueman, 1996). However, it has been proposed that wing characters show a higher degree of convergent evolution than previously expected (Fleck et al., 2008a). This is especially true for the order Odonata (Bybee et al., 2008; Carle et al., 2008; Fleck et al., 2008a). Authors have shown that effects of wing size reduction and different flight styles may be responsible for parts of the wing vein characterstics in Odonata, thus potentially biasing phylogenetic signal. For example, functional dependencies between e.g. the costal region (the leading edge of the wing) are believed to have an influence on the configuration of more posteriorly located wing parts (Wootton, 1992).

Concerning Anisoptera (dragonflies) two main goals were pursued in this thesis. First, it was aimed to compile an updated reliable morphological character matrix to infer a hopefully robust phylogeny of dragonflies. It was tried to achieve this by a review and extension of the currently largest morphological data matrix covering all parts of the dragonfly body. Focus for the addition of new characters was the head region since this character system is underrepresented in dragonfly phylogenetics (only 13 of 153 characters, i.e. 8,5% (Bybee et al., 2008)), but has proven useful to infer relationships among various groups of other insects (Blanke et al., 2012a; Blanke et al., 2012b; Wipfler et al., 2011; Wipfler et al., 2012). Secondly, the degree of concerted convergence in this extended data matrix was investigated in order to explore potential confounding signal within morphological characters with Holland's et al. (2010) approach. Subsequently, it is analysed which functional groups of characters are prone to concerted convergence.

MicroCT allows analysing a wide range of taxa in reasonable timeframes

Many morphology based phylogenetic analyses suffered to a great extend from limited taxon sampling and time consuming exploration of the structures in question (Staniczek, 2000; Staniczek, 2001; Wheeler et al., 2001). The morphological examination of muscles and exo- and endoskeletal features in insects benefited to a great

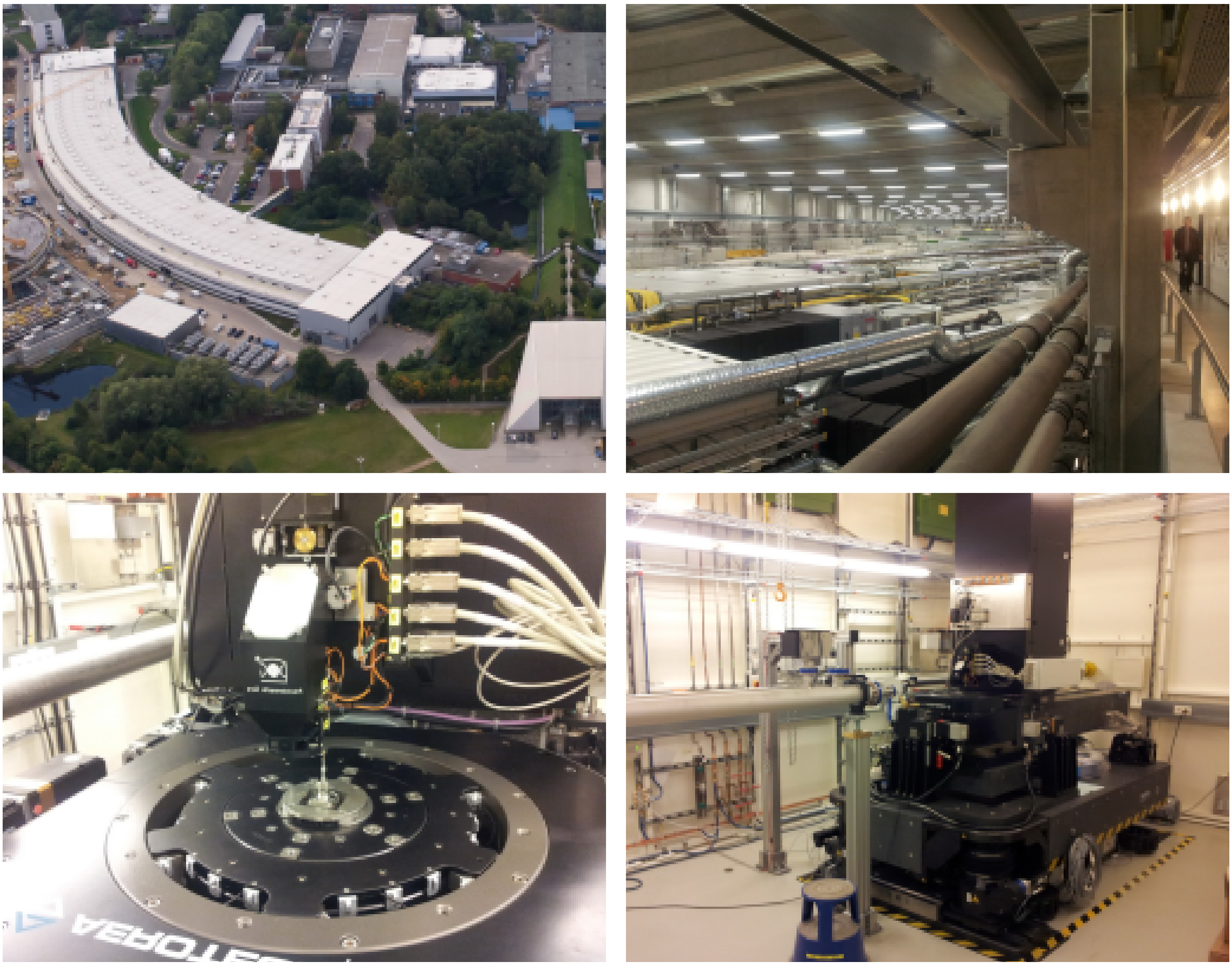

Figure 3 Pictures of the particle accelerator at the Deutsches Elektronen Synchrotron (DESY, Hamburg, Germany) illustrating the necessary effort to obtain tomographic images of small insects with a high density dependent tissue resolution. Upper left: the new building of PETRA III housing the latest extension stage of the DESY synchrotron facilities. Upper right: The beamlines inside the PETRA III building. Lower left: the sample manipulation stage inside the hutch of beamline IBL P05. The sample is located in the center of the image on the small metal pin. Lower right: the beamline hutch illustrating the general setting. The black device is the sample stage allowing for exact sample positioning with micron resolution.

extend from the availability of micro computer tomography (microCT) devices (Beutel and Friedrich, 2008). The principle of microCT imaging can be compared to medical CT imaging, where an electron beam penetrates the sample and the absorbtion of the beam by the sample is measured for each sensor pixel (Betz et al., 2007). Medical CT scanners reach resolutions of 500 micron whereas current microCT scanners deliver effective pixel resolutions of 1 micron. These devices combine quick image aquisition times with high resolution. However, the density dependent resolution of samples, i.e. the tissue dependent display of different grey values is poor.

SR-microCT is based on synchrotron radiation as beam source. The radiation is very brilliant i.e. contains a high quantity of photons per energy range and area. It is, imonochromatic and has a parallel beam geometry. As already stated (Friedrich and Beutel, 2008a) this can result in images with high tissue dependent density resolution. SR-microCT is well suited for phase-contrast imaging but also delivers density dependent resolution in attenuation-contrast mode when special settings are used (Beckmann 2008). However, the experimental setups (beam energy range, sensor, etc.) between facilities vary. This can lead to very different results regarding image quality. The usage of these facilities is bound to successful project applications due to the quantity of working groups interested in research at these experimental stations and the limited available time. Usually the application is restricted to shifts of several hours up to three days, which is nonetheless enough to investigate up to 140 different samples, depending on sample size and desired scan quality, therefore allowing to explore muscles and endoskeletal features of many taxa to the level of figure ready data in a matter of days.

This quick high quality data acquisition aided some major contributions concerning long standing problems of entomological research: a robust phylogeny of holometabola (Beutel et al., 2011), a first cladistic assessment of polyneopteran phylogeny based on cephalic characters (Wipfler, 2012; Wipfler et al., 2011), the morphological rejection of the Halteria concept (Friedrich and Beutel, 2010), and numerous contributions concerning other insect groups (Beutel et al., 2008a; Beutel et al., 2008b; Friedemann et al., 2012; Friedrich and Beutel, 2008b; Wipfler et al., 2012).

Due to its focus on muscles and skeletal features the present thesis solely uses micro- and SR-microCT for the acquisition of inner anatomy data. Scanning electron microscopy (SEM) is used for the documentation of the outer anatomy. A total of 118 specimens could be explored, in the case of SR-microCT performed at DESY also with a high density resolution.

The data from these facilities are provided as image stacks in a defined cutting plane (sagittal, transverse, frontal). The perfect alignment of the stacks allows to “browse” through the object while paging through the images. By using programs like Reconstruct ® (Fiala, 2005) it is possible to segment structures in each image. After this a mesh is generated between each segmentation which results in a three dimensional image. This allows to explore the spatial arrangement of structures.

Goals and structure of this thesis

The aims of this disseration are (i) to illustrate the evolution of the head in the first insect lineages, (ii) to point out potential pitfalls in the interpretation of structures, (iii) to provide a formal approach to identify convergence, and (iv) to illustrate current developments in the field of SR-microCT data aquisition.

This thesis is divided into 14 chapters. In chapter 2 a promising method for SR-microCT imaging of internal features on the nanoscale level is described. Chapter 3 serves as an introduction to the second main topic of this thesis – the phylogenetic relationships of the orders Odonata, Ephemeroptera, and Neoptera. In chapter 4 evidence for Palaeoptera is provided for the first time based on analyses of cephalic characters. This included a detailed description of odonatan head structures, a comparison to ephemeropteran cephalic features, and the compilation of a data matrix including a sizeable taxon sampling with data partly gathered from the literature. In chapter 5 the same data set is analysed applying a formal approach to detect concerted convergence in morphological matrices. The study corroborated Palaeoptera and provided objective means to exclude certain characters from phylogenetic analyses.

Chapter 6 is a short overview on the third main topic of this thesis - an analysis of the morphology and phylogenetic relationships among Odonata.

Chapter 7 is a study focused on the adult head of *Epiophlebia superstes*. In chapter 8 the gathered morphological data for Odonata are analysed phylogenetically. A published morphological data matrix is extended by characters mainly related to the internal cephalic structures. Subsequently, the character matrix is used for tree reconstruction and concerted convergence analysis.

In Chapter 9 the inner and outer head anatomy of *Tricholepidion gertschi* the up to now sole representative of the relic family Tricholepididae is described. This chapter will serve as an important basis for subsequent analyzes of Zygentoma, the sistergroup of all winged insects. Chapter 10 is a general discussion of the framework presented in this thesis including an outlook to further projects planned.

2

X-ray Mosaic Nanotomography of Large Microorganisms

X-ray Mosaic Nanotomography of Large Microorganisms

X-ray mosaic nanotomography of large microorganisms

R. Mokso [a], L. Quaroni [a], F. Marone [a], S. Irvine [a,b], J. Vila-Comamala [c], A. Blanke [d], M. Stampanoni [a,e]

[a] Swiss Light Source, Paul Scherrer Institut, 5232 Villigen, Switzerland
[b] School of Biology and Medicine, University of Lausanne, Switzerland
[c] Laboratory for Micro-and Nanotechnology, Paul Scherrer Institut, 5232 Villigen, Switzerland
[d] Zoologisches Forschungsmuseum Alexander Koenig, Adenauerallee 160, 53113 Bonn, Germany
[e] Institute for Biomedical Engineering, University of Zürich and ETH Zürich, 8092 Zürich, Switzerland

This is the author’s version of a work originally published in the Journal of Structural Biology (2012) 177: 233-238

Abstract

Full-field X-ray microscopy is a valuable tool for 3D observation of biological systems. In the soft X-ray domain organelles can be visualized in individual cells while hard X-ray microscopes excel in imaging of larger complex biological tissue. The field of view of these instruments is typically 103 times the spatial resolution. We exploit the assets of the hard X-ray sub-micrometer imaging and extend the standard approach by widening the effective field of view to match the size of the sample. We show that global tomography of biological systems exceeding several times the field of view is feasible also at the nanoscale with moderate radiation dose. We address the performance issues and limitations of the TOMCAT full-field microscope and more generally for Zernike phase contrast imaging. Two biologically relevant systems were investigated. The first being the largest known bacteria (Thiomargarita namibiensis), the second is a small myriapod species (Pauropoda sp.). Both examples illustrate the capacity of the unique, structured condenser based broad-band full-.eld microscope to access the 3D structural details of biological systems at the nanoscale while avoiding complicated sample preparation, or even keeping the sample environment close to the natural state.

Introduction

The penetrating power of X-rays coupled to the high photon flux of 3rd generation synchrotron sources makes X-ray tomography outperform other imaging techniques in particular when large, opaque samples need to be investigated with high spatial and temporal resolution. Standard synchrotron-based-microtomography, reaching about 1 μm spatial resolution (Stampanoni et al., 2010), does not allow the imaging of samples down to the cellular level in sufficient detail. There is a general need to overcome this limitation and to further develop imaging techniques reaching sub-micrometer spatial resolution. The performance of full-field X-ray microscopy instruments relies on the fabrication of X-ray optical components, like Fresnel zone plates (FZP) used as beam shapers, condensers or magnifying lens, similar to visible light microscopes. The main difference is that for a FZP-based X-ray microscope, the spatial resolution is mainly affected by the size of the outermost zone of the lens rather than by the diffraction constraints. The fabrication of X-ray lenses is technologically challenging especially for hard (>10 keV) X-rays. This explains the apparently paradox situation of state-of-the-art X-ray microscopes, where the best achieved spatial resolution is inversely proportional to the X-ray wavelength at which the full-field microscope operates. Soft X-ray full-field microscopes look back to a longer history and can currently achieve a spatial resolution of about 20 nm routinely (Parkinson et al., 2008). They are typically designed to work in the water window (283–530 eV) and the contrast is based on absorption using the significant difference in photoelectric cross-section between carbonized structure and the aqueous medium. The small penetration depth – typically less than 15 μm for biological soft tissue – is sufficient to study single cells. On the other hand, hard X-ray microscopes with efficient tomographic capabilities usually operate in projection mode (Mokso et al., 2007) or full-field mode (Andrews et al., 2010; Neuhausler et al., 2003) and typically in the range of 6–20 keV with a penetration depth of up to several millimeters, granting therefore insight into larger samples made of materials with higher atomic numbers. In projection mode at 17–29 keV, with inherent propagation-based phase contrast, a spatial resolution of 180 nm in 3D has been reported in Requena et al. (2009). In full-field mode and Zernike phase contrast a spatial resolution of 30 nm was demonstrated for the 2D case in Chen et al. (2011) and beyond 200 nm for 3D in Stampanoni et al. (2010) and Takeuchi et al. (2011). As a consequence and differently from soft X-ray microscopes these instruments are well suited for both biological and material science applications. A more detailed review on X-ray microcopy can be found in Sakdinawat and Attwood (2010). Here, we highlight two biological applications of a full-field hard X-ray Zernike phase contrast microscope based on a structured condenser and its corresponding, custom-designed X-ray phase shifting optical component. We fully exploit the large penetration length and depth of focus as well as the short exposure times to perform full-field 3D nanoimaging of large biological objects that we will refer to as ‘‘mosaic tomography’’.

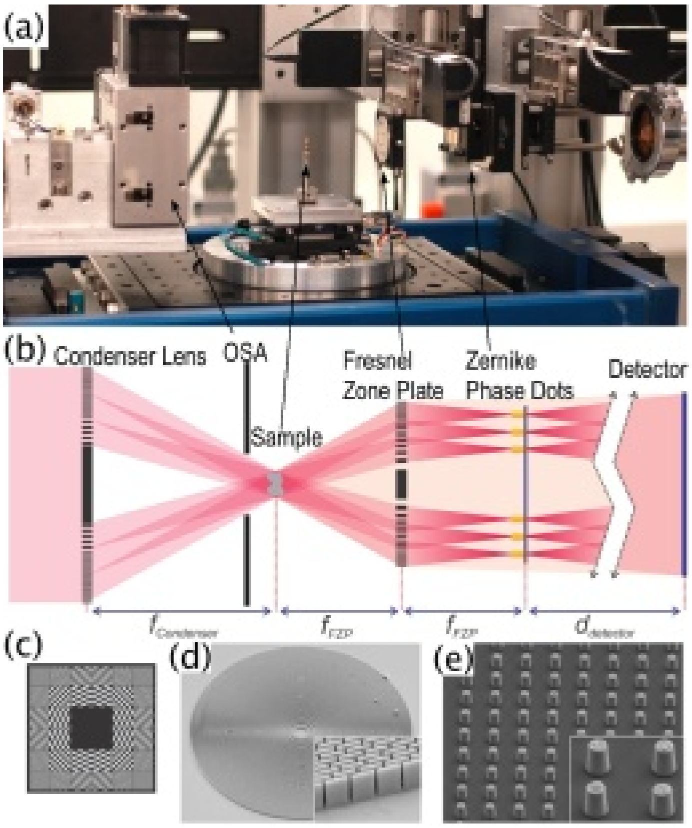

Fig.1. The TOMCAT nanoscope (a) with the schematic drawing of the layout (b) and the structured condenser (c). SEM images of the objective Fresnel zone plate and (d) and the phase dots (pillars) (e)

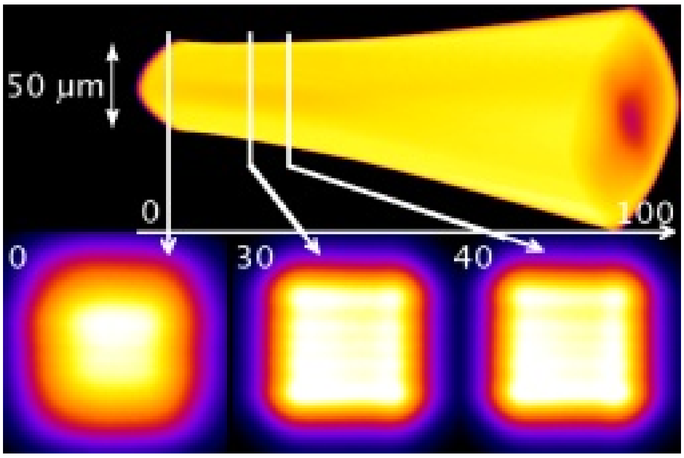

Fig.2. The illumination cone near the focal plane of the condenser acquired using a high resolution X-ray detector over 100 mm in beam direction with a step size of 1 mm. The three transversal beam profiles in the lower part of the Figure are shown for the positions 0, 30 and 40 mm.

Instrumentation and methods

The TOMCAT beamline of the Swiss Light Source (Stampanoni et al., 2010) operates a full-field microscope with moderately monochromatic X-ray beam from a double crystal multilayer monochromator ($\Delta\lambda / \lambda = 10^{-2}$). The advantage of this unusual choice for the energy bandwidth is the high photon flux from the multilayer ensuring short exposure times and therefore fast data collection. The benefit is evident, in particular for tomographic acquisitions, where a large number of angular projections is required and therefore shorter exposure times results in relaxed requirements on the instrumentation's long term stability. Fast data acquisition is a particularly important prerequisite for realizing full-field raster scanning in order to extend the effective field of view of the microscope. This can be done in either 2D (Andrews et al., 2008) or, as introduced in this work, in 3D (mosaic tomography).

The optical layout

The TOMCAT full-field microscope is operated optimally between 8 and 12 keV, since for this energy range the efficiency of each diffractive optical element lies between 6% and 9% while it significantly decreases at higher energies. For this work in particular, we adjusted the X-ray energy to 10 keV. As described in detail in Stampanoni et al. (2010) and schematically shown in Fig. 1, the beam condenser installed 20 m downstream from the source (13 m from the Ru/C multilayer monochromator) collects 1 x 1mm2 of the X-ray beam and creates a sample illumination of 0.05 x 0.05 mm^2 at a distance of $f_{condenser}$ = 760 mm further downstream. The unconventional design by Jefimovs et al. (2008) of this structured condenser results in a square top-flat illumination spot instead of the most common circular one with an Airy disk profile. We use a condenser with an outermost zone width of 70 nm. Gold structures of 900 nm in height have been fabricated by electroplating into a polyimide mould. The resulting aspect-ratio of 13 ensures about 8% diffraction effciency. To obtain a homogeneous, top-flat illumination with this structured condenser (Fig. 1b), the transverse coherence length of the incoming X-rays should be smaller than the size of one single element within the condenser lens. In our case, one structural element is 50 50 μm^2 in size and therefore, at 20 m from the superbend source, the above mentioned condition is satisfied along both the vertical and horizontal direction. For broad bandwidth illumination, the depth of focus of the condenser is several hundreds of micrometers long. This can be verified experimentally (Fig. 2) by recording a through-focus series around the condenser focal plane. As a consequence, large samples are illuminated uniformly not only along the lateral but even along the direction of the optical axis. To produce a magnified image of the sample ($d_{detector}$ = 9.95 m downstream of the lens), an objective zone plate is inserted 56.8 mm downstream the sample. We use a Fresnel zone plate with 70 nm outermost zone width and 900 nm high gold structures, this time lithographically prepared on a thin SiN membrane. With a diameter of 100 μm the focal distance at 10 keV is f_{FZP} = 56.4 mm. The numerical aperture is matched to that of the condenser ensuring therefore best performance (Goodman, 1988). A 14-bit dynamic range and high sensitivity Photonics Science VHR water cooled CCD detector is coupled via a fiber optics taper (with 3-fold magnification) to the scintillator screen (GdOS:Tb). The geometrical pixel size at the scintillator plane is 4 μm. Accounting for the magnification of the X-ray microscope of M = 175, the pixel size of the full-field X-ray microscope is 23 nm. In this configuration the (absorption) contrast in the images arises through the variation of the photoelectric cross section of the elements composing the sample. However, the majority of small samples investigated at submicrometer resolution exhibit naturally very little attenuation contrast at 10 keV due to their small size. Especially for biological samples, an alternative, more sensitive, approach is desired. Zernike phase contrast (ZPC) (Zernike, 1934) offers improved sensitivity. We generate ZPC by inserting an array of phase shifting gold pillars in the back-focal plane of the Fresnel zone plate. These are lithographically fabricated on a thin SiN membrane and consist of 25 x 25 pillars spaced by 3.56 μm. Their diameter is 0.9 μm and their height 3 μm. This specific array scheme is required to match the shape of the condenser's illumination in the Fourier space, where each of its individual structural element corresponds to a light spot. In the following, we will refer to this optical element as Zernike phase dots as introduced in Stampanoni et al. (2010).

Formation and interpretation of Zernike phase contrast images

Zernike phase contrast is an interferometric technique where the reference and object wave are spatially not separated and belongs therefore to the common-path interferometric methods. The reference wave is the part of the beam which is not affected by the sample: it constitutes the transmitted, undiffracted part of the beam.

There are three distinct arrangements which give rise to ZPC-type interference. The first – most commonly used – is by retardation of the reference wave (positive ZPC), the second is by retardation of the diffracted part of the beam (negative ZPC) and the last option is by attenuating the reference wave. In Stampanoni et al. (2010) we showed the performance of a full-field microscope operated in negative ZPC mode while in the current study we present a combination of the first and third option to produce positive ZPC images enhanced by reference beam attenuation. The positive ZPC image is produced with a $\pi/2$ phase shift combined with the attenuation of the reference wave via the Zernike phase dots and – at the same time – by letting the beam diffracted by the sample travel unchanged and in turn create interference with the delayed diffracted branch. Different phase shifting dots (e.g. $p=\pi/4$ or $3\pi/4$) can also be used to manipulate the image contrast. In this paper, for the sake of simpler interpretation of the intensity values, we use the $\pi/2$ phase shift. If we write the complex object function as $T(x,y) = A\ x\ exp(i\ \phi)$ and suppose a pure phase object satisfying the weak phase approximation (sometimes referred to as smallscale phase approximation) then the complex object function can be approximated by the Taylor expansion to the first order as $T(x,y) = 1 + i\ \phi$. The intensity in the images may then be linearly mapped to the actual phase of the object. In the case of a $\pi/2$ phase dots it becomes $I = i + 2\ \phi$.

Sample requirements

When using 10 keV X-rays the penetration depth in biological tissue is as great as several millimeters. Furthermore, because the depth of focus for the X-ray lenses is several hundred micrometers too, an X-ray projection image (2D) of large (several hundred micrometers) samples can therefore be acquired and interpreted. In standard X-ray Zernike Phase Contrast microscopy meaningful 3D images are obtained, if the samples' lateral dimensions are restricted to approximately the field of view of the microscope, in our case 40 µm. As discussed above, the image contrast generated by a Zernike type microscope can – under the condition of weakly absorbing objects – be linearly related to the phase shifting properties of the sample.

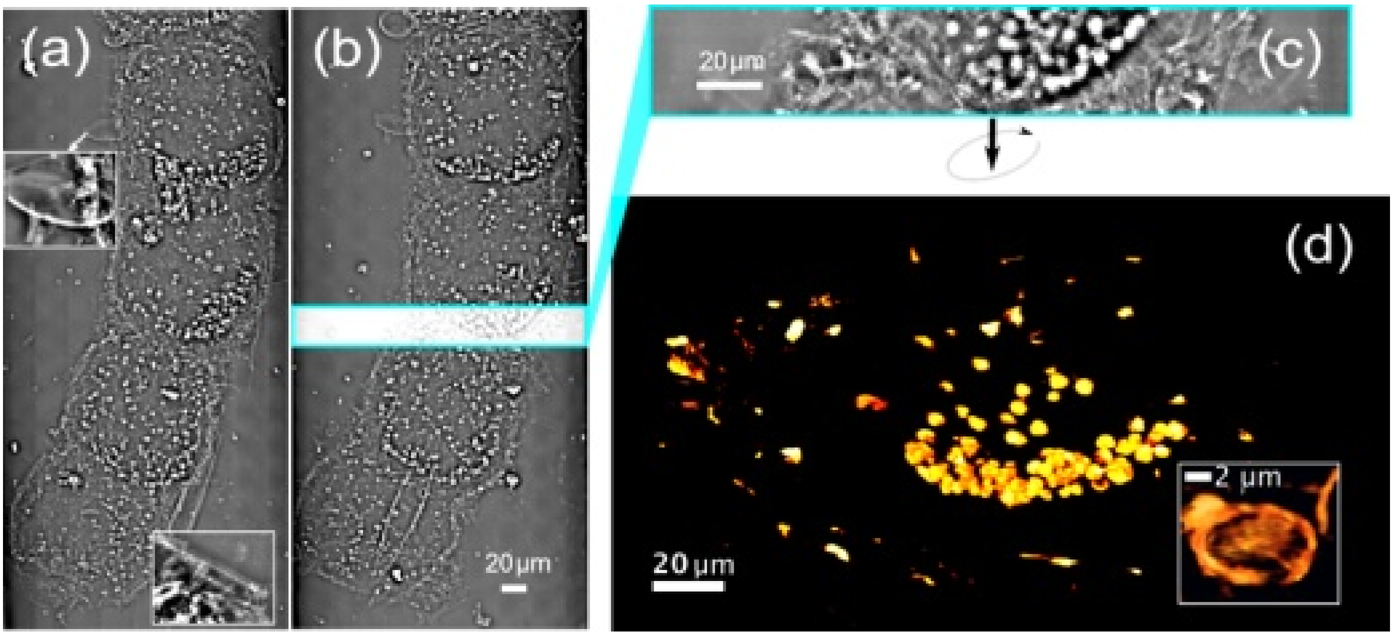

Fig.3. Mosaic tomographic nanoimaging of the Thiomargarita namibiensis bacteria. In (a) and (b) are depicted the 2D mosaic images, at 0° and 45°, respectively, consisting of 9 x 20 radiographic images obtained through raster scanning the sample in full-field microscopy mode. In (c), we show an example of the row of 1 x 6 images used for the tomography. By combining 73 angular positions, the result is a 3D reconstruction with rendering shown in (d). Amongst other information, we are able to see for the first time an accurate distribution in 3D of the inclusions at the periphery of the cell. The insets in (a) represent zoomed-in projection images of diatoms attached to the surface of the bacteria. The inset in (d) highlights a 3D rendering of a diatom zoomed in at the tomographic reconstruction to appreciate its fine structure.

Practically, this condition means that the sample must produce a phase shift smaller than $\pi/3$(Goodman, 1988) for the first order Taylor expansion to be valid. If such requirements are not met and the object is violating the first-order Taylor approximation, then it is no longer straightforward to extract quantitative information from ZPC images either in 2D or in 3D.

The possibility to use a Taylor expansion to higher orders was theoretically investigated by Teschke and Sinzinger (2009). An alternative method based on Fourier decomposition was attempted by Glückstad and Palima (2009). It is mainly in visible light microscopy where efforts are put into the quantitative interpretation of ZPC images of strong phase objects while for ZPC with X-rays the imaging of strong phase objects remains in many studies rather qualitative than quantitative.

Data processing

The raw tomographic projections are corrected for the background and detector dark current using the usual expression (Image-dark)/(background-dark). Other than this the projections do not undergo further processing prior to the tomographic reconstruction. In the case of the mosaic tomography the projections corresponding to a given angular position are stitched to form a single projection image. The stability of the microscope and the precision of the sample stages allow one to feed the angular projections directly into the standard tomographic reconstruction algorithms. The Fourier based tomographic reconstruction routine (Marone et al., 2008) used for parallel beam tomography at the TOMCAT beamline was applied to all data. The resulting volumes capture the spatial distribution of structures based on their phase retardation action on the probing X-rays. The images shown in the figures are raw data without further manipulation.

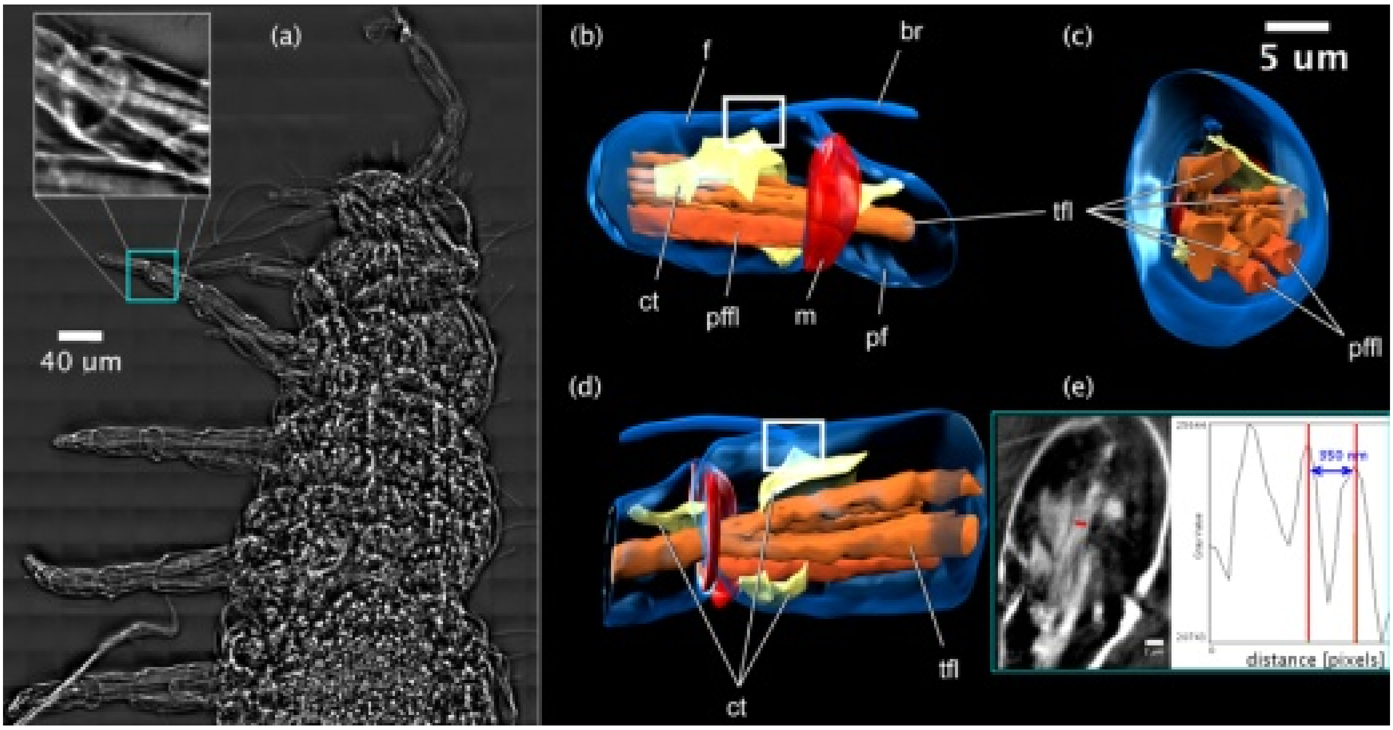

Fig.4. Stitched 2D image of the Pauropus sp. (Myriapoda) showing the habitus of the animal. The inset in (a) represents a projection image of the selected region of interest for the tomographic acquisition. On the right the volume rendering of the tomographic reconstruction of the femur-postfemur articulation with detailed labeling of the different muscle groups are shown. The colormap highlights the cuticle (blue, partly transparent), muscles (orange), connective tissue (yellow), and membranes (red). The three dimensional reconstruction is visualised by the anterior view (b), mesolateral view (c) and posteroir view (d). White square highlights the connection between bristle and connective tissue. Further explanations see text. Abbreviations: br, bristle; ct, connective tissue; f, femur; m, membrane; pf, post-femur; pffl, post-femur flexor; tfl, tarsal flexor. In (e) the spatial resolution and tissue contrast is demonstrated. The line profile (on the right) along a 2 lm long line (in red) on a tomographic slice (on the left) highlights the resolved fine structure of the connective tissue. The Y-axis represents the normalized gray value in the reconstructed 16 bit tomographic slice.

Radiation dose

One important issue to address in X-ray microscopy is the deposited dose and its effects on the samples. It has been established that the deposited dose is a function of the desired spatial resolution (Howells et al., 2009). Particularly for biological samples, images are strongly affected by radiation issues and are mainly showing the damaged tissue rather than its natural state. Specifically for our experiment at 10 keV, the photon flux incident on the condenser is approximately 10^{11} photons/s/mm^2. Accounting for the efficiency and focal spot size of the condenser as well as the 0.6 x 0.6 mm^2 beam blocker, the total photon flux within the illumination plane reaches 10^{12} photons/s. Because only about 8% of these photons at 0.12 nm wavelength are absorbed in the bacteria, the deposited dose rate – calculated according to the simplified model reported by Howells et al. (2009) – is below 1 Gy/s. According to the empirical formula D_m [Gray] = 10^8 x *res* [nm] (Howells et al., 2009), where *res* is the spatial resolution, the maximum tolerable dose for a spatial resolution of 100 nm is $D_{mt} = 10^{10}$ Gray. To verify the non-destructive features of our hard X-ray 3D microcopy technique, we captured an image of the sample (T. namibiensis as discussed in Section 3.1) before and after the tomographic acquisition and compared them in order to investigate eventual damage in the structure. Taking into account the total exposure time during the tomographic acquisition as described below the calculated dose deposited into the bacteria is less than 70 Grays, i.e. well below the tolerable radiation.

Results

In this work, we focus on two examples of large (several hundreds of micrometers) biological specimens to demonstrate the unique capabilities of mosaic, hard X-ray full-field microscopy in Zernike phase contrast mode. The first example is a bacterium (*T. namibiensis*), the second is a myriapod insect (*Pauropoda* sp.). The experiments were performed with a pixel size of 46 nm. For this configuration the 3D spatial resolution previously evaluated in Stampanoni et al. (2010) is 144 nm. In each of the two applications the spatial resolution was addressed separately in a similar way.

T. namibiensis *bacteria*

Thiomargarita bacteria are the largest known bacteria, with individual cells typically 100–300 μm in diameter, but reaching a size of up to 700 μm (Schulz et al., 1999; Schulz and Schulz, 2005). The cells are often gathered to form chains that are visible to the naked eye. Thiomargarita are lithotrophic organisms living in oceanic sediments, where they survive by oxidizing hydrogen sulfide using nitrate stored in a large vacuole. The cell structure is dominated by the vacuole, with the cytoplasm limited to a thin (about 2 μm) surrounding layer. Strings of bacterial cells are further enveloped by a gelatinous sheath. The sheath is believed to protect the cell from mechanical damage arising from contact with sediment particles. As part of their metabolism, the bacteria accumulate inclusions of elemental sulfur, polyphosphate and polyglucose, ranging in size from 1 to 10 μm, distributed over a roughly spherical surface at the periphery of the cell. We observed that the larger inclusions are spherical and their size distribution in the studied bacteria was very monodisperse with a diameter of 4 μm. The absorption of such particles, presumably sulfur according to their size, at 10 keV is only about 4%. They shift the phase by $\pi/4$ at most (when X-rays travel through their center) satisfying locally the condition for quantitative ZPC imaging at 10 keV, yet their transmission for soft X-rays (water window) would still be less than 1% making their observation with a soft X-ray microscope practically impossible.

The bacteria are not mobile, so no mobility preventing substances such as gels or fixatives had to be used. The sample preparation consists therefore only of inserting the bacteria into a capillary of 300 μm in diameter, containing seawater and marine sediment, and placing the capillary onto the sample stage. Nonetheless some sporadic movements of the cell have been occasionally observed, probably due to convection processes within the medium in the capillary.

Fig. 3a depicts a 2D mosaic image resulting from raster scanning the sample in full-field microscopy mode. A total of 9 x 20 = 180 radiographic images were collected covering the whole area of the sample with a lateral extension of approximately 200 μm. The exposure time for each radiographic projection was 1.4 s (for 2 x binning and a pixel size of 46 µm). This procedure can be applied at any selected angular position (Fig. 3b is rotated 45° around the tomographic rotation axis as compared to Fig. 3a). For the demonstration of the proposed low dose mosaic tomography mode we selected a horizontal ‘stripe’ of 1 x 6 fields of view Fig. 3c to form a single, stitched projection for 73 angular positions, i.e. one stripe every 180/72°. Finally, we combined the raster scanning of 1 x 6 FOV with the rotation of the bacteria around the vertical tomographic axis. This results in a set of 73 radiographic projections each of 700 x 4200 pixels corresponding to the physical dimensions of 35 x 210 lm for the final FOV. The total exposure time during which the bacteria was irradiated was 12 min for the whole tomographic set, not including overheads introduced by the movement of the linear stages and the readout time for the CCD.

Applying the standard reconstruction routine (Marone et al., 2008) we obtain a tomogram of the entire horizontal size of the bacteria. In this particular application we chose to minimize the deposited radiation dose on the bacteria and compromise the true 3D spatial resolution as it is affected by the angular undersampling (small amount of tomographic projections). The power spectrum method applied on the whole reconstructed 3D volume gives a spatial resolution of 150 and 210 nm in the directions parallel and perpendicular to the tomographic rotation axis, respectively. The image (Fig. 3b) shows in detail the distribution of inclusions at the periphery of the cell. This is the first time that the accurate mapping of the inclusions of Thiomargarita in 3D has been reported. Previous measurements used confocal fluorescence microscopy to visualize the distribution of the cytoplasm. TEM experiments also provided high resolution images of the cytoplasm (Schulz, 2006), but at the expense of dissolving sulfur grains during the fixation process. Rotation of the image clearly shows the distribution of the inclusions along a spherical surface, which cannot be appreciated from a single 2D projection. Spherical inclusions larger than 3 microns in size are expected to be mostly elemental sulfur. Smaller irregular inclusions could be either polyphosphates or polyglucose deposits.

The inorganic components of the sheath are also imaged with high contrast and high resolution. Several diatom and foraminifera skeletons attached to the gelatinous sheath have been easily identified. For some of them, fine structural patterns of the skeleton could be appreciated with submicron resolution as highlighted in the insets of Fig. 3a and d. In addition to these well identified structures, numerous small structures are seen embedded in the sheath, probably representing fragments of shells.

We also investigated the radiation damage and, as all images before and after the scanning procedure were identical, we therefore conclude that no obvious radiation induced damage was observed on the bacteria.

Micro-arthropods (Pauropoda sp.)

The aim of our second example is the visualization of internal structures in micro-arthropods. Nanotomography can be particularly useful for imaging muscles and cuticular structures in these animals. It delivers fast, consistent results with good resolution allowing for structure comparison between many taxa in a reasonable timeframe. In particular, this feature was used here to study soil dwelling micro-arthropods. The single species shown in the present work forms a part of a bigger framework aiming at a detailed comparison of the leg and trunk musculature of all major myriapod taxa. Leg and trunk musculature has proven useful to infer phylogenies of other Arthropoda (Bäcker et al., 2008). Myriapoda (centipedes) are a subphylum of the megadiverse arthropods (a phylum containing also insects, arachnids and crustaceans, approximately 1.2 million of described species). Despite numerous molecular research activities (Gai et al., 2006; Regier et al., 2005) the phylogeny of Arthropoda, in particular the location of myriapods is still heavily disputed. Myriapods are composed of four main taxa (Chilopoda, Diplopoda, Pauropoda and Symphyla) whose intrarelationships are also not clear. This situation requires a broad taxon sampling, so that character polarisation can be developed robustly.

As an example, we present here *Pauropus* sp. (Pauropoda), a particular small taxon of Myriapoda (approximately 0.5 x 1mm body size). The legs of these species are extremely small (ca. 0.2 x 0.1 mm). Prior to scanning, samples were dried at the critical point (CPD) (Model E4850, BioRad) and mounted on dedicated specimen holders. Similarly to the previous example, we raster scanned and stitched the images of the whole insect to identify the regions of interest for the individual nanotomographic acquisitions (Fig. 4a). The scale bar of 40 µm is chosen to highlight the standard field of view of the instrument. When the regions of interest were identified, a tomographic set of the femur articulation was acquired. Differently from the previous example, the scanning procedure here was the standard one consisting of 460 projections (without raster scanning). The tomographic reconstruction was performed using the standard algorithm for parallel beam. Subsequent segmentation and rendering was accomplished with GPL license packages Reconstruct (Fiala, 2005) and Blender (blender.org). The 3D spatial resolution evaluated on tomographic slices of various orientation using the power spectrum analysis corresponds to 140 nm similarly to the previously published results Stampanoni et al., 2010. The high 3D spatial resolution allows one to observe fine structural details as demonstrated in Fig. 4e.

The 3D reconstructions clearly show the cuticle and musculature at the femur-postfemur articulation (Fig. 4b-e) as well as connective tissue and membranes. The last accounts of these body parts date back several decades (Tiegs, 1947). From the rendering on Fig. 4b–d and the movie in the Supplementary material it becomes obvious that the muscle equipment differs from the literature record. The tarsal flexor (tfl) originates clearly not in the femur. The post-femur flexor (pffl, ‘‘.fl.tb’’) in Tiegs (1947) is composed of two muscle bundles instead of three (Tiegs, 1947). This gives important information for the development of character matrices which can be subsequently used for phylogenetic analysis. Moreover, it became apparent that the large bristle at the dorsal side of the femur is connected to the large tarsal flexor (Fig. 4d); t.) by connective tissue. The structural linkage may be of importance for rapid motions of the leg, not controlled by the nervous system, but by indirect stimuli. If the bristle is deflected by an obstacle in the way of this leg part, the deflection is transferred via the connective tissue to the tarsal flexor. This induces a contraction of this muscle so that the tarsus is flexed rapidly to react to objects which are in the way of the leg. Such indirectly controlled movements are frequently reported for arthropods, but are not known for Pauropoda, yet (Koditschek et al., 2004). It remains to be tested by further studies which precise impact this morphological linkage, identified here for the first time, has for the functional biology of pauropod legs.

Conclusions

In this paper, we discuss the performance and limitations of the hard X-ray full-field microscope in Zernike phase contrast mode. With two biologically relevant examples we show how large samples can be characterized in 3D at the nanoscale. This type of sample has so far been visualized with mostly surface sensitive methods in 2D (visible light microscopy, SEM) or with limited spatial resolution in 3D (parallel beam X-ray imaging). For both cases the fast mosaic radiographic imaging is first used to identify the regions of interest. This is followed either by standard nanoscale tomography or (as introduced in this paper) by mosaic tomography to access the spatial distribution of relevant features in 3D within the selected region of interest. With the study of *T. namibiensis* we demonstrated the capability to perform 3D nanoscale imaging with an extended field of view up to the lateral dimension of the sample rather than performing local tomography. The Thiomargarita bacteria was scanned in an environment of seawater with sediments, i.e. very close to its natural condition. This fact can be of utmost importance for many biological studies where complicated sample preparation can impair the purpose of the study, since biological systems do often change their structure/functionality when extracted from their natural environment. Hard X-rays are a highly efficient probe for sub-micrometric 3D imaging of relatively large biological samples and in particular when anorganic compounds are part of the inner structure. It must be pointed out that today there is no alternative technique to hard X-ray microscopy to extract the 3D structural details at the nanoscale for these two kinds of applications.

Outlook

In our setup it is straightforward to switch between positive and negative ZPC simply by substituting the phase pillars by phase 'holes'. As shown in this and in an earlier work (Stampanoni et al., 2010) both configurations give similar image quality. Therefore the linear combination of a doublet of positive and negative ZPC images could further enhance the image contrast if desired. For the low dose mosaic tomography, iterative tomographic reconstruction methods may bring improvement in image quality.

Acknowledgments

We greatly acknowledge G. Mikuljan of the SLS-TOMCAT beamline staff for his fundamental support in setting up the experiment. This study was supported by Centre d'Imagerie BioMedicale (CIBM) of the UNIL, UNIGE, HUG, CHUV, EPFL and the Leenaards and Jeantet Foundations.

3 SR-microCT-data helps to develop a phylogenetic character matrix for head structures of lower Pterygota

SR-microCT-data helps to develop a phylogenetic character matrix for head structures of lower Pterygota.

SR-microCT-data helps to develop a phylogenetic character matrix for head structures of lower Pterygota

Alexander Blanke, Manuela Thelen

Zoologisches Forschungsmuseum Alexander Koenig, Zentrum für molekulare Biodiversität, Adenauerallee 160, 53113 Bonn, Germany

This is the author's version of a work originally published in the HASYLAB annual report 2011

The basal branching patterns of pterygote insects - Odonata, Ephemeroptera and neopterans - are one of the major unsolved problems of insect systematics (Klass 2007). All three possibilities are subject of the discussion and are favoured by studies (Haas and Kukalová-Peck 2001; Hennig 1969; Kristensen 1981; Kristensen 1991; Kukalová-Peck 1991; Staniczek 2000; Staniczek 2001). One major setback of morphologic analyses in the past were incomplete studies and an insufficient taxon sampling. Especially the odonatan head was rarely studied (Mathur and Mathur 1961; Short 1955). In contrast, the head has proven to be a highly informative character system (Beutel et al. 2010), especially addressing the pterygote base (Wipfler et al. 2011). Since the odonatan thorax with its direct flight musculature highly diverges from all other pterygote insects, it is of limited use in our context. The present study will address the basal pterygote relationships by providing a comprehensive morphological data set: 200 cephalic characters for a total of 26 species of all major pterygote insect lineages and two outgroups (Archaeognatha and Zygentoma) are studied. Evolutionary scenarios for all three possible clades (Metapterygota, Palaeoptera, Chiastomyaria) will be presented.

Prior to scanning samples were critical point dried (CPD) (Model E4850, BioRad) and mounted on sample holders. Except for Siphlonurus and Lepisma all specimens were scanned using the beamline BW2 of the storage ring DORIS III at DESY (operated by HZG) with a stable energy of 8 keV and a high density resolution (Beckmann et al. 2008). For scanning electron microscopy (SEM) species were transferred to 100% ethanol, CP-dried (Model E4850, BioRad) and subsequently sputter coated (Model Anatech Hummer VII). Microscopy was performed on a Hitachi S-2460N using a special sample holder (Pohl 2010).

Some of the results obtained by SR-microCT scanning at BW2 are shown below (Fig 1, B). We received detailed images of the inner anatomy of our taxon set. The muscle equipment and our results from the external analysis (Fig 1, A) will be incorporated into a data matrix for phylogenetic analysis and subsequently analysed with TNT and Winclada.

With the help of SR-microCT at DESY we plan to conduct studies on the functional anatomy of pterygote heads. The 3D models generated from the CT-data will be the basis for developing physically realistic simulations of mouthpart movement. This will aid us in reconstructing a scenario for the mouthpart evolution which is robust and testable against conflicting hypotheses.

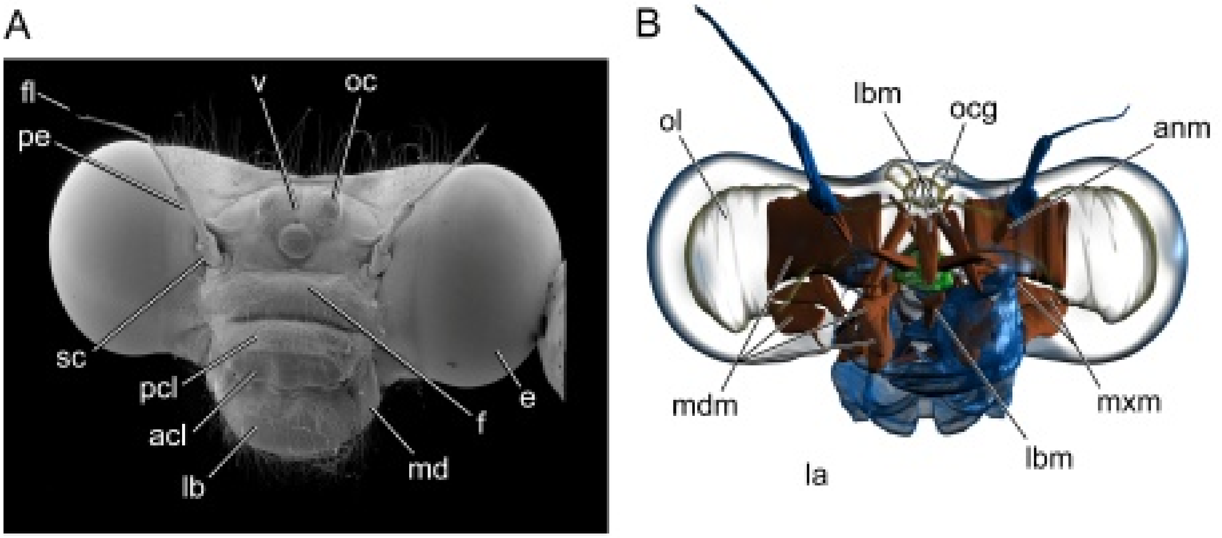

Figure 1 The head of L. virens in frontal view. A SEM picture show relevant head structures and general organisation. B 3D-reconstruction from SR-microCT data showing head muscles, brain and ocellar ganglia. acl anteclypeus, anm antennal muscles, e eye, fl flagellum, la labium, lb labrum, lbm labral muscles, md mandible, mdm mandibular muscles, mxm maxillar muscles, oc ocellus, ocg ocellar ganglion, ol optical lobe, pcl postclypeus, pe pedicellus, sc scapus, v vertex

4

Revival of Palaeoptera – head characters support a monophyletic origin of Odonata and Ephemeroptera (Insecta)

Revival of Palaeoptera – head characters support a monophyletic origin of Odonata and Ephemeroptera (Insecta)

Revival of Palaeoptera – head characters support a monophyletic origin of Odonata and Ephemeroptera (Insecta)

Alexander Blanke [a,*], Benjamin Wipfler[b], Harald Letsch[c], Markus Koch[d], Felix Beckmann[e], Rolf Beutel[b], Bernhard Misof[a]

[a] Forschungsmuseum Alexander Koenig, Zentrum für molekulare Biodiversität, Adenauerallee 160, 53113 Bonn, Germany

[b] Entomology Group, Institut für Spezielle Zoologie und Evolutionsbiologie, Friedrich-Schiller-Universität Jena, Erbertstraße 1, 07743 Jena, Germany

[c] Department für Tropenökologie und Biodiversität der Tiere, Universität Wien, Rennweg 14, A-1030 Vienna, Austria

[d] Institute of Evolutionary Biology and Animal Ecology, University of Bonn, An der Immenburg 1, 53121 Bonn, Germany

[e] Institute of Materials Research, Helmholtz-Zentrum Geesthacht, Max-Planck-Str. 1, 21502 Geesthacht, Germany

*Corresponding author, e-mail adress: blanke@uni-bonn.de

This is the author's version of a work originally published in the journal Cladistics (2012) 28: 560-581

Abstract

The earliest branching event in winged insects, one of the core problems regarding early insect evolution, was addressed using characters of the head. The head is arguably one of the most complex body regions in insects and the phylogenetic information content of its features has been demonstrated. In contrast, the wings and other body parts related to the flight apparatus and sperm transmission are not useful in the context of this problem, since the outgroups (silverfish and bristletails) are wingless and transmit spermatophores externally. Therefore they show profound differences in the organisation of the postcephalic body, and the homology assessment and subsequent phylogenetic analysis of features of these body regions is extremely difficult. The core of this study is the investigation of head structures of representatives of the major clades of dragonflies. A detailed description of the head of Lestes virens is presented and was used as starting point for the compilation of a character set and a character state matrix for the entire Dicondylia (winged insects + silverfish), with a main focus on the placement of dragonflies and consequently the basal branching event within winged insects. Our results indicate a sistergroup relationship between a clade Palaeoptera (dragonflies + mayflies) and the megadiverse monophyletic lineage Neoptera. We show that despite of considerable structural similarity between the odonate and neopteran mandible, the muscle equipment in dragonflies is more plesiomorphic with respect to Dicondylia than previously known. Odonata and Ephemeroptera also share presumably derived features of the antenna, maxilla, and labial musculature. Parsimony analyses of the head data unambiguously support a clade Palaeoptera.

Introduction

Whole segments tagmata have been successfully used to infer insect phylogenies (Beutel et al., 2010; Friedrich and Beutel, 2010). Generally, head, thorax and abdomen each provide a rich set of phylogenetically informative characters. However, in the case of the earliest branching events within winged insects (Pterygota), i.e. the relationships between dragonflies (Odonata), mayflies (Ephemeroptera) and all remaining winged insects (Neoptera), fundamental problems become apparent. As a consequence of the flight apparatus evolution a drastic redesign of the thoracic morphology took place. This makes a reliable homologisation of several thoracic elements between wingless (apterygote) and winged (pterygote) lineages very problematic (Beutel and Gorb, 2006). In a phylogenetic context, the definition of characters (primary homology hypotheses) is often difficult or impossible. This greatly impedes a formal phylogenetic evaluation of thoracic features using the outgroup criterion. A similar dilemma exists with characters related to the reproductive system due to the drastically different mode of sperm transfer, i.e. externally deposited spermatophores versus internal fertilization using an intromittent organ (Boudreaux, 1979; Witte and Doring, 1999). Moreover, homologising reproductive elements between some neopteran taxa, i.e. within the same functional assemblage showing direct sperm transfer, is problematic (Klass, 2009). Again, this causes fundamentally impedes the homologisation between wingless and winged insect lineages and character state polarisation. Nonetheless, exactly these character systems have been constantly used for decades to reconstruct the basal splitting in winged insects (Boudreaux, 1979; Kristensen, 1975; Kristensen, 1998; Kukalová-Peck, 1997; Kukalová-Peck, 2008; Soldán, 2003).

Basically, our approach is to infer the general evolutionary trends of these problematic organ systems indirectly by choosing another organ system body region. The head is perfectly suitable as it is not directly affected by the evolution of the flight apparatus or the modified sperm transfer. The homologisation of head structures between bristletails (Archaeognatha), silverfish (Zygentoma) and the winged lineages of insects (Pterygota) is straightforward and unproblematic, with the possible exception of the hypopharyngeal complex. It was demonstrated, that the homology of head muscles between primarily apterygote and winged groups of insects can be assessed without particular problems (Wipfler et al. 2011) (Denis and Bitsch, 1973; Matsuda, 1965). Therefore, it is surprising that insect head structures have not yet been systematically evaluated in the context of the basal pterygote splitting events. A considerable number of detailed morphologic investigations have been carried out concerning Ephemeroptera and Odonata (Mathur and Mathur, 1961; Short, 1955; Staniczek, 2000; Staniczek, 2001; Strenger, 1952; Strenger, 1954; Strenger, 1970; Strenger, 1975), but with a limited taxon sampling, randomly chosen taxa in different studies, and without a formal, numerical evaluation. Consequently, in this comparative study of head structures it was attempted not only to acquire detailed data for the hitherto under-represented taxa dragonflies (Odonata) and mayflies (Ephemeroptera), but also a broad spectrum of representatives of other insect lineages.

The relationships of the three basal winged lineages (Odonata, Ephemeroptera and Neoptera) is one of the major unsolved problems in entomology (Klass, 2007; Kristensen, 1991). All three possible solutions have been proposed and are still under discussion. A sistergroup relationship between Ephemeroptera and Odonata (Palaeoptera hypothesis) is mostly supported by has been advocated based on characters of the wing venation and articulation as well as the maxillary configuration (Bechly et al., 2001; Brauckmann and Zessin, 1989; Haas and Kukalová-Peck, 2001; Hennig, 1969; Hovmöller et al., 2002; Kukalová-Peck, 1997; Kukalová-Peck, 2008; Soldán, 2003; Wheeler et al., 2001; Willkommen and Hörnschemeyer, 2007).

A sistergroup relationship between Ephemeroptera and Neoptera (Chiastomyaria hypothesis) is suggested by the mode of direct sperm transfer, the indirect flight musculature, and molecular analyses based on rRNA genes (Boudreaux, 1979; Kjer, 2004; Mallatt and Giribet, 2006; Matsuda, 1970; Simon et al., 2009). A sistergroup relationship between Odonata and Neoptera (Metapterygota hypothesis) is hypothesized e.g. by features of the mandibles and the tracheal respiratory system, and also by molecular data (Beutel and Gorb, 2006; Kristensen, 1991; Ogden and Whiting, 2003; Pass et al., 2006; Staniczek, 2000; Staniczek, 2001; Terry and Whiting, 2005; Wheeler et al., 2001). Finally, most recent studies based on primary sequence data of complete mitochondrial genomes (Lin et al., 2010; Zhang et al., 2010) supported a clade Ephemeroptera + Plecoptera as sistergroups to all remaining pterygotes, thus challenging the monophyly of Neoptera.

Issues concerning the relationships between Ephemeroptera, Odonata and Neoptera have often been addressed as the “Palaeoptera problem” (Hovmöller et al., 2002; Ogden and Whiting, 2003; Whitfield and Kjer, 2008), which implies a problematic grouping of Ephemeroptera + Odonata. The appearance of Ephemeroptera, Odonata and the neopteran orders in a geologically relatively short time span - probably some time during or after the Devonian (Engel and Grimaldi, 2004; Gaunt and Miles, 2002; Grimaldi and Engel, 2005) - has been followed by a long period, in which these lineages have evolved separately. This specific evolutionary pattern, previously described as an "ancient rapid radiation", has been assumed to necessarily hamper phylogenetic reconstructions (Kjer et al., 2006; Rokas and Carroll, 2006; Whitfield and Kjer, 2008; Whitfield and Lockhart, 2007) as all evolutionary changes useful to display the branching patterns of Ephemeroptera, Odonata and Neoptera must have been accumulated in the short branches linking these lineages, whereas subsequent changes occurring in the branches leading to the terminal groups do not provide information about their relationships. Consequently, characters evolving convergent on these branches leading to the terminals might be erroneously interpreted as synapomorphies in parsimony based methods (the "long-branch attraction" phenomenon discussed by Felsenstein (1978)). In contrast, model based methods like maximum likelihood and Bayesian inference have a chance to find the correct topology, as the applied models expect a certain amount of homoplasy (Whitfield and Kjer, 2008).

To contribute to a resolution of this persistent problem, we studied the complex head anatomy of representatives of all major insect lineages including a bristletail, a silverfish, eight species of mayflies, seven species of dragonflies, and 30 representatives of all major neopteran lineages. Eighteen taxa are represented by original data.

In terms of available morphological data dragonflies are an unusual case. Whereas the thoracic (Pfau, 1986; Pfau, 1991; Willkommen, 2009; Willkommen and Hörnschemeyer, 2007) and abdominal morphology (Klass, 2008; Matushkina, 2008a; Matushkina, 2008b; Pfau, 2002; Pfau, 2005; Whedon, 1918) have been intensively studied, the head has been largely neglected. The last treatments of dragonfly head anatomy date back several decades (Asahina, 1954; Hakim, 1964; Mathur, 1962; Mathur and Mathur, 1961; Short, 1955; Strenger, 1952) were insufficient for a clarification of the systematic position of the order (Wipfler et al., 2011). Consequently, our primary aim is a detailed examination and documentation of dragonfly head structures. The obtained data, combined with information from specific morphological studies and comparative investigations, form the basis of a new assessment of the systematic position of dragonflies, which is crucial for the understanding of the early evolution of the most successful group of organisms.

Material and methods

The anatomy was investigated using synchrotron micro-Computer Tomography (SR-microCT) (Betz et al., 2007). Prior to scanning, samples were dried at the critical point (CPD) (Model E4850, BioRad) and mounted on specimen holders. Except for *Siphlonurus lacustris* and *Thermobia domestica*, all specimens were scanned at the beamline BW2/DORIS III at the Deutsches Elektronen-Synchrotron (DESY, Hamburg, Germany) using a monochromatic X-ray beam at 8 keV photon

Table 1 Scanning parameters used for the investigated taxa; for the scans at BW2 (DESY) and TOMCAT (SLS at PSI) monochromatic X-rays are used

Taxon	**Species**	**Beamline**	**microCT specifications**		
			Energy [keV]	Magnification	Pixel size (µm)
Archaeognatha	*Machilis sp.*	BW2 (DESY) and TOMCAT (SLS)	8	2.7 and 10	5.01 and 10
Zygentoma	*Thermobia domestica*	TOMCAT (SLS)	8.5	10	0.74
Ephemeroptera	*Siphlonurus lacustris*	vtomex (Steinmann)	20.5	4	7.87
	Ephemera danica	BW2 (DESY)	8	2.9	6.06
	Heptagenia sulphurea	BW2 (DESY)	8	2.9	6.06
Odonata	*Lestes virens*	BW2 (DESY)	8	3.4	4.69
	Epiophlebia superstes	BW2 (DESY) and TOMCAT (SLS)	8 and 10	1.9 and 2	9.46 and 3.7
	Onychogomphus forcipatus	BW2 (DESY)	8	1.9	9.46
Plecoptera	*Perla marginata*	BW2 (DESY)	8	1.9	9.46

Higher ranking taxon	**Species**		**Data source**
Archaeognatha	*Machilis germanica* Janetschek 1953		SR-microCT (HZG, DESY and SLS at PSI)
Zygentoma	*Thermobia domestica* (Packard, 1837)		SR-microCT (SLS at PSI)
	Thermobia domestica (Packard, 1837)		Chaudonneret 1948, 1950
Ephemeroptera	*Siphlonurus lacustris* (Eaton 1870)	(larva)	microCT (vtomex at Steinmann)
	Oniscigaster wakefieldi McLachlan, 1873		Staniczek 2001
	Heptagenia sulphurea (Müller 1776)	(larva)	SR-microCT (HZG, DESY)
	Ephemera danica (Müller, 1764)	(larva)	SR-microCT (HZG, DESY)
Odonata	*Lestes virens* (Charpentier, 1825)		SR-microCT (HZG, DESY)
	Mnais pruinosa Selys, 1853		Asahina 1954
	Onychogomphus forcipatus (Linnaeus, 1758)		SR-microCT (HZG, DESY)
	Davidius nanus (Selys, 1896)		Asahina 1954
	Ictinogomphus angulosus (Selys, 1854)		Mathur & Mathur 1961
	Aeshna cyanea (Müller, 1764)		Short 1955
	Epiophlebia superstes (Selys, 1889)		SR-microCT (HZG, DESY and SLS at PSI)
	Epiophlebia superstes (Selys, 1889)		Asahina 1954
Plecoptera	*Perla marginata (*Panzer 1799)	(larva)	SR-microCT (HZG, DESY)
	Nemoura cinerea (Retzius, 1783)		Moulins 1968
Grylloblattodea	*Grylloblatta campodeiformis* Walker, 1914		Walker 1931
	Galloisiana yuasai Asahina, 1959		Wipfler et al. 2011 (SR-microCT at HZG, DESY)
Mantophasmatodea	*Karoophasma sp.*		Baum et al. 2007
	Austrophasma sp.		Wipfler et al. 2011 (BESSY)
Blattodea	*Periplaneta americana* Linnaeus, 1758		Wipfler et al. 2011 (BESSY)
Mantodea	*Hymenopus coronatus* (Olivier 1792)		Wipfler et al. subm.
Phasmatodea	*Timema christinae* Vickery, 1993		Tilgner et al. 1999
	Agathemera crassa (Blanchard, 1851)		Wipfler et al. 2011 (BESSY)
	Megacrania batesii Kriby, 1896		Friedemann et al. 2012 (BESSY)
	Phyllium siccidifolium (Linnaeus, 1758)		Friedemann et al. 2012 (BESSY)
	Sipyloidea sipylus (Westwood, 1859)		Friedemann et al. 2012 (BESSY)
Embioptera	*Embia ramburi* Rimsky-Korsakow, 1906		Rähle 1970
Dermaptera	*Labidura riparia* (Pallas, 1773)		Kadam 1961
Orthoptera	*Locusta migratoria* (Linnaeus, 1758)		Albrecht 1953
Zoraptera	*Zorotypus hubbardi* Caudell, 1918		Beutel & Weide 2005
Psocoptera	*Stenopsocus stigmaticus* (Imhoff & Labram, 1846)		Badonnel 1934
Hymenoptera	*Macroxyela sp*.		Beutel & Vilhelmsen 2007

Table 2 Taxa used in the morphological data matrix and the corresponding data source; original data from Friedemann et al. (2012) and Wipfler et al. (2011, 2012) were available to the authors

energy. The tomography station operated by Helmholtz-Zentrum Geesthacht (HZG, Geesthacht, Germany) is optimized for performing high-density resolution microtomography (Beckmann et al., 2008). *T. domestica* was scanned at beamline TOMCAT at Swiss Light Source, Paul Scherrer Institut (PSI, Villigen, Switzerland) and *S. lacustris* at the high resolution computed tomography scanner v|tome|x s (GE phoenix|x-ray, Steinmann-Institut, Bonn, Germany) (Table 1). Subsequent segmentation and rendering was accomplished with Reconstruct (Fiala, 2005) and Blender (blender.org). Both software packages are distributed under the GPL license. Final tables were edited with GIMP, Adobe Photoshop® and Adobe Illustrator®.

Readers not familiar with insect head morphology are encouraged to open electronic supplement ES4. A 3D model of the head of *Lestes virens* is presented in this file, which facilitates the identification of internal structures. The underlying program "Blender" can be downloaded free of charge under the GPL license from www.blender.org. For instructions http://wiki.blender.org/index.php/Doc:Manual can be used.

For scanning electron microscopy (SEM) specimens were transferred in a series of steps into 100% ethanol, dried at the critical point (Model E4850, BioRad), and sputter coated (Model Anatech Hummer VII). Microscopy was performed on a Hitachi S-2460N using a new type of rotatable sample holder (Pohl, 2010). Additional information for the taxon sampling was obtained from the literature (Table 2).

Concerning usage of the terms "sutures" and "ridges" we consistently use the term "suture" for ecdysial cleavage lines (DuPorte, 1946; DuPorte, 1957; Snodgrass, 1947) and "ridge" for any cuticular strengthening lines or ridges (Snodgrass, 1935; Snodgrass, 1947; Strenger, 1952). We avoid the term "sulcus" completely since this refers to a fissure between bones. Morphological definitions and structure designations follow Seifert (1995).

Literature sources were partly used for character 19 (Staniczek, 2000) and for characters 35, 36, 37, 38, 39, 40, 45, 46 (Pass et al., 2006; Pass, 2000).

Phylogenetic Analyses

Parsimony analyses of the morphological character set and Bremer as well as bootstrap support calculations were carried out with TNT (Goloboff et al., 2008) using 1000 heuristic searches starting with random addition of taxa (TBR branch swapping). All characters were equally weighted and unordered. Only unambiguous changes were mapped on the tree. Optimizations were analyzed with WinClada version 1.00.08 (Nixon, 2002). To explore evolutionary implications of alternative hypotheses we used constrained tree reconstruction (CTR) executing the "move branch mode" in WinClada. These CTRs were Metapterygota (Ephemeroptera (Odonata + Neoptera)), Chiastomyaria (Odonata (Ephemeroptera + Neoptera)) and paraphyletic Neoptera (Odonata + ((Ephemeroptera + Plecoptera) + other Neoptera))) (Lin et al., 2010). The following abbreviations are used for these hypotheses: Palaeoptera = PP; Metapterygota = MP; Chiastomyaria = CM; paraphyletic Neoptera = PN.

In addition to the parsimony approach, we also conducted maximum likelihood (ML) and Bayesian inference (BI) analyses. To model morphological characters by these methods, the Mk (for Markov with k-states) model has been introduced by Lewis (2001). The Mk model is a generalization of the Jukes-Cantor model (Jukes et al., 1969), assuming all states having the same frequency and all transitions between different states occurring at the same rate (Allman et al., 2009; Lewis, 2001). In the present study, maximum likelihood analyses were conducted with RAxML v7.2.6 (Ott et al., 2007; Stamatakis, 2006; Stamatakis et al., 2005). The Mkv model was applied, with all model parameters estimated from the data, and rate heterogeneity across characters considered by applying the gamma-model of Yang (1994) with four discrete categories. Node support was estimated with 1000 Bootstrap replicates.

Bayesian inference was conducted using MrBayes v3.2 (Huelsenbeck and Bollback, 2001; Ronquist and Huelsenbeck, 2003). Again, the Mk model was applied, with among character rate variation modelled with gamma distributed rates across characters with four discrete rate categories. Priors were set adopting the default settings of MrBayes v3.2. Two parallel analyses were run with random starting trees and four Metropolis coupled Markov chains for 1.000.000 generations. Every 100th generation was sampled to yield a posterior probability distribution of 10.000 trees. After discarding the first 1000 trees of each run as burn-in trees, a 50 % majority rule consensus tree was calculated from the concatenated sample trees of both runs.

The matrix is based on those presented in Wipfler et al. (2011) and Friedemann (2012) (electronic supplement ES2+3), extended by 38 new characters. Eighteen characters of Wipfler et al. (2011) were excluded from our analysis since their homologisation between taxa is unclear (electronic supplement ES3). In the descriptions and tree figures, species are referred to by the generic names only.

Results

Head morphology of **Lestes virens**

The orthognathous head (mouthparts ventrally oriented) is strongly sclerotised and the surface is covered with a moderately dense vestiture of setae (Fig. 1A+B). It is more than twice as wide as long. Approximately 40% of its width is occupied by the large, dome-shaped, laterally positioned compound eyes. They are placed on sockets formed by the enlarged postgenae, thus facing slightly forward. Anteriorly the eyes are approximately twice as broad as posteriorly (Fig. 2A). Each eye is composed of more than 20.000 ommatidia and is internally enclosed by a strongly developed, wide circumocular ridge (cor). Mesally, the compound eyes do not touch each other.

The short coronal (cs) and frontal sutures (fs) or ecdysial cleavage lines are visible as an inverted "Y" on the dorsal head region in frontal view (Fig. 1A, 2A). Three ocelli (moc, loc) are present between these sutures close to their junction point. The frontal sutures do not reach the circumantennal ridges (car). The coronal suture (cs) is confluent with the transversely oriented occipital ridges (ocr), which are continuous with the internal circumocular ridges (cor). Posterior to the occipital ridge lies an occipital bar (ocb), which has a transverse orientation and is about as long as the width of the vertex (v, Fig. 2A). The occiput (oc) forms the major part of the backside of the head and bears the cephalic part of the arresting system, which is responsible for the support and fixation of the head in different situations (see Gorb 1999). It is composed of two vertically oriented oval fields of microtrichia on both sides of the foramen occipitale.

The postocciput around the posterior head opening or foramen occipitale is small and partly separated from the other head regions by an incomplete postoccipital ridge, which forms an incomplete arch above the foramen occipitale. It is dorsolaterally interrupted on both sides, thus represented by a dorsal nearly horizontal part and two lateral vertical parts. The foramen is roughly oval and narrow. The narrowed neck region and cervical membrane result in a high mobility of the head in the roll, pitch and yaw planes.

The oval antennal foramina are surrounded by complete circumantennal ridges (car) and interconnect by a distinct interantennal ridge (iar, Fig. 1A). An antennifer, frequently ecountered in other insects, is absent. The large clypeus is divided into an ante- and postclypeus. The latter apears broader and horizontally oriented in lateral view, whereas the anteclypeus has a vertical orientation (Fig. 2C). The anteclypeus is not membranous, but as heavily sclerotised as the postclypeus (same thickness and material density in the microCT data). Despite this, the anteclypeus is "softer" than the stiff postclypeus and therefore well distinguishable from the latter (see also Asahina, 1954). The frons (fr) is seperated from the postclypeus (pcl) by a strong, transverse epistomal ridge (er, Fig. 1A). The interantennal ridge (iar) subdivides the frons into an anterior bead-like part and a posterior flat and more vertically oriented region in lateral view (Fig. 2C). In frontal view the entire clypeus has a trapezoid shape (Fig. 1A). The anterior tentorial pits (atp) are continuous with the pleurostomal ridge, which is curved posteriorly and confluent with the hypostomal ridge. The subgenal ridge (=hypostomal + pleurostomal ridge) is not connected with the circumoccular ridge.

The anterior elements of the cuticular head exoskeleton (anterior tentorial arms "ata", Fig. 6D) are short, massive and twisted. Protuberances emerge at their ventral base and extend into the lumen of the mandibles. They serve as origin for mandibular muscles (0md6 and 0md8, Fig. 6C). The dorsal tentorial arms (dta) also originate from the basal part of the anterior arms (Fig. 6D). They are thin, twisted and merge with the head capsule directly dorsad the antennal origin. The attachment points are externally recognizable as dorsal tentorial pits (dtp, Fig. 1A). All antennal muscles originate from the dorsal tentorial arms. The corpotentorium (ct, Fig 6A) is compact and cylinder-shaped. Oesotendons are absent. The posterior tentorial arms are very short and originate from the head capsule, directly proximad the articulation of the basal maxillary element (cardo). This is externally visible by deepened posterior tentorial pits. Short but thick apodemes, the trabeculae tentorii, originate from the ventral side of the posterior tentorial pits. They serve as attachment areas for the tentoriostipital muscles 0mx4 and 0mx5.

The anteriorly rounded, parabolic labrum partly covers the mandibles and is movably connected with the slightly rounded anterior anteclypeal margin by a membranous fold allowing movement. It bears a vestiture of setae (Fig. 1B).

The short and thin antennae are composed of scapus, pedicellus and three flagellomeres (Fig. 1A). Articulations

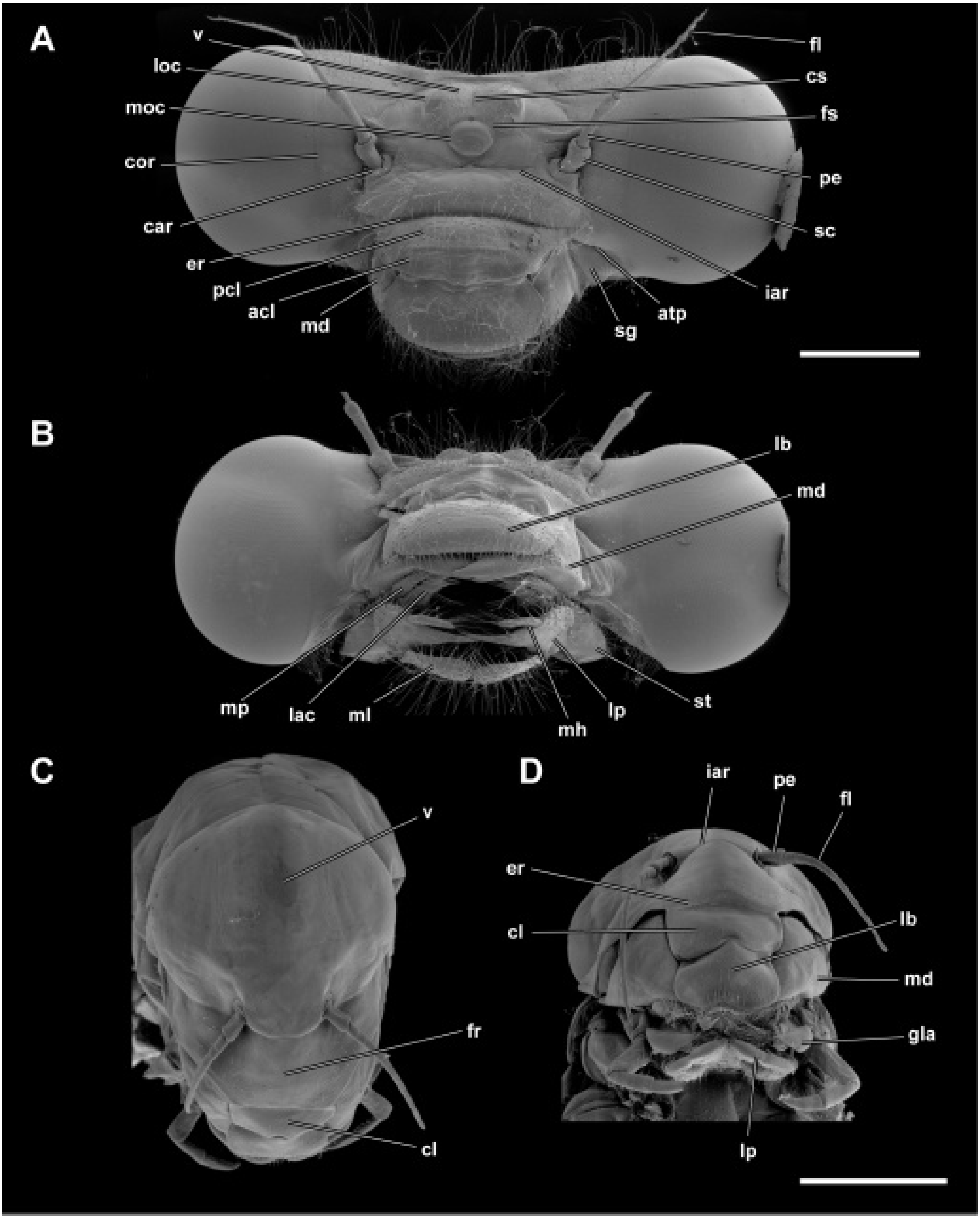

Fig. 1. SEM micrographs of *Lestes virens* (a, b) and *Siphlonurus lacustris* (c, d). (a, c) frontal view; (b, d) ventral view. Abbreviations: acl, anteclypeus; atp, anterior tentorial pit; car, circumantennal ridge; cl, clypeus; cor, circumoccular ridge; cs, coronal sulcus; er, epistomal ridge; fl, flagellum, fr, frons; fs, frontal sulcus; gla, galeolacinia; iar, interantennal ridge; lb, labrum; lp, labial palpus; md, mandible; mh, moveable hook; ml, median lobe; moc, median ocellus; mp, maxillar palpus; loc, lateral ocellus; pcl, postclypeus; pe, pedicellus; sc, scapus; sg, subgena; st, stipes; v, vertex. Scale bar = 1 mm.

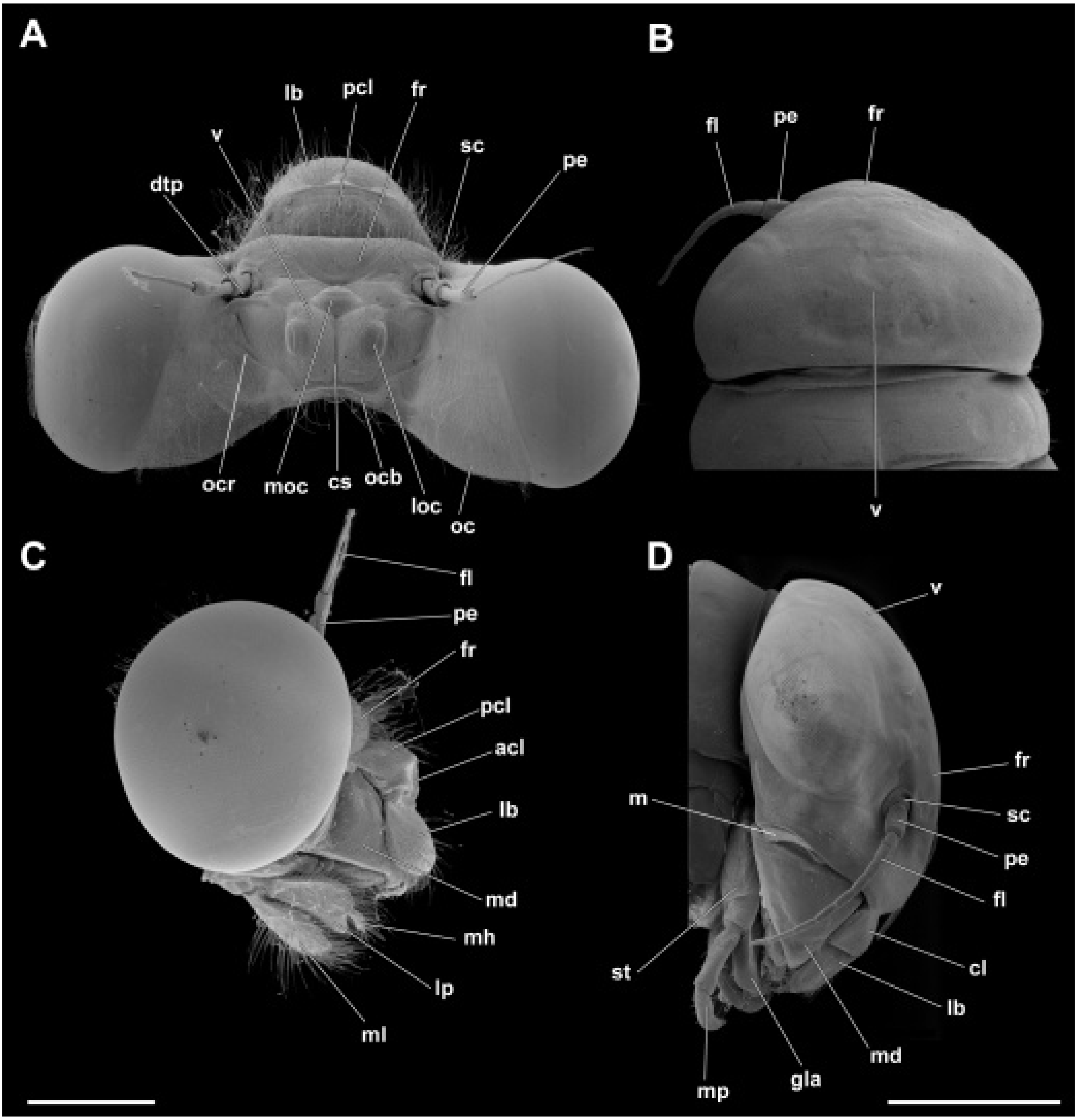

Fig. 2. SEM micrographs of *Lestes virens* (a, c) and *Siphlonurus lacustris* (b, d). (a, b) dorsal view; (d, e) lateral view. Abbreviations: acl, anteclypeus; cl, clypeus; cs, coronal sulcus; fl, flagellum; fr, frons; gla, galeolacinia; lb, labium; loc, lateral ocellus; lp, labial palpus; m, membrane; md, mandible; mh, moveable hook; ml, median lobe; moc, median ocellus; mp, maxillar palpus; oc, occiput; ocb, occipital bar; ocr, occipital ridge; pcl, postclypeus; pe, pedicellus; sc, scapus; st, stipes; v, vertex. Scale bar = 1 mm.

between scapus, pedicellus and flagellum are absent. The scapus is about half as long as the pedicellus but twice as wide. The first and second flagellomere are equally long. The terminal one is very short. All antennomeres are entirely devoid of sensilla. Antennal circulatory organs (ampullary formations and antennal vessels) as well as the corresponding muscles are also absent. We found no indication of any other structure which might be responsible for transportation of haemolymph into the antennae.

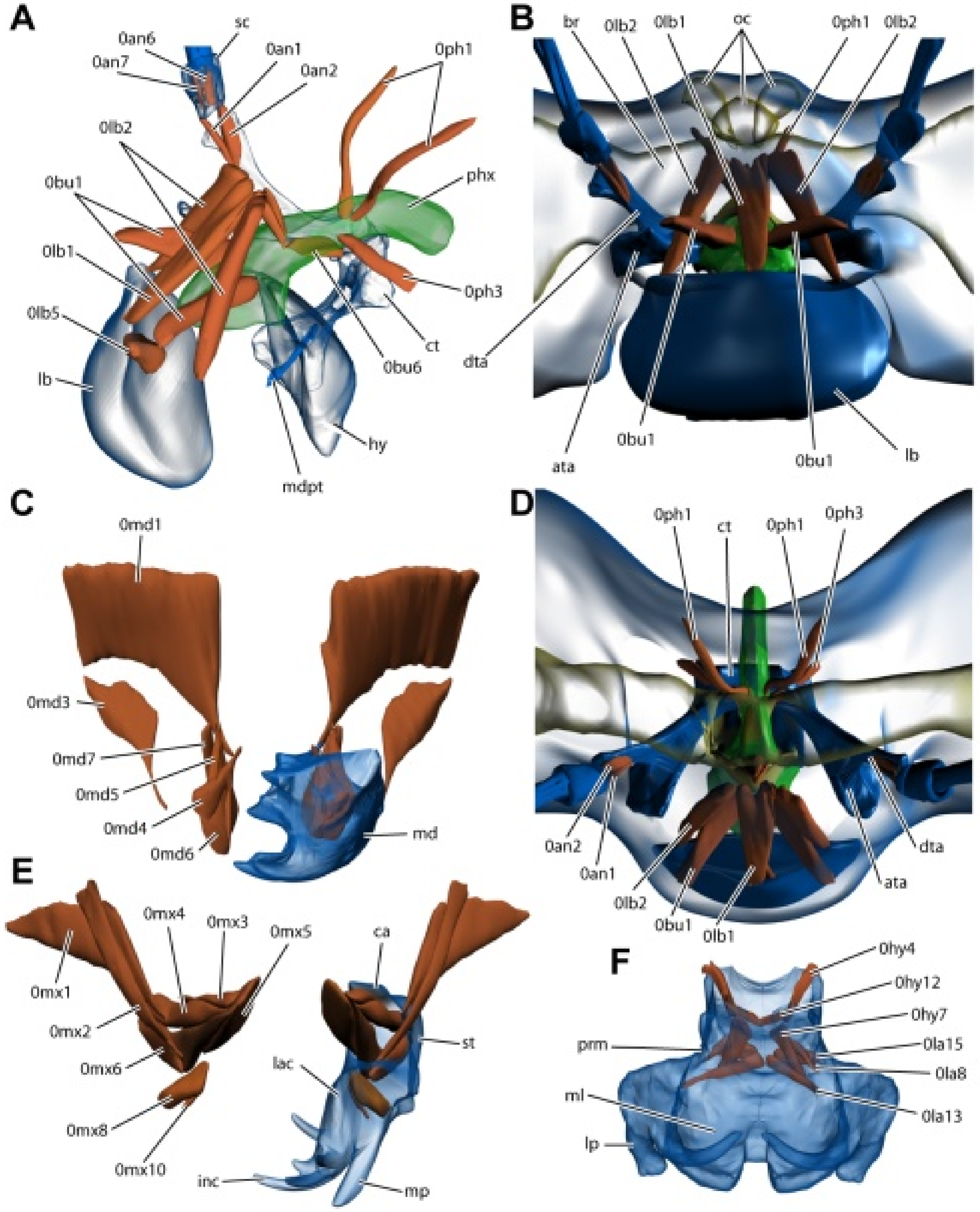

Fig. 3. *Lestes virens*, cephalic musculature and endoskeleton. Three-dimensional reconstructions; cuticle (blue) partly transparent. (a) head, dorsolateral view, head cuticle removed; (b) head, frontal view; (c) mandible and corresponding musculature, frontal view; (d) head, dorsal view; (e) maxillae, frontal view; (f) labium, frontal view. Muscles orange; cuticular structures blue; pharynx and oesophagus green. Abbreviations: ata, anterior tentorial arms; br, brain; ca, cardo; ct, corpotentorium; dta, dorsal tentorial arms; hy, hypopharynx; inc, incisivus; lac, lacinia; lb, labrum; lp, labial palpus; md, mandible; mdpt, mandibular process of tentorium; ml, median lobe; mp, maxillar palpus; oc, ocellus; phx, pharynx; prm, prementum; sc, scapus; st, stipes. For muscle references see Data S1.

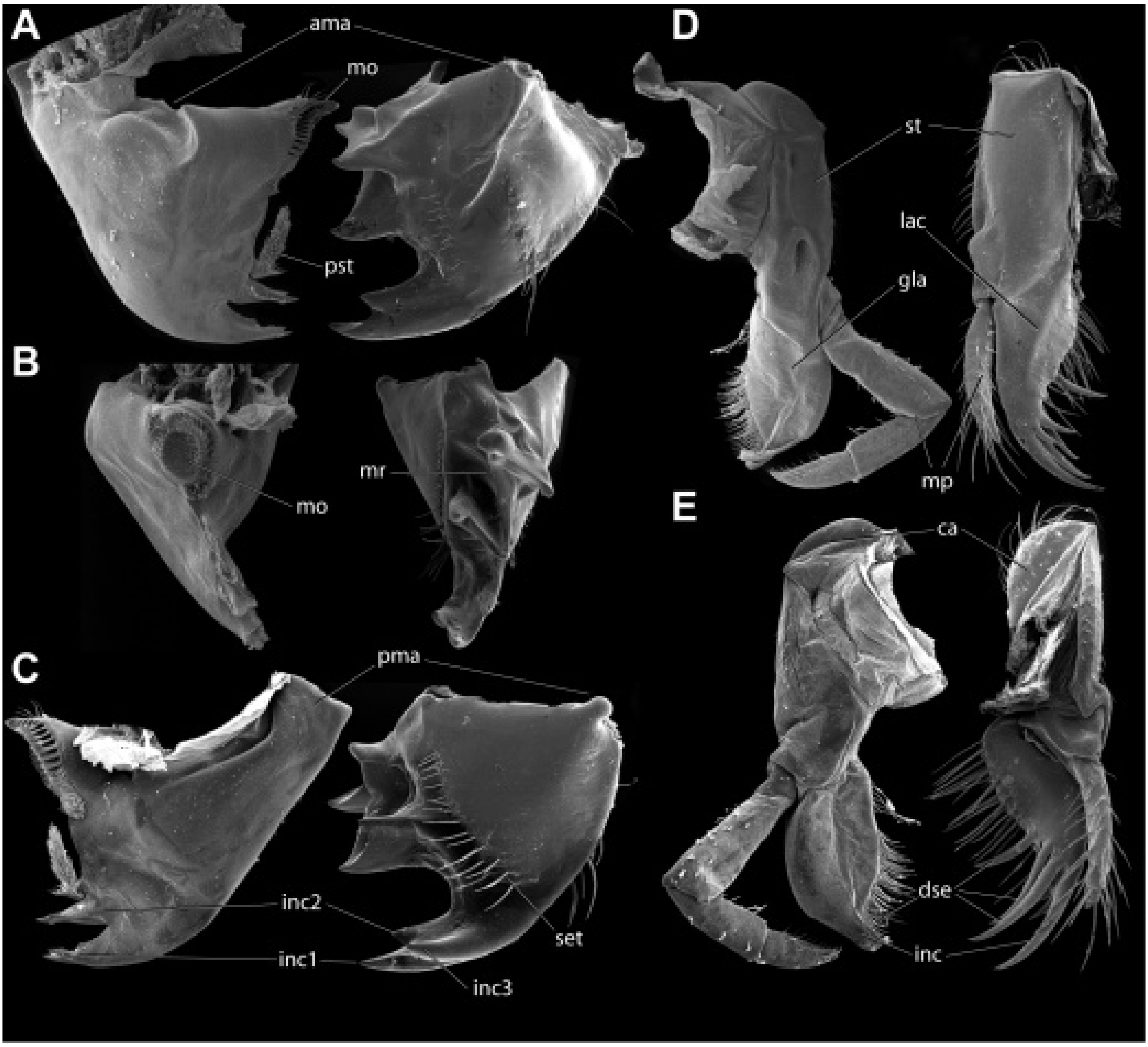

Fig. 4. Mandible and maxilla of *Lestes virens* and *Siphlonurus lacustris* in direct comparison. Left mouthpart always from *S. lacustris*, right mouthpart always from *L. virens*. SEM micrographs. (a) mandibles frontal view; (b) mandibles lateral view; (c) mandibles posterior view; (d) maxillae ventral view; (e) maxillae dorsal view. Abbreviations: ama, anterior mandibular articulation; ca, cardo; dse, dentisetae; eh, end hook of labial palp; gl, glossa; gla galeolacinia; hy, hypopharynx; inc, incisivus; inc1, frist incisivus of mandible; inc2, second incisivus of mandible; inc3, third incisivus of mandible; lac, lacinia; lp, labial palp; mh, moveable hook of labial palp; ml, median lobe; mo, mola; mp, maxillar palp; mr, mesal ridge; pma, posterior mandibular articulation; pgl, paraglossa; prm, prementum; pst, prostheca; set, setae; sli, superlinguae; st, stipes. Mouthparts not to scale among each other.

The articulation of the heavily sclerotized, slightly asymmetric mandibles is of the dicondylic (two articulations) ball-and-socket type (Fig. 3A+C). The mandibular shape is triangular in dorsal view. At the mandible base the anterior articulation (ama, Fig. 3A) is a socket while the posterior one (pma, Fig. 3C) is a distinct knob with their respective counterparts (socket and knob) at the head. The gnathal edges of the left and right mandibles are almost symmetrical. Each mandible bears 3 incisivi and a z-shaped mesal edge formed by 4 strongly sclerotised prominences connected by sharp ridges (Fig. 3B). Additionally, the mandible bears several rows of setae on the anterior and posterior surfaces.

The maxillae are long and slender. The undivided triangular cardo is clearly separated from the stipes by a well-developed cardostipital ridge by a groove

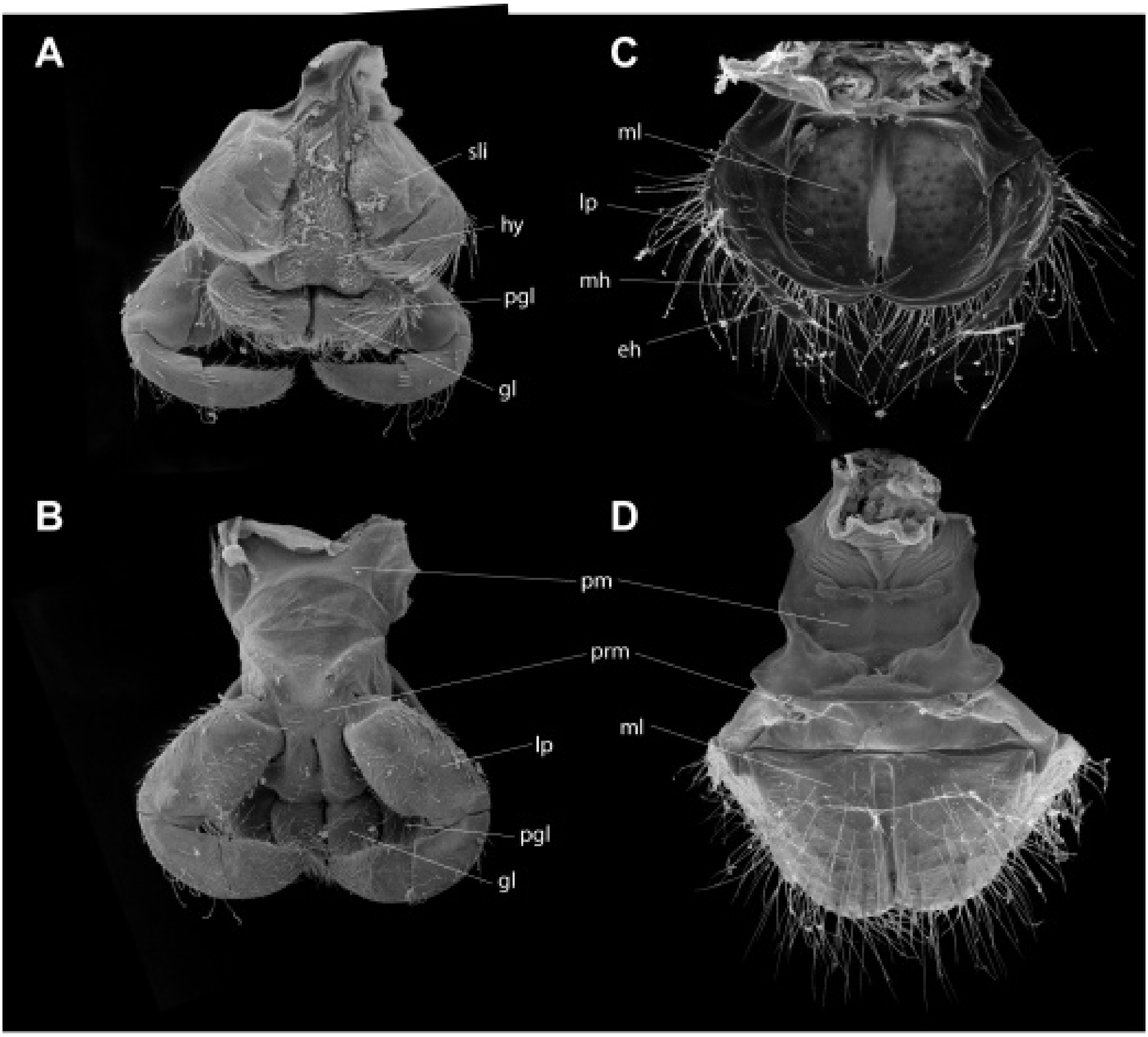

Fig. 5. Labium of *Lestes virens* and *Siphlonurus lacustris* in direct comparison. Left mouthpart always from *S. lacustris*, right mouthpart always from *L. virens*. (a, c) dorsal view; (b, d) ventral view. eh, end hook of labial palp; gl, glossa; gla, galeolacinia; hy, hypopharynx; lp, labial palp; mh, moveable hook of labial palp; ml, median lobe; pgl, paraglossa; pm, postmentum; prm, prementum; sli, superlinguae. Mouthparts not to scale among each other.

harbouring a very narrow membrane. The stipes is a rectangular plate subdivided by the stipital ridge into a narrow basistipes and a much larger mediostipes (Fig. 3D+E). Its distal part bears an unsegmented palpus covered with setae (mp, Fig. 3D). Mesally an oblique ridge separates the sickle-shaped lacinia from the stipes. The lacinia is not moveably connected to the stipes. The Its mesal side of the lacinia is armed with a row of long setae, two apical incisivi and five subapical, paramesal dentisetae. A galea is absent.

The labium consists of a basal postmentum (pm) and a distal prementum (prm, Fig. 4D). The postmentum is a rectangular plate and reinforced dorsally, ventrally and laterally by heavily sclerotised bars. The short and broad prementum forms a right angle with the postmentum visible in lateral view. Apically it bears paired 1-segmented palps and paired median lobes. The palps are flat and densely covered with setae, especially on the outer side. Apicomesally they bear a fixed subapical hook (eh, Fig. 4C). A second movable hook (mh) is present distad of this hook (Fig. 4C). The median lobes are a fusion product of glossae and paraglossa; (see discussion). Mesally the two lobes are connected by a sclerotised stripe which is approximately 2/3 as long as the lobes themselves. The ventral side of the lobes is densely covered with setae. The palps and median lobes together form a cavity for reception of the hypopharynx and maxillae.

The hypopharynx is a ventrally oriented tongue-like structure in front of the prementum. It is weakly sclerotised and bears no anterior or posterior plates. A conspicuous row of setae is present on the lateral surfaces. Mandibular glands are absent. The oral arm forms a rounded bar directly posterad the anatomical mouth opening. Its serves as attachment site for M. oralis transversalis (0hy9). The loral arm is thin and bears no linguactual tendon or apodeme.

The epipharynx is weakly sclerotised and not subdivided. It bears one lateral row of setae on the left and right side. The tormae are formed like an inverted "Y" in posterior view. They serve as attachment areas of M. frontoepipharyngalis (0lb2).

The salivary glands are paired, mesally connected globular structures located directly ventrad the deutocerebrum and dorsad the salivary receptacle. The paired salivary ducts fuse before opening into the salivary receptacle, which is anteriorly continuous with an unpaired salivary channel. The channel opens into the salivarium posterad of the hypopharynx.

Pharynx and oesophagus have a wide lumen. Several dorsal, lateral and ventral folds serve for muscle attachment.

Comparison with **Siphlonurus lacustris**

The following statements are restricted to features differing from descriptions in earlier studies and characters relevant for the discussion. A detailed description of ephemeropteran head morphology with comparisons between several taxa can be found in Staniczek (Staniczek, 2000; Staniczek, 2001).

Head distinctly longer than wide and oval in frontal view (Fig. 1C). Compound eyes not protruding but integrated in the outline of the head capsule (Fig. 1C+2B). Coronal and frontal sutures very delicate, scarcely recognisable. Labrum (lb) parabolic (Fig. 1D). Clypeus (cl) not subdivided into ante- and postclypeus. Epistomal ridge (er) present, confluent with anterior tentorial arms and separating frons (fr) from clypeus (cl). Frons (fr) wide, subdivided by an interantennal ridge (iar), turned inwards laterally of the epistomal ridge on both sides, thus in contact with the anterior mandibular articulation complex. Infolded frontal region gradually narrowing towards posterior mandibular articulation and continuous with it (see Staniczek 2000 for a detailed description of this structure). Ocelli sunk below cuticular and epidermal surface, not visible externally. Vertex (v) without protuberances and not clearly separated from the rest of the head capsule. Scapus very short and sunk into lumen of head capsule (Fig. 2D); pedicellus five times longer than scapus; flagellum 10-segmented. Occiput without transverse bar. Head arrester system absent.

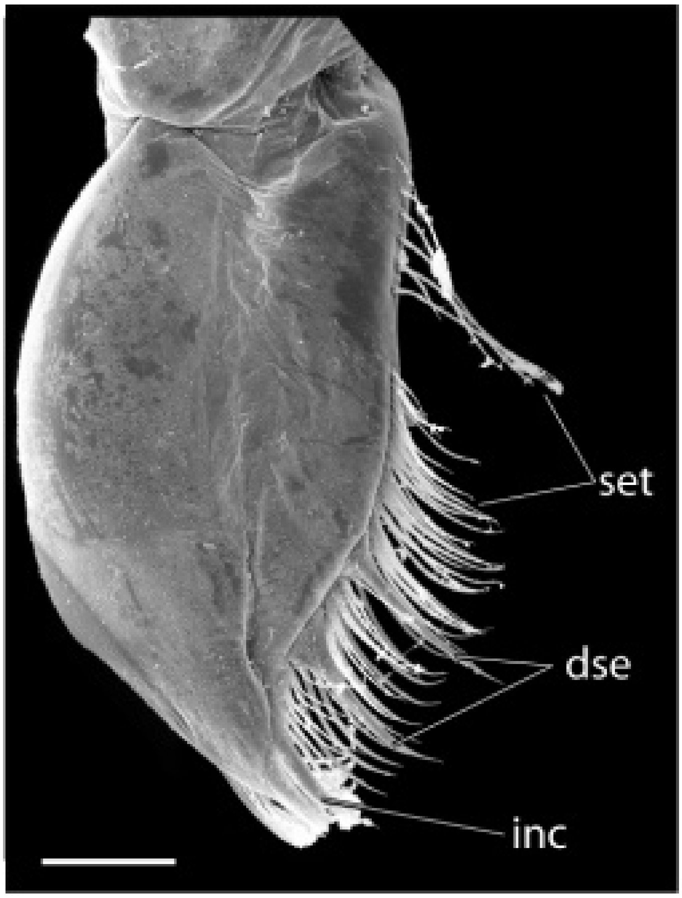

Fig. 6. The fused apical lobes of the maxilla (galea + lacinia = galeolacinia) of *Siphlonurus lacustris* showing clearly the dentisetae and the single incisivus of the lacinia. Abbreviations: dse, dentisetae; inc, incisivus of lacinia; set, setae. Scale bar = 100 lm.

Mandible with movable prostheca (pst), lamellar mola (mo) and two incisivi (inc1+2); mesal ridge absent (Fig. 3A-C). Posterior articulation (pma) formed by heavily sclerotised bar; anterior articulation complex (ama) with hollow concavity for reception of inflected frontal part of head. Saddle-like, ventrally bent groove originates immediately caudad the paratentorial joint (Fig. 3A, see also Staniczek 2000, 2001). Cardo undivided; stipes divided into basi- and mediostipes; mediostipes with distinct indentation (attachment for tentoriostipital muscles) on its ventral side near the three-segmented palp (Fig. 3E). First palpomere nearly twice as long as second and third, respectively. Galea and lacinia connected by membrane along entire length and still discernible as separate structures (Fig. 3E; see discussion). Lacinia with one apical incisivus and subapical dentisetae (Fig. 5). Labium composed of pre- and postmentum and paired glossae and paraglossae (Fig. 4A). Premental cleft absent but ventral premental apodeme present (Fig. 4B). Labial palpus three-segmented; first palpomere 2x as wide and 1.5x longer than second and third, respectively. Glossae and paraglossae separated from each other, short and globular. Hypopharynx composed of median lingua and paired lateral superlinguae (Fig. 4A). Superlinguae flat and spoon-shaped, apically with mesally directed setae. Lingua densely covered with setae.

Phylogenetic analyses

External and internal characters were scored for two outgroup and 31 ingroup taxa covering Archaeognatha, Zygentoma, Ephemeroptera, Odonata, several polyneopteran lineages, Acercaria, Zoraptera and Endopterygota (Table 2). The matrix comprises 19 characters of the head capsule, six labral characters, 22 characters of the antennae, 13 tentorial characters, 13 mandibular characters, 17 characters of the maxillae, 33 labial characters and 16 characters of the hypopharynx, salivarium and oesophagus (electronic supplement ES2). Our morphological investigation clarifies many seemingly ambiguous features used in earlier studies (e.g. the presence (20) and shape of the tormae (21), dentisetae (83), glossae (96) and paraglossae (99, 100); see also Wipfler et al., 2011, characters 34, 35, 52, 61, 62 and 63). In the following support values will be stated in parentheses with the following order: (Bremer support | parsimony bootstrap | Bayes posterior probability | RaxML bootstrap value).

All analyses recover Pterygota with strong support (Fig. 7; 12|99|1.0|100). Parsimony analyses with TNT result in two equally parsimonious trees. In a strict consensus (298 steps; Ci = 57; Ri = 73) **Pterygota** (winged insects) are divided into two clades Palaeoptera (dragonflies + mayflies, 3|59|.94|83) and Neoptera (all remaining winged insects, 1|X|X|59). Maximum likelihood and Bayesian inference analyses produced the same branching pattern for all taxa except *Labidura* (Dermaptera) and *Embia* (Embioptera), which are sistergroups in these analyses (Fig. 7). Embioptera is recovered as sister to Phasmatodea and Dermaptera as sister to Embioptera + Phasmatodea in the parsimony analysis.

The monophyly of Pterygota is strongly supported in our parsimony analyses by a series of unique autapomorphies (Fig. 8A): subdivided clypeus (15:1), absence of a postcerebral circumesophageal vessel branching off the dorsal aorta (35:1), M. tentoriobuccalis posterior (0bu6) arising at the corpotentorium (138:0), and loss of M. epistoepipharyngealis (0lb3, 22:1), M. tentoriofrontalis posterior (0te1, 56:1), M. posteriotentorialis (0te4, 57:1), M. tentoritentorialis longis (0te5, 58:1), M. tentoritentorialis brevis (0te6, 59:1), M. tentorioglandularis (0la7, 114:1), M. postmentomembranus (0la9, 117:1) and M. postmentoloralis (0hy6, 130:1). With the exception of the clypeal subdivision (16:1) these features turned out as robust autapomorphies of Pterygota even if the monophyly of Chiastomyaria (CM) or Metapterygota (MP) is enforced, or alternatively under a scenario with paraphyletic Neoptera (PN), all of which are retrieved as suboptimal resolutions (Fig. 8B-D). The fusion of the posterior and anterior tentoria (47:1) optimizes as another unique autapomorphy of Pterygota in our analysis but likely is homoplastic as it seems to be paralleled in Maindroniidae among zygentomans (Koch 2003), which we have not yet included into our taxon sampling.

All insect orders sampled by more than one species are

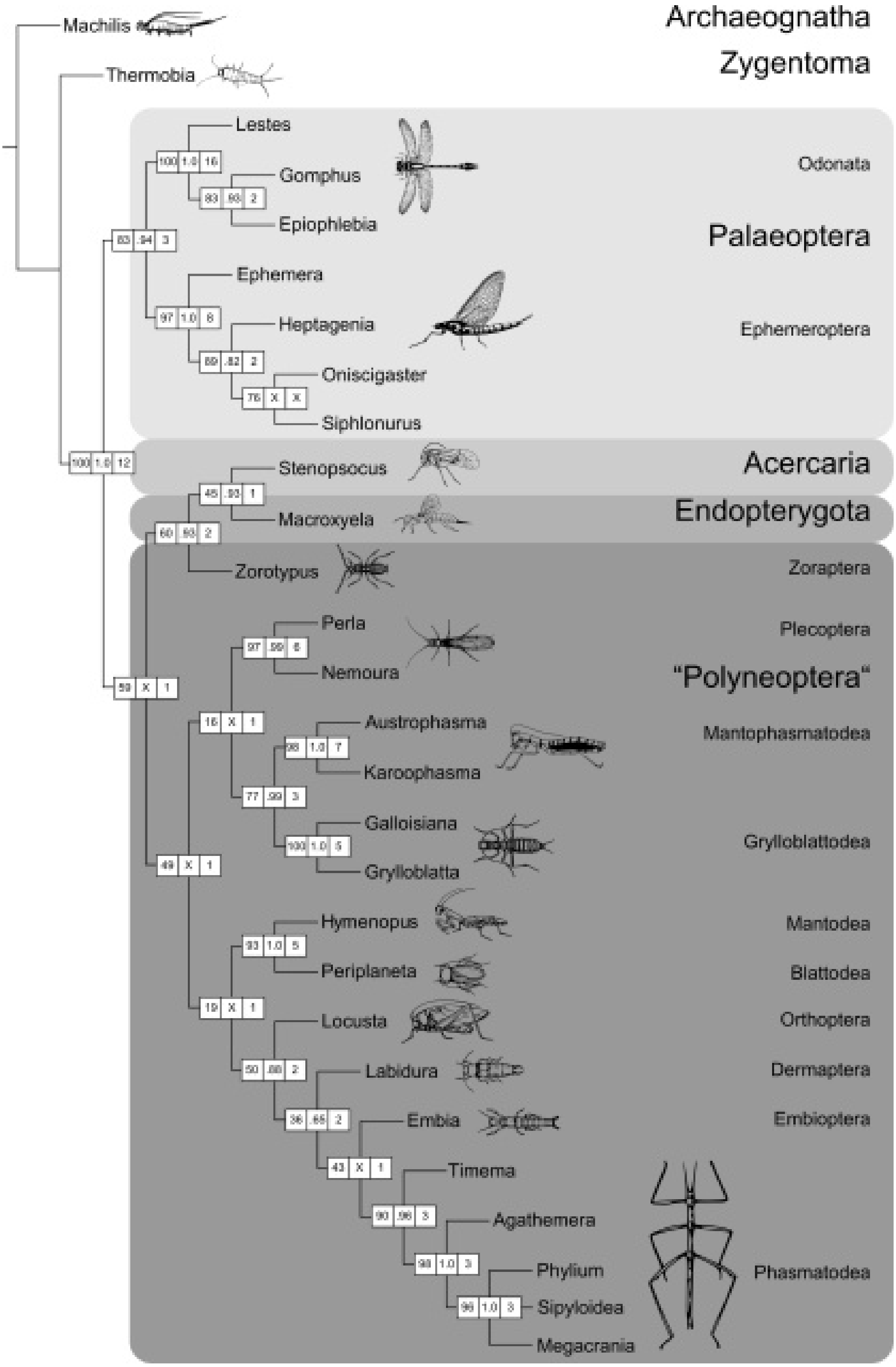

Fig. 7. Strict consensus tree derived from the TNT parsimony analysis of the morphological data matrix. Support values derived from parsimony, likelihood and Bayesian inference analyses. ''X'' indicates no support or a bootstrap support lower 50 and a posterior probability lower than 0.5, respectively.

monophyletic. **Odonata** are monophyletic (16|100|1.0|100) with Zygoptera (damselflies) as sistergroup of a clade Epiophlebioptera + Anisoptera (=Epiprocta fide Lohmann (1996)). Odonata are supported by the following autapomorphies (Fig. 6A): loss of the galea (76:1), presence of movable-hooks on the labial palpi (106:1) and absence of 0la5 (111:1) and 0la11 (120:1). CTRs (MP, CM and PN) produced additional homoplasious characters for the alternative hypotheses (Fig. 6B-D).

Ephemeroptera were confirmed as monophyletic (8|98|1.0|97). Our analysis revealed four potential autapomorphies (Fig. 8A): non-functionality of adult mouthparts (18:1), a channel-like anterior mandibular joint (66:1), a lacinia with one incisivus (82:2) and the absence of salivary glands and ductus (126:1). CTRs resulted in one additional autapomorphic feature for Ephemeroptera, the fusion of the galea and lacinia (77:1). The channel-like anterior mandibular joint (66) was not retrieved as an autapomorphy under this scenario. CTR for the CM hypothesis produced the same apomorphies like MP, and a regain of the channel-like anterior mandibular joint (66:1) as a potential autapomorphy. Under the PN hypothesis non-homoplasious characters of the CM hypothesis remained stable, but the number of homoplasious character transformations was drastically increased (Fig. 8D).

The monophyly of **Neoptera** is unambiguously supported by the loss of M. tentorio-mandibularis lateralis superior (0md5; 71:1). CTRs of Metapterygota and Chiastomyaria optimise a membranous anteclypeus (17:0), the origin of the antennal muscle 0an1 at the anterior and dorsal tentorial arms (31:4) and the absence of 0md5 (71:1) as neopteran autapomorphies. If Neoptera are enforced as paraphyletic (Lin et al., 2010), the origin of the antennal muscle 0an1 at the anterior and dorsal tentorial arms (31:4) is the only potential autapomorphy of a restricted neopteran clade excluding Plecoptera.

A clade **Palaeoptera** is favoured by all shortest trees and is unambiguously supported by the following autapomorphies (Fig. 8A): a pedicellus longer than the scapus (27:0), the loss of antennal circulatory organs in adults (38:1), dentisetae (83:0), and the loss of labral muscle 0la14 (122:1). Support for Palaeoptera is lower in the parsimony based tree reconstructions (Bremer and bootstrap) and higher in model based approaches (likelihood and Bayes)

CTR of the MP hypothesis produced a tree four steps longer (Fig 8B). These suboptimal tree optimizes the loss of the anterolateral part of the anterior mandibular articulation (paratentorial joint; 67:1) and M. craniomandibularis externus anterior (0md2; 69:1) as autapomorphies of Metapterygota.

CTR of CM resulted in a tree eight steps longer and is not supported by any head character (Fig 8C). Simulated PN following the hypothesis of Lin (2010) (Fig. 8D) requires twelve additional steps and is also not supported by any character.

Discussion

Pterygota are also strongly supported by head characters

A single origin of winged insects (Pterygota) is generally accepted, even though it was disputed in several earlier publications (La Greca, 1980; Matsuda, 1981, Manton 1977). However, the monophyly of Pterygota was until now poorly supported by characters of the head. The fusion of the anterior and posterior tentorial elements was the only autapomorphy mentioned in previous works (Bitsch and Bitsch, 2002; Grimaldi and Engel, 2005; Koch, 2003) but occurs at least in Mandroniidae (Zygentoma) as well.

Our investigation shows that a clade Pterygota is indeed well supported by derived features of the head (see Fig. 8 and appendix5). Apomorphic groundplan character states are the subdivided clypeus (16:1), the absence of a circumesophageal vessel ring (35:1) (Bitsch and Bitsch, 1998; Kristensen, 1997), a fused anterior and posterior tentorium (47:1), and the loss of an entire series of head muscles (23:1, 34:1, 57-60:1, 115:1, 118:1, 131:1, 133:1).

Evidence for palaeopteran monophyly

A sistergroup relationship between the two most ancestral pterygote lineages dragonflies and mayflies

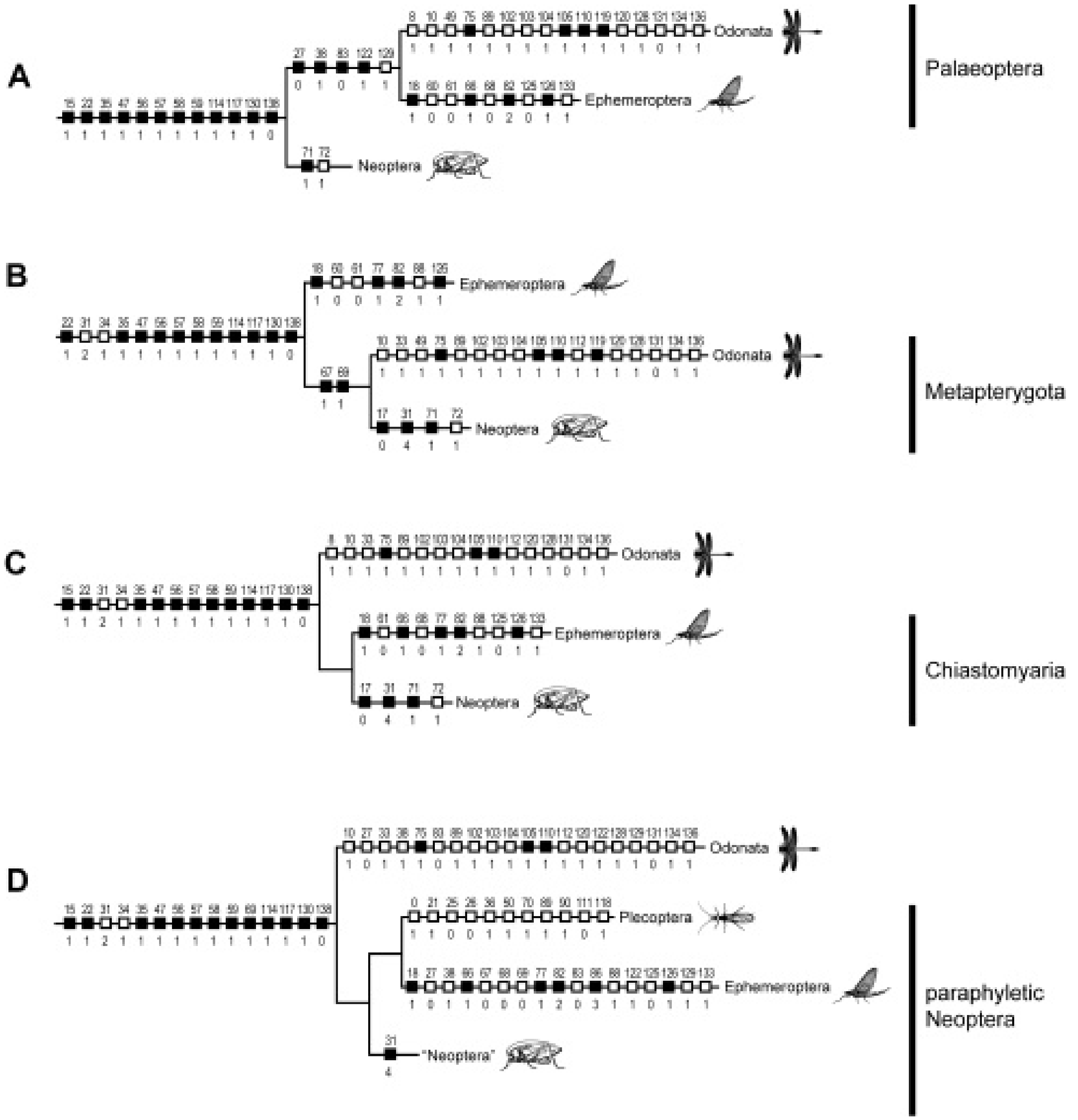

Fig. 8. Character optimizations on optimal tree resolution and CTRs of the four main hypotheses concerning basal splits of pterygotes. (a) strict consensus of the two equally parsimonious cladograms (length = 298 steps, CI = 57, RI = 73) focused on Palaeoptera received from the unconstrained analysis. B, strict consensus enforcing Metapterygota (length = 301 steps, CI = 56, RI = 73). C, strict consensus with enforced Chiastomyaria (length = 303 steps, CI = 56, RI = 72). D, strict consensus with enforced paraphyletic Neoptera (Lin, 2010) (length = 310 steps, CI = 55, RI = 71). Non-homoplasious character changes are indicated with black squares, homoplasious characters with white squares. Trait numbers are indicated above squares, state changes below. For trait reference see Data S2 and S3.

was up to now not supported by any character of the head. Features of the mandibular articulation and muscle equipment strongly pointed towards a clade Metapterygota (Staniczek, 2000; Staniczek, 2001). In the present study, all characters potentially supporting alternative concepts (e.g., Metapterygota, Chiastomyaria) are taken into account. Nevertheless, a clade Palaeoptera (Odonata + Ephemeroptera) is consistently supported in all analyses using the entire set of characters of the head, although support levels are lower in parsimony based tree reconstructions (Fig. 7).

A clade Palaeoptera comprising Odonata, Ephemeroptera and some extinct Palaeozoic insect groups was first proposed by Martynow (1924) and Crampton (1924). Since then, various potential synapomorphies were presented, including shortened antennae (Hennig, 1969), aquatic larvae (Ax, 1999), the distinct wing joint (Haas and Kukalová-Peck, 2001; Kukalová-Peck, 1997; Willkommen and Hörnschemeyer, 2007), and a paired penis (Bechly et al., 2001). Palaeoptera was also supported in several molecular studies (Hovmöller et al., 2002; Ishiwata et al., 2011; Kjer et al., 2006; Simon et al., 2010; Wheeler et al., 2001). Most of the morphological arguments are problematic: Palaeozoic dragonflies, mayflies and other palaeopterans possessed multisegmented antennae (Brauckmann and Zessin, 1989; Klass, 2007; Kukalová-Peck, 1983; Soldán, 1997), which implies that the antennal shortening of mayflies and dragonflies occurred independently. Paired penises also occur in Grylloblattodea and Dermaptera (Bechly et al., 2001; Klass, 2007) and the homology in all groups concerned is problematic due to differences in ontogeny and structure (Bechly et al., 2001). Characters related to the wing or wing joint suffer from unclear character polarity since all potential outgroups are wingless (Beutel and Gorb, 2006; Whitfield and Kjer, 2008). Fossil stem group representatives of winged insects may clarify the ancestral articulation and mode of flight, but are not known yet. The argument of aquatic larvae is weak. Aquatic immature stages also occur in stoneflies (Plecoptera) and have evolved several times independently in Holometabola (Grimaldi and Engel, 2005).

Palaeopteran autapomorphies revealed in our study are a pedicellus longer than the scapus (28:0), the loss of antennal circulatory organs in the adults (38:1), a lacinia with a single incisivus (83:2) and dentisetae (84:0), and the loss of M. praementopalpalis externus (123:1; 0la14). We are aware that the presumptive apomorphies for Palaeoptera (Fig. 8A) need further scrutiny and critical re-evaluation using well documented morphological characters of all body parts and/or extensive molecular data. Variations of the antennal organisation frequently occur in pterygotes (Kristensen, 1991; Soldán, 1997) and generally seem to correlate with antennal size reduction. The study of more recent and extinct taxa may reveal whether an elongated pedicel is obligatorily correlated with antennal size reduction or an independent character synapomorphic for Ephemeroptera and Odonata. Presently available information supports the view that the distinct length ratio of the scapus and pedicellus is a unique feature of Palaeoptera and evolved only once.

The entire lack of antennal vessels in Ephemeroptera and adult Odonata was already discussed by Pass (Pass, 1991; Pass et al., 2006): in early instar immatures of Odonata a sac-like frontal sinus is present and connected to the antennal vessels. However, apparently this structure cannot be homologised with the antennal vessels of other taxa (Pass et al., 2006). Since aquatic larvae originated multiple times (Grimaldi and Engel, 2005) the antennal vessels of odonate larvae may have evolved independently (Pass, 2000) and may represent another specialisation and autapomorphy of this group.

The structure of the lacinia is an apparent autapomorphy of Palaeoptera. Especially the mesally directed dentisetae are unique among winged insects. Mesally directed hyaline lamellae at similar position are usually present in Zygentoma (Koch pers. obs.), but these are flat, unsclerotized, strictly arranged in one row along the mesal edge, and more numerous than the dentisetae in palaeopterans. The hyaline lamellae in Zygentoma show more structural correspondences to the aboral row of setae in Ephemeroptera (Staniczek 2001) that occur at the same position on the lacinia besides dentisetae.

Rejection of alternative hypotheses

Two recent studies of the mitochondrial genome (Lin et al. 2010; Zhang et al. 2010) placed a clade Ephemeroptera + Plecoptera as sistergroup to all the remaining neopterans, thus rendering Neoptera paraphyletic. The authors claim that “the non-monophyly of the Neoptera is not strongly supported and needs further investigation” (Lin et al. 2010). Considering the arguments in favour of a monophyletic Neoptera and the weak support of a clade Ephemeroptera + Plecoptera, paraphyletic Neoptera appear extremely unlikely considering the data set presented here (twelve additional steps in the parsimony analysis; see Fig. 8D).

Boudreaux (1979) proposed direct sperm transfer and the dominant role of indirect flight muscles as potential synapomorphies of Ephemeroptera + Neoptera (=Chiastomyaria). As pointed out above, it is not possible to determine the polarity of the latter character due to the lack of a suitable outgroup. The indirect sperm transfer of all primarily wingless hexapods is definitely not homologous to the indirect sperm transfer of Odonata (Witte and Doring, 1999). Therefore, also in this case, the polarity of the character remains ambiguous. None of the characters analysed here turned out as a potential autapomorphy of “Chiastomyaria” and to enforce this clade requires eight additional steps in our analysis (Fig. 8C).

Weakened support for Metapterygota

The third possible combination, a clade comprising Neoptera and Odonata (=*Metapterygota*; Fig. 6B) (Staniczek 2001) is favoured by most morphologists (Grimaldi and Engel, 2005; Klass, 2007; Kristensen, 1981; Kristensen, 1991) and was also supported in several molecular studies (Plazzi et al., 2011; Terry and Whiting, 2005; Zhang et al., 2008). Arguments in favour of this hypothesis are the suppression of the imaginal molt, the additional tracheal supply of each wing and pterothoracic leg from the spiracle of the following segment, paired female gonopores, a posteriorly closed heart, the loss of long terminal filaments, the suppression of the hypopharyngeal superlinguae, and a series of interrelated modifications of the mandible. The Palaeoptera hypothesis supported by the characters analysed here implies that the presumptive metapterygote apomorphies have evolved independently or represent character reversals. It is conceivable that the winged subimago was lost independently in Odonata and Neoptera, and it was even discussed that this mode of development may have evolved several times in the winged stages (Kristensen, 1991; Kukalova-Peck, 1978). Paired female gonopores are a secondary feature of Ephemeroptera (Boudreaux, 1979). A posteriorly closed heart also occurs in Collembola and Protura, which makes the polarity assessment ambiguous (Klass, 2007; Pass et al., 2006). Superlinguae-like structures also appear in dermapterans and parallel loss appears likely in this case but their homology to superlinguae in basal hexapods is highly controversial. A double tracheal supply of each wing and leg stated as an autapomorphy for Metapterygota is also present in some ephemeropterans (Klass, 2007; Kristensen, 1975), and the mayfly *Epeorus* possesses a short and slender posterior leg trachea, which is not connected to the anterior one (Chapman, 1918). Staniczek (2000, 2001) proposed an entire series of characters concerning the mandibular articulation including anterior (66) and posterior ball-and-socket joints (68), a lateral shift of the anterior tentorial pit resulting in the presence of a subgenal ridge (8), and the loss of three mandibular muscles (69, 0md2; 71, 0md5; 72, 0md7). In contrast to Staniczek’s findings our reinvestigation of head structures of three odonatan representatives shows that the muscle equipment is the same as in mayflies, with the exception of M. craniomandibularis externus anterior (70, 0md2). Besides this, odonatans possess an entire series of muscles, which belong to the insect groundplan (0hy4, 0hy5, 0hy12, 0la15) but are absent in Ephemeroptera. Additionally, Archaeognatha also possess a posterior mandibular ball-and-socket joint. Therefore, this character complex is ambiguous and does not support Metapterygota (or an alternative concept). The aquisition of a cylinder-shaped joint in the stem group of Dicondylia would require a modification to a ball-and-socket joint in Metapterygota. A cylinder-shaped posterior joint as an independent modification in Zygentoma and Ephemeroptera, respectively, would imply the presence of a ball-and-socket joint in the entire stemgroup of Pterygota.

Mayfly head morphology partly reassessed

Numerous studies addressed the anatomy of the ephemeropteran head [Siphlonuridae: Schonmann (1981); Heptageniidae: Strenger (1954); Palingeniidae: Strenger (1970); Ephemeridae: Strenger (1975); Euthyplociidae: Strenger (1977)] and selected substructures (Hudson, 1951). Staniczek (2000, 2001) reviewed and homologised head structures of Ephemeroptera and reconstructed the groundplan based on an investigation of *Oniscigaster wakefieldi* McLachlan, 1873. Staniczek (2000, 2001) had to rely on the larval morphology, as the mouthparts of adult mayflies are strongly reduced (Edmunds, 1988; Simm, 1914), and we followed this approach here. Generally, the comparison of characters of different life stages is problematic and a potential source of phylogenetic misinterpretations. However, the alternative, i.e. the use of adult head structures, would have been more problematic, as many characters would have been inapplicable for mayflies.

Our data corroborates that a distinct channel-like anterior mandibular joint (“Rinnengelenk” fide Staniczek 2000; “slider” fide Kukalova-Peck, 1991) and the absence of a salivary system are defining features of ephemeropteran head organisation. An orthognathous head orientation, together with 3-segmented maxillary palps (muscles 0mx13-15 absent) and the fusion of galea and lacinia are additional features of the ephemeropteran head groundplan.

In contrast to Staniczek (2000) we consider the cuticular ridge interconnecting the anterior tentorial pits an epistomal ridge (er, Fig. 1). MicroCT data clearly show a strengthening of the cuticle in this region. The clypeus by definition is a part ventral to the epistomal ridge (Jacobs and Seidel, 1975; Seifert, 1995; Torre-Bueno et al., 1989), which implies that Staniczeks "postclypeus" belongs to the frons. We hypothesise that the change from a cuticular hardening of the mandibular depression (Zygentoma) towards an anterior mandibular articulation complex (Ephemeroptera) requires the modification of other head parts. We hypothesise that the evolution of dicondyly requires the modification of other head parts as well. The formation of an epistomal ridge is one of these modifications. In agreement with Staniczek (2000, 2001), we found no indication of a subgenal ridge in Zygentoma and Ephemeroptera as it is present in Odonata and Neoptera. This structure seems to be directly associated with a ball-and-socket articulation resulting in a fixed axis of movement and increased biting forces in the transverse plane (Staniczek, 2001).

A partly revised interpretation of odonate head morphology

As already pointed out in the introduction, the cephalic morphology of Odonata is understudied and its interpretation subject to controversy (Asahina, 1954; Mathur and Mathur, 1961; Short, 1955; Staniczek, 2000; Strenger, 1952; Tillyard, 1917). In contrast to the present contribution (see electronic supplement ES1), in all earlier studies only subsets of the musculature are described. With the exception of M. craniomandibularis externus anterior (0md2), which is absent in Odonata and Neoptera, the mandibular muscle equipment is similar in both Ephemeroptera and Odonata (Fig. 6, electronic supplement ES1+4).

As active predators which feed during flight, Odonata are characterised by some unique specialisations such as the head arrester system (Gorb, 1999), the extremely large compound eyes with a very high number of ommatidia, and mouthparts with fused lobes (75:1), shortened palps (86:2, 102:1) and moveable labial hooks (105:1). The homology of the labial and maxillary lobes was discussed for example by Tillyard (1928) and Asahina (1954). Our data support Asahina’s view (1954) that the labial lobes represent a pair of fused glossae and paraglossae. In the anisozygopteran *Epiophlebia superstes*, the distal edge of these lobes bears two appendages on each side. We interpret these as vestiges of glossae and paraglossae based on the incomplete fusion of these structures. Asahina (1954) referred to the labial part bearing the lateral lobes as "mentum" and the more proximal part as the "submentum". This view implies a bilobed prementum (the lobe and the prementum as termed in the present article) and the loss (instead of a fusion) of the galea and lacinia. We do not follow this interpretation based on the insertion of M. submentopraementalis (0la8), which generally defines the posterior margin of the prementum.

The labial palps of odonates underwent some unique specialisations, more conspicuous in the larvae, but still distinct in the adult despite of the strongly modified function. They are characterized by the reduction of the number of palpomeres (102:1) together with a dorsoventral flattening (103:1), a drastically increased length (104:0), and moveable spine-like hooks (105:1) devoid of muscles. Due to their flat shape and the increased stiffness (realised by palpomere reduction) the palps are very well suited to counter the high transverse mechanical strain produced when catching and clamping prey. The hooks function as spines for penetrating and fixing the prey.

In the maxilla the outer lobe can be homologised with the palpus based on the muscle insertions (0la13, 0la14). We consider the mesal lobe as the lacinia. It was shown in a developmental study that no galea is formed in the embryo (Ando, 1962). Additionally, there is no trace of muscles in the adult or larval stages. Thus, we conclude that the galea is completely reduced in Odonata. Accordingly, we refute the term “galeolacinia”, which implies a fusion of the outer and inner endite lobes (Ax, 1999). Staniczek (2000, 2001) demonstrated that mayflies, albeit also lacking galeal muscles, exhibit a "real" galeolacinia containing elements of both endite lobes. Both are clearly distinguishable and connected along their entire length by a membranous field. Thus, the loss of M. stipitogalealis (0mx7; 88:1) is a potential synapomorphy of Ephemeroptera and Odonata.

Wing-like tentorial processes reaching inside the lumen of the mandible (49:1) have not been encountered in neopterans yet. They are shared with *Lepisma* and other Zygentoma (Koch, 2003), but we found no comparable structures in the examined ephemeropterans and there are no records in the literature (Staniczek, 2001; Strenger, 1952; Strenger, 1954; Strenger, 1970; Strenger, 1975). Consequently, these tentorial protuberances are a potential autapomorphy of Odonata.

In summary, incomplete, inaccurate and misinterpreted information on the head of Odonata was one of the main reasons for the widely accepted Metapterygota hypothesis. Our reassessment of the odonate head morphology clearly shows that dragonflies lack some of the metapterygotan features formerly proposed in the literature.

Conclusions and Outlook

The present investigation shows - in contrast to earlier studies - that characters of the head support a clade Palaeoptera. The three main alternatives Palaeoptera, Chiastomyaria and Metapterygota are supported by arguments derived from different body parts. Each option implies homoplasy in some of these characters. A principal problem related to far reaching evolutionary transformations in the early evolution of Pterygota is the problematic or impossible polarity determination of characters of the head and thorax several thoracial and abdominal characters, due to the absence of corresponding features in all potential apterygote outgroups. These problems can be avoided by evaluating characters of the head, the approach followed in this study. As shown earlier (see e.g. Beutel and Baum 2008; Beutel et al., 2010) the evaluation of a limited character system can easily lead to erroneous phylogenetic results. Therefore, the results presented here should be critically re-evaluated in the framework of very broad analyses, especially of extensive molecular data. Past morphological studies gave the impression that the basal splitting events of winged insects are based on robust theories derived from mandible anatomy. The present study shows that this is by no means true. Even though the phylogenetic hypothesis presented here may be preliminary, the well documented data will allow a better understanding of character transformations in the early evolution of Pterygota. A stepwise progress in this direction will also reveal possible interconnections of different characters and character systems (hidden character weighing) and features which require more detailed investigations. This process will very likely lead to a well-founded and detailed evolutionary scenario of the winged insects, arguably the most successful group of organisms.

Acknowledgement

We thank Dr. A. Staniczek and Prof. Ryu Machida for providing valuable specimens for this study. Sincere thanks also go to Fabian Wilde (HZG, Geesthacht) and Sebastian Thieß, Wolfgang Drube (DESY, Hamburg) as well as Marco Stampanoni and Peter Modregger (both SLS, Villigen, Switzerland) for the ability to conduct SR-microCT investigations at a high quality level. The SR-microCT investigations were conducted through successful project applications I-20080169 and I-20090211 (DESY, Hamburg) and 20110069 (SLS, Villigen, Switzerland). Irina Ruf (Steinmann Institute, Bonn, Germany) made microCT investigations at the device of the Steinmann Institute possible. Claudia Etzbauer, Manuela Thelen and Johannes Dambach (all ZFMK) provided excellent support in lab and field.

5 The Identification of Concerted Convergence in Insect Heads Corroborates Palaeoptera

The Identification of Concerted Convergence in Insect Heads Corroborates Palaeoptera

The Identification of Concerted Convergence in Insect Heads Corroborates Palaeoptera

Alexander Blanke[a,*], Carola Greve[a], Benjamin Wipfler[b], Rolf Beutel[b], Barbara Holland[c] and Bernhard Misof[a]

[a] Zoologisches Forschungsmuseum Alexander Koenig, Zentrum für molekulare Biodiversität, Adenauerallee 160, 53113 Bonn, Germany
[b] Entomology Group, Institut für Spezielle Zoologie und Evolutionsbiologie, Friedrich-Schiller-Universität Jena, Erbertstraße 1, 07743 Jena, Germany
[c] Theoretical Phylogenetics Group, School of Mathematics & Physics, University of Tasmania, Private Bag 37, Hobart, Tasmania 7001, Australia
*Corresponding author: Alexander Blanke, Zoologisches Forschungsmuseum Alexander Koenig, Adenauerallee 160, 53113 Bonn, Germany; e-mail adress: blanke@uni-bonn.de; Tel.: +49 (0)228 9122-421; Fax: +49 (0)228 9122-295

This is the author's version of a work accepted for publication in the journal Systematic Biology doi:10.1093/sysbio/sys091

Abstract

The relationships of the three major clades of winged insects - Ephemeroptera, Odonata and Neoptera - are still unclear. Many morphologists favour a clade Metapterygota (Odonata+Neoptera), but Chiastomyaria (Ephemeroptera+Neoptera) or Palaeoptera (Ephemeroptera+Odonata) have also been supported in some older and more recent studies.

A possible explanation for the difficulties in resolving these relationships is concerted convergence, convergent evolution of entire character complexes under the same or similar selective pressures.

In this study we analyse possible instances of this phenomenon in the context of head structures of Ephemeroptera, Odonata and Neoptera. We apply a recently introduced formal approach to detect the occurrence of concerted convergence.

In particular characters of the tentorium and mandibles, but also some other head structures, have apparently not evolved independently, and thus can cause artefacts in tree reconstruction. Our analyses, taking into account identified character sets that may be affected by concerted convergence, corroborate the Palaeoptera concept. We show that the analysis of homoplasy and its influence on tree inference can be formally improved with important consequences for the identification of incompatibilities between data. Modified weighting (or exclusion of characters) in cases of formally identified correlated cliques of characters may generally improve morphology based tree reconstruction.

Within winged insects (Pterygota), systematists distinguish three major clades: Ephemeroptera (mayflies), Odonata (damselflies and dragonflies) and Neoptera (all remaining winged insects, figure 1). The monophyly of each of the three groups is generally accepted and supported by rich sets of morphological and molecular data (Carapelli et al., 2006; Klass, 2009; Meusemann et al., 2010; Ogden et al., 2009; Rehn, 2003; Simon et al., 2009). The relationships, however, are still unresolved (Klass, 2009; Kristensen, 1981). All 3 possible topologies have been proposed: (a) Palaeoptera (Ephemeroptera plus Odonata; figure 1a) has been advocated based on characters of the wing venation and articulation (Bechly et al., 2001; Brauckmann and Zessin, 1989; Haas and Kukalová-Peck, 2001; Hennig, 1969; Hovmöller et al., 2002; Kukalová-Peck, 1997; Kukalová-Peck, 2008; Soldán, 2003; Wheeler et al., 2001; Willkommen and Hörnschemeyer, 2007); (b) Metapterygota (Odonata plus Neoptera; figure 1b) is supported by characters of the mandibles and tracheal system and also by molecular data (Beutel and Gorb, 2006; Kristensen, 1981; Ogden and Whiting, 2003; Pass et al., 2006; Staniczek, 2000; Staniczek, 2001; Terry and Whiting, 2005; Wheeler et al., 2001); and (c) Chiastomyaria (Ephemeroptera plus Neoptera; figure 1c) is supported by the presumably apomorphic mode of direct sperm transfer, the pterothoracic locomotor system dominated by indirect flight muscles, and molecular analyses based on rRNA genes and EST data (Carle, 1982; Kjer, 2004; Mallatt and Giribet, 2006; Matsuda, 1970; Simon et al., 2009).

Why is the Reconstruction of the Early Evolution of Winged Insects such a Challenge?

The sister group of Pterygota is Zygentoma (the silverfish) and both groups together form a clade Dicondylia (Figure 1a-c). Because silverfish are primarily wingless, homology assessments of thoracic skeletal elements and muscles related to flight are problematic, and consequently character polarisation within the early pterygote lineages is ambiguous. This also applies to sperm transfer, which changed from an indirect external mode (Zygentoma, Archaeognatha) to a direct transfer via an intromittent organ (Ephemeroptera & Neoptera). Odonata evolved a secondary copulatory apparatus at abdominal segments II and III and exhibit a unique form of "indirect" sperm transfer completely different from the condition in all other insects. Again, robust homology hypotheses and character polarisations covering winged and wingless groups are impossible (Witte and Doring, 1999), even though more data became available in recent years (Dallai et al., 2011; Klass, 2008; Matushkina, 2008a; Matushkina, 2008b). Due to this situation, most of the aforementioned arguments for either Chiastomyaria or Palaeoptera are affected by unclear homology assessments and character polarisation.

In contrast, the Metapterygota hypothesis is supported by mandibular characters with widely accepted homology and polarity assessment (Staniczek, 2001). Nevertheless, it has been shown that characters of the entire head including all mouthparts and the head capsule do not support this hypothesis (Blanke et al., in

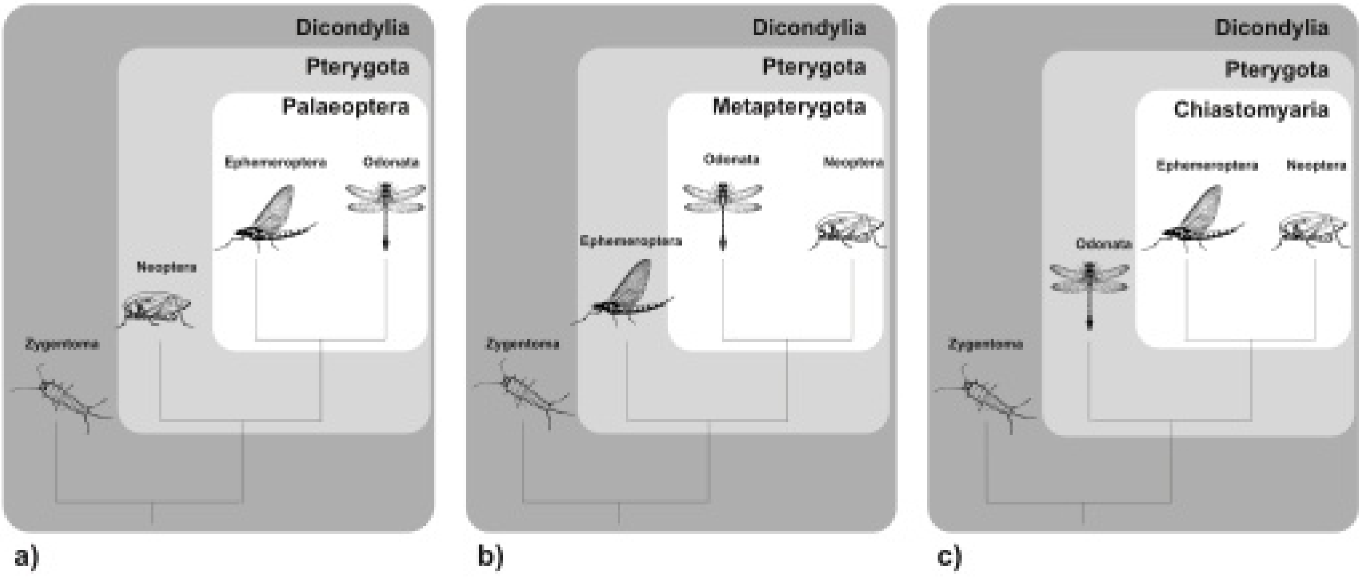

Figure 1 The most frequently encountered hypotheses concerning relationships of Ephemeroptera, Odonata and Neoptera. a) Palaeoptera (Odonata + Ephemeroptera); b) Metapterygota (Odonata + Neoptera); c) Chiastomyaria (Ephemeroptera + Neoptera).

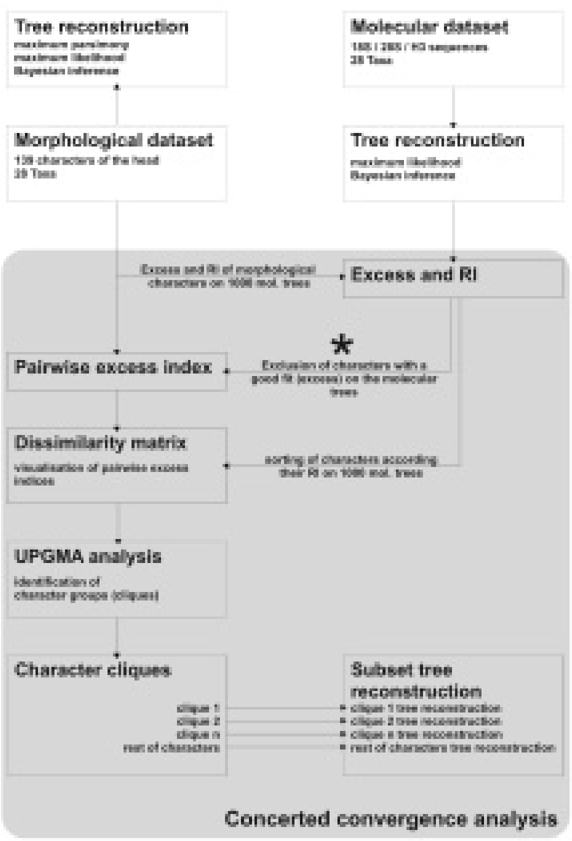

Figure 2 Principal workflow of the analysis to identify concerted convergence conducted by Holland et al. (2010) which is adapted herin. The asterisk indicates the analysis step of Holland et al. (2010) which is not followed in this contribution. For further explanations see text.

press). It turns out that formerly proposed presumptive synapomorphies in the literature (loss of certain head muscles and sutures) are in fact not groundplan features of Odonata, and data from the literature on seemingly well-known and important taxa like Zygentoma are ambiguous. Examples are the conflicting statements of Chaudonneret (1950) and Staniczek (2000) regarding the presence of a subgena in *Thermobia* (Zygentoma) which is generally considered an important structure in the context of the evolution of the mandibular articulation.

Dealing with Homoplasy

Phylogenetic hypotheses based on morphological and molecular characters frequently contradict each other (Giribet and Edgecombe, 2012; Giribet et al., 2001; Trautwein et al., 2012) although remarkable congruence has been reached in many areas (Beutel et al., 2011; Wiegmann et al., 2009). Consequently, the robustness of tree reconstruction techniques and the signal strength of molecular data and morphological characters become essential aspects of phylogenetic analyses (Letsch et al., 2010; Wägele and Mayer, 2007). Basically, causes for high statistical support despite incongruence between results have to be investigated.

One potential reason for extensive morphological homoplasy among lineages is a phenomenon called concerted convergence (Patterson and Givnish, 2002). This describes a process in which several traits, for instance the character complexes "wings", "mouthparts" or "genitalia", are exposed to the same shared set of environmental conditions or functional requirements. In each of these cases a given selective pressure might influence the whole character system such that the evolution of many individual characters occurs in a "concerted" manner. In phylogenetic analyses this can result in an artificially increased number of presumptive synapomorphies, which are in fact not independent, and consequently in clades with unjustified support.

As a solution to this problem, Holland et al. (2010) proposed to identify groups - or cliques - of characters evolving in a concerted manner. Applying permutation tests of character compatibility (Figure 2), Holland et al. (2010) were able to detect cliques of mutually compatible characters in water birds and demonstrated the impact of this phenomenon on phylogenetic inference.

In this study we analyze the possible homoplasy of cephalic characters and concerted convergence obscuring the earliest divergences within Pterygota. We show that a cephalic character state matrix used to reconstruct the early evolution of winged insects contains considerable evidence of concerted convergence, which negatively affects the results of phylogenetic analyses. We address whether (i) character groups show concerted convergence and (ii) how these characters influence tree inference.

Data

Due to the inherent problems of homology and polarity of thoracic and abdominal characters, the data assembled here are exclusively based on features of the head. The taxon sampling covers Archaeognatha, Zygentoma, Ephemeroptera, Odonata and 12 orders of Neoptera including all major polyneopteran clades (Table 1). The matrix is composed of a total of 139 characters including 19 characters of the head capsule, six labral characters, 22 antennal characters, 13 tentorial characters, 13 mandibular characters, 17 maxillary characters, 33 labial characters and 16 characters of the hypopharynx, salivarium and fore gut. A character discussion is presented in Blanke et al. (in press). Although the focus of this study is the Palaeoptera problem it was necessary to include a wide taxon sampling of Neoptera as well. As it is currently impossible to define a cephalic groundplan for Neoptera, the homology hypotheses implied by the present character matrix have been carefully evaluated across a wide range of neopteran taxa. Moreover, the reliability of our concerted convergence analysis partly depends on the relationships within Neoptera. Additionally, we compiled a molecular data set with a corresponding taxon selection in which we used 18S and 28S rRNA genes and sequences of the protein-coding gene Histone H3 (Table 1). All sequences were downloaded from NCBI Genbank. Taxa were only included if represented by at least two genes. We considered 18S sequences with at least 1700 base pairs (bp), 28S sequences with at least 1400 bp and complete or nearly complete sequences of Histone H3. If sequence data of a certain taxon were not publicly available or did not match our selection criteria, we chose sequences of a species of a different genus but within the same insect order (Table 1).

Definitions

Several terms related to the analytical steps proposed by Holland et al. (2010) are frequently used throughout this manuscript. These are briefly defined as follows.

Clique: a set of mutually pairwise compatible characters.

Compatible: characters are compatible if they can be displayed on the same tree without homoplastic changes. Note that pairwise compatibility guarantees overall compatibility of a set of characters for two-state characters but not for multi-state characters.

Concerted convergence: the convergent evolution of groups of characters.

Dissimilarity: a measure, $d(i,j)$, of the difference between two objects i and j, that is symmetric, i.e. $d(i,j) = d(j,i)$, and non-negative, i.e. $d(i,j) \geq 0$, and where $d(x,x) = 0$.

Excess index: the extra number of character changes required to explain a character on a given tree above the minimum number possible (the number of character states minus 1).

Pairwise excess index (Holland et al., 2010): the dissimilarity between 2 characters i and j is defined as the difference between the parsimony score of the most parsimonious tree constructed using only that pair of characters and the minimum possible parsimony scores for i and j. Thus the index is equal to $P - m_i - m_j$, where P is the parsimony score for the most parsimonious tree for the alignment containing characters i and j and m_i and m_j are the minimum possible parsimony score for characters i and j, respectively. A pair of compatible characters has a dissimilarity of 0.

Parsimony score: the sum of implied character changes along a given tree topology.

Retention index: defined as $(M-s)/(M-m)$, where M and m are respectively the maximum and the minimum possible parsimony scores and s the actual parsimony score of the character on the tree.

Alignment Procedure

18S and 28S rRNA sequences were aligned separately with RNAsalsa software (Stocsits et al., 2009). The prealignment for RNAsalsa was conducted with the E-INS-i algorithm of MAFFT, using default settings (Katoh et al., 2005; Katoh et al., 2002). As structure constraints, we employed the nuclear 18S and 28S structure models of *A. albimanus* and *A. mellifera*, respectively, both retrieved from the European Ribosomal Database. The stringency settings for adoption of secondary structures in different alignment steps were relaxed (0.51), as we wanted to retain as much structure information as possible. Histone H3 was aligned with MAFFT choosing the G-INS-i algorithm (Katoh et al., 2005). Subsequent

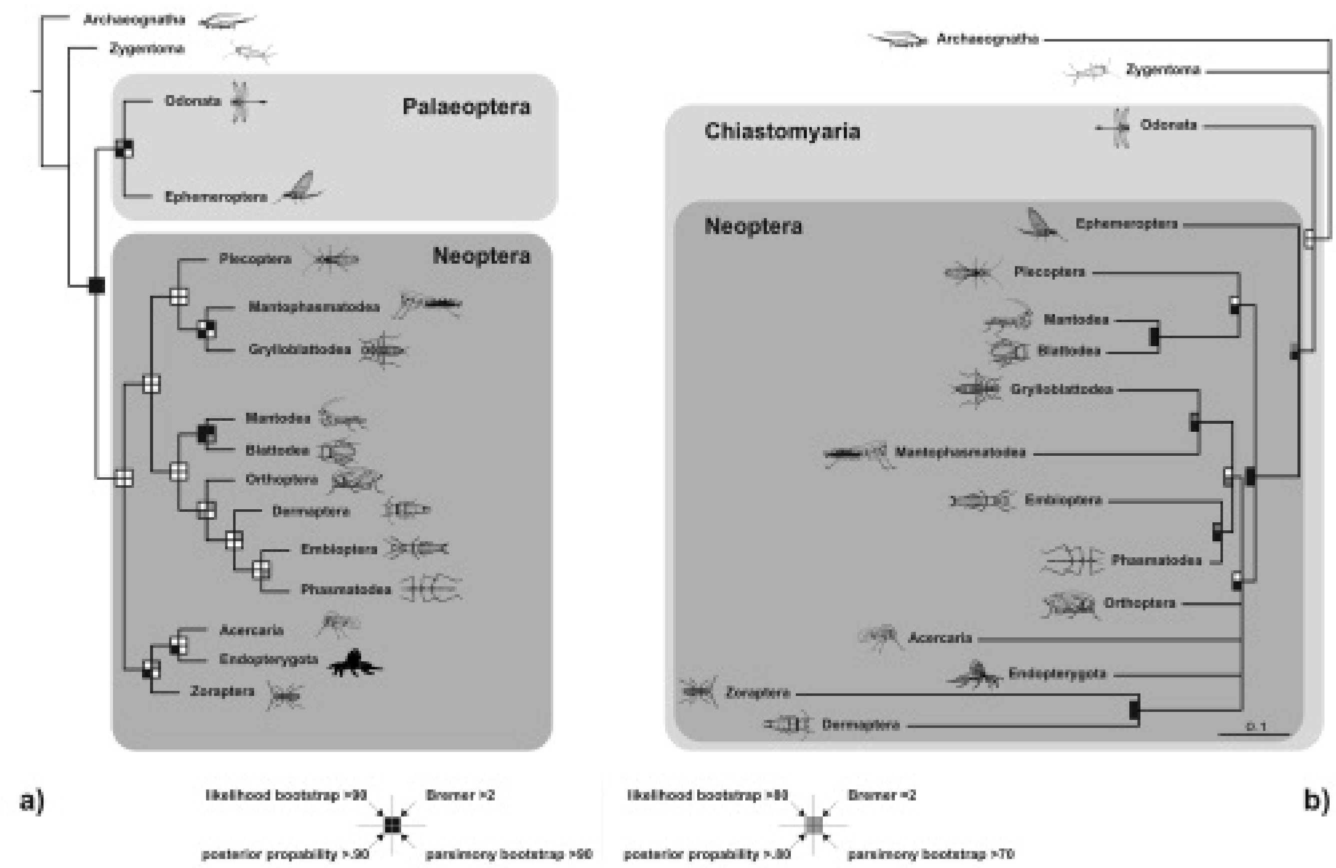

Figure 3 Tree inference from analysis of the morphological and molecular data. a) Consensus tree of the morphological data analysed with Bayesian inference, maximum likelihood, maximum parsimony and parsimony bootstrapping. Tree topology derived from the parsimony analysis. b) Consensus tree from the analysis of the molecular data using Bayesian inference and maximum likelihood (Bremer support and parsimony bootstrap were not calculated). Branch lengths and tree topology are derived from the Bayes analysis. White squares indicate support below the respective boundary values indicated below the trees. The underlying morphological data can be found at doi:10.5061/dryad.1q3b6 in Electronic supplement (ES) 1. Detailed trees for each reconstruction method are available at doi:10.5061/dryad.1q3b6 in Electronic supplement (ES) 2 and Electronic supplement (ES) 3.

masking of the alignments was done with Aliscore v.0.2 (Misof and Misof, 2009) which identifies putative ambiguously aligned regions in multiple sequence alignments using a sliding window approach. For gap treatment (g), window size (ws) and random pairwise comparisons (pc), the following settings were used: g = ambiguous characters, ws = six positions, pc = 4 x number of taxa. Aliscore is currently not able to detect base pairings. In case of 18S and 28S rRNA sequences, positions which are part of the consensus structure of the RNAsalsa alignments were considered as structurally conserved and were retained as paired positions in the data set. The complete molecular data set comprised 4258 sites, of which the 18S partition accounted for 1854 sites, the 28S partition for 2041 sites and the Histone H3 partition for 363 sites.

Tree Reconstruction of the Morphological Data

The morphological data were analysed using maximum parsimony, Bayesian inference and maximum likelihood.

Parsimony analyses and Bremer/bootstrap support calculations of the morphological data were carried out with TNT (Goloboff et al., 2008) using 1000 heuristic searches starting with random addition of taxa (TBR branch swapping).

Bayesian inference of the morphological data was conducted using MrBayes v3.2 (Huelsenbeck and Ronquist, 2001; Ronquist and Huelsenbeck, 2003). The MK model was applied, with among-character rate variation modelled with gamma-distributed rates across characters with four discrete rate categories. Priors were set adopting the default settings of MrBayes v3.2 (all state frequencies (change rates) set equal, all topologies with equal probabilities, unconstrained branch length). Two parallel analyses were run with random starting trees and four Metropolis coupled Markov chains (MCMC) for 1,000,000 generations. Every 100th generation was sampled to yield a posterior probability distribution of 10,000 trees. After discarding the first 1000 trees of each run as burn-in trees, a 50 % majority rule consensus tree was calculated from the sampled trees of both runs. Convergence diagnostics implemented in MrBayes, potential scale reduction factors (PSRF), and average standard deviation of split frequencies were used as guidelines for assessing convergence. In the Bayesian analysis (BA) the average standard deviation of split frequencies had a final value of 0.0046 and the PSRF approached 1 for all parameters. The MKV model was applied in the maximum likelihood (ML) analysis of the morphological data using RAxML v7.0.3 (Stamatakis, 2006), with all model parameters estimated from the data, and rate heterogeneity across characters modelled using the gamma-model of Yang (Yang, 1994) with four discrete categories. Support was estimated with 1000 bootstrap replicates with identical tree-search settings.

Tree Reconstruction based on Molecular Data

For molecular tree inference the concatenated data set was divided into four partitions: (1) 18S + 28S loops, (2) 18S + 28S stems, (3) 1st + 2nd codon position of Histone H3 and (4) 3rd codon position of Histone H3. The consensus structures of the RNAsalsa alignments were used to define paired and unpaired partitions of 18S and 28S, respectively. According to the results of the Akaike Information Criterion in MrModeltest v2.3 (Nylander, 2004), the GTR + Γ + I model was selected as the best model of nucleotide substitution for partition (1) + (2) + (3). The GTR + Γ model was chosen for partition (4). Based on the selected models, a BA was carried out with MrBayes v3.1.2. (Huelsenbeck and Ronquist, 2001; Ronquist and Huelsenbeck, 2003) using two parallel runs each with 4 simultaneous Markov chains (one cold and three heated) for 10,000,000 generations. Trees were sampled every 100th generation. Excluding the first 25,000 trees of each run as burn-in, a 50 % majority-rule consensus tree with posterior probabilities was constructed from the remaining 150,002 trees.

Tracer v1.4.1 (Rambaut and Drummond, 2008) was used to determine the burn-in and to check convergence of parameter estimates by inspecting effective sample size (ESS) values and traces of the MCMC samples. The average standard deviation of split frequencies had a final value of 0.003, the PSRF approached 1 for all parameters, the ESS value of each parameter exceeded the recommended threshold of 200, and the traces of corresponding parameters in independent runs converged to the same optimum.

The ML analysis of the molecular data was conducted with RAxML v7.3.2. (Stamatakis 2006). The data set was partitioned into (1) 18S + 28S loops, (2) 18S + 28S

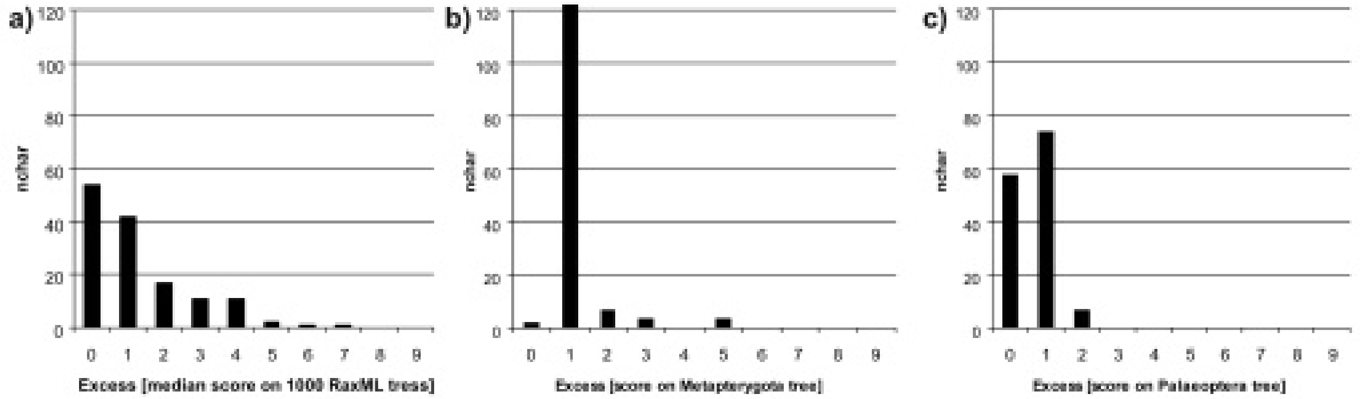

Figure 4 Frequency histograms of the median excess indices for the 139 characters derived by Blanke et al. (in press) on a) the set of 1000 RaxML trees sampled from the molecular analysis; b) an artificial metapterygotean tree and c) an artificial palaeopteran tree.

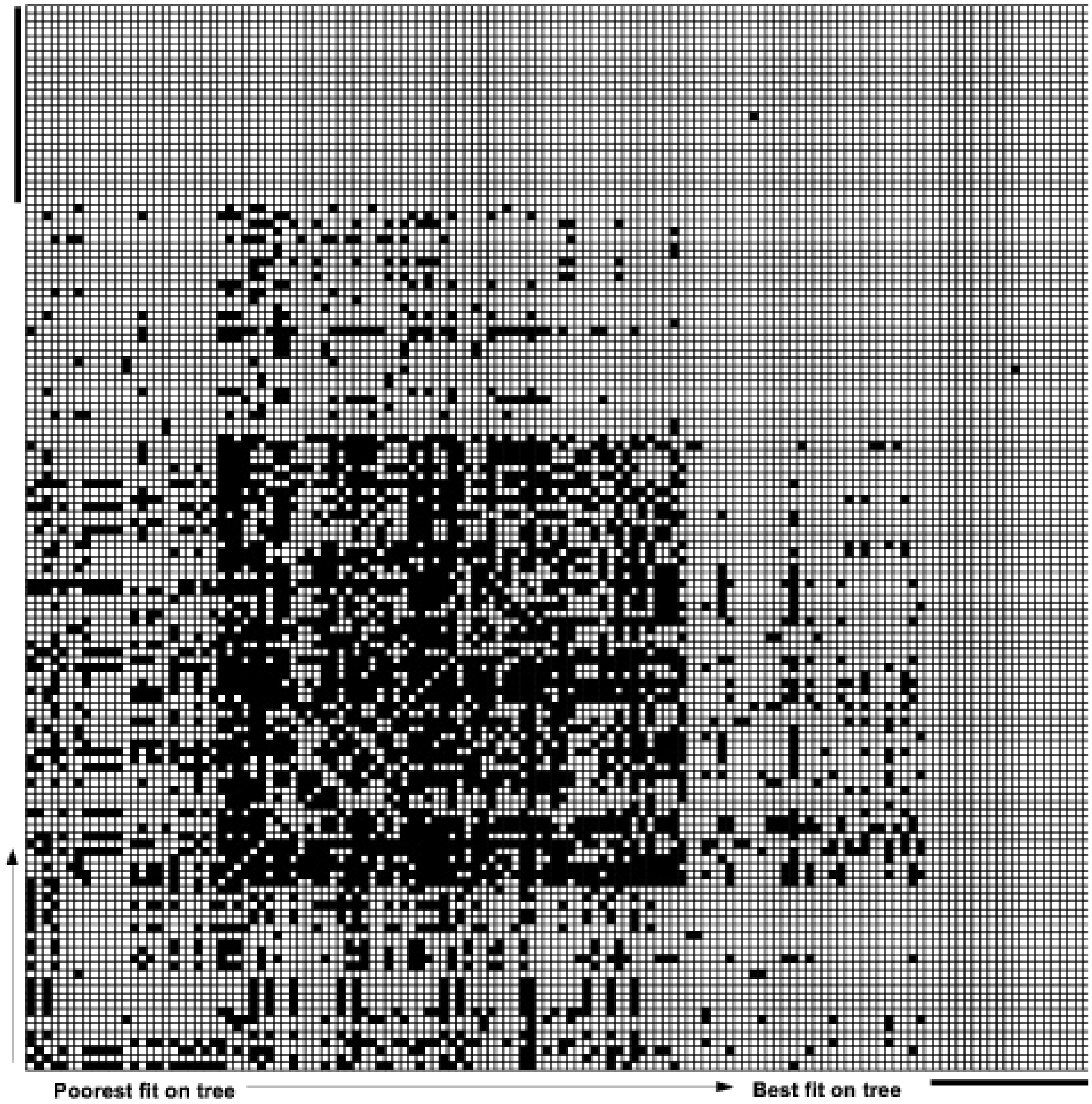

Figure 5 Excess index matrix showing the pairwise excess indices for each character pair of the morphological data matrix sorted according to their fit (retention index) on the 1000 RaxML trees of the molecular data (vertical and horizontal arrows). White dots show compatible pairs of characters. Black dots indicate incompatible pairs of characters. The black bars indicate parsimony uninformative characters (apomorphies). A detailed pairwise excess matrix is available at doi:10.5061/dryad.1q3b6 in electronic supplement (ES) 4.

stems, (3) 1st + 2nd codon position of Histone H3, and (4) 3rd codon position of Histone 3. The consensus structures of the RNAsalsa alignments were used to define paired and unpaired partitions. The GTR+ Γ + I model was used for all four partitions. Node support for the best–scoring ML tree was evaluated with 1000 rapid bootstrap replicates (Stamatakis et al., 2008). ML analyses were computed on HPC Linux clusters at the Regionales Rechenzentrum Köln (RRZK) using Cologne High-Efficient Operating Platform for Science (CHEOPS). Support values are given in parentheses in the following order: (RaxML bootstrap value (BS) / Bayes posterior probability (PP) / Bremer support (BR) / parsimony bootstrap(PB)). As Bremer support values are still frequently shown in morphology based phylogenetic studies, we decided to present them here despite of inherent problems pointed out by DeBry (DeBry, 2001). For the molecular tree node support is given in the following order: BS / PP.

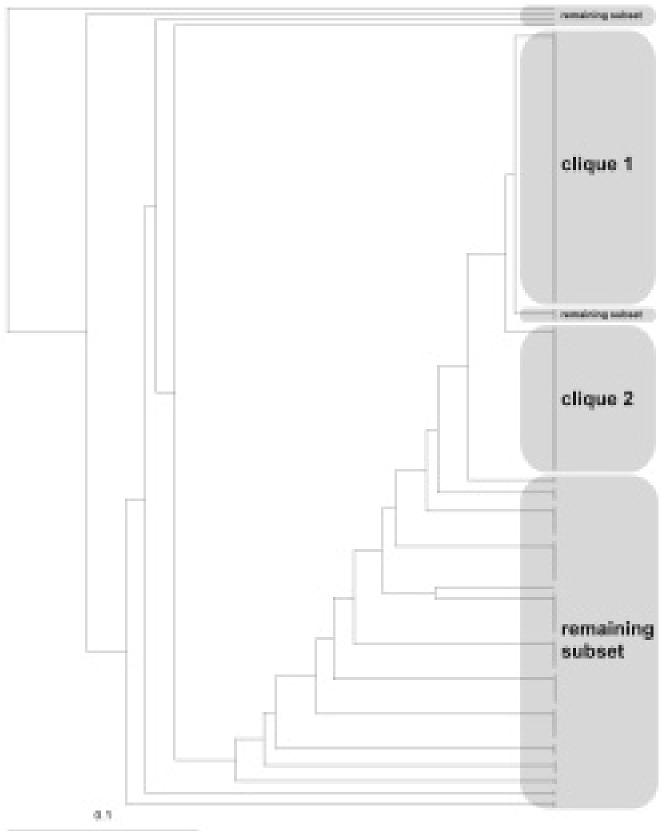

Figure 6 UPGMA clustering of the pairwise excess index matrix calculated in PAUP. Clustered characters are indicated by a vertical terminal line. The two cliques and the remaining subset of characters are indicated with grey boxes. For a detailed tree with all characters mapped see doi:10.5061/dryad.1q3b6.

Conflict Between Molecular data and Morphology

Morphological data (Figure 3a) provide consistent support (BS .83 / PP .94 / BR 3 / PB 59) for a clade Palaeoptera (Ephemeroptera + Odonata) while the molecular approach (Figure 3b) partly yields Chiastomyaria (Ephemeroptera + Neoptera; BS X / PP .99). The monophyly of Neoptera is weakly supported in the morphology based analysis of the cephalic data (BS 59 / PP x / BR 1 / PB 32) and the Bayesian analysis of the molecular data (BS X / PP .74). An obvious explanation is that the evolutionary diagnostic changes are thoracic and wing joint characters, which are not included in our data.

Some of the unorthodox results of the molecular analysis can be explained by the limited taxon sampling. However, for the specific analytical approach applied here, an identical or at least very similar taxon sampling was required. The purpose of the molecular analysis was not to provide a reliable tree of Neoptera, but to provide a reference tree for the earliest pterygote branching events. Focusing on the Palaeoptera problem, Chiastomyaria partly supported by molecular evidence is a hypothesis frequently encountered (Kjer, 2004; Misof et al., 2007; Simon et al., 2009; von Reumont et al., 2009).

Identifying Morphological Characters with the Highest Incompatibility with the Molecular Results

In the workflow of Holland et al's (2010) analysis (Figure 2) morphological characters are identified that agree least with the molecular trees by calculating their excess indices. These characters are further analysed by calculating their pairwise excess indices. The basic idea of this formalized approach is to subsequently identify cliques of characters that are more compatible with each other than to either the molecular or the morphological trees. If this is the case, at least some of these cliques may represent instances of concerted convergence and thus violate the assumption of character independence. The inclusion or treatment of these characters in tree reconstruction then has to be reconsidered.

As a starting hypothesis, we assume that Chiastomyaria are a natural clade. Based on the molecular tree we identified the morphological characters responsible for the incongruence between the molecular and morphological trees (Holland et al., 2010). First, we recorded the fit of the morphological characters to the trees derived from the molecular data. We took a random sample of 1000 trees from the RaxML bootstrap analysis of the molecular data and calculated the excess index as a measure of fit for each morphological character on these trees (Figure 4a). We also tested the excess distribution on the alternative hypotheses (Figure 4b+c) by changing only the sistergroup relationship between Ephemeroptera and Odonata (Figure 4b = Metapterygota; Figure 4c = Palaeoptera). The rest of the tree was left unchanged, i.e. identical to the molecular tree reconstruction. The excess index of a particular character is defined as the number of extra state changes above the minimum number possible (which is the number of character states minus 1) (Holland et al., 2010). Thus, a character with two states (0 and 1) and 5 state changes on a given tree has an excess of 4 (5 minus 1). The median excess index is derived from the excess index of each character calculated for all bootstrap trees. The median excess index is thus a measure of the average fit for each single character over all molecular trees. High excess values indicate a poor fit.

The excess indices derived from the molecular data (Figure 4a) show an exponential decrease. This implies that most of the characters fit the bootstrap trees quite well (peaks 0 & 1), while some characters with higher excess indices do not match the branching pattern implied by the molecular data. Basically, calculation of the excess indices already allows identification of characters with a poor fit to the molecular trees. However, this procedure alone is not sufficient for an exploration of possible character interdependencies, i.e. a higher compatibility with each other than to either the molecular or the morphological trees.

The excess distribution of the characters can be used as a decision basis for choosing cutoff values so that specific groups of characters can be analysed further. In contrast to Holland et al's (2010) study we decided to proceed with all morphological characters (see also figure 2), since characters important for the estimation of the basal pterygote splits have a good fit on both the molecular trees (excess index of 0-1; figure 4a) and on theoretical alternative trees supporting Metapterygota (Figure 4b) or Palaeoptera (Figure 4c). Excess frequencies in both cases show maximum peaks at either 0 or 1 indicating that most of the characters have a good fit on the respective hypotheses. For example the anterior ball-and-socket joint of the mandible has an excess index of zero under the Metapterygota hypothesis, and an excess of 1 under either the Palaeoptera or Chiastomyaria hypothesis.

Analysing Incongruent Groups of Characters

To identify mutually compatible morphological characters we calculated their dissimilarity as pairwise excess indices. We then plotted the dissimilarity values on the matrix representation of characters and ordered them according the median retention index the characters have on the 1000 RAxML bootstrap trees ("Dissimilarity matrix"; figure 4). The matrix shows that there are

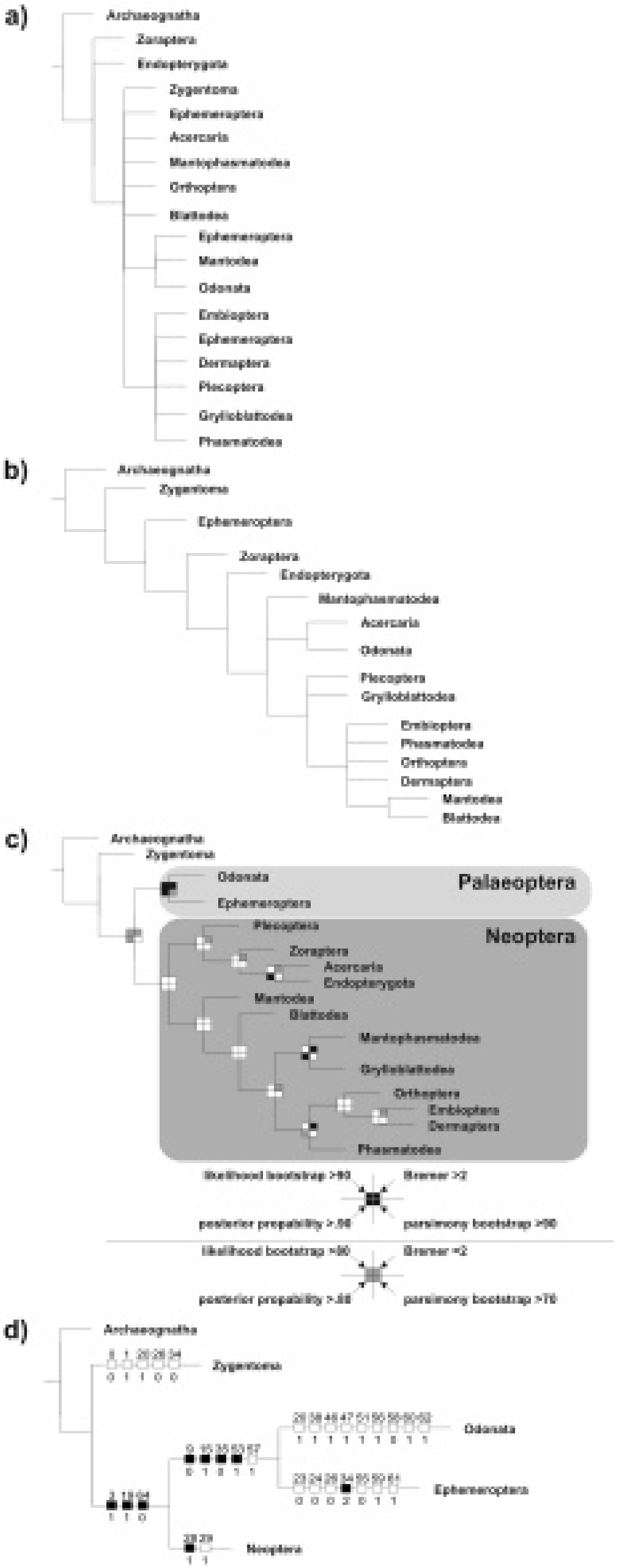

Figure 7 Phylogenies calculated from the two cliques of characters (a & b) and from the remaining character subset (c) of the morphological data matrix. a) Strict consensus of 25 trees; 48 characters; tree length = 56; RI = 88; CI = 89. b) Strict consensus of 16 trees; 26 characters; tree length = 38; RI = 93; CI = 86. c) The single most parsimonious tree derived from parsimony analysis; 65 characters; tree length = 192; RI = 71; CI = 45. The support values are mapped on the parsimony tree. d Detail of tree C showing the specific characters for each node focused on the Palaeoptera problem. Details for each clique and the remaining character set can be found at doi:10.5061/dryad.1q3b6 in electronic supplement (ES) 5. Trees for each reconstruction method used in Figure 7C are available at doi:10.5061/dryad.1q3b6 in electronic supplement (ES) 6.

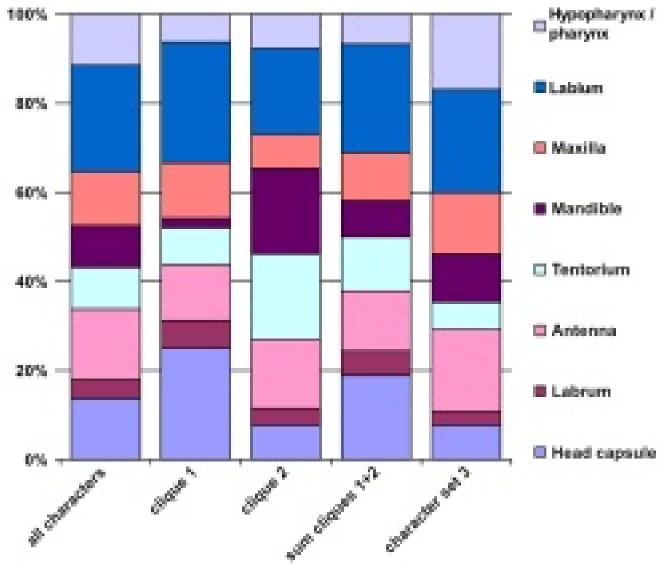

Figure 8 Distribution of characters in the complete data matrix (leftmost bar) and in each of the derived character cliques (bars 2-5) and in the remaining amount of characters (rightmost bar)

several character groups that are highly compatible to each other but have a rather poor fit on the molecular bootstrap trees (see arrows in figure 4). Furthermore, as could be expected, several characters with a good fit to the trees are also highly compatible to each other.

Identification of Character Cliques

We next selected cliques of mutually compatible characters by performing a cluster analysis (UPGMA in Paup Version 4.0b10) of the dissimilarity matrix. The rationale behind this was that sets of mutually compatible characters represent instances of potentially concerted convergence. The analysis yielded two larger cliques of characters (Figure 6). We ran separate parsimony analyses with these two cliques (size 48 and 26 characters) in TNT using 1000 heuristic searches with random addition of taxa and TBR branch swapping (Figure 7a+b). Separate analyses of the characters in cliques 1 and 2 both yielded incongruent results to those obtained with both the molecular data and the entire morphological character set. In fact, these trees are incompatible with classical and generally accepted concepts like the monophyly of Pterygota, Holometabola, Odonata, and Ephemeroptera. We thus conclude that the characters in these two cliques represent instances of concerted convergence. If we take this into account, the amount of convergence in the remaining characters (65 characters; excluding cliques 1 and 2) should be substantially lower. A tree calculated from the remaining characters (henceforth referred to as character set 3) is compatible with the Palaeoptera hypothesis, the monophyly of Odonata, Ephemeroptera, Xenonomia (Grylloblattodea + Mantophasmatodea), and Phasmatodea. The second major clade shows a sistergroup relationship between Zoraptera and Acercaria + Holometabola and Plecoptera as sister to this assemblage.

Clique Composition

Cliques 1 and 2 account for 53% of the original characters (clique 1 = 35%; clique 2 = 18%). We further analysed the character composition concerning morphological units in cliques 1 and 2 and character set 3 (Figure 6). The morphological data matrix was divided into character groups representing mouthparts (labrum, mandibles, maxillae, labium), head capsule, tentorium, antennae and hypopharynx/pharynx. Finally, the percentage of characters in each character group in both of the cliques and character set 3 was calculated (Figure 8).

Clique 1 contains a high number of head capsule characters (25%) while mandibular characters are underrepresented (2%). In contrast, mandibular characters group together in clique 2 (19%), which also contains more tentorial characters (19%). Only two characters of the head capsule (8%) are contained in this clique.

The remaining characters (set 3) contains more hypopharyngeal/pharnygeal and antennal characters relative to the complete dataset. Again head capsule characters are underrepresented (8%).

Discussion

Our study demonstrates that at least two sets of cephalic characters - clique 1 and 2 - are apparently affected by concerted convergence and are therefore potentially biasing tree inference. Trees derived from the remaining morphological characters support the clade Palaeoptera,

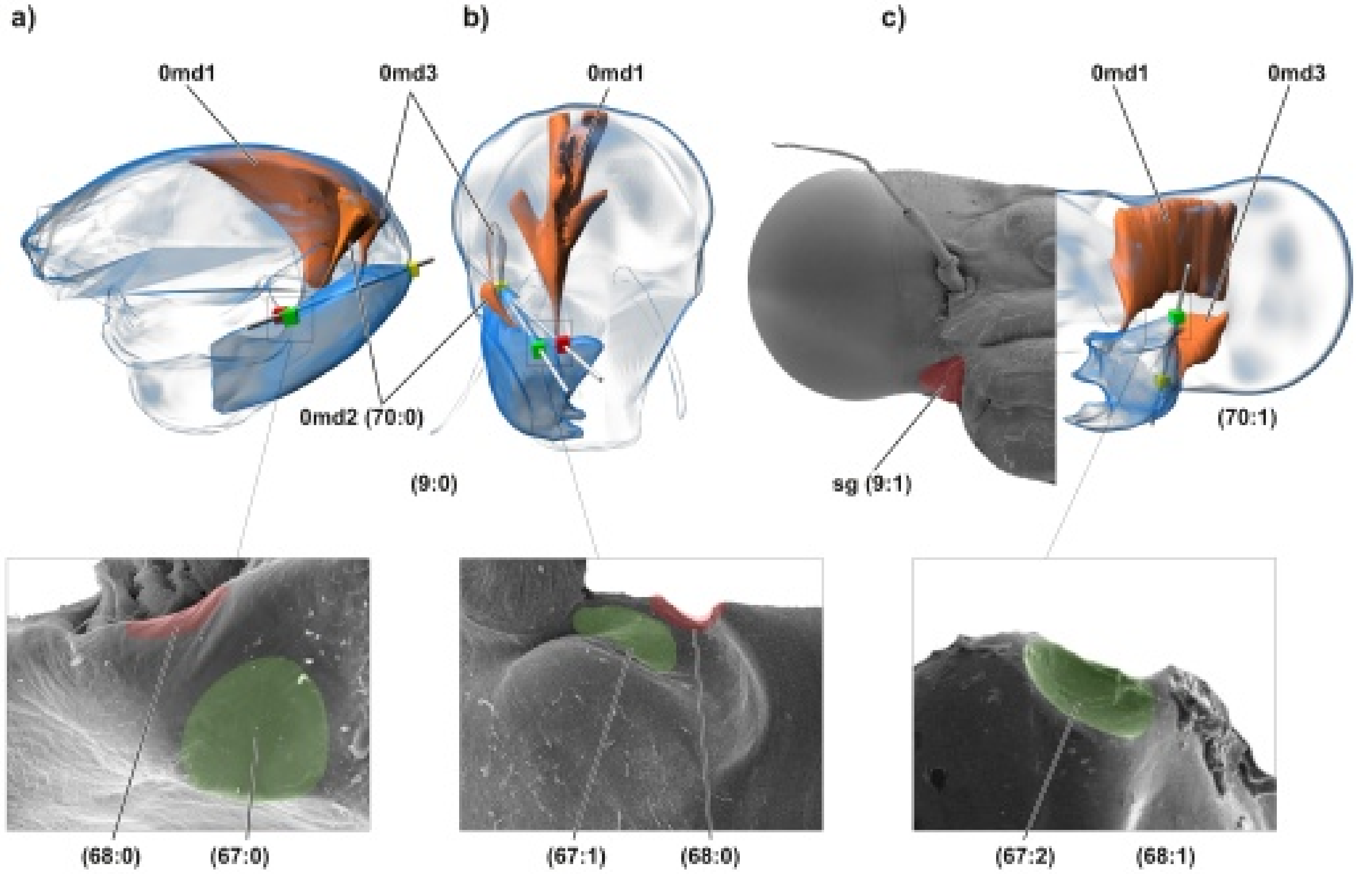

Figure 9 3D reconstructions and SEM micrographs of a part of the problematic head characters which clustered in clique 2. Character numbers and states in brackets, heads and mouthparts in frontal view. Red, green and yellow cubes indicate the location of the mandibular articulation complexes, grey bars the assumed rotation axis of the mandible. a) *Tricholepidion gertschi* (Zygentoma); b) *Siphlonurus lacustris* (Ephemeroptera); c) *Lestes virens* (Odonata). The corresponding character states for Neoptera are identical to the situation in Odonata. Character 9: Subgenal ridge (sg): (0) absent; (1) present; Character 67: Anterior mandibular joint: (0) cuticular hardening on the mandibular depression; (1) channel-joint (2) ball-and-socket joint; Character 68: Anterolateral part of the anterior mandibular articulation (paratentorial joint): (0) present; (1) absent; Character 70: Musculus craniomandibularis externus anterior (0md2): (0) present; (1) absent. 0md1: Musculus craniomandibularis internus; 0md3: Musculus craniomandibularis externus.

whereas the molecular data partly support the Chiastomyaria concept, an incongruence that will be evaluated in the following.

It is well known that molecular data are not free of homoplasy. Phylogenetically independent shifts in base composition can be considered as cases of concerted convergence. Holland et al. (2010) used a tree based on molecular data as a null hypothesis to identify candidate morphological characters with a high excess index on the molecular trees. We also tested the morphological data against the molecular trees (see figure 4), but took a different approach afterwards by including all morphological data into the subsequent analyses. This was necessary as the characters relevant in the context of the Palaeoptera problem (subgena [8], anteclypeus [17], antennal configuration [27], antennal circulatory organs [38], mandibular [66, 67, 69] and lacinial structure [83]) fit well on the molecular trees. These characters change only once or twice (depending on the underlying tree) at the basal-most pterygote node. This is fundamentally different to the situation described in Holland et al. (2010), where the relationships of nine groups of water birds were explored. Characters in the Holland et al. (2010) study had higher excess values than those we evaluated here. We also tested the exclusion of characters that fit well on the molecular trees (those with an excess of 0 or 1), but this eroded the signal for the deep pterygote nodes completely (see electronic supplement (ES) 7).

Moreover, by retaining all morphological characters we rule out the selection of high-excess characters based on a questionable molecular hypothesis; selecting only high-excess characters could heavily influence clique formation and clique composition.

Based on the present analysis, the mutually compatible characters of cliques 1 and 2 are indicative of concerted convergence. Convergence is a well known and frequent pattern in insect evolution (Carapelli et al., 2007; Grimaldi, 2001). Concerted convergence - the congruent evolution of entire character groups in relatively distantly related taxa - can give rise to biased inference and/or inflated tree support, ultimately resulting in misleading phylogenies (Givnish et al., 2006; Patterson and Givnish, 2002; Sanderson and Doyle, 1992).

The detection of cliques of characters is straightforward but the interpretation of concerted convergence is a decision based on additional information.

In our case we showed that character cliques 1 and 2 support highly implausible relationships and represent biased subsets of the total character matrix. For example, analysis of clique 1 resulted in a comb-like tree with Zoraptera and Holometabola as the first split after Archaeognatha. Clique 2 shows some more plausible relationships with Zygentoma as sistergroup to Pterygota and monophyletic Ephemeroptera as sistergroup to the clade Neoptera (=Chiastomyaria). However, clique 2 characters support implausible relationships inside Neoptera, for instance Zoraptera as sistergroup to all other Neoptera, and Odonata as sister to Acercaria deeply nested inside Neoptera. All other resulting relationships within Neoptera are morphologically equally implausible and not encountered in any literature sources.

Based on these results, we interpret that the signal within both cliques is affected by concerted convergence. Consequently, these characters should be down-weighted or omitted in future tree reconstructions.

Several additional conclusions follow from this result. First, the dissimilarity score of Holland et al. (2010) indeed helped to identify patterns of concerted convergence. Second, character set 3 potentially represents a data set with a better signal-to-noise ratio in the morphological data. These characters as well as the characters of both cliques should be carefully investigated to assess their potential phylogenetic signal.

Clique composition (Figure 8) shows that especially characters of the head capsule, tentorium, and mandible are prone to concerted convergence. Characters of the head capsule are mainly related to ridges or sutures (37% of the characters in the complete matrix) and the general shape of the head (42%). All characters related to ridges and sutures (6-11) appear in the cliques (character 9 in clique 2, the rest in clique 1). Head shape characters (1, 5, 12) cluster also in clique 1. The phylogenetic value of ridges and sutures has been a matter of controversy (Beutel et al., 2008; Klass and Eulitz, 2007; Kristensen, 1981; Strenger, 1952). Apparently, their possible correlation with the general head shape is still not well understood. Staniczek (2000, 2001) assumed that the presence of the subgenal ridge is a synapomorphy of Metapterygota. In conjunction with the formation of a subgenal ridge, he considered a lateral shift and broadening of the anterior tentorial arms as further synapomorphies and as responses to enhanced forces resulting from reduced degrees of freedom at the mandibular base (anterior articulation modified as ball-and-socket joint in Odonata + Neoptera). However, if the Palaeoptera hypothesis is correct the subgenal ridge (9), the anterior ball-and-socket joint (67), and the tentorial modifications are independent developments of Odonata and Neoptera. This scenario also implies the independent reduction of the paratentorial joint (68) and the M. craniomandibularis externus anterior (70), which are both present in Ephemeroptera (Figure 9). All these characters are represented in the morphological data matrix (9, 67, 68, 70) and they group together in clique 2. Based on the present analysis, it appears highly advisable to treat the four characters as one (or to exclude three of them) to prevent a hidden weighting of structural transformations associated with the evolution of the anterior mandibular articulation. Likewise, the fusion of the anterior and posterior tentorium (48, set 3) and the reduction of all intratentorial muscles (57-60; clique 2) are closely correlated. This set of muscles should therefore be treated similarily as one character in future analyses. The tentorial fusion already accounts for the entire complex of structural modifications.

In this study, we use a character matrix which is based on widely accepted and established homology hypotheses. However, the concerted convergence approach applied here may also point towards non-homology of characters thereby exposing putatively homologous character states as non-homologous. The application of Holland et al's (2010) convergence assessment on the Palaeoptera problem, however, is not completely unproblematic. It has been shown that exclusion of characters obviously related to each other may not remove all the homoplasy involved (Worthy and Lee, 2008). Formal convergence assessments also do not release investigators from the task of working out primary homology hypotheses for each morphological character. No automated procedure can determine if, for instance, the lacinia mobilis is homologous across Crustacea, Myriapoda and Hexapoda (Richter et al., 2002). Thus, the principal responsibilities of evolutionary morphologists regarding character identification and homology assessment remain untouched by the concerted convergence approach. Nevertheless, the analytical framework tested here is a useful step towards downweighting (or removing) convergent characters using a formal procedure.

The corroboration of Palaeoptera by our convergence assessment does not settle the deep-rooted problem of basal splits in Pterygota. The dataset contains only cephalic characters and the taxon sampling is limited. However, it is now evident that in future studies addressing this issue, attention should be paid to the evolutionary dependence of characters of the head capsule and mandibles. Character systems that seem to be less problematic are those related to the antennae, labrum, maxillae, labium, hypopharynx and pharynx. For a better understanding of character evolution related to the early pterygote splits, it will also be necessary to obtain more detailed and well documented data for the two key taxa, Zygentoma and Archaeognatha.

Funding

BRH acknowledges the Australian Research Council grant FT100100031.

Acknowledgements

We thank the lab members of the ZFMK for their support in the field and lab. Karen Meusemann is thanked for support in setting up the molecular analyses on an external computer cluster. Furthermore, we acknowledge Viktor Achter and Volker Winkelmann for help with ML analyses on the CHEOPS, HPC cluster at the RRZK, University of Cologne, Cologne, Germany, http://rrzk.uni-koeln.de/cheops.html. The anatomy of species was mainly investigated with SR-microCT done at DESY (Hamburg, Germany) and PSI (Villigen, Switzerland) through grants I-20080169, I-20090211 (both DESY) & 20100137 (PSI) which is gratefully acknowledged. Sincere thanks also go to Felix Beckmann, Fabian Wilde (HZG, Geesthacht), Sebastian Thieß, and Wolfgang Drube (DESY, Hamburg). Felix Beckmann, Fabian Wilde (both HZG), Marco Stampanoni, Peter Modregger and Rajmund Mokso (all PSI) provided valuable support at the beamlines.

6 Contributions to the phylogeny of Anisoptera from SRµCT-data of internal head morphology

Contributions to the phylogeny of Anisoptera from SRµCT-data of internal head morphology.

Contributions to the phylogeny of Anisoptera from SRµCT-data of internal head morphology. Article published in the HASYLAB annual report 2011

Alexander Blanke[1], Bernhard Misof[2], and Felix Beckmann[3]

[1] Zoologisches Forschungsmuseum Alexander Koenig, Adenauerallee 160, 53113 Bonn, Germany
[2] Biozentrum Grindel & Zoologisches Museum, Martin-Luther-King Platz 3, 20146 Hamburg, Germany
[3] GKSS-Research Centre, Max-Planck-Str. 1, 21502 Geesthacht, Germany

This is the author’s version of a work originally published in the HASYLAB annual report 2011

Background

Experiments at DESY HASYLAB BW2 are carried out in the framework of an extensive project on the phylogeny of selected arthropod groups. Besides elucidating the possibilties of SRµCT for our studies, we were aiming at a muscle equipment study of selected damselfly (Zygoptera) and dragonfly (Anisoptera) heads in a first step. This study worked also as an indicator whether µCT studies are suited to reveal morphological details at the family level inside hexapods. In subsequent projects covering a broader taxon scale we aim to extend our scope to the phylogeny of the four major arthropod groups (see our other HASYLAB report for more details). The morphological data we have gathered at HASYLAB so far will be incorporated into a data matrix for subsequent phylogenetic analysis of odonatan internal head anatomy.

Material and specimen preparation

Adult specimens of Aeschnidae, Libellulidae, Gomphidae, Cordulidae, Lestidae and Calopterygidae were freshly collected into Bouin's solution (Dubosq-Brasil), transferred to 70% EthOH after a few days and subsequently critical point dried to avoid image noise due to fluids influencing the scan process. For maximum field of view appendages like antennae were cut off. Specimens were mounted on metal holders with superglue and acclimatised in the scan chamber to avoid any movements due to unintended specimen movement

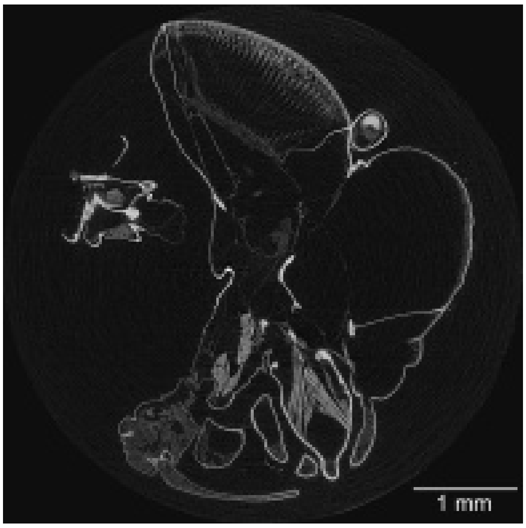

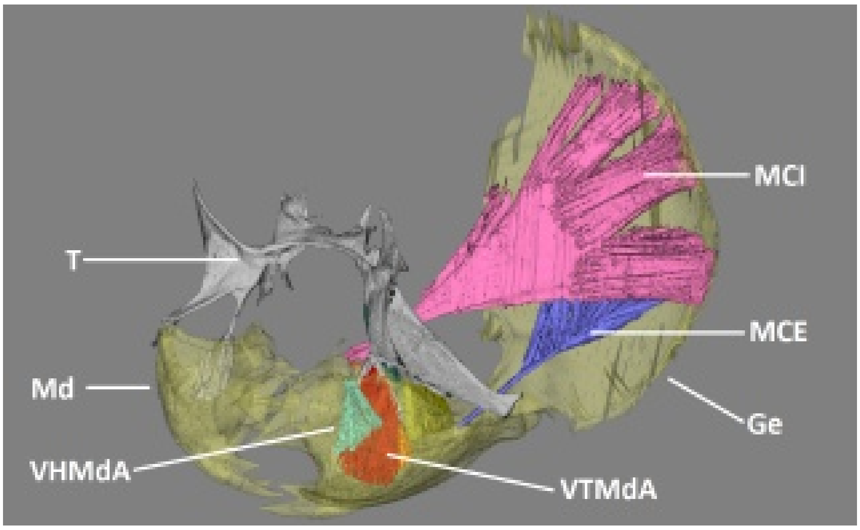

Figure 1: Sympetrum sanguineum (Hexapoda: Odonata) head. Parasagittal image at height of the right mandible. Image from DESY HASYLAB beamline BW2. Scantime: 3 hours for the whole head. Figure 2: Part of the mandible musculature of Sympetrum sanguineum (Odonata) reconstructed from SR-microCT images. Unpublished prelimnary data. Scantime: 3 hours; reconstruction time: ca. 8 hours; voxelsize: 2,34 µm (isotropic voxels). Ge Gena; MCI Musculus craniomandibularis internus; Md Mandible; MCE Musculus craniomandibularis externus; T Tentorium;; VHMdA ventral hypopharyngo-mandibular adductor; VTMdA ventral tentorio-mandibular adductor. Muscles named according to Kéler (Kéler 1963).

or temperature changes.

Results

SRµCT of dragonfly heads resulted in image data of excellent quality. Besides reconstruction of hard parts like the body wall, apodemes and tentorial structures, it was possible to reconstruct and discern muscles, tendons, nerves and even membranes of the tracheal system from each other (Fig 1). Due to the density dependent graytone range of each tissue we were able to reconstruct structures semi-automatically sparing the time consuming step of tissue designation by hand in each image. This also aided to the resolution of volume rendering yielding more realistic and precise structures for the final 3D-image (Fig 2).

Outlook

We plan to use SRµCT extensively in the future for our broader approach to arthropod relationships. Our taxon sampling will encompass Chelicerata, Crustacea, Hexapoda and “Myriapoda”. In our opinion SRµCT is THE method to receive information on very different structures at the same time. For example it is possible to infer muscles as well as the inervation in one methodological step (albeit information on sensoric and motoric neurons is lacking). Unlike cLSM larger non-transparent structures are scanable. Information retrieval is greatly reduced compared to classic histological work or micro-taxidermy.

7

The head anatomy of *Epiophlebia superstes* (Odonata: Epiophlebiidae)

The head anatomy of *Epiophlebia superstes* (Odonata: Epiophlebiidae)

The head anatomy of *Epiophlebia superstes* (Odonata: Epiophlebiidae)

Alexander Blanke [1,*] , Felix Beckmann[2] and Bernhard Misof[1]

[1] Zoologisches Forschungsmuseum Alexander Koenig, Adenauerallee 160, 53113 Bonn, Germany
[2] Institute of Materials Research, Helmholtz-Zentrum Geesthacht, Max-Planck-Str. 1, 21502 Geesthacht, Germany
* Corresponding author e-mail adress: blanke@uni-bonn.de

This is the author's version of a work originally published in the journal Organisms, Diversity & Evolution (2012) DOI 10.1007/s13127-012-0097-z

Abstract

The relic dragonfly family Epiophlebiidae is recovered as sistergroup of Anisoptera (=Epiprocta) by most molecular and morphological analyses. However, in a recent study it was placed as sistergroup of Cordulegastridae. In another contribution numerous affinities to Zygoptera in the morphology of the ovipositor and the egg laying behaviour were pointed out. Here we present a detailed study of the head of *Epiophlebia superstes* with a focus on its internal structures. Compared to the last detailed literature account three additional mandibular muscles were discovered as well as additional buccal and pharyngeal muscles. The results are compared to features of Zygoptera and Anisoptera. A preliminary phylogenetic analysis of characters of the head confirms the sistergroup relationship of Epiophlebiidae and Anisoptera.

Introduction

The dragonfly *Epiophlebia superstes* is one of three species of the relict family Epiophlebiidae (Odonata: Anisoptera). These species are restricted to the oriental region with *E. superstes* occurring only in Japan and *E. laidlawi* found only in the Himalaya region. The third species – *E. siniensis* - was discovered very recently in China in a habitat similar to that of the other two species (Li et al. 2012).

Molecular as well as morphological studies consistently retrieve extant species of Epiophlebiidae as sistergroup of all other extant anisopteran families (Bybee et al. 2008; Misof et al. 2001; Lohmann 1996; Bechly 1996; Carle 1982; Trueman 1996; Gade et al. 2011), with the exception of Dumont *et al.* (Dumont et al. 2010) who recovered Epiophlebiidae as the sistertaxon to Cordulegastridae.

Due to its assumed phylogenetic position species of this family is crucial in comparative studies. Epiophlebiidae exhibit zygopteran as well as anisopteran features: like in Zygoptera the shape of the fore- and hindwings is similar and the wings are held back over the abdomen at rest. Anisopteran features are the shape of the abdominal tergites, the presence of a transverse carina, and the morphology of the larva (except the pronymph) (see Asahina 1954, page 119 for a complete overview).

Due to its specific phylogenetic position the morphology of *E. superstes* has been intensively investigated (Asahina 1954; Ando 1962). A recent detailed account of the ovipositor of *E. superstes* revealed numerous affinities with Zygoptera, especially concerning internal features, and similarities of the egg laying behaviour were also pointed out (Matushkina 2008). The author also found additional muscles and characteristic muscle branches compared to those described in the earlier study of Asahina (1954).

Despite of intensive investigations, several morphological character complexes have not been adequately described yet, especially internal structures, as for instance the muscles of the head appendages.

Thus, the aim of the present study is a detailed description of the head morphology with a special focus on the musculature. The characters will be evaluated with respect to their implications for the phylogenetic placement of Epiophlebiidae within Odonata.

Material and Methods

We used freshly collected specimens of *E. superstes*. They were fixed in Bouin (Romeis 1989) for several days. Afterwards, specimens were washed several times in 70% EthOH and also stored in ethanol. The anatomy was investigated using synchrotron micro-Computer Tomography (SR-microCT) (Betz et al. 2007). Prior to scanning, the sample was critical point dried (CPD) (Model E4850, BioRad) to avoid shrinking artefacts and mounted on specimen holders. Scanning was performed at the German electron synchrotron accelerator (DESY, Hamburg, Germany) (Beckmann et al. 2008) and at the Paul Scherrer institute (PSI, Villigen, Switzerland) TOMCAT beamline with a stable energy beam of 8 keV. Subsequent segmentation and rendering was accomplished with Reconstruct (Fiala, 2005) and Blender (blender.org). Both software packages are distributed under the general public license (GPL). Final tables and figures were edited with GIMP, Inkscape and Scribus (all GPL).

A 3D model of the head of *E. superstes* is available (Online resource 1 [OR 1]), which facilitates the identification of internal structures. The underlying program "Blender" can be downloaded free of charge under the GPL license from www.blender.org. A manual can be found at http://wiki.blender.org/index.php/Doc:Manual.

For scanning electron microscopy (SEM) the specimen was transferred in a series of steps into 100% ethanol, dried at the critical point (Model E4850, BioRad), and sputter coated (Model Anatech Hummer VII). Microscopy was performed on a Hitachi S-2460N using a new type of rotatable specimen holder (Pohl 2010). We consistently use the term "suture" for ecdysial cleavage lines (DuPorte 1946, 1957; Snodgrass 1947) and "ridge" for any cuticular strengthening lines or ridges as suggested by Wipfler et al. (2011; see also Snodgrass 1935, 1947; Strenger 1952). We avoid the term "sulcus" completely since this refers to a fissure between bones. Muscles are named after the nomenclature introduced by Wipfler et al. (2011), structural descriptions follow Seifert (1995).

Results

External head capsule

The orthognathous head is strongly sclerotised and the surface is covered with a moderately dense vestiture of long setae (Fig. 1). It is slightly compressed anterio-posterad and dominated by the large, strongly convex, laterally placed compound eyes. They face almost completely forward since the occipital region covers the entire backside of the head (Fig. 1b). They are enclosed by a complete but barely recognisable circumoccular ridge which continues internally as a complete circumoccular apodeme encircling the optic lobes. Seen from above, the eyes appear drop-shaped with tips not touching each other. They are connected by an occipital bar. Directly anterad the occipital bar lies the occipital ridge. It proceeds posterad the lateral occelli, touches the antennal ridge and is confluent with the dorsal tentorial pits directly posterad the antennal base.

The lateral occelli lie anterad the occipital ridge at the level of the dorsal tips of the compound eyes. They are enclosed in the groove formed between the compound eyes and the grossly enlarged vertex which protudes between the three occelli. The vertex is formed like a semiparabolic “dish” oriented ventrally with its “opening” at a 45° angle to the dorsoventral axis (Fig. 1a). Its dorsal part is moderately indented by the coronal suture (cs, Fig. 1b) which continues anterad over the edge of the vertex “dish” and splits after passing the edge into the frontal sutures (fs, Fig. 1a). The frontal sutures continue parallel to the dorsal edges of the vertex and obliterate at its lateral edges. Consequently they do not reach the antennal bases.

The occipital region (oc, Fig. 1e) forms the major part of the backside of the head and bears the cephalic part of

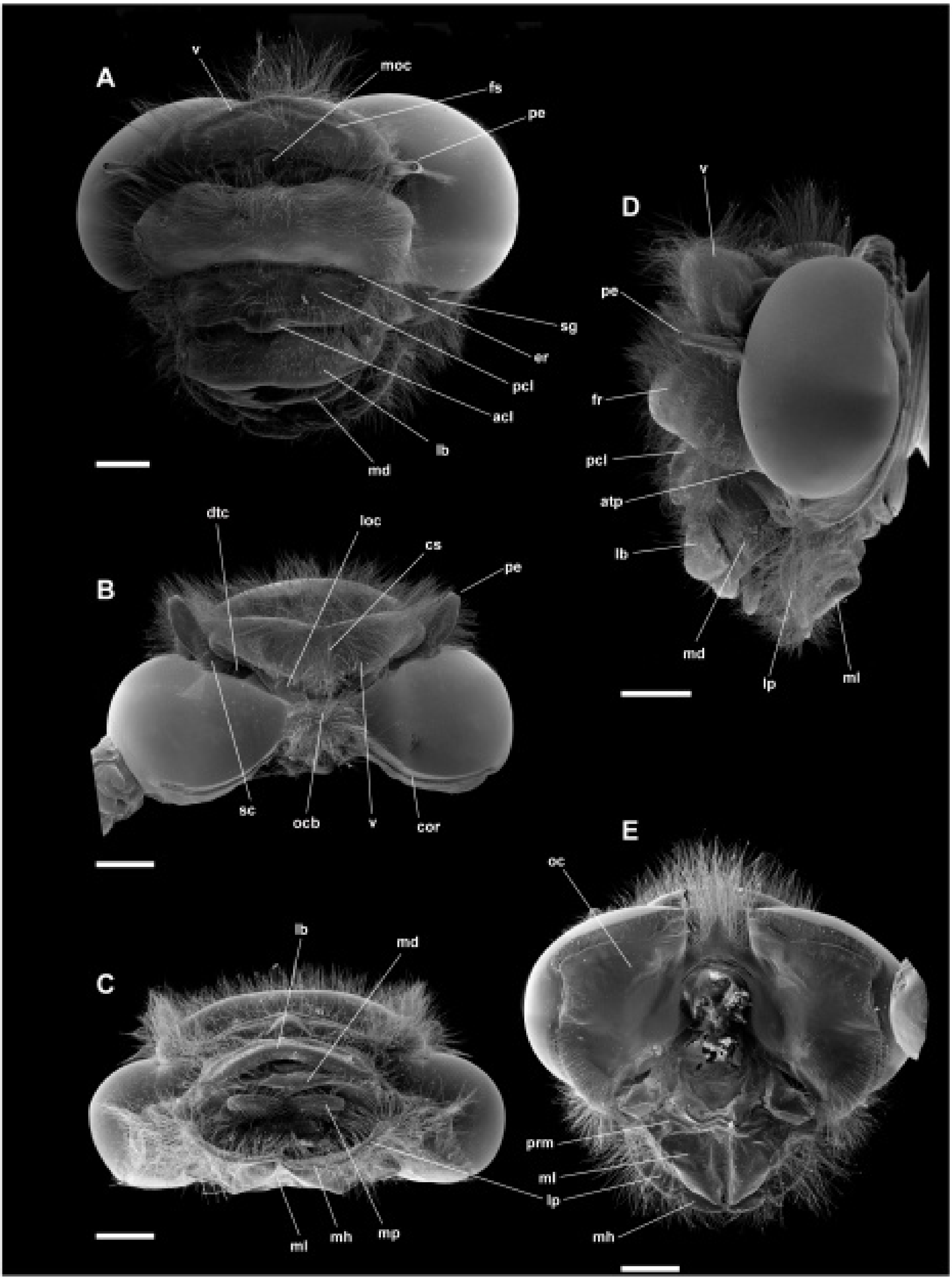

Fig 1 SEM micrographs of the head of *E. superstes* A, frontal view; B, dorsal view; C, ventral view; D, lateral view; E, posterior view. Abbreviations: acl, anteclypeus; atp, anterior tentorial pit; cor, circumoccular ridge; cs, coronal sulcus; er, epistomal ridge; fr, frons; fs, frontal sulcus; lb, labrum; loc, lateral ocellus; lp, labial palpus; md, mandible; mh, moveable hook; ml, median lobe; moc, median ocellus; mp, maxillar palpus; oc, occiput; pcl, postclypeus; pe, pedicellus; prm, prementum;sc, scapus; sg, subgena; v, vertex. Scale bars: 1 mm

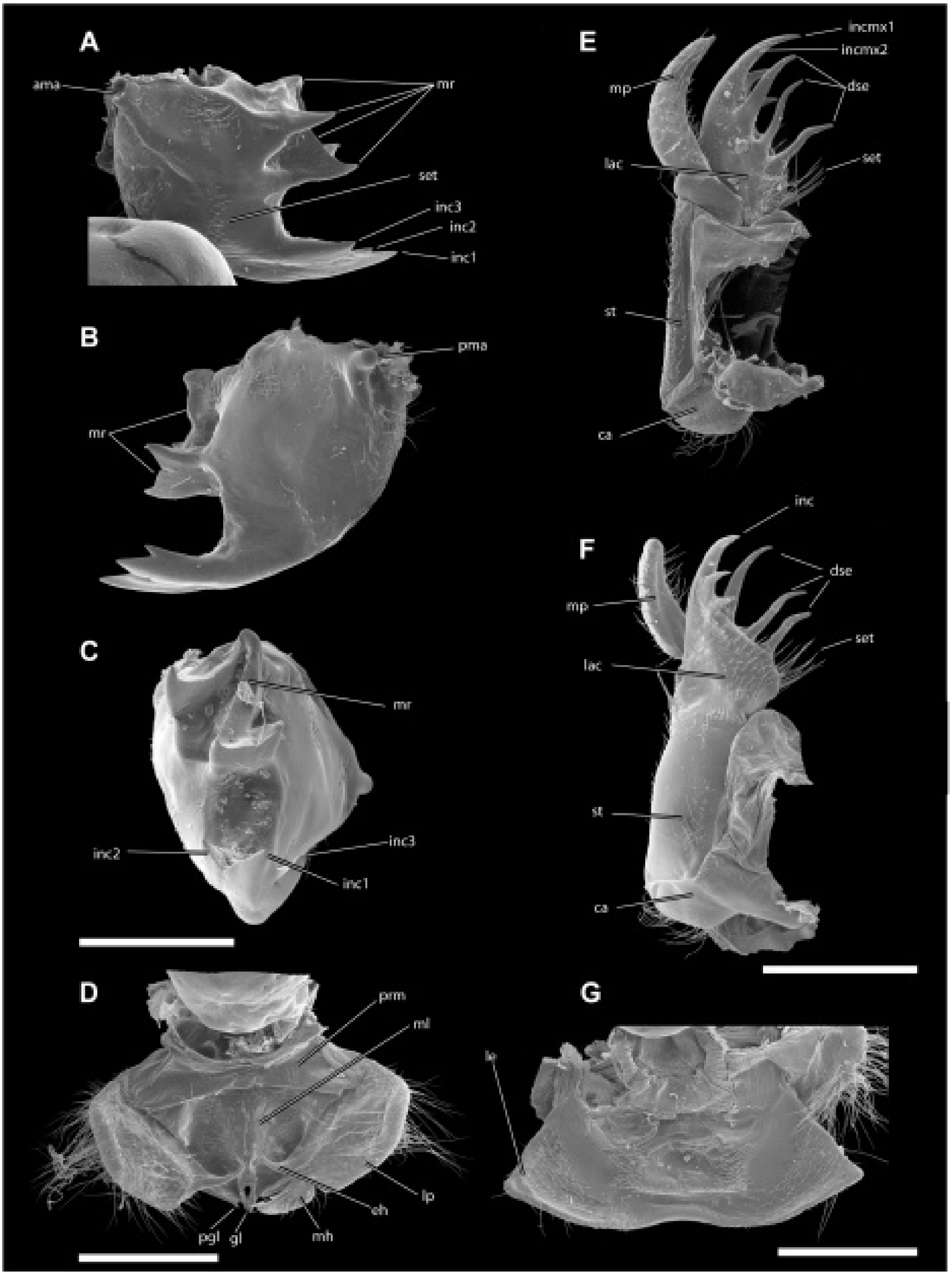

Fig 2 Mouthparts of *E. superstes*. SEM micrographs. A, mandible frontal view; B, mandible posterior view; C, mandible lateral view; D, labium dorsal view; E, maxilla dorsal view; F, maxillae ventral view; G, labrum posterior view. Abbreviations: ama, anterior mandibular articulation; ca, cardo; dse, dentisetae; eh, end hook of labial palp; gl, glossa; inc1, frist incisivus of mandible; inc2, second incisivus of mandible; inc3, third incisivus of mandible; incmx1, frist incisivus of maxilla; incmx2, second incisivus of maxilla; lac, lacinia; le, lateral extensions of labrum; lp, labial palp; mh, moveable hook of labial palp; ml, median lobe; mp, maxillar palp; mr, mesal ridge; pma, posterior mandibular articulation; pgl, paraglossa; prm, prementum; set, setae; st, stipes. Scale bars: 1 mm

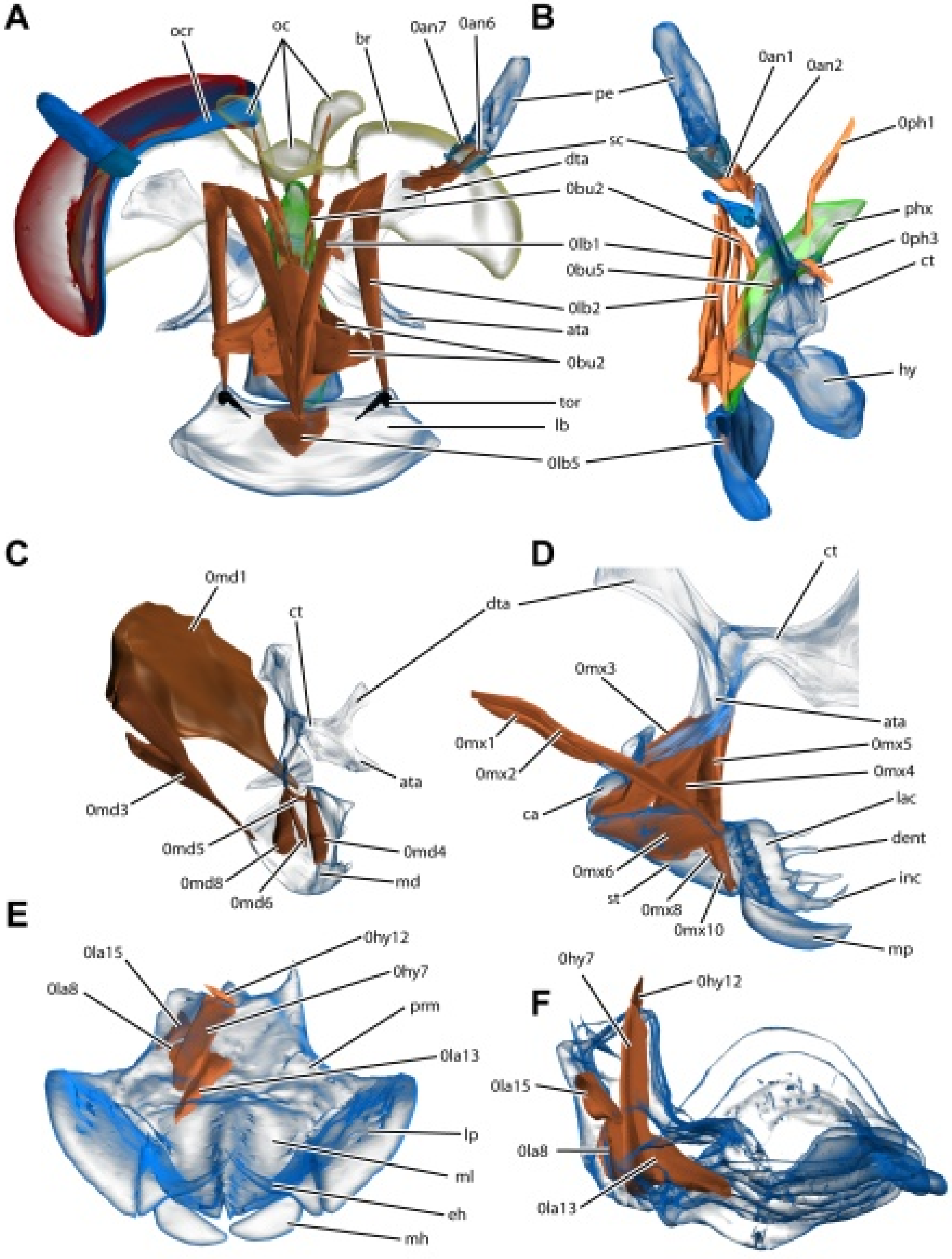

Fig 3 Head muscle system of *E. superstes*. A, frontal view with all labral and pharyngeal muscles; B, the same muscles in lateral view; C, frontolateral view of the mandibular muscle system; D, frontal view of maxillar muscle system; E+ F, frontal and lateral view of labial muscle system. Blue, chitinous structures (tentorium, mouthparts, ridges/sutures); orange, muscles; green, digestive tract; red, eye. Abbreviations: ata, anterior tentorial arm; br, brain; ca, cardo; ct, corpotentorium; dent, dentisetae; dta, dorsal tentorial arm; eh, end hook; hy, hypopharynx; inc, inscisivus; lac, lacinia; lb, labrum; lp, labial palpus; md, mandible; mh, moveable hook; ml, median lobe; mp, maxillar palpus; oc, ocellus; ocr, occipital suture; pe, pedicellus; phx, pharynx; prm, prementum; sc, scapus; st, stipes; tor, tormae

the arresting system, which is responsible for the support and fixation of the head in different situations (see Gorb 1999). The arresting system is composed of trichoid sensillae and sparsely distributed microtrichia. The part of the occipital region directly posterad the occipital bar bears numerous long, upwards directed setae (Fig. 1e).

The postocciput is small and divided into three parts: a half moon shaped dorsal part and two lateral indented parts on both sides of the oval foramen occipital, directly above the posterior tentorial pits. The postoccipital ridge encircles the postoccipital parts but does not reach the posterior tentorial pits.

The large trapezoid clypeus is divided into an ante- and postclypeus. Both regions are heavily sclerotised (Fig. 1e). The anteclypeus is one third as long as the postclypeus, which encloses it on both sides. Both parts face anteriorly. A strong epistomal ridge (=transverse frontoclypeal strengtheneing ridge) separates the frons from the postclypeus. The frons is globular, protuding anteriorly, and transversely elongated when seen in frontal view. Together with the enlarged vertex it forms a groove with the middle occellus at its base (moc, Fig. 1a). The anterior tentorial pits are continous with the epistomal and pleurostomal ridges. The pleurostomal and hypostomal ridge (=subgenal ridge) are not continous. The pleurostomal ridge is confluent with the circumoccular ridge. The hypostomal ridge arises posterad the posterior tentorial pits, passes the maxillary articulation, and bends towards the posterior mandibular articulation with which it is confluent.

Cephalic endoskeleton

The anterior tentorial arms ("ata", Fig. 3c) are short, massive and twisted. Wing-like protuberances emerge at their ventral base and extend into the lumen of the mandibles. They serve as attachment areas for mandibular muscles (0md6 and 0md8, Fig. 3c). The dorsal tentorial arms (dta, Fig. 3a) also originate from the basal part of the anterior arms. They are massive, not twisted, and they merge with the head capsule directly dorsad the antennal origin. The attachment points are externally recognizable as dorsal tentorial pits (dtp, Fig. 1b). All antennal muscles originate from the dorsal arms. The corpotentorium (=tentorial bridge; ct, Fig 3c) is compact and cylinder-shaped. The posterior tentorial arms are very short and originate from the head capsule, directly proximad the articulation of the cardo. Short but thick apodemes, the trabeculae tentorii, originate from the ventral side of the posterior tentorial pits. They serve as attachment areas for the tentoriostipital muscles 0mx4 and 0mx5.

Musculature (Fig. 3; OR 1): M. tentoriofrontalis posterior (**0te1**) – absent. M. tentoriofrontalis anterior (**0te2**) – absent. M. tentoriofrontalis dorsalis (**0te3**) – absent. M. posteriotentorialis (**0te4**) – absent. M. tentoritentorialis longis (**0te5**) – absent. M. tentoritentorialis brevis (**0te6**) – absent.

Labrum

The anteriorly rounded, parabolic labrum almost completely covers the mandibles and is movably connected with the slightly rounded anterior anteclypeal margin by a membranous fold. It bears a vestiture of setae (Fig. 1). The labrum is trapezoid in shape when seen in frontal view and laterally strongly extended, so that a “spike” is present on both sides. The labrum is ventrally wider than dorsally.

Musculature (Fig. 3; OR 1): M. frontolabralis (**0lb1**) – broad, appearing unpaired over almost its entire length, but with paired subcomponents distinguishable posteriorly; O: mesally at the interantennal ridge; I: external wall of the labral base. M. frontoepipharyngalis (**0lb2**) – O: laterad of 0lb1 at the interantennal ridge; I: posterolateral edge of labrum, on short tormae. M. epistoepipharyngealis (**0lb3**) – absent. M. labralis transversalis (**0lb4**) – absent. M. labroepipharyngalis (**0lb5**) – O: ventral of insertion point of 0lb1, median at the anterior labral wall; I: median at the dorsal part of the epipharyngeal wall. M. labrolabralis (**0lb6**) – absent.

Antenna

The short antennae are composed of scapus, pedicellus and three flagellomeres. The antennal base is strongly protuding from the head capsule and surrounded by a complete circumantennal ridge. An interantennal ridge, an antennifer and an antennal circulatory system, frequently ecountered in other insects, are absent. The scapus is short, cylindrical and thick, and the pedicellus three times as long. It is dorsoventrally flattened but as thick as the scapus and densely covered with long hairs only along the lateral edges. The flagellormeres are thin; the first one is half as long as the pedicel, the second one one third of the latter, and the third one half as long as the second.

Musculature (Fig. 3; OR 1): M. tentorioscapalis anterior (**0an1**) – weakly developed; O: mesal wall of the dorsal tentorial arm just below the connection to the head, with a punctual origin; I: anteriorly on the scapal base. M. tentorioscapalis posterior (**0an2**) – weakly developed; O: directly dorsad 0an1, with a punctual origin; I: posteromesally on the scapal base. M. tentorioscapalis lateralis (**0an3**) – absent. M. tentorioscapalis medialis (**0an4**) – absent. M. frontopedicellarius (**0an5**) – absent. M. scapopedicellaris lateralis (**0an6**) – O: anterolaterally from the scapal base; I: anterolaterally on the base of the pedicellus; M. scapopedicellaris medialis (**0an7**) – O: mesally from the scapal base; I: posteriorly on the base of the pedicellus; M. intraflagellaris (**0an8**) – absent. M. interampularis (**0ah1**) – absent. M. ampulloaortica (**0ah2**) – absent. M. ampullopharyngealis (**0ah3**) – absent. M. ampullofrontalis (**0ah4**) – absent. M. frontofrontalis (**0ah5**) – absent.

Mandibles

The articulation of the heavily sclerotized, slightly asymmetric mandibles is of the dicondylic (two articulations) ball-and-socket type (Fig. 2a+b). The mandibular shape is triangular in dorsal view. The anterior mandibular articulation (ama, Fig. 2a) is a socket while the posterior one (pma, Fig. 2b) is a distinct knob. The gnathal edges of the left and right mandibles are almost symmetrical. Each mandible bears 3 incisivi and a z-shaped mesal edge formed by 4 strongly sclerotised prominences connected by sharp ridges (mr, Fig. 2a, b, c). Additionally, the mandible bears several rows of setae on the anterior surface.

Musculature (Fig. 3; OR 1): M. craniomandibularis internus (**0md1**), by far the largest muscle of the head – O: large parts of the posterodorsal and posterolateral areas of the head capsule; I: adductor tendon. M. craniomandibularis externus anterior (**0md2**) – absent. M. craniomandibularis externus posterior (**0md3**) – O: laterally from the head capsule, composed of two major bundles, one of them originating below 0md1 and the other one above it; I: abductor tendon. M. hypopharyngomandibularis (**0md4**) – O: suspensorial bar of the hypopharynx; I: anterior inner wall of the mandible. M. tentoriomandibularis lateralis superior (**0md5**) – O: posterior side of the anterior tentorial arm; I: posterior edge of the mandible between the insertion of 0md1 and the primary condylus. M. tentoriomandibularis lateralis inferior (**0md6**) – well developed, two parallel bundles, – O: anterior tentorial arm with a tendon; I: anterior inner wall of the mandible ventrad 0md4. M. tentoriomandibularis medialis superior (**0md7**) – absent. M. tentoriomandibularis medialis inferior (**0md8**) – O: anterior tentorial arm sharing the tendon with 0md6; I: posterior inner wall of the mandible.

Maxillae

The maxillae are long and slender. The undivided triangular cardo is clearly separated from the stipes by a well-developed cardostipital ridge. The stipes is a rectangular plate subdivided by the stipital ridge into a narrow basistipes and a much larger mediostipes (Fig. 2e). Its distal part bears an unsegmented palpus covered with setae (mp, Fig. 2e, f). Mesally an oblique ridge separates the sickle-shaped lacinia from the stipes. Its mesal side is armed with a row of long setae, two apical incisivi and five subapical, paramesal dentisetae (dse, Fig. 2e, f). The galea is absent.

Musculature (Fig. 3; OR 1): M. craniocardinalis (**0mx1**), fan shaped – O: ventrolateral area of the head capsule between 0md1 and 0md3; I: basal process of the cardo with a tendon. M. craniolacinialis (**0mx2**), a long and slender muscle with two bundles – O: head capsule, dorsally to 0mx1; I: basal edge of lacinia. M. tentoriocardinalis (**0mx3**), O: ventrolaterally on the corpotentorium; I: inner surface of the cardo; M. tentoriostipitalis anterior (**0mx4**) – O: along the entire ventral side of the corpotentorium and the tentorial ridge, anterad 0mx2; I: broadly on the ventral stipital wall; M. tentoriostipitalis posterior (**0mx5**) – O: ventrolateral side of the corpotentorium, anterior to M. tentoriocardinalis (0mx3); I: basal outer stipital wall , close to the stipitocardinal ridge. M. stipitolacinialis (**0mx6**), well developed, fan-shaped – O: ventrolateral surface of the stipital base; I: proximal base of lacinia. M. stipitogalealis (**0mx7**) – absent. M. stipitopalpalis externus (**0mx8**) – O: lateral inner wall of the stipital ridge; I: posteriorly on the base of the palpus. M. stipitopalpalis medianus (**0mx9**) – absent. M. stipitopalpalis internus (**0mx10**) – well developed; O: lateral inner wall of the stipital ridge; I: anteriorly on the base of the palpus. M. stipitotransversalis (**0mx11**) – absent. M. palpopalpalis maxillae primus (**0mx12**) – absent. M. palpopalpalis secundus (**0mx13**) – absent. M. palpopalpalis tertius (**0mx14**) – absent. Musculus palpopalpalis quartus (**0mx15**) – absent.

Labium

The labium consists of a basal postmentum and a distal prementum (prm, Fig. 1e, Fig. 2d). The postmentum is a rectangular plate and reinforced by heavily sclerotised bars dorsally, ventrally and laterally. The short and broad prementum forms a right angle with the postmentum, which is visible in lateral view. Apically it bears paired 1-segmented palps and paired median lobes. The palps are flat and densely covered with setae, especially on the outer side. Apicomesally they bear a fixed subapical hook (eh). A second movable hook (mh) is present distad of this hook (Fig. 2d). The median lobes are a fusion product of glossae and paraglossae. Mesally the two lobes are connected by a sclerotised stripe which is as long as the lobes themselves. Only the tips of the glossae and paraglossae are visible (Fig. 2d). The palps and median lobes together form a cavity for reception of the hypopharynx and maxillae.

Musculature (Fig. 3; OR 1): M. postoccipitoglossalis medianus (**0la1**) – absent.M. postoccipitoglossalis lateralis (**0la2**) – absent. M. postoccipitoparaglossalis (**0la3**) – absent. M. postoccipitoprementalis (**0la4**) – absent. M. tentoriopraementalis (**0la5**) – absent; M. tentorioparaglossalis (**0la6**) – absent. M. tentorioglandularis (**0la7**) – absent. M. submentopraementalis (**0la8**) – O: medially on the posterior submentum, I: dorsally on the inner wall of the premental base. M. postmentomembranus (**0la9**) – absent. M. submentomentalis (**0la10**) – absent. M. praementoparaglossalis (**0la11**) – absent. M. praementoglossalis (**0la12**) – absent. M. praementopalpalis internus (**0la13**) – O: medially on the prementum; I: mesally on the anterior base of the palpus. M. praementopalpalis externus (**0la14**) – absent. M. praementomembranus (**0la15**) – O: medially on the prementum; I: dorsal membrane of prementum. M. palpopalpalis labii primus (**0la16**) – absent. M. palpopalpalis labii secundus (**0la17**) – absent.

Hypopharynx

The hypopharynx is a ventrally oriented tongue-like structure in front of the prementum. It is weakly sclerotised and bears no anterior or posterior plates. A conspicuous row of setae is present on the lateral surfaces. The oral arm forms a rounded bar directly posterad the anatomical mouth opening. Its serves as attachment site for M. oralis transversalis (0hy9). The loral arm is thin.

Musculature (Fig. 3; OR 1): M. frontooralis (**0hy1**) – absent. M. tentoriooralis (**0hy2**) – absent. M. craniohypopharyngealis (**0hy3**) – absent. M. postoccipitalohypopharyngealis (**0hy4**) – absent. M. tentoriosuspensorialis (**0hy5**) – absent. M. postmentoloralis (**0hy6**) – absent. M. praementosalivaris anterior (**0hy7**) – O: anterolaterally on the prementum; I: ventrally on the sclerotised floor of the anteriormost salivary duct. M. praementosalivaris posterior (**0hy8**) –

Fig 4 Phylogram summarizing the characters of the head supporting a sistergroup relationship of Epiophlebiidae with the rest of Anisoptera

absent. M. transversalis buccae (**0hy9**) – O: oral arm of suspensorial sclerite; I: oral arms of the suspensorial sclerite on the opposite side. M. loroloralis (**0hy10**) – absent. M. lorosalivarialis (**0hy11)** – absent. M. hypopharyngosalivaris (**0hy12**) – O: hypopharyngeal suspensorium; I: suprasalivarial sclerite, close to the salivarial orifice. M. annularis salivarii (**0hy13**) – absent.

Epipharynx

The epipharynx is weakly sclerotised and not subdivided. It bears a single lateral row of setae on both sides. The tormae are formed like an inverted "Y" in posterior view. They serve as attachment areas of M. frontoepipharyngalis (0lb2).

Salivarium and salivary glands

The salivary glands are paired, mesally connected, globular structures. They are located directly ventrad the deutocerebrum and dorsad the salivary receptacle. The paired salivary ducts fuse before opening into the salivary receptacle, which is anteriorly continuous with an unpaired salivary channel. The channel opens into the salivarium posterad the hypopharynx at about ¾ of its total length.

Pharynx and oesophagus

The pharynx and oesophagus have a wide lumen. Several dorsal, lateral and ventral folds serve for muscle attachment.

Musculature (Fig. 3; OR 1): M. clypeopalatalis (**0ci1**) – absent. M. clypeobuccalis (**0bu1**) – present. M. frontobuccalis anterior (**0bu2**) – O: interantennal ridge posterior to the 0lb1; I: dorsal buccal wall, posterior to the ganglion frontale. M. frontobuccalis posterior (**0bu3**) – absent. M. tentoriobuccalis lateralis (**0bu4**) – absent. M. tentoriobuccalis anterior (**0bu5**) – one muscle bundle; O: anterior wall of corpotentorium; I: ventral buccal wall. M. tentoriobuccalis posterior (**0bu6**) – absent. M. verticopharyngalis (**0ph1**) – O: posterior head capsule, posterad the brain, mediad of 0md1; I: dorsal pharyngeal wall. M. tentoriopharyngalis (**0ph2**) – absent. M. postoccipitopharyngealis (**0ph3**) – O: head capsule, close to the posterior tentorial pit; I: ventral pharyngeal wall, below the attachment of M. verticopharyngalis (0ph1).

Comparison and Discussion

The morphology of *E. superstes*, the Japanese species of Epiophlebiidae, was already investigated more than six decades ago (However, the account of internal structures remained fragmentary.

Our study revealed three additional mandible muscles (0md4 "M. hypopharyngo mandibularis", 0md6 "M. zygomaticus mandibulae anterior", 0md8 "M. zygomaticus mandibulae posterior"), which are also consistently found in Zygoptera and Anisoptera. M. tentoriomandibularis medialis superior (0md7) is absent in adults of *E. superstes*. It is also missing in Calopterygidae, Neopetaliidae, Aeshnidae, Libelullidae, Macromiidae and Corduliidae, but is present in Lestidae, Austropetaliidae, Cordulegastridae, Petaluridae and Gomphidae. This muscle belongs to the groundplan of Ephemeroptera and Zygentoma and apparently also of Odonata. The loss apparently occurred several times independently. Based on the available data we postulate the primary absence of 0md7 in Anisoptera (Fig. 4).

The composition of M. craniomandibularis externus (0md3) is unusual. The abductor comprises one major muscle package and a smaller one with different origin. The smaller part originates above M.craniomandibularis internus (0md1), the larger part below it. Both packages insert at the abductor tendon. This situation is similar to the condition found in Ephemeroptera (Staniczek 2001) for 0md2 and 0md3. In contrast to Odonata, these two muscles are discernible as separate bundles from origin to insertion in Ephemeroptera, although they have the same function and their insertion points are almost adjacent (Staniczek 2000, 2001). Due to the peculiar structure of 0md3 in Odonata, we assume a fusion of 0md2 and 0md3 based on our data (see Figs 3 and 4).

The antennal musculature is typical for Odonata, with two tentorio-scapal muscles moving the scapus. Two scapo-pedicellar muscles move the pedicellus. The available data suggest that antennal circulatory system are absent in adults of *E. superstes* and other adult odonatans, whereas they were reported by Pass (Pass 1991) for some odonatan larvae.

The bucca and pharynx of *E.superstes* are equipped with more muscles than those illustrated by Asahina (1954). Our study revealed a second M. frontobuccalis originating very close to the M. frontobuccalis anterior medially on the interantennal ridge. More posteriorly the pharynx is dorsally connected with the head by M. verticopharyngalis (0ph1).

The ventral dilators of the bucca and pharynx are M. tentoriobuccalis anterior (0bu5) and M. postoccipitopharyngalis (0ph3). The muscular equipment of the bucca and pharynx is the same as in all other studied odonatans. It is a reduced type compared to the condition in Ephemeroptera (see OR 2).

In the majority of studies Ephiophlebiidae are placed as sister taxon to extant Anisoptera (=Epiprocta). Matuskina (2008) found that the ovipositor and the egg laying behaviour of *E. superstes* are very similar to the corresponding conditions in Zygopteran, suggesting possible phylogenetic affinities. Dumont (2010) placed Epiophlebiidae as sister taxon to Cordulegastridae based on molecular data.

The head musculature of *E. superstes* is similar to what is found in Lestidae and Gomphidae (Fig. 3 & 4, table ES 1). Possible groundplan features of Odonata are a fused M. craniomandibularis externus anterior (0md2) and M. craniomandibularis externus (0md3), and the absence of M. tentoriopraementalis inferior (0la5) and M. praementoparaglossalis (0la11). The two labial muscles are present in all studied Zygentoma, Ephemeroptera and Neoptera (Blanke et al. subm). The head morphology of *E. superstes* shows more affinities with conditions found in Anisoptera (Fig. 4) than in Zygoptera. However, we agree only partly with the cephalic synapomorphies proposed for Epiprocta previously (Asahina 1954; page 121). Due to the enlargement of the vertex the position of the antennal foramen is shifted to a dorsolateral position. The enlargement and globular shape of the compound eyes in Epiprocta restricts the size of the dorsal portion of the occiput. It is apparent that several derived features are linked with these major changes in the cephalic construction. Considering all these characters as independent synapomorphies would in phylogenetic analyses would be equivalent with artificially increased weight.

Instead, we propose the following head synapomorphies for Epiprocta (Fig. 4): the primary loss of 0md7 (8), eyes separated by less than their own width (9), anteclypeus and postclypeus facing anteriorly (10) and a strongly convex vertex (15).

Anisoptera (Epiprocta excl. Epiophelbiidae) is supported by the presence of an epistomal and interantennal ridge (17 + 18) which is absent in Epiophlebiidae, Zygoptera and Ephemeroptera.

Our study shows that supposedly detailed anatomical studies (Asahina 1954) several decades old have to be seen with caution. Re-analyses may be important in some case to avoid errors in phylogenetic analyses which may be caused by incomplete or wrong morphological data (Wipfler et al. 2011; Blanke et al. subm). Especially Odonata and Ephemeroptera are interesting subjects because of their essential role in answering the evolution of flight in insects and their phylogenetic relation to Neoptera which is still not resolved. The detailed knowledge of the head morphology of *E. superstes* is apparently crucial for the reconstruction of the groundplan of Odonata.

Acknowledgement

Felix Beckmann and Fabian Wilde provided excellent support at the DESY synchrotron facilities. The scanning was done in the course of proposals no. I-20080169 and I-20090211. Marco Stampanoni and Peter Modregger are sincerely thanked for their support at the PSI SLS TOMCAT beamline (proposals 20100137 and 20110069). We would like to express our gratitude to Prof. Ryu Machida (University of Tsukuba, Japan) who kindly provided specimens of *E. superstes*. Benjamin Wipfler and Rolf Beutel (University of Jena, Germany) are thanked for useful advise. The lab members of the ZFMK are sincerely thanked for their support.

8

An updated phylogeny of Anisoptera including formal convergence analysis of morphological characters

An updated phylogeny of Anisoptera including formal convergence analysis of morphological characters

An updated phylogeny of Anisoptera including formal convergence analysis of morphological characters

Alexander Blanke [1]*, Carola Greve [1], Rajmund Mokso [2], Felix Beckmann [3], & Bernhard Misof [1]

[1] Zoologisches Forschungsmuseum Alexander Koenig, Zentrum für Molekulare Biodiversität, Adenauerallee 160, 53113 Bonn, Germany
[2] Swiss Light Source, Paul Scherrer Institut, 5232 Villigen, Switzerland
[3] Institute of Materials Research, Helmholtz-Zentrum Geesthacht, Max-Planck-Str. 1, 21502 Geesthacht, Germany
*Correspondence: Alexander Blanke, Zoologisches Forschungsmuseum Alexander Koenig, Zentrum für Molekulare Biodiversität, Adenauerallee 160, 53113 Bonn, Germany. E-mail: blanke@uni-bonn.de

This is the author's version of a work accepted for publication in the journal Systematic Entomology

Abstract

Deep level relationships among Anisoptera (dragonflies) are unresolved. Molecular markers applied have not been particularly useful to resolve the relationships at the family level. Previous morphological studies depend heavily on characters of wing venation and articulation which are believed to display considerable degrees of homoplasy due to adaptations to different flight modes. Here, we present the most comprehensive anatomical dataset of the head morphology of Anisoptera with focus on muscle organisation and endoskeletal features covering nearly all families. The characters are illustrated in detail and incorporated into an updated morphological character matrix covering all parts of the dragonfly body. Phylogenetic analysis recovers all families as monophyletic clades except Corduliidae, Gomphidae as sistergroup to all remaining Anisoptera, and Austropetaliidae as sistergroup to Aeshnidae (=Aeshnoidea). The position of Petaluridae and Aeshnoidea to each other could not be resolved. Libelluloidea is monophyletic with Neopetalia and Cordulegastridae branching off first. Chlorogomphidae is sister to an assemblage of monophyletic (Synthemistidae + ("Corduliidae" + Libellulidae). In addition, we applied a recently published formal approach to detect concerted convergence in morphological data matrices to uncover possible homoplasies. Analyses show that especially head and thorax characters may harbour homoplasies. After exclusion of possible homoplastic characters Gomphidae is corroborated as sister group to all remaining Anisoptera.

Introduction

Vein branching patterns and wing base sclerite configuration have been routinely used in insect phylogenetics and proved an invaluable tool to compare fossils with the recent insect fauna (Trueman, 1996). However, it has been proposed that wing characters display a considerable degree of convergence (Fleck et al., 2008a). This is especially true for Odonata (Bybee et al., 2008; Carle et al., 2008; Fleck et al., 2008a). Authors have shown that effects of wing size reduction and different flight styles may be responsible for parts of the wing vein characterstics in Odonata, thus potentially biasing phylogenetic signal. For example, functional dependence between e.g. the costal region (the leading edge of the wing) are believed to have an influence on the configuration of more posteriorly located wing parts (Wootton, 1992).

The effect of convergent evolution of groups of characters is called concerted convergence (Patterson and Givnish, 2002). It is assumed that similar selective pressures result in convergent evolution of character groups which may inflate node support values in tree reconstructions. Recently, Holland et al. (2010) proposed an approach to detect these character groups in morphological data matrices by applying permutation tests of character compatibility.

In this study we pursue two main goals. First, we aim to compile a comprehensive morphological character matrix to infer a robust deep-level phylogeny of dragonflies by extending the currently largest morphological data matrix covering all parts of the dragonfly body (Bybee et al., 2008; Rehn, 2003). Our focus for addition of new characters is the head region. The head as a character system is underrepresented in dragonfly phylogenetics (only 13 of 153 characters, i.e. 8,5% (Bybee et al., 2008)), but has proven useful to infer relationships among various other groups of insects (Blanke et al., 2012a; Blanke et al., 2012b; Wipfler et al., 2011; Wipfler et al., 2012).

Secondly, we investigate the degree of concerted convergence in this extended data matrix in order to explore potential confounding signal within morphological characters with Holland's et al. (2010) approach. Subsequently, we analyse which functional groups of characters are prone to concerted convergence.

Background

Odonata are classified into two major groups: Zygoptera (damselflies) and Epiprocta (fide Lohmann (1996)) comprising the sistergroups Anisoptera (dragonflies) and Anisozygoptera, containing one family, Epiophlebiidae, with three relict species (Li et al., 2012).

The monophyly of the families within Anisoptera is generally accepted except for the morphologically very heterogeneous Corduliidae. However, the relationships of these families to each other are not congruently resolved. In molecular studies especially the positions of Gomphidae (clubtails), Aeshnidae+Austropetaliidae (=Aeshnoidea), Petaluridae (petaltails) and Cordulegastridae (spiketails) are incongruently resolved depending on molecular markers chosen analysis (Fig. 1). For example, Misof et al. (2001) recovered a clade Gomphidae + Petaluridae which is sister to the remaining Anisoptera. In this study, Aeshnoidea were recovered as the sistergroup to Libelluloidea (Chlorogomphidae + Neopetaliidae + Cordulegastridae + Macromiidae +

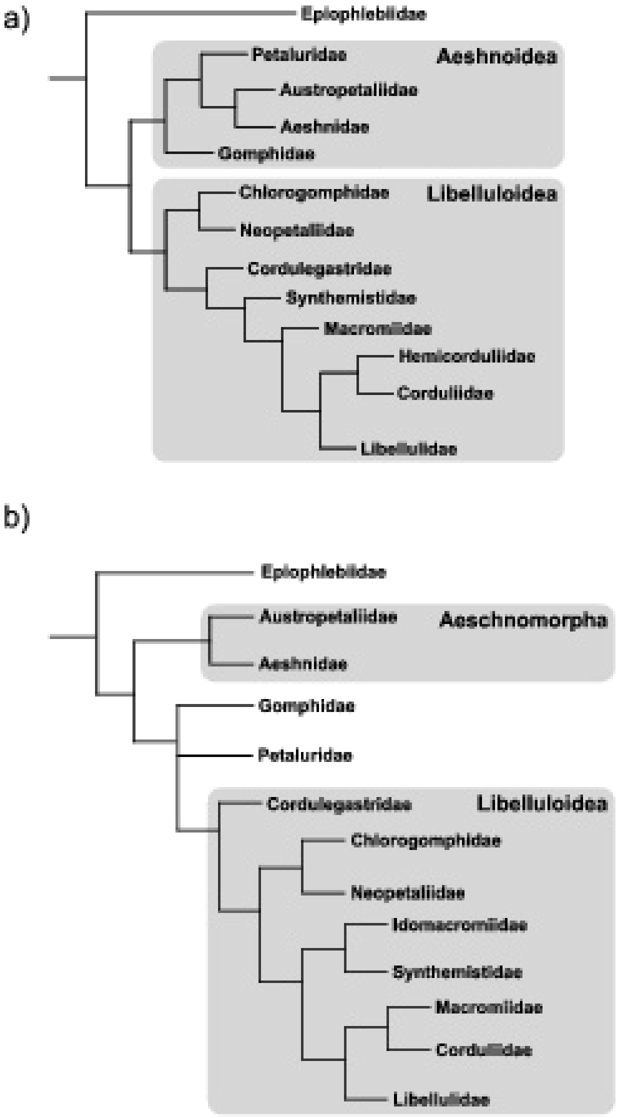

Fig. 1 The two principal hypotheses concerning the deep splits inside Anisoptera. a) Tree reconstruction of Fleck et al. (2008b) based on mtRNA sequences and RNA secondary structure information. b) Tree reconstruction of Letsch et al. (2009) using mtRNA and rRNA sequences and improved RNA secondary structure models.

Corduliidae + Libellulidae). Carle et al. (2008) based on nuclear and mitochondrial rRNAs and EF1-α markers proposed Aeshnoidea as sister to all remaining Anisoptera and Gomphidae as sistergroup to Petaluridae + Libelluloidea. Taking secondary structure information of mtRNA gene sequences into account, Fleck et al. (2008b) suggested monophyletic Aeshnomorpha (Gomphidae + Petaluridae + Aeshnoidea) as sistergroup to Libelluloidea. Letsch et al. (2009) analyzed mitochondrial as well as nuclear sequence data and refined the secondary structure analysis approach by identifying local structure constraints of each sequence thereby uncovering phylogenetic signal in folded RNA structures. Basically, this analysis pointed towards the results of Carle et al. (2008), although the position of Gomphidae and Petaluridae did not receive strong support.

Morphological analyses of the interfamily relationships within Anisoptera are equally plagued by incongruent results. Based on wing characters Trueman (1996) proposed Petaluridae as sistergroup to the remaining Anisoptera and Aeshnidae + Chlorogomphidae as sister to Gomphidae + the remaining Libelluloidea. Carle (1982) using a less exclusive set of characters including thorax and abdominal characters proposed Gomphidae as sistergroup to the remaining Anisoptera, while Chlorogomphidae and Cordulegastridae were placed as basal Libelluloidea. In contrast Pfau (1991) placed Aeshnidae as sister to the remaining Anisoptera based on functional morphological analyses of genitalia. Using a groundplan approach, Bechly (1995) placed Petaluridae as sister to extant Anisoptera and Gomphidae as sister to Libelluloidea. Rehn (2003) proposed Petaluridae as sister to all remaining Anisoptera and Gomphidae as sister to Aeshnidae + Libelluloidea using characters from the whole dragonfly body. Rehns' (2003) analysis put a strong focus on the relationships of Zygoptera therefore lacking some anisopteran families (eg. Austropetaliidae, Neopetaliidae, and Chlorogomphidae). Bybee et al. (2008) used the matrix of Rehn (2003) in his combined molecular and morphological analysis and extended it by several characters and many taxa to cover outgroup taxa and to increase resolution within Anisoptera.

All morphological data matrices used in formal cladistic analyses of odonatan relationships are largely dependent on characters of wing venation and articulation (Ballare and Ware, 2011; Rehn, 2003; Trueman, 1996; von Ellenrieder, 2002) which have also been used in a combined molecular and morphological approach (Bybee et al., 2008). The last comprehensive account on odonate phylogeny derived 81 out of 153 characters (53%) from wing venation or wing articulation (Rehn, 2003).

Additionally, the majority of other characters are derived from the copulatory system. Dragonflies exhibit a unique mode of sperm transfer via a secondary copulatory system located at the 2nd and 3rd abdominal segments of males. Spermatophores are transferred to this apparatus by males prior to copulation. Females are then grasped at the neck by males with the claspers of the abdominal tip (copulatory tandem) and collect sperm from the male secondary copulatory system. Due to the absence of the secondary copulatory apparatus outside of Odonata, polarization of characters associated with this character system is impossible. The situation is different for the female ovipositor: monophyly of Zygoptera and Anisoptera could be corroborated, the position of Epiophlebiidae and the phylogenetic relationships between anisopteran families, however, remain unclear (Klass, 2008; Matushkina, 2008a; Matushkina, 2008b).

Material and Methods

We collected data of the outer and inner head anatomy for all currently recognized families except Gomphomacromiidae and Synthemistidae resulting in 31 data sets (see supporting information file_SI_1). Additional data for adults and nymphs were gathered from the literature. For brevity terminals are mentioned only with their generic name in the following.

SEM and visual observations

The outer morphology was assessed with SEM and observation with a Zeiss Stemi 2000C binocular (Carl Zeiss AG, Oberkochen, Germany). For SEM specimens were transferred in a series of steps into 100% ethanol, critical point dried (Model E4850, BioRad, Hercules, CA, USA), and sputter coated (Model Hummer VII, Anatech, Union City, CA). SEM was performed on a Hitachi S-2460N (Hitachi Ltd., Chiyoda, Tokyo, Japan) using a new type of rotatable sample holder (Pohl 2010).

Computer tomography

The anatomy of specimens was investigated using synchrotron micro-Computer Tomography (SR-microCT) (Betz et al., 2007). Prior to scanning, samples were critical point dried (CPD) (Model E4850, BioRad, Hercules, CA, USA) and mounted on specimen holders. Generally, X-ray imaging has a high penetrating power and allows visualizing large specimens without need for sectioning. SR-microCT offers a true 3D spatial resolution of up to 1 µm with moderate resolving power of tissues and tissue interfaces.

Specimens were scanned either at the German electron synchrotron accelerator (DESY, Hamburg, Germany; Beckmann et al., 2008), at the Swiss Light Source electron synchrotron accelerator (SLS, Villigen, Switzerland; (Stampanoni et al., 2010)) or at the high resolution computed tomography scanner v|tome|x s (GE phoenix|x-ray, Steinmann-Institut, Bonn, Germany) (Table 1). The DESY and SLS X-ray sources were optimized for high density and spatial resolution (1-10 um) imaging with monochromatic X-rays. A single 3D volume of typically 3.7mm³ can be acquired in about 12 min at SLS.

The tomography station BW2 (DESY) operated by Helmholtz-Zentrum Geesthacht (HZG, Geesthacht, Germany) is optimized for performing high-density resolution microtomography (Beckmann et al., 2008). All facilities provide floating point data as well as 16bit TIFF image files and volume data files (.vgi-format) ready for analysis in the free and the proprietary Volume Graphics software packages (Volume Graphics, Heidelberg, Germany).

Datasize for each specimen ranges between 1500-3000 images (or 3-12 GB of raw data) depending on specimen size, magnification and quality of the back projections. The raw data is available upon request from the corresponding author and will be deposited in MorphDbase (https://www.morphdbase.de/).

The provided volume data (.vgi-files) was analyzed with the free myVGL 2.0 64bit viewer (Volume Graphics, Heidelberg, Germany). Segmentation and rendering of single structures was accomplished with Reconstruct (Fiala, 2005) and Blender (http://www.blender.org). Both software packages are distributed under the General Public License (GPL) licence. Final tables and figures were edited with GIMP, Iinkscape and Scribus (all GPL). A table showing the homologised cephalic musculature of the investigated odonates can be found in supporting information file SI_2.

Testing for concerted convergence

For concerted convergence analysis (CCA) we applied the formal approach proposed by Holland et al. (2010) which aims to identify groups of characters upon which convergent evolution probably acted (concerted convergent characters). The proposed workflow (Fig. 2) has been successfully used to detect concerted convergence among morphological characters coding deep pterygote splits (Blanke et al., accepted). The workflow is only roughly explained in the following, details on the general procedure can be found in Holland et al. (2010), on the modifications used in the present study in Blanke et al. (accepted).

In principle, the method performs permutation tests of pairwise character compatibility of a morphological character matrix (see supporting information file SI_3 & 4) using the pairwise excess index (PEI) as a measure of fit of two randomly chosen characters on a tree constructed from just these two characters (see supporting information file_SI_5). Pairwise compatible characters can be grouped into clusters depending on their PEI using a standard clustering method (UPGMA, see supporting information file_SI_6). The significance of the cluster size is assessed using a cutoff value derived from testing (PEI and UPGMA) of 1000 shuffled character matrices with equal size and parsimony index (for details see Holland et al. 2010). All cliques of the empirical dataset, which are larger than the smallest clique size generated with the shuffled artificial character matrices, are significant. These character clusters, which are larger than expected by chance alone, can then be used for tree inference. The plausibility of hypotheses supported by trees reconstructed from the clique characters as well as the remaining character set can be used to interpret the pairwise compatibility of characters. An analysis of the type of characters and their distribution among cliques may uncover groups of characters with a high probability of interdependence. The whole test needs no initial tree and is therefore independent of morphological and molecular tree inferences. However, it is possible to identify potentially problematic morphological characters by calculating the homoplasy excess for each character on a random subset of 1000 molecular trees (Holland et al., 2010). We did not follow this approach here, since the characters relevant for the phylogenetic placement of Gomphidae and Aeshnoidea have low excess values. Therefore exactly the characters relevant for the main questions of this paper would have been excluded by testing against the molecular tree inference (see supporting information file_SI_7 for a detailed molecular tree and SI_8 for the excess distribution of the morphological characters on the molecular trees).

In an UPGMA analysis (using PAUP version 4.0b10) we calculated a tree of the pairwise excess matrix received from PEI calculation of the complete dataset (see supporting information SI_6) to identify character cliques. The significance value for the largest randomly generated clique was size 23, therefore indicating one significant character clique in the complete empirical dataset. The character clique as well as the remaining character set were used for tree reconstruction using maximum parsimony. Reconstructed strict consensus trees of these character subsets were compared with the initial strict consensus tree of the complete dataset.

We also classified all characters into seven groups: head, thorax, wing, abdomen, genitalia, anatomic characters and nymphal characters and recorded which characters grouped together in cliques and whether whole groups clustered together in cliques.

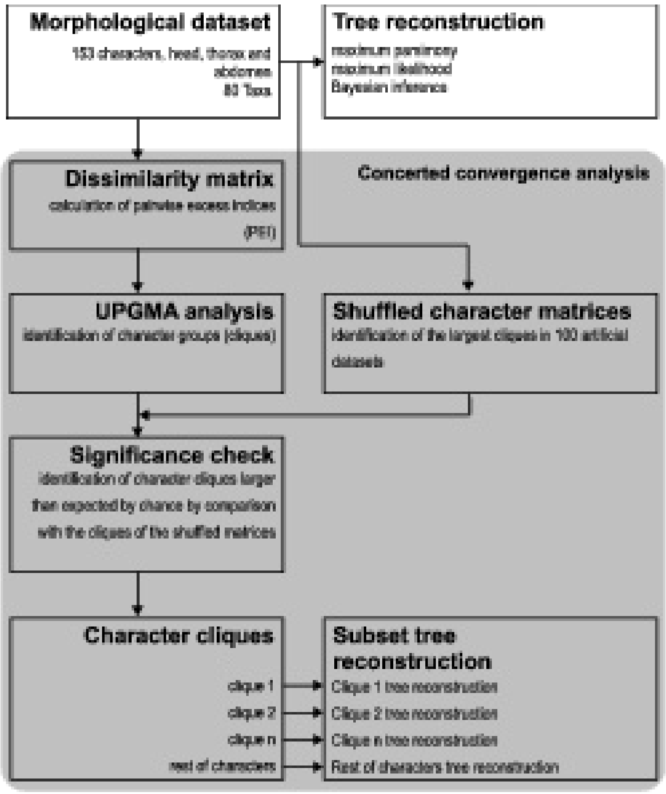

Fig. 2 Principal workflow of the data analysis after character compilation derived from the study of Holland et al. (Holland et al., 2010). Note that tree reconstruction of the complete data and convergence analysis are performed independently of each other.

Molecular data

For the initial excess distribution test we compiled a molecular data set with corresponding taxon selection to our morphological data matrix in which we used 12S, 16S, 18S and 28S rRNA sequences and sequences of the protein-coding genes Histone H3 and cytochrome c oxidase subunit II (COII) (supporting information file_SI_1). All sequences were downloaded from NCBI Genbank. Taxa were only included if represented by at least three genes (considering each mitochondrial gene as independent). We only considered 12S sequences with at least 313 base pairs (bp), 16S sequences with at least 393 bp, 18S with at least 560 bp, 28S with at least 1019 bp, COII with at least 458 bp and complete or nearly complete sequences of Histone H3. If molecular data of taxa were not publicly available or did not pass our selection criteria, we chose sequences of other species, preferably within the same genus, or within the same family (see supporting information SI_1).

Alignment procedure

All genes were aligned separately with MAFFT (Katoh et al., 2002) choosing the L-INS-i algorithm for 12S, 16S, 18S rRNA sequences and COII, the E-INS-i algorithm for

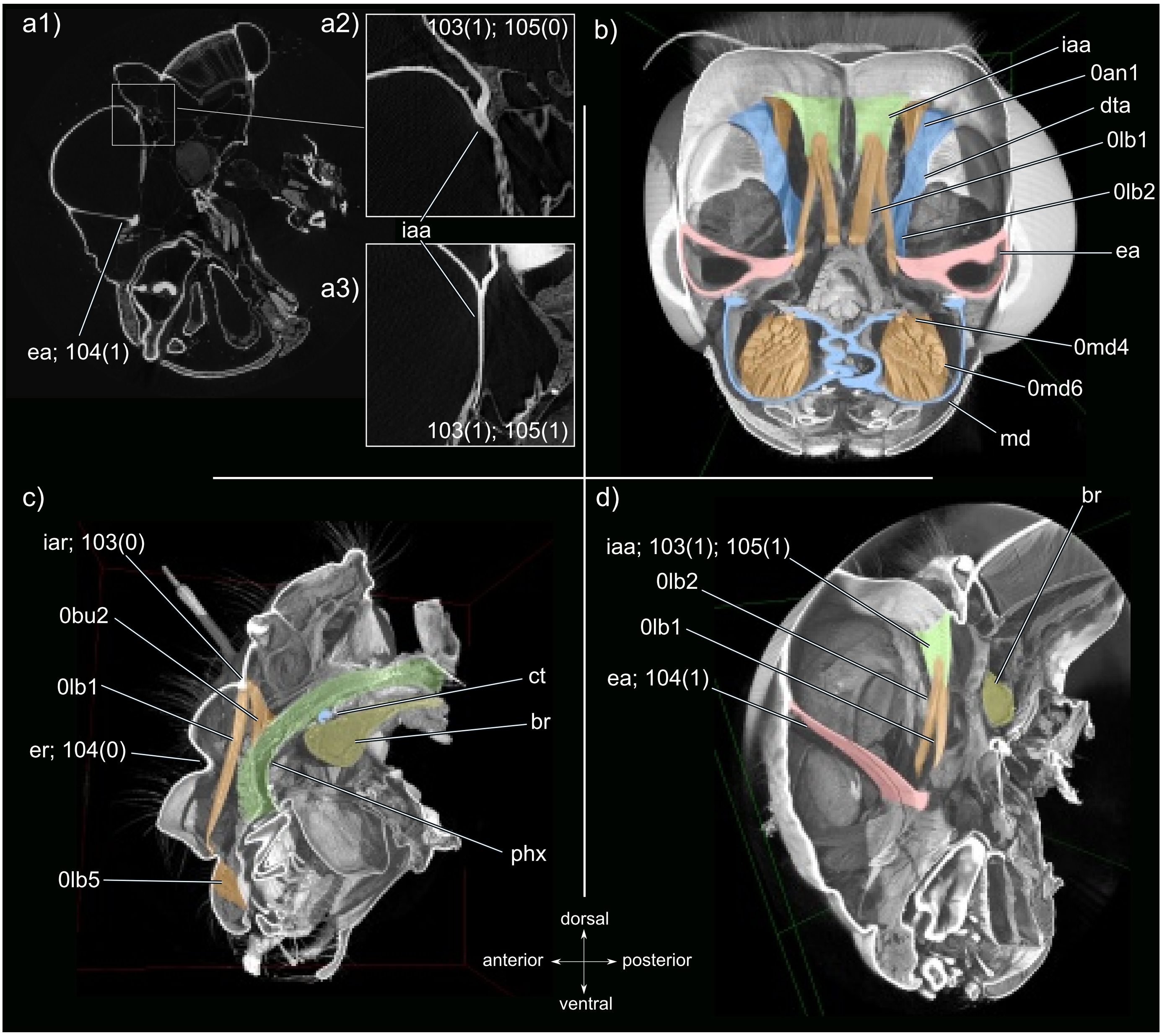

Fig. 3 General overview of the anatomic organisation in Zygoptera and Anisoptera and illustration of characters 103-105 (character states in brackets). a1) Sagittal section of *L. depressa* at height of the left mandible illustrating the interantennal and the epistomal ridge and the respective apodemes. a2) Detail of the interantennal ridge in *L. depressa*. a3) Detail of the interantennal ridge in *A. mixta*. b) Frontal section of *A. mixta* at height of the mandibular incisivi showing the interantennal apodemes and respective muscle attachments. c) Sagittal section of *C. virgo* showing the absence of the interantennal and epistomal apodemes. d) Sagittal section of *A. mixta* showing the epistomal and interantennal apodemes as well as muscle attachments. Abbreviations: 0lb1, M. frontolabralis; 0lb2, M. frontoepipharyngalis; 0lb5, M. labroepipharyngalis; 0md4, M. hypopharyngo mandibularis; 0md6, M. tentoriomandibularis lateralis inferior; 0bu2, M. frontobuccalis anterior; br, brain; dta, dorsal tentorial arm; ea, epistomal apodeme; er, epistomal ridge; iaa, interantennal apodeme; iar, interantennal ridge; md, mandible; phx, pharynx. a) SR-microCT image, b)-d) volume renderings of SR-microCT image stacks. Images not to scale.

28S rRNA sequences and the G-INS-i algorithm for Histone H3 (Katoh et al., 2005). Subsequent masking of the alignments was done with Aliscore v.0.2 (Misof and Misof, 2009), which identifies putative ambiguously aligned regions in multiple sequence alignments using a sliding window approach. For gap treatment (g), window size (ws) and random pairwise comparisons (pc), the following settings were used: g = ambiguous characters, ws = six positions, pc = 4 x number of taxa. Ambiguous positions were masked and the masked alignments were concatenated using FASconCAT version 1.0 {Kück, 2010 #2714}. Finally, the complete molecular data set comprised 5773 characters, of which the 16S partition accounted for 466, the 18S partition for 1821, the 28S

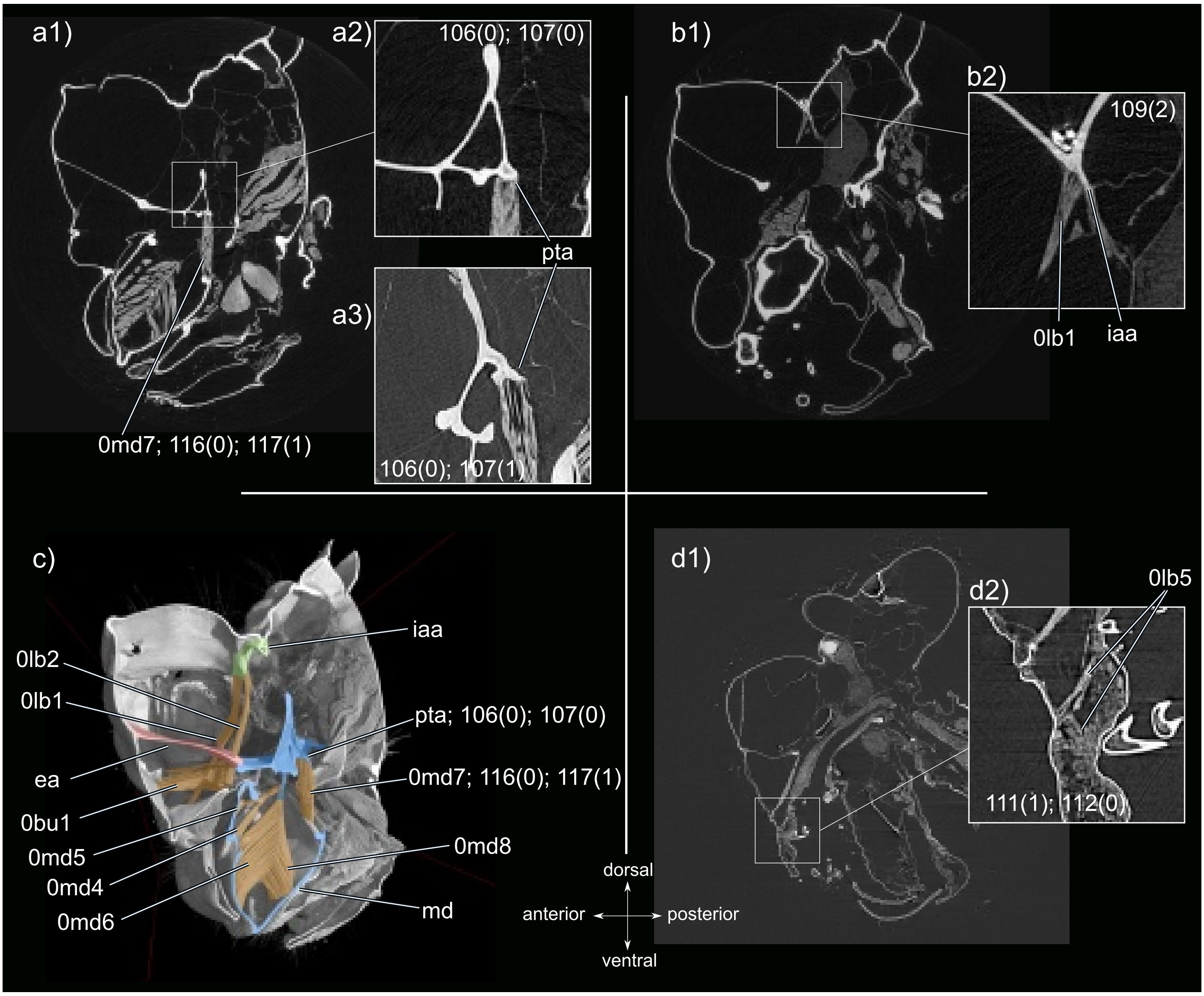

Fig. 4 Illustration of characters 106, 107, 109, 111, 112, 116 and 117 with SR-microCT data (character states in brackets). a1) Sagittal section of *G. pulchellus* showing the posterior tentorial apodeme (pta) at the posterior base of the anterior tentorial arms and the location of M. tentoriomandibularis medialis superior (0md7). a2) Detail of the pta in *G. pulchellus*. a3) Detail of the pta in *T. pryeri*. b1) Section of *G. pulchellus* showing M. frontoepipharyngalis (0lb2) originating at the interantennal ridge as well as on the interantennal apodeme. b2) Detail of b1). c) Sagittal section of *G. pulchellus* showing the configuration and location of the pta in relation to other head structures. d1) 3D reconstruction of the labrum of *P. gray* showing the peculiar configuration of the M. labroepipharyngalis (0lb5). a)+b) SR-microCT images; c) volume rendering of a SR-microCT image stack. Abbreviations: 0lb1, M. frontolabralis; 0lb2, M. frontoepipharyngalis; 0lb5, M. labroepipharyngalis; 0md4, M. hypopharyngo mandibularis; 0md5, M. tentoriomandibularis lateralis superior; 0md6, M. tentoriomandibularis lateralis inferior; 0md7, M. tentoriomandibularis medialis superior; 0md8, M. tentoriomandibularis medialis inferior; 0bu1, M. clypeobuccalis anterior; ct, corpotentorium; ea, epistomal apodeme; iaa, interantennal apodeme; md, mandible; phx, pharnyx; pta, posterior tentorial apodeme. Images not to scale.

partition for 2152, the 12S partition for 361, the COII partition for 647 and the Histone H3 partition for 326 sites.

Tree calculations

The morphological data were analyzed using maximum parsimony and Bayesian inference. Parsimony analyses and Bremer/bootstrap support calculations of the morphological data were carried out with TNT (Goloboff et al., 2008) using 1000 heuristic searches starting with random addition of taxa (TBR branch swapping; all characters treated as unordered). Bayesian inference of the morphological data was conducted using MrBayes v3.2 (Huelsenbeck and Ronquist, 2001; Ronquist and Huelsenbeck, 2003). The MK model was applied, with among character rate variation modelled with gamma

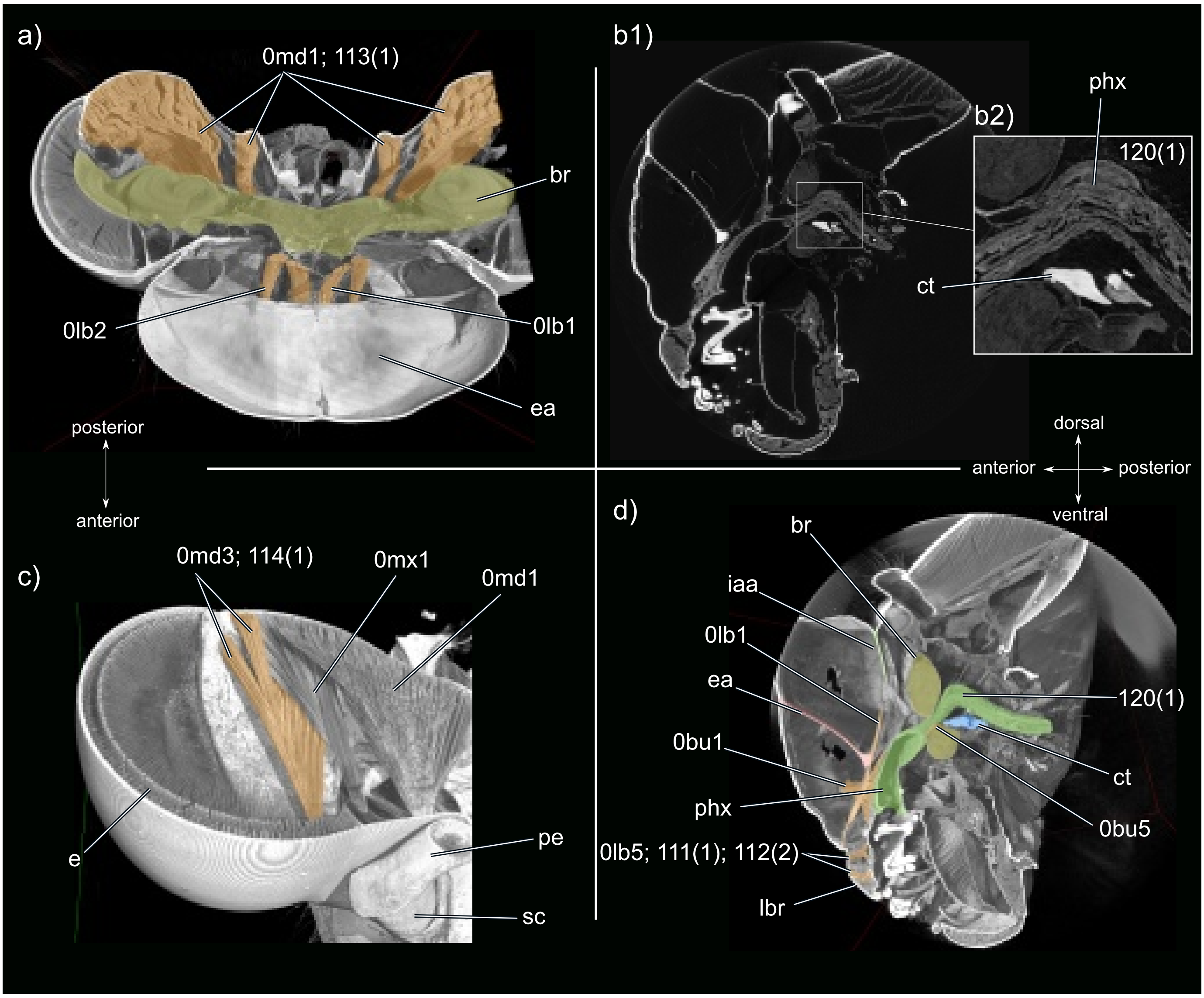

Fig. 5 Illustration of characters 111-114 and 120 with SR-microCT data (character states in brackets). a) Transversal section of *G. pulchellus* showing the origins of M. craniomandibularis internus (0md1). b1) Sagittal section of *A. mixta* showing the peculiar progression of the pharynx at height of the corpotentorium. b2) Detail of b1). c) Transversal section of *C. virgo* showing the second origin of the M. craniomandibularis externus (0md3). d) Sagittal section of *A. mixta* showing the origins and insertions of M. labroepipharyngalis (0lb5) and the progression of the pharynx. Abbreviations: 0lb1, M. frontolabralis; 0lb2, M. frontoepipharyngalis; 0lb5, M. labroepipharyngalis; 0md1, M. craniomandibularis internus; 0md3, M. craniomandibularis externus; 0bu1, M. clypeobuccalis; br, brain; ct, corpotentorium; ea, epistomal apodeme; iaa, interantennal apodeme; lbr, labrum; pe, pedicellus; phx, pharnyx; sc, scapus. Images not to scale.

distributed rates across characters with four discrete rate categories. Priors were set adopting the default settings of MrBayes v3.2. Two parallel analyses were run with random starting trees and four Metropolis coupled Markov chains (MCMC) for 10,000,000 generations with the temperature set to 0.3. Every 100th generation was sampled to yield a posterior probability distribution of 100,000 trees. After discarding the first 25,000 trees of each run as burn-in trees, a 50 % majority rule consensus tree was calculated from the sampled trees of both runs. Support values are given in parentheses with the following order: (Bremer support (BR) / parsimony bootstrap (PB) / Bayes posterior probability (PP)).

We used constrained tree reconstruction (CTR) executing the "move branch mode" in Winclada ver. 1.00.08 (Nixon, 2002) to explore the character state implications of alternative hypotheses encountered in the literature. These alternative hypotheses were: *Epiophlebia* is sister to Cordulegastridae (EC hypothesis; Dumont et al. (2010)), Aeshnomorpha as sister to all other Anisoptera (AA hypothesis; Letsch et al. (2009)), and Aeshnoidea as sistergroup to Libelluloidea (AL hypothesis; Fleck et al. (2008b)).

The ML analysis of the molecular data (Supporting information SI_7) was conducted using the GTR + Γ + I model. To optimize model parameter estimation for each gene, the data set was partitioned into (1) 16S, (2) 18S, (3) 28S, (4) 12S, (5) COII and (6) Histon H3. Node support for the best–scoring ML tree was evaluated with 1000 rapid bootstrap replicates (Stamatakis et al., 2008).

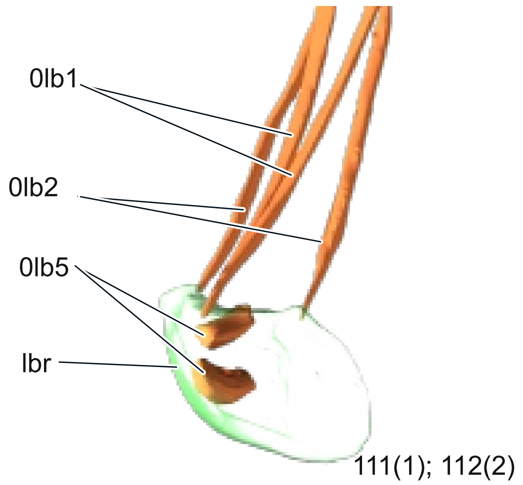

Fig. 6 3D.reconstruction of the labrum and associated muscles of *A. mixta* illustrating the double origin of M. labroepipharnygalis (0lb5). Abbreviations: 0lb1, M. frontolabralis; 0lb2, M. frontoepipharyngalis; 0lb5, M. labroepipharyngalis; lbr, labrum.

Results

Morphological data matrix

The morphological data matrix is based on that of Rehn (2003) and the proposed extensions of Bybee et al. (2008). A character discussion can be found in Rehn (2003), a complete character list is included in the supporting information (file_SI_3). Several characters of the matrices of Rehn (2003) and Bybee (2008) were not included in the phylogenetic analyses, since they are specific for fossil taxa or zygopteran relationships. Characters for which homology hypotheses are unclear were also not included in the analyses. Please refer to SI2 for a complete commented list. We recoded several characters according to the suggestions of Lee & Bryant (1999) by splitting up character parts (coded as absent or present) and character variables (e.g. colours schemes)

The present matrix is composed of 13 head characters, 5 thorax characters, 47 characters related to wing articulation and venation, 4 abdominal characters, 13 male copulatory characters, 18 nymphal characters and 20 characters related to the inner anatomy (mainly derived from the head).

Proposed phylogenetic characters

Characters 0-11 are derived from Rehn (2003).

12. Shape of vertex and location of ocelli: (0) transverse protuberance with lateral ocelli located at the lateral border and middle ocellus anteriorly; (1) small protuberance with all ocelli located on the vertex covering it almost completely; (2) large transverse oriented plate with middle ocellus located anteriorly and lateral ocelli located at the posterior side at the base; (3) flat with all ocelli located on the vertex; (4) two protuberances or horn like structures with lateral ocelli located at distal sides and middle ocellus anteriorly; (5) conical with all ocelli located on the vertex. This character is a modification of character 13 of the Rehn (2003) matrix taking into account the relative position of the ocelli and refining the structure definitions of the vertex. The vertex is a large transverse oriented plate with a distinct ocellus organisation in *Epiophlebia*, whereas it is a transverse protuberance in all studied Aeshnidae, Cordulegastridae, Libellulidae, Synthemistidae and most Corduliidae. The vertex forms a small protuberance with all ocelli located on the vertex in Austropetaliidae. In Gomphidae, Macromiidae, *Tachopteryx* and *Procordulia* it forms two protuberances or horn-like structures. All Petaluridae except *Tachopteryx* show a conical vertex with all ocelli located on the vertex.

Characters 13-55 & 57 & 58 are derived from Rehn (2003).

Character 56 is derived from Bybee (2008).

59. Wings with several reddish spots in the C-Sc-Ra area: (0) absent; (1) present. Several distinct reddish spots in the C-Sc-Ra area of the wings are present in the Neopetaliidae and Austropetaliidae studied.

Characters 60, 64-66; 68; 70;71 & 73-76 are derived from Rehn (2003).

Characters 61; 62 & 77 are derived from Bybee (2008).

63. Male mesotibial spines: (0) not quadrangular; (1) quadrangular (Garrison et al., 2006). The male mesotibial spines are quadrangular in all studied Cordulegastridae.

67. Anterior hamuli directed medially: (0) no; (1) yes (Carle and Louton, 1994). The anterior hamuli are directed medially in all Aeshnoidea studied.

69. Anterior lamina with elongate medial cleft: (0) absent; (1) present (Carle and Louton, 1994). An elongate medial cleft is present in all Aeshnoidea studied. It is absent in all other odonates.

72. Posterior hamules: (0) present; (1) vestigial (Carle and Louton, 1994). The posterior hamules are vestigial in all Aeshnoidea studied.

Characters 78 & 79 are derived from Rehn (2003).

80. Abdominal terga 5-8 with ventroapical tufts of long black hairs: (0) absent; (1) present (Carle and Louton, 1994). Ventroapical tufts of long black hairs on the abdominal terga 5-8 are present in Neopetalia and absent in all other odonates studied.

Character 81 is derived from Bybee (2008).

82. Nymph with pyramidal to spike-like horn between the eyes: (0) absent; (1) present (Needham and Westfall, 1955). A conspicuous spike-like horn between the eyes is present in the Macromiidae investigated.

Characters 83-88 are derived from Rehn (2003).

Character 89 is derived from Bybee (2008).

90. First flagellum of nymphal antenna: (0) thinner than pedicellus; (1) thicker or at least as thick as pedicellus (Needham and Westfall, 1955). All studied Gomphidae and Petaluridae possess a first flagellum which is at least as thick or thicker as the pedicellus.

91. Fourth antennal segment very short or vestigial in nymph: (0) absent; (1) present (Needham and Westfall, 1955). The fourth antennal segment is very short in all studied Gomphidae.

Characters 92 & 93 are derived from Bybee (2008).

94. Spur of moveable hook: (0) robust; (1) thin and setae-like (Fleck, 2011). The spur of the moveable hook is thin and setae like in all Cordulegastridae studied and Neopetalia, while it is robust in all Petaluridae (Fleck, 2011).

Character 95 is derived from Bybee (2008).

96. Hind legs of nymph: (0) at least twice as long as abdomen; (1) longer than abdomen, but less than twice as long; (2) at most as long as abdomen (Needham and Westfall, 1955). The nymphal hind legs are more than twice as long as the abdomen in all studied Macromiidae and *Zygonyx*. The hind legs are shorter or as long as the abdomen in *Epiophlebia*, Neopetaliidae, Aeshnidae, Cordulegastridae, Gomphidae, Petaluridae, and the libellulids *Brachydiplax, Libellula, and Trithemis*. All other Libellulidae, Corduliidae, and Synthemistidae posses hind legs which are longer but not twice as long as the abdomen.

97. Lateral spines or lobes on segment 5-9 in nymph: (0) absent; (1) present (Needham and Westfall, 1955). Lateral spines on the last segments of the nymphal abdomen are present in the studied Aeshnidae, Austropetaliidae, and Petaluridae. In all other studied taxa possessing lateral abdominal spines these are not present from segments 5-9.

98. Shape of distal margin of nymphal prementum: (0) with two apical, strong teeth flanked laterally by a rectangular tooth; (1) not as in (0). The distal margin of the nymphal prementum possesses two teeth flanked by a rectangular tooth in Neopetaliidae and Cordulegastridae (Fleck, 2011).

99. Nymphal molar lobes of left and right mandible: (0) moveable; (1) only left molar lobe moveable (flexible area present); (2) both molar lobes fixed (no flexible area present). The nymphal molar lobe is moveable on both mandibles in *Epiophlebia* and

Gomphidae (Fleck, 2011), whereas it is only moveable on the left mandible in Chlorogomphidae (Fleck, 2011).

100. Dorsal spines or hooks on abdominal segments of nymph: (0) absent; (1) present (Needham and Westfall, 1955). Dorsal projections on the nymphal abdominal segments are present in all studied Libellulidae, Macromiidae and Synthemistidae.

101. Number of dental folds in proventriculus: (0) 16; (1) 8; (2) 4. Fleck (2011) describes the proventriculus as follows: "...(it) is an internal bulbshaped structure of the alimentary canal making the junction between the foregut and the midgut. The part in contact with the lumen is essentially formed by longitudinal folds, the totality or a part of them carrying denticles placed on a sclerotized excrescence (= dental folds)." According to Fleck (2011) all Zygoptera (except *Lestes*) and *Epiophlebia* were coded as state (0) possessing 16 dental folds. Petaluridae (excluding *Phenes*) and *Lestes* possess a proventriculus with 8 dental folds. All remaining Anisoptera have four dental folds in their proventriculus (Fleck, 2011).

102. Ventral dental folds of proventriculus with median elongated rasp-like dentition: (0) present; (1) absent. An elongated rasp-like dentition is present in all included Zygoptera, *Epiophlebia*, Chlorogomphidae, and Gomphidae (Fleck, 2011).

103. Internal part of the interantennal ridge (interantennal apodeme; Fig. 3): (0) absent; (1) present. An interantennal apodeme (iaa) originating at the interantennal ridge is present in Neopetaliidae, Aeshnidae, Gomphidae, Petaluridae (except *Tachopteryx*), Libellulidae (except *Zygonyx*), Macromiidae, and Corduliidae (except *Procordulia*). The situation in Chlorogomphidae and Synthemistidae is unclear (coded as "?"). The interantennal apodeme frequently serves as an attachment site for labral muscles (see characters 103 and 104).

104. Internal part of the epistomal ridge (epistomal apodeme; Fig. 3): (0) absent; (1) present. An epistomal apodeme (ea) originating at the epistomal ridge is present in all studied Anisoptera and absent in *Epiophlebia* and Zygoptera.

105. Internal part of the interantennal ridge (interantennal apodeme; Fig. 3): (0) short, no longer than one third the length of epistomal apodeme; (1) longer than one third of epistomal apodeme. The interantennal apodeme is short in Neopetaliidae, Gomphidae, Petaluridae, Libellulidae, Macromiidae, Corduliidae, and the aeshnid *Oligoaeschna*. All other studied taxa exhibit an apodeme which is longer than one third of the epistomal apodeme.

106. Apodeme posteriorly of the anterior tentorial arm (attachment for 0md7; Fig. 4): (0) present; (1) absent. An apodeme serving as attachment site for 0md7 is present in all studied Aeshnidae, Gomphidae, *Phyllopetalia, Anotogaster,* and all Petaluridae except *Uropetala*.

107. Apodeme posteriorly of the anterior tentorial arm (attachment for 0md7; Fig. 4): (0) proximally in contact with the base of the anterior tentorial arm; (1) seperated at the entire length. The apodeme for attachment of 0md7 is proximally in contact with the anterior tentorial arms in Aeshnidae, Gomphidae, *Anotogaster, Phenes* and *Tachopteryx*.

108. M. tentorioscapalis lateralis (0an3): (0) present; (1) absent. Present in *Calopteryx*, Aeshnidae, Corduliidae, *Zonophora* (Gomphidae), *Libellula*, and *Sympetrum* (both Libellulidae). Absent in all other studied taxa.

109. Origin of M. frontolabralis (0lb1; Fig. 4): (0) at the interantennal ridge; (1) at the interantennal apodeme; (2) partly at the interantennal ridge, partly at the interantennal apodeme. The M. frontolabralis (0lb1) originates at the interantennal ridge in all Zygoptera, *Epiophlebia*, Neopetaliidae, Austropetaliidae, *Tachopteryx,* and *Procordulia*. The muscle originates at the interantennal ridge in all studied Aeshnidae, Cordulegastridae, Petaluridae (except *Tachopteryx*), Libellulidae, Macromiidae, and *Cordulia* (Corduliidae).

110. Origin of M. frontoepipharyngalis (0lb2): (0) partly

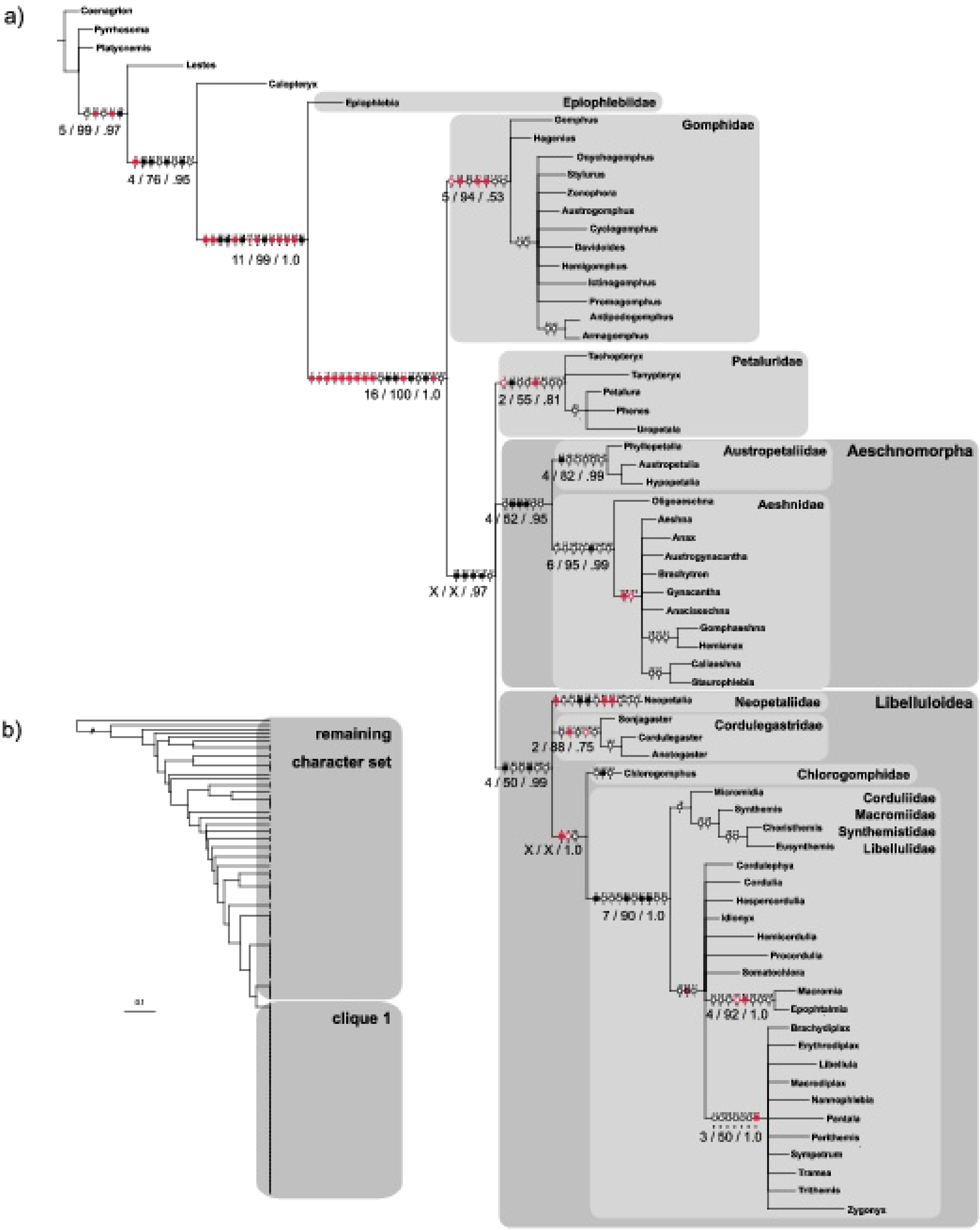

Fig. 7 Strict consensus (length = 409; CI = 39; RI = 83) of the 4680 equally parsimonious trees derived from maximum parsimony analysis of the complete morphological dataset. Support values from maximum parsimony and Bayesian inference are mapped on the tree. Bremer support=first node value, bootstrap support=second node value, posterior probability=third node value. X indicates Bremer support below 2, bootstrap support below 50 or a posterior probability below 0.7, respectively. b) UPGMA clustering of the pairwise excess index matrix calculated in PAUP. Clustered characters are indicated by a vertical terminal line. For a detailed tree with all characters mapped see Electronic supplement (ES) 4.

on the interantennal ridge, partly on the interantennal apodeme; (1) only on the interantennal apodeme; (2) only on the interantennal ridge. The M. frontoepipharyngalis (0lb2) originates partly on the interantennal ridge in all Zygoptera, *Epiophlebia*, and Gomphidae. It originates completely on the interantennal apodeme in Neopetaliidae, Aeshnidae, Petaluridae (except *Tachopteryx*), Libellulidae, Macromiidae, *Cordulia*, and *Sonjagaster*.

111. M. labroepipharyngalis (0lb5; Figs 5+6): (0) one muscle bundle; (1) two distinct muscle bundles. The M. labroepipharyngalis (0lb5) is split up into two distinct muscle bundles in Aeshnidae and the corduliid *Procordulia*.

112. M. labroepipharyngalis (0lb5; Figure 4+5): (0) originating directly ventral of the labral ridge; (1) originating centered on the labium; (2) one bundle centered on the labium, the other directly ventral to the labral ridge. The M. labroepipharyngalis (0lb5) originates directly ventral of the labral ridge in Neopetaliidae, Cordulegastridae, Corduliidae, and *Phenes* (Petaluridae). The muscle originates further ventral in the center of the labium in all studied Zygoptera, Austropetaliidae, Gomphidae, and all remaining Petaluridae.

113. M. craniomandibularis internus (0md1; Figure 5): (0) without second origin; (1) with two clearly seperated, well defined origins. The main adductor of the mandible (0md1) possesses a clearly seperated second origin in all studied Gomphidae, Libellulidae, Corduliidae, and the petalurid *Tachopteryx*.

114. M. craniomandibularis externus (0md3; Figure 5): (0) with one origin; (1) with two clearly seperated, well defined origins. The abductor of the mandible (0md3) possesses a clearly seperated second origin further proximal in all studied Gomphidae, Neopetaliidae, *Calopteryx, Epiophlebia, Oligoaeshna,* and *Tachopteryx.*

115. Origins of M. craniomandibularis externus (0md3): (0) only ventral of M. craniomandibularis internus (0md1) and M. craniolacinialis (0mx2); (1) one origin ventral of 0md1 & 0mx2, one dorsal of 0mx2; (2) one origin ventral of 0md1, one origin dorsal of 0md1. The origin of the abductor of the mandible (0md3) is ventral of the 0md1 in all studied Zygoptera (except *Calopteryx*), Aeshnidae, Austropetaliidae, Cordulegastridae, Libelluloidea, and all Gomphidae except *Gomphus.* If composed of two bundles this muscle originates with one bundle ventral of 0md1 and with the other one dorsal of 0md1 in *Epiophlebia*, Neopetaliidae, and *Gomphus.*

116. M. tentoriomandibularis medialis superior (0md7; Figure 4): (0) present; (1) absent. The M. tentoriomandibularis medialis superior (0md7) is absent in *Calopteryx, Epiophlebia*, Aeshnidae, Libellulidae, Corduliidae, and Macromiidae.

117. Insertion of M. tentoriomandibularis medialis superior (0md7; Fig. 4): (0) on the ventral side of the anterior tentorial arms near the base; (1) on separate apodeme posterior of the anterior tentorial arms; (2) on the posterior side of the dorsal tentorial arm base. In those taxa where the 0md7 is present its insertion varies. It inserts near the base of the anterior tentorial arm on its ventral side in *Lestes*, on a separate apodeme posterior of the anterior tentorial arms in Gomphidae and all Petaluridae (except *Uropetala*), and on the posterior side of the base of the dorsal tentorial arms in all remaining Zygoptera, Austropetaliidae, Cordulegastridae, and the petalurid *Uropetala*.

118. M. craniocardinalis (0mx1): (0) with only one origin; (1) with two clearly seperated, well defined origins. The M. craniocardinalis (0mx1) possesses a second origin in *Uropetala* (Petaluridae) and *Zygonyx* (Libellulidae).

119. M. tentoriobuccalis anterior (0bu5): (0) present; (1) absent. The M. tentoriobuccalis anterior (0bu5) is absent in all studied Aeshnidae except *Oligoaeschna*.

120. Location of pharynx (Figs 5+6): (0) in touch with the corpotentorium ; (1) not in touch with the corpotentorium. The pharynx is not in contact with the corpotentorium in all studied Aeshnidae,

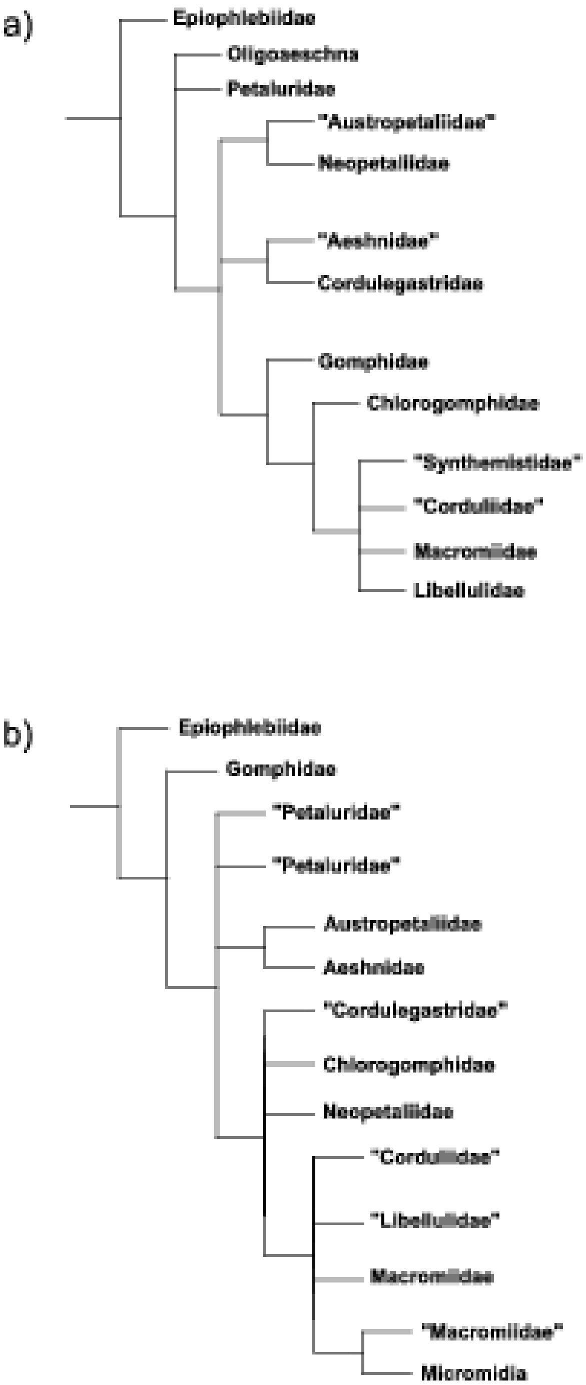

Fig. 8 Phylogenies calculated from the significant clique of characters (a) and from the remaining characters (b) of the morphological data matrix. Parsimony analyses in TNT, 1000 heuristic searches with random addition of taxa (TBR branch swapping). a) Strict consensus of 37 trees; 50 characters; tree length = 70; RI = 98; CI = 91. b) Strict consensus of 3750 trees; 69 characters; tree length = 398; RI = 73; CI = 24. Para- or polyphyletic groups are put in quotation marks.

Cordulegastridae, *Lestes*, and *Tachopteryx*.

Phylogenetic results

Phylogenetic analysis of the morphological data (Fig. 7) resulted in 4680 equally parsimonious trees. In the following we will only focus on the interfamily relationships. Generally, all currently recognized anisopteran families except Corduliidae were recovered as monophyletic. In a strict consensus (length=409; Ci=39; Ri=83) *Epiophlebia* is recovered as sister to all Anisoptera (= Epiprocta fide Lohmann (1996)) with high support (BR11 / PB99 / PP1.0). The head morphology of Epiprocta is characterized by an enlarged frons and vertex (3:1; 12:0,1,2,4,5), a globular shape of the head (9:0), and a distance between the eyes never greater than their own width (10:0,2,3). Apomorphies related to the wing are the relative size of the anterior and posterior lobes of the FxC sclerite (14:1), the general shape of the wing (17:1), the position of the arculus (24:1), the wing position at rest (52:0), and the obliquity of the thorax (64:0). The shape of the anterior hamules (68:3), presence of an epiproct (74:0), and the configuration of the paraprocts (76:0) are potential apomorphies of Epiprocta related to the copulatory system, while presence/absence of nymphal caudal (83:0) and rectal gills (84:1), and the absence of nymphal raptorial setae (86:0) are the larval characters supporting monophyletic Epiprocta.

Monophyletic Anisoptera (BR16 / PB100 / PP1.0) split into monophyletic Gomphidae (BR5 / PB94 / PP.53) which are sister to all remaining Anisoptera. Unique head

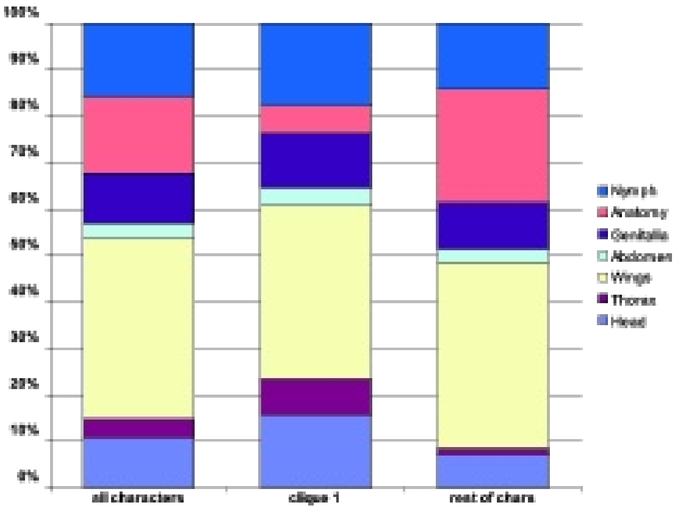

Fig. 9 Distribution of characters in the complete data matrix (left bar) and in the derived character clique (middle bar) and in the remaining amount of characters (right bar).

characters of Anisoptera are the arrangement of the anteclypeus and postclypeus (0:1) and the presence of an interantennal (103:1) and epistomal apodeme (104:1). Wing characters are the shape of the BxC sclerite (13:2), the origin of the MP vein (23:3), the structure of the quadrangle (32:2; 37:2), presence of a costal nodal kink (39:1), a membranule (40:1), a secondary CuP-vein (51:1), and an anal triangle (54:1) as well as the width of the MA-MP field (48:1). Further apomorphies are the segmentation of the vesica spermalis (71:1) and the presence of auricles (78:1).

Gomphidae are supported by one head apomorphy, the peculiar origin of the M. frontolabralis (0lb1; 109:2) and several nymphal characters: the structure of the antennae (89:1; 91:1) and mesotarsi (92:1). All other Anisoptera group together through the following synapomorphies: the configuration of the hamules (68:2), the fixed molar lobes of the nymphal mandible (99:2), the loss of rasp-like dentitions in the ventral dental folds of the proventriculus (102:1), and origin of the M. frontoepipharyngalis (0lb2) at the interantennal apodeme (110:1).

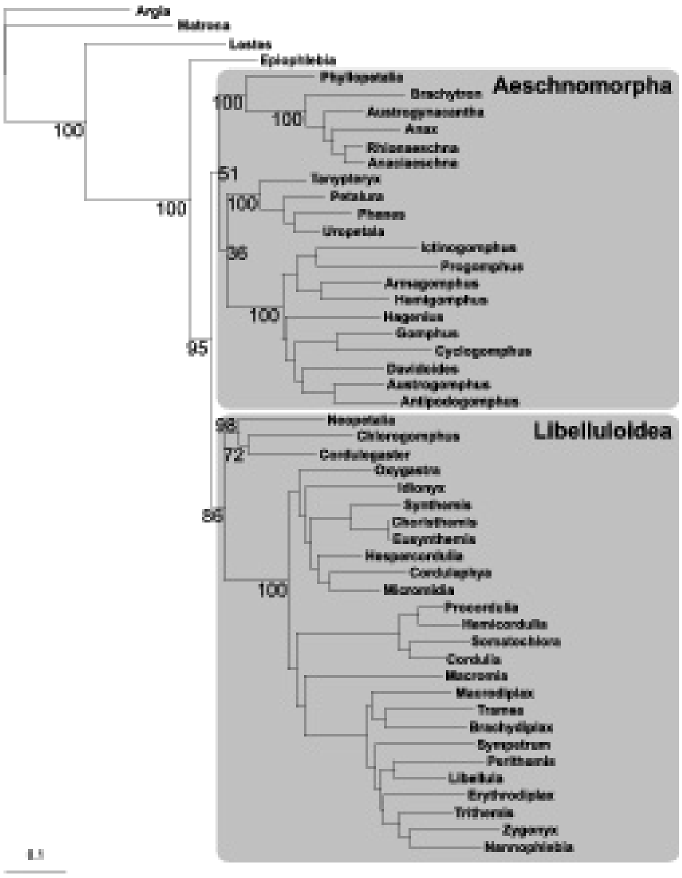

Fig. 10 RaxML analysis of the molecular data showing unsupported Aeshnomorpha, Petaluridae + Gomphidae and Chlorogomphidae + Cordulegastridae. Support values are only shown for the deep level relationships. See Supporting Information (SI) 5 for a tree with all support values mapped.

The position of Petaluridae (BR2 / PB55 / PP81) could not be resolved with the available data. Apomorphies supporting monophyletic Petaluridae are the shape of the vertex and the location of the ocelli (12:5) and the length of the pterostigma (56:1). Austropetaliidae are the sistergroup of Aeshnidae (BR4 / PB52 / PP.95) through the orientation of the anterior hamuli (67:1), the structure of the anterior lamina (69:1) and vestigial posterior hamules (72:1). Monophyletic Austropetaliidae (BR4 / PB82 / PP.99) are supported by the shape of the vertex and the location of the ocelli (12:1), monophyletic Aeshnidae (BR6 / PB95 / PP.99) by the origin of the bundles of the M. labroepipharyngalis (0lb5; 112:2). Libelluloidea (BR4 / PB50 / PP.99) are supported by the scoop-shaped form of the labium (85:1) and the toothed distal margin of the prementum (95:1) with *Neopetalia* as sister to all remaining Libelluloidea. Potential autapomorphies of *Neopetalia* are the triangular shape of the labial palp (1:3), the U-shaped external hamules (68:5), the undivided epiproct (75:4), the ventroapical tufts of long hairs on abdominal segments 5-8 (80:1), and the number of raptorial setae (1-3) on the prementum (87:2). The position of Cordulegastridae (BR2 / PB88 / PP.75) inside Libelluloidea is unresolved. The data support a basal position and the monophyly of the group through the quadrangular form of the male mesotibial spines (63:1). Chlorogomphidae is recovered as the sistergroup of Corduliidae, Synthemistidae, Macromiidae and Libellulidae (BR7 / PB 90 / PP1.0) which is supported by the well-developed anal loop (50:2). Corduliidae are polyphyletic, Macromiidae (BR4 / PB92 / PP1.0) are supported by the presence of horns between the eyes (82:1), Libellulidae by the triquetral abdomen (81:1).

Concerted convergence analysis (CCA) of the morphological dataset yielded one significant clique (Fig. 7b) containing 51 characters (the clique threshold size for significance was 24 characters). Parsimony analysis of the characters contained in this clique yielded 37 equally parsimonious trees. In a strict consensus (Fig.

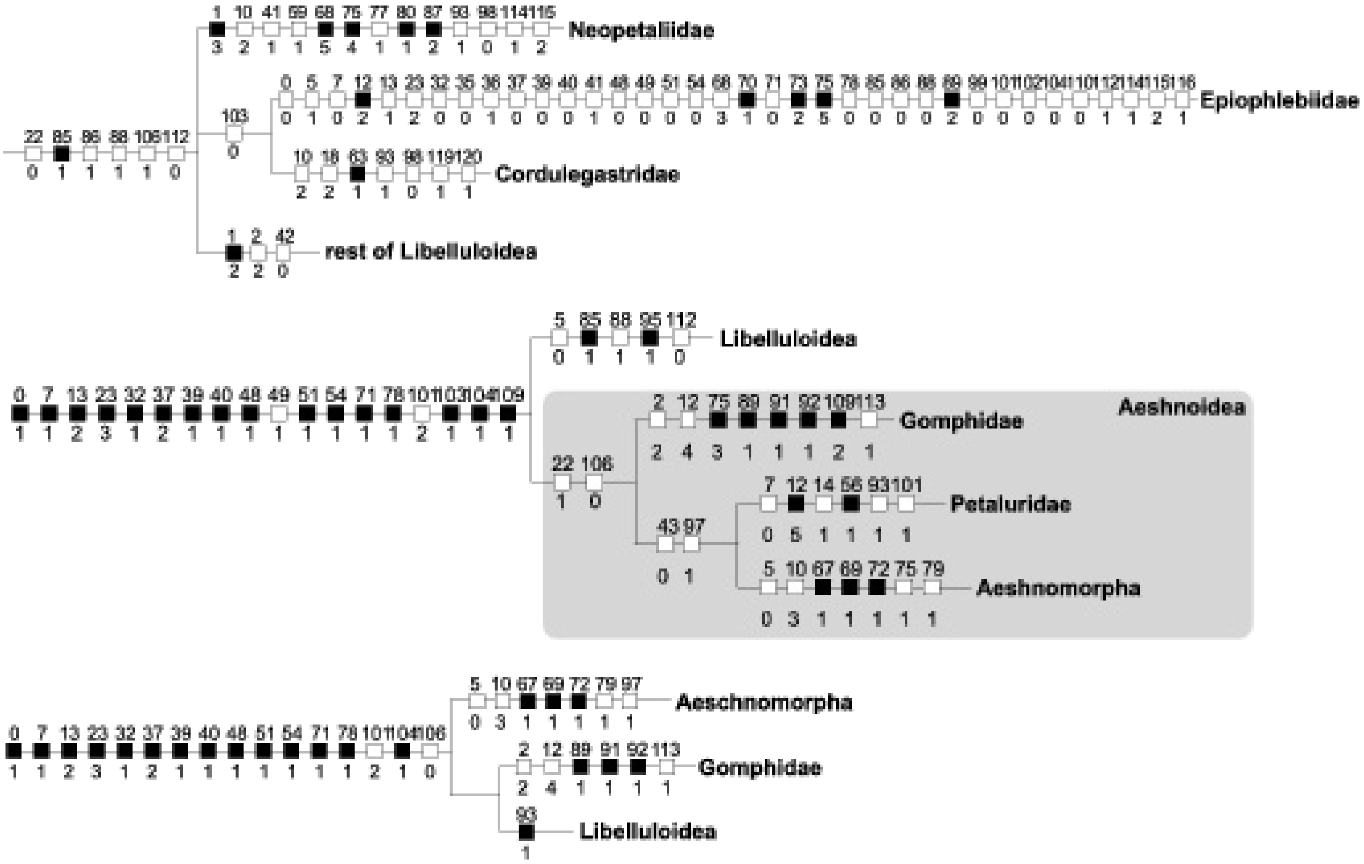

Fig. 11 Character optimizations on the CTRs (suboptimal tree resolutions) of the three enforced hypotheses concerning the deep splits inside Anisoptera. (a) strict consensus enforcing a sistergroup relationship of Ephiophlebiidae + Cordulegastridae (EC hypothesis (Dumont et al., 2010); length = 436 steps, CI = 37, RI = 81). b) strict consensus with enforced Aeshnomorpha as sister to all remaining Anisoptera (AA hypothesis (Letsch et al., 2009); length = 413 steps, CI = 39, RI = 83). c) strict consensus with enforced Aeshnoidea as sister to Libelluloidea (AL hypothesis (Fleck et al., 2008b); length = 410 steps, CI = 39, RI = 83). Non-homoplasious character changes are indicated with black squares, homoplasious characters with white squares. Trait numbers are indicated above squares, state changes below. For trait reference see Supporting Information (SI) 2 or the Appendix.

8a; length=70; Ci=91; Ri=98) Anisoptera are monophyletic with *Oligoaeschna* and Petaluridae branching off first. Paraphyletic Austropetaliidae group together with *Neopetalia*, ’Aeshnidae‘ with monophyletic Cordulegastridae. Gomphidae are the sistergroup to all remaining Libelluloidea, Synthemistidae and Corduliidae are retrieved as paraphyletic groups.

Parsimony analysis of the remaining character set excluding clique 1 produced 3750 equally parsimoneous trees. The strict consensus (Fig. 8b, length=398; Ci=24; Ri=73) resulted in Gomphidae as sistergroup to all remaining Anisoptera. ’Petaluridae‘ are polyphyletic, Austropetaliidae and Aeshnidae are sistergroups. Libelluloidea are monophyletic, however, the position of ’Cordulegastridae‘, Chlorogomphidae, and *Neopetalia* could not be resolved, whereas ’Corduliidae‘, ’Libellulidae‘ and Macromiidae form a clade. The character distribution among the clique and the remaining characters (Fig. 9) showed a higher number of head and thorax characters in the clique compared with the number of head characters in the complete matrix, while fewer anatomical characters are represented in the clique.

Discussion

Epiophlebiidae is the sistergroup to Anisoptera

A study based on the morphology of the ovipositor of *Epiophlebia* (Matushkina, 2008a) stated that *Epiophlebia* exhibits some similarties with the ovipositor organisation in Zygoptera, and Dumont (2010) recovered *Epiophlebia* as the sistergroup to Cordulegastridae (EC hypothesis) based on the analysis of 18S, 5.8S and ITS1 & 2 sequences. Klass (2008), in an overview of ovipositor bearing Odonata, found no abdominal characters resolving the position of *Epiophlebia.*

From a morphological perspective (Blanke et al., 2012a) the above mentioned groupings seem to be unlikely and they are neither found in the phylogenetic analysis of the present study. A CTR of the EC hypothesis resulted in a tree 17 steps longer than the most parsimonious strict consensus with multiple homoplastic changes for Epiophlebiidae and Cordulegastridae (Fig. 11). Also, after concerted convergence analysis (CCA) *Epiophlebia* remains sistergroup to Anisoptera. Most other molecular studies also support this position (Bybee et al., 2008; Fleck et al., 2008b; Letsch et al., 2009)

Gomphidae is the sistergroup of all remaining Anisoptera

Gomphidae as sistergroup to all other Anisoptera was always recovered and the family retained its position after concerted convergence analysis (CCA). A sistergroup relationship of Gomphidae with all remaining Anisoptera was first proposed by Carle et al. (1982). In the present study this position is supported by the internal and hooked-like structure of the anterior hamules (68:3), the moveable molar lobes of the left and right mandible (99:0), the presence of rasp-like dentitions on the ventral dental folds of the proventriculus (102:0; Fleck (2011)), and the peculiar origin of the M. frontoepipharyngalis (0lb2) on the interantennal ridge as well as on the interantennal apodeme (110:0; Fig. 4). Although these character states are plesiomorphic since they are shared with Epiophlebiidae, Gomphidae share the states of characters 0, 7, 13, 23, 32, 37, 39, 40, 48, 51, 54, 71, 78, 103, and 104 with Anisoptera (see Fig. 7 and SI2 [?] for details). The remaining Anisoptera except Gomphidae are supported by several potential autapomorphies: the internal and folded anterior hamules (68:2), the fixed molar lobes of the mandibles (99:2), the absence of rasp-like dentitions on the ventral dental folds of the proventriculus (102:1), and the origin of M. frontoepipharyngalis solely on the interantennal apodeme (110:1).

A recent molecular study using mitochondrial sequence data and secondary RNA structure information suggested a clade Aeshnoidea comprised of Gomphidae, Petaluridae, Austropetaliidae, and Aeshnidae (Fleck et al., 2008b). With the exception of *Neopetalia* which was transferred to Libelluloidea (Carle and Louton, 1994) this clade was already proposed by Fraser (1957). However, this pre-Hennigian classifications was based on symplesiomorphies. Fleck et al. (2008b) already pointed out that a hypothetical clade Aeshnoidea is only backed up by one putative synapomorphy, the fusion of sternites and postpleurites in larval abdominal segments 9. Instead, the grouping Aeshnoidea would imply an independent reduction of the ovipositor in Gomphidae and libelluloid lineages. A position of Gomphidae within ’Aeshnoidea‘ is equally not supported by any character of the present matrix and requires one additional step in CTR (Fig. 11).

Other morphological (Bechly, 1996; Lohmann, 1996) and molecular (Misof et al., 2001) studies proposed a sistergroup relationship Gomphidae + Libelluloidea which was not favoured by Carle (1995), since he considered larval characters and structures related to the male copulatory apparatus as homoplastic. Again, a relationship of Gomphidae with Libelluloidea is not supported by any character of the present matrix and a CTR enforcing this relationship requires 4 additional steps (Fig. 11). In our study the position of Gomphidae as sister to all other Anisoptera was also corroborated by CCA and this results in an additional putative synapomorphy for the remaining Anisoptera, the internal and folded structure of the anterior hamules (68:2).

Aeshnoidea and Libelluloidea are monophyletic

The present study supports Aeshnomorpha, Aeshnidae + Austropetaliidae. Besides the characters presented herein, monophyletic Aeshnidae are supported by the well developed median and radial planates of the wings (Bechly, 1996; Carle, 1996; Lohmann, 1996). In contrast to Bechly we consider the well developed "interocellar lobe" (=vertex) not as an autapomorphy of Aeshnidae, since several taxa, especially Libellulidae and Cordulegastridae also possess a well developed vertex.

Aeshnomorpha are well supported by molecular and morphological studies, since the establishment of Austropetaliidae and placement of *Neopetalia* inside Libelluloidea (Carle and Louton, 1994). *Neopetalia* is

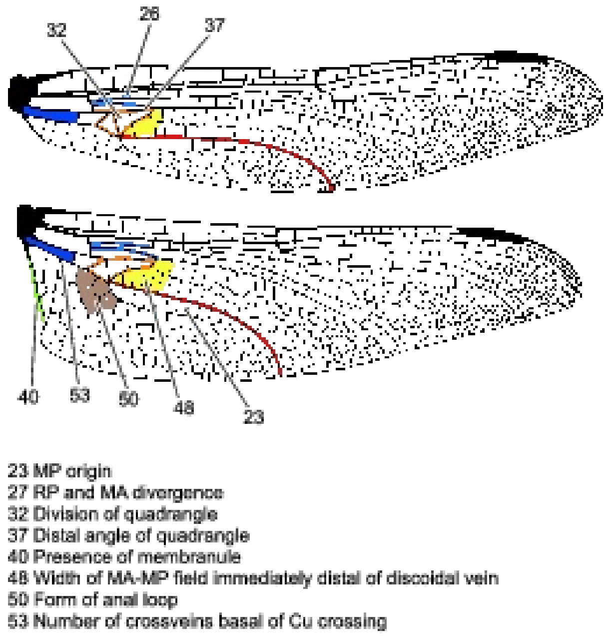

Fig. 12 Illustration of a part of the wing characters which clustered in the clique. For a complete overview of the characters which clustered in the clique please refer to supporting information. For a complete character list including the character numbering of Rehn 2003 and Bybee et al. 2008 see the supporting information as well.

only superficially resembling Austropetaliidae in wing colour pattern (Garrison et al., 2006) and a quadrate epiproct (Carle et al., 2008). Accordingly, similarities between Aeshnidae and Libellulidae like the contiguous eyes and the structure of the anal loop are homoplasies (see also Carle et al. (2008)).

Our analyses support monophyly of Libelluloidea albeit with low bootstrap support. The result is in line with many molecular studies, where Libelluloidea are recovered with low support values (Fleck et al., 2008b; Letsch et al., 2009). Morphologically the clade is supported by the spoon-shaped labial mask of the nymph as was already proposed by others (Carle, 1995; Lohmann, 1996). Still, convincing imaginal synapomorphies are lacking and the anatomical characters included here provide no further support for this clade.

The position of Petaluridae remains unresolved

The position of Petaluridae is not robustly resolved in other studies and could not be resolved in the present study either. Molecular studies recovered the family either as sister to Gomphidae (Misof et al., 2001), as sister to Aeshnomorpha (Fleck et al., 2008b), as sister to Libelluloidea (Carle et al., 2008), or as sister to Chlorogomphidae + Cordulegastridae (Bybee et al., 2008).

Using wing characters, Trueman (1996) proposed Petaluridae as sister to all remaining Anisoptera as did Rehn (2003) based on characters of the whole body. Pfau (1991) focused on genitalic characters and proposed a sistergroup relationship of Petaluridae to a clade consisting of Gomphidae, Cordulegastridae, and Petaluridae. Recently, Fleck (Fleck, 2011) hypothesized a sistergroup relationship of Petaluridae with Aeshnomorpha based on the structure of the mandibles, the proventriculus, and the anal pyramid in nymphs as well as the styli of the ovipositor and the terminalia. However, as the author himself stated, these characters are prone to convergence or their status in certain taxa is unclear. We adopted those characters for which homology hypotheses are clear and taxon sampling was sufficient (characters 94, 98, 99, 101, 102) but they did not serve to clarify the position of Petaluridae.

Potential homoplasy in head characters

CCA of the complete dataset yielded one character clique of significant size (Fig. 7b). This clique contained a high amount of head characters while the amount of anatomical characters is reduced compared to the character distribution in the remaining matrix (Fig. 9). Head characters of the clique are mainly related to the general head structure and the configuration of the labium. The ante- and postclypeus facing anteriorly (0:1), the grossly enlarged shape of the frons (3:1), and presence of an epistomal apodeme (ea, 104:1) are characters influencing the general globular shape of the head (9:0). According to the present CCA the characters seem to be correlated to each other and should therefore be excluded from further analyses. The globular head shape already accounts for the modifications of certain substructures (clypeus, frons, ea).

Wing base characters evolved concerted convergent

The number of wing characters did not differ significantly between the three datasets (original matrix, clique and remaining subset), however, character distribution in the clique is interesting. A high amount of characters (8 out of 19 = 42%) are related to the wing base (Fig. 11), specifically to the quadrangle area (23 / 26 / 32 / 37 / 48) and the anal loop area (40 / 50 and probably 53).

Wootton & Kukalová-Peck (2000) already identified two areas in the palaeopteran wing - the leading edge-nodus complex and the arculus - which are responsible for the flight capabilities in modern Odonata. Based on this Bybee et al. (Bybee et al., 2008) mapped wing characters onto their inferred tree and identified the pterostigma-nodal brace complex as well as the costal wing base & costal-ScP junction complex as areas where key innovations during the transition from ancient flight styles only represented by fossils to modern" flight styles took place (modern including all extant odonate groups plus fossil Tarsophlebiidae). According to the authors, these complexes also showed convergent evolution (Bybee et al., 2008).

Concerning extant taxa [+ Tarsophlebiidae?], we propose that especially the wing base venation may have evolved concerted convergent (Fig. 11). Changes in the origin of the MP vein (23) and the width of the MA-MP field (48), as well as the divergence of the RP and MA veins (26) and several characters of the quadrangle (32, 37), anal loop (50), and membranule (40) seem to be correlated to each other. However, we judge it too early to map these wing characters on the strict consenus tree reconstructed. First wing character state shifts within families are present, and second the resolution within families using the present character set is too low. This hampers estimation of a wing venation pattern common to e.g. all Gomphidae (compare e.g. presence of an anal loop in different taxa of Gomphidae and Petaluridae, or the changing division of the quadrangle within all families). Therefore, a drastically increased taxon sampling within studies focused on reconstructions of wing venation patterns among anisopteran families is warranted.

The present CCA analysis shows that the amount of concerted convergence is high in the wing base area (Fig. 11). To further corroborate these results by an independent data set, functional analyses are needed simulating the effect of single vein changes on the vein system. These functional analyses can also be done with the wing venation pattern of fossil taxa, since the wing preservation status is often excellent (Bechly, 1995).

Conclusion

A sistergroup relationship of Gomphidae + remaining Anisoptera is most parsimoneous when taking into account all currently available characters. Analyses of concerted convergence reveal the presence of a single clique of characters which support an alternative but implausible tree. Tree reconstruction using the remaining character set corroborated the position of Gomphidae. Analysis of the significant *clique* showed that especially head - and to a minor extend - thorax characters need extensive reevaluation with regards to possible interdependence of characters. Moreover, characters related to wing venation showed an unusual distribution among the significant character clique. Results suggest that especially the wing base venation may harbour concerted convergent characters.

Character distribution analysis shows that characters of internal anatomy do not group into cliques, meaning that interdependencies are not likely for these characters. Further studies, especially focused on the internal anatomy of the copulatory apparatus will likely yield new phylogenetically informative characters which can be analysed with the analysis framework presented herein.

Acknowledgment

Ryuchiro Machida kindly provided specimens of *E. superstes*. The morphological data was mainly gathered at the Deutsches Elektronen Synchrotron (DESY, Hamburg, Germany) with support from grants I-20080169 and I-20090211, the Paul-Scherrer Institut (PSI, Villigen, Switzerland) through grant no. 20110069 and at the Steinmann Institut (Bonn, Germany) which is gratefully acknowledged. We sincerely thank Barbara Holland who provided useful assistance with the implementation of her concerted convergence analysis and Jessica Ware who gave useful comments throughout the preparation of this paper.

9

The head anatomy of *Tricholepidion gertschi* (Zygentoma)

The head anatomy of Tricholepidion gertschi (Zygentoma)

The head anatomy of Tricholepidion gertschi: head morphology points towards a sistergroup relationship with Zygentoma.

Alexander Blanke[1]*, Markus Koch[2], Benjamin Wipfler[3], and Bernhard Misof[1]

[1]Zoologisches Forschungsmuseum Alexander Koenig, Zentrum für molekulare Biodiversität, Adenauerallee 160, 53113 Bonn, Germany;
[2]Institute of Evolutionary Biology and Animal Ecology, University of Bonn, An der Immenburg 1, 53121 Bonn, Germany;
[3]Entomology Group, Institut für Spezielle Zoologie und Evolutionsbiologie, Friedrich-Schiller-Universität Jena, Erbertstraße 1, 07743 Jena, Germany
*Corresponding author: E-mail address: blanke@uni-bonn.de

This is the author’s version of a manuscript prepared for publication in the journal Arthropod Structure & Development

Abstract

The relic silverfish Tricholepidion gertschi is the sole surviving representative of the family Lepidotrichidae and is considered a "living fossil". Its phylogenetic position is unclear: a basal position within silverfish (Zygentoma) as well as a position as sister to all Dicondylia (silverfish and winged insects) have been discussed.
This makes Tricholepidion of special interest, since it may deliver insights into the evolutionary history at the stemline of Dicondylia, containing the most successful lineage of insects, the Pterygota.
Here we present the so far most detailed description of the head of Tricholepidion. A strong focus is put on the documentation of mouthparts and the anatomy of the endoskeleton as well as the muscle equipment. Based on this documentation we discuss its phylogenetic position. The presented results indicate a sistergroup relationship with the remaining zygentomans.

Introduction

The relic silverfish *Trichlepidion gertschi* occuring occurs only in the coastal region of northern California and is the sole representatitve of the family Lepidotrichidae (sensu Wygodzinsky (1961)). The species is characterized by a number of plesiomorphies such as …. And was therefore considered to represent an ancient lineage. This is also reflected in the discussion concerning its phylogenetic placement Wygodzinsky (1961) placed *Trichlepidion* together with Lepidothrix in the family Lepidotrichidae based on the lack of ocelli in all other Zygentoma (see also Boudreaux (1979) and Sharov (1966)) and favoured a sistergroup relationship with Nicoletidae within Zygentoma. The monophyly of Zygentoma was argued through the occurrence of sperm conjugation (or sperm pairing) (Kristensen, 1991)(Wingstrand 1973, Kristensen 1991), although the former author also emphasized doubts as to the monophyly of Zygentoma. Large abdominal sterna with posteriorly attached coxopodites and a large number of pregenital styles and eversible sacs were interpreted as primitive traits not shared with other Dicondylia (BELEG). Lepidotrichidae were also hypothesized as sister to all Dicondylia rendering Zygentoma as paraphyletic (Kristensen, 1997; Stys and Zrzavy, 1994). In a detailed study on the sperm ultrastructure and sperm pairing mode of *Trichlepidion* Dallai et al. (2001a; 2001b) found that the sperm pairing

Head Structures of Dicondylia

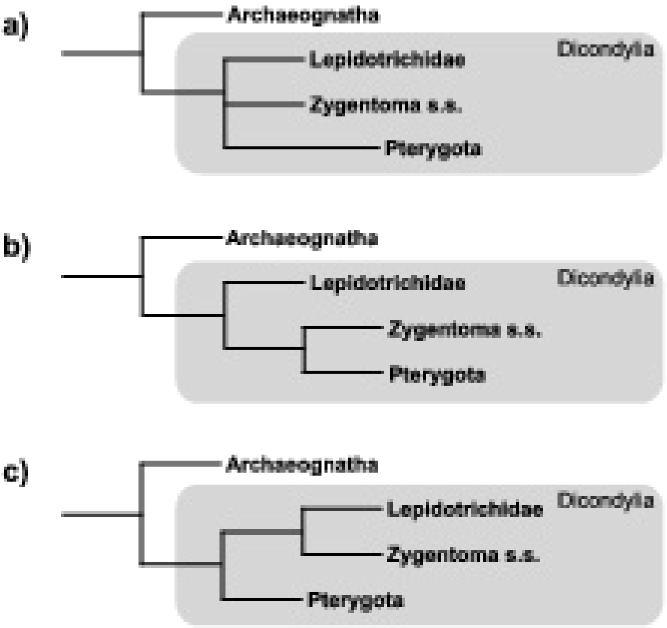

Figure 1 Hypotheses concerning the phylogenetic position of Lepidotrichidae. a) the position of Lepidotrichidae remained unclear after analysis of cephalic characters (Staniczek, 2000; Staniczek, 2001) and characters of the whole body with a focus on attachment structures (Beutel and Gorb, 2006). b) Lepidotrichidae as the sistergroup to all remaining Dicondylia were hypothesized by Kristensen (1997) and Stys & Zrzavy (1994). c) Lepidotrichidae as the sistergroup to the remaining Zygentoma (however, with varying families as the closest relative) were hypothesized by Engel (2006), Sturm (1997), and Wygodzinsky (1961).

mechanism is not directly comparable to the one in other Zygentoma.

In contrast, Sturm (1997) pointed out the analogies between the mating behaviour of *Trichlepidion* & Lepismatidae. Finally, Engel placed *Trichlepidion* in its own family Tricholepidiidae as sister to all other Zygentoma (including Lepidothrix = Neozygentoma Engel (2006)). In contrast to Wygodzinsky, he proposed the dorsoventral flattening of the body as a synapomorphy uniting all Zygentoma and the loss of ocelli as the synapomorphy uniting Neozygentoma.

Knowledge of the exact phylogenetic position of *Trichlepidion* would provide valuable information to understand the evolution of several morphologic characters at the stemline of Dicondylia, e.g. presence of a proventriculus (Wygodzinsky, 1961), sperm configuration, the general organisation of the head (Staniczek, 2000; Staniczek, 2001) and thorax (Barlet, 1981) including muscle equipment, and the number of ovarioles (Wygodzinsky, 1961).

So far cephalic data failed to deliver a definitive hypothesis for the phylogenetic relationships (Staniczek, 2000; Staniczek, 2001), as did a study of the whole body with a focus on attachment structures (Beutel and Gorb, 2006). Consequently, the present contribution aims to provide a detailed description of the head morphology of *Trichlepidion* with a strong focus on the documentation of mouthparts, endoskeleton and muscle equipment. With this, we hope to clarify the up to now unclear position of *Trichlepidion* regarding this character system.

Material and Methods

The anatomy was investigated using synchrotron micro-Computer Tomography (SR-microCT) (Betz et al., 2007). Prior to scanning, the sample was dried at the critical point (CPD) (Model E4850, BioRad) and mounted on specimen holders. Scanning was performed at the Paul-Scherrer Institut (PSI, Villigen, Switzerland) with a stable energy beam of 8 keV (Stampanoni et al., 2010). Subsequent segmentation and rendering was accomplished with Reconstruct (Fiala, 2005) and Blender (blender.org). Both software packages are distributed under the general public license (GPL). Final tables and figures were edited with GIMP, Inkscape and Scribus (all GPL).

A 3D model of the head of *Tricholepidion* is available (Online resource 1 [(OR 1])), which facilitates the identification of internal structures. The underlying program "Meshlab" can be downloaded free of charge under the GPL license from http://meshlab.sourceforge.net/, any other VRML97 file viewer should work as well but was not tested by us. Please use the "import function" in Meshlab to open the file.

For scanning electron microscopy (SEM) the specimen was transferred in a series of steps into 100% ethanol, dried at the critical point (Model E4850, BioRad), and sputter coated (Model Anatech Hummer VII). Microscopy was performed on a Hitachi S-2460N using a new type of rotatable sample holder (Pohl 2010).

Phylogenetic analyses

Parsimony analyses of the morphological character set (see Appendix 1) and Bremer, as well as bootstrap, support calculations were carried out with TNT (Goloboff

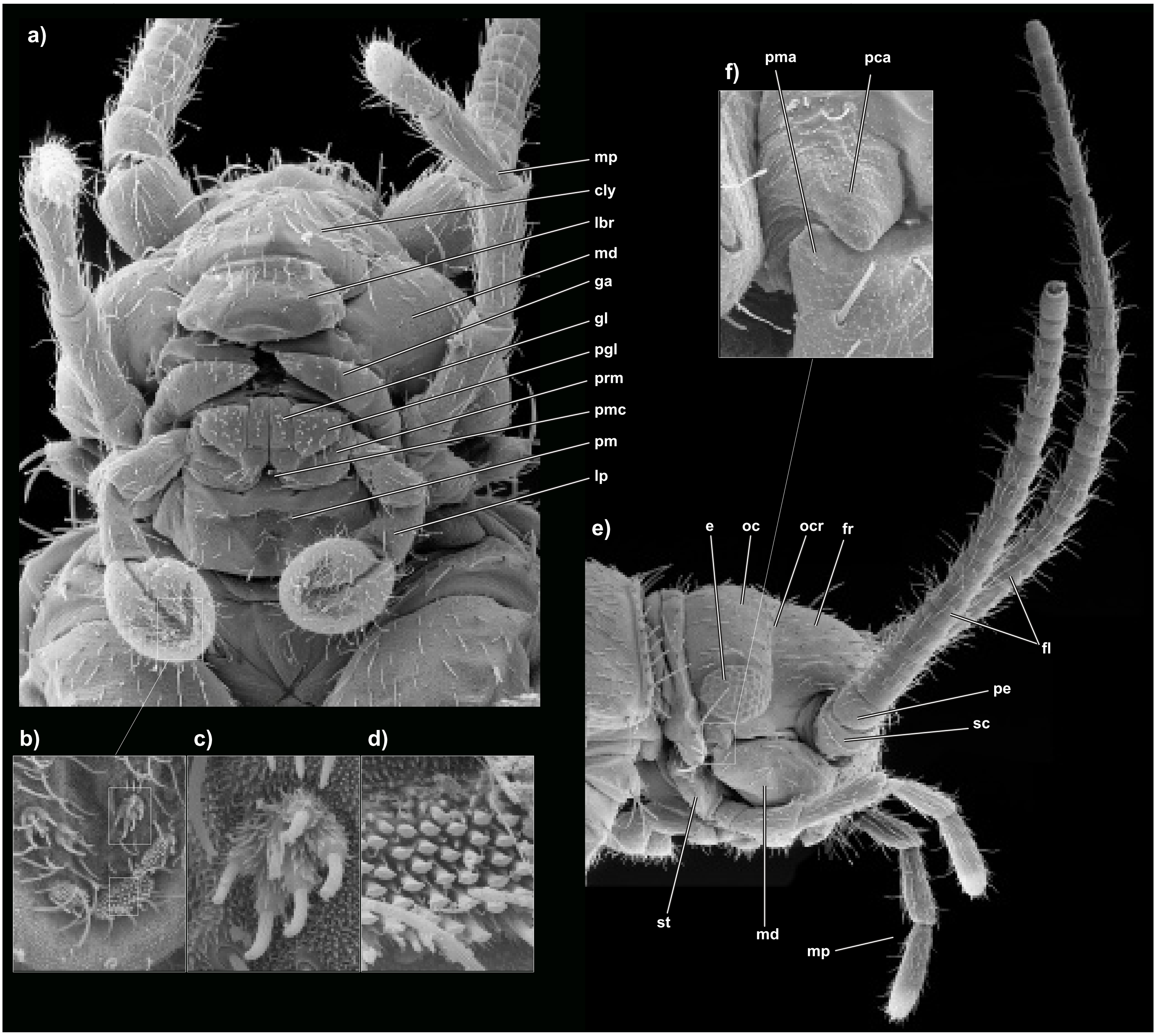

Figure 2 SEM micrographs of *Tricholepidion gertschi* a) ventral overview of the head; b) detail of the ventral side of labial palpus segment four; c) detail of the first sensilla type; d) detail of the second sensilla type; e) lateral overview of the head; f) detail of the posterior mandibular articulation. Abbreviations: cly, clypeus; e, eye; fl, flagellum; fr, frons; ga, galea; gl, glossa; lbr, labrum; lp, labial palpus; md, mandible; mp, maxillar palpus; oc, occiput; ocr, occipital ridge; pca, posterior cephalic articulation; pe, pedicellus; pgl, paraglossa; pma, posterior mandibular articulation; pmc, premental cleft; prm, prementum; sc, scapus; st, stipes. Scale bar = 1 mm.

clypeo-labral ridge where it is devoid of setae.

The epistomal ridge is located at half height of the antennal bases. An interantennal ridge is absent. The frons is of rounded form in lateral view. It continues ventral of the eyes until the postocciput. Thus, the frons forms the head part of the posterior mandibular articulation, a gena is absent. In dorsal view the frons appears like a semi cycle, its corners almost meeting the eyes anteriorly.

on the anterior arms and the tentorial plate. They are not in contact with the head capsule but instead connected to it by two muscle bundles (xx & YY). Posterad the dorsal arms the anterior plate narrows and gets again as wide as the anterior arms at height of the posterior mandibular articulation, where the posterior tentorial plate begins.

The posterior plate is connected to the anterior plate by

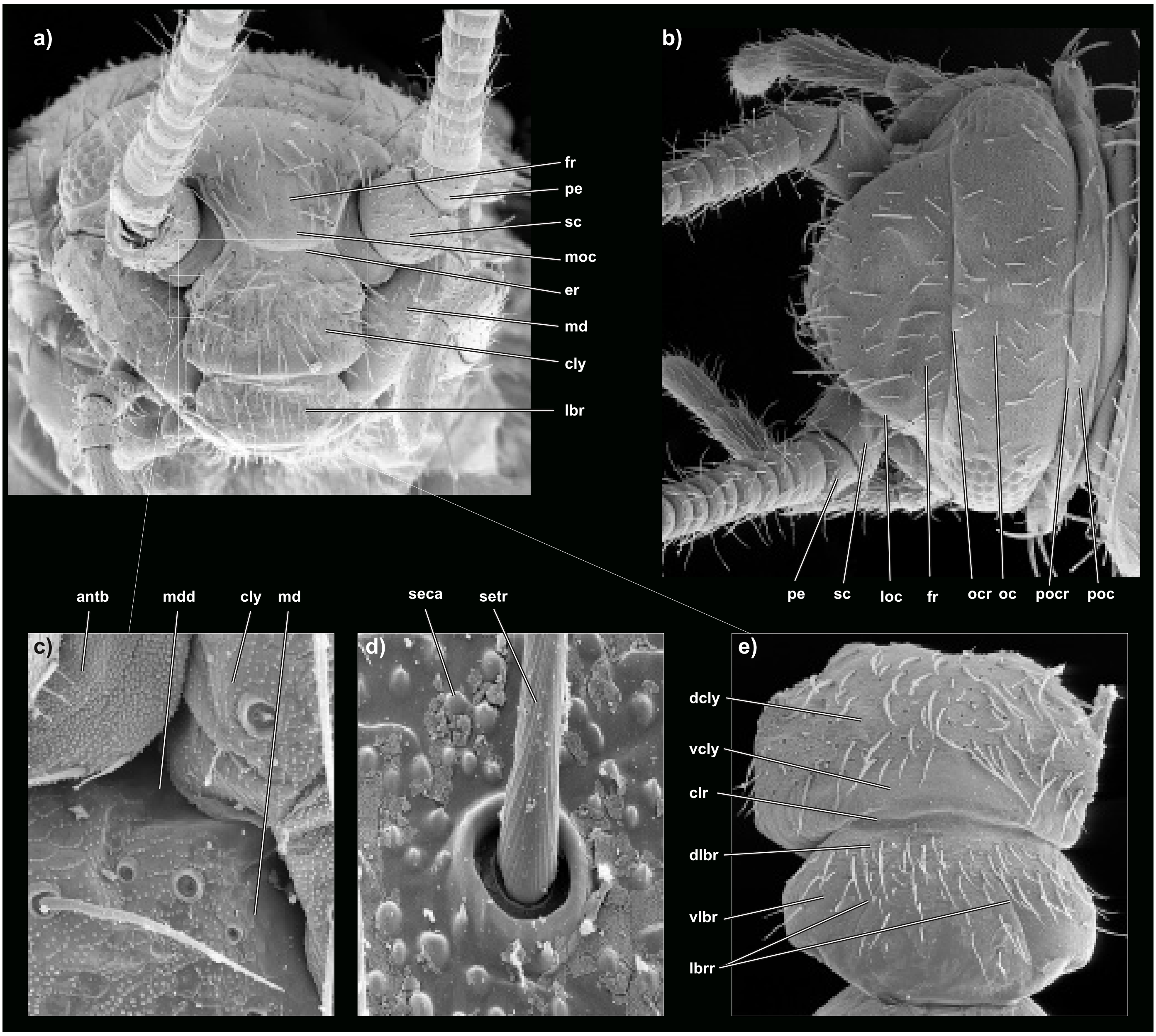

Figure 3 SEM micrographs of *Tricholepidion gertschi* a) frontal overview of the head; b) dorsal overview of the head; c) detail of the externally visible part of the anterior mandibular articulation; d) detail of a trichoid sensillium; e) detail of the clypeal region and the labrum. Abbreviations: antb, antennal base; clr, clypeo-labral ridge; cly, clypeus; dcly, dorsal clypeal region; dlbr, dorsal labral region; er, epistomal ridge; fr, frons; lbr, labrum; lbrr, labral ridge; loc, lateral ocellus; md, mandible; mdd, mandibular depression; moc, middle ocellus; ocr, occipital ridge; pe, pedicellus; pocr, postoccipital ridge; sc, scapus; seca, campaniform sensillium; setr, trichoid sensillium; vcly, ventral clypeal region; vlbr, ventral labral region. Scale bar = 1 mm.

muscles (XX & YY) and continues into the posterior tentorial arms. The posterior tentorial pits are not externally visible. They are located directly posterad the maxillar articulation.

Labrum

The convex labrum (Figure 3e) is covered with a stripe of trichoid and campaniform sensillae directly ventral the clypeolabral ridge. On the remaining labrum trichoid sensillae occur sporadically. The labrum partly covers the mandibles in frontal view and is moveably connected to the clypeus. Two thin dorsoventral ridges occur on the frontal side of the labrum but do not reach the apex.

Antennae

The antennal foramina are located XXX and directed

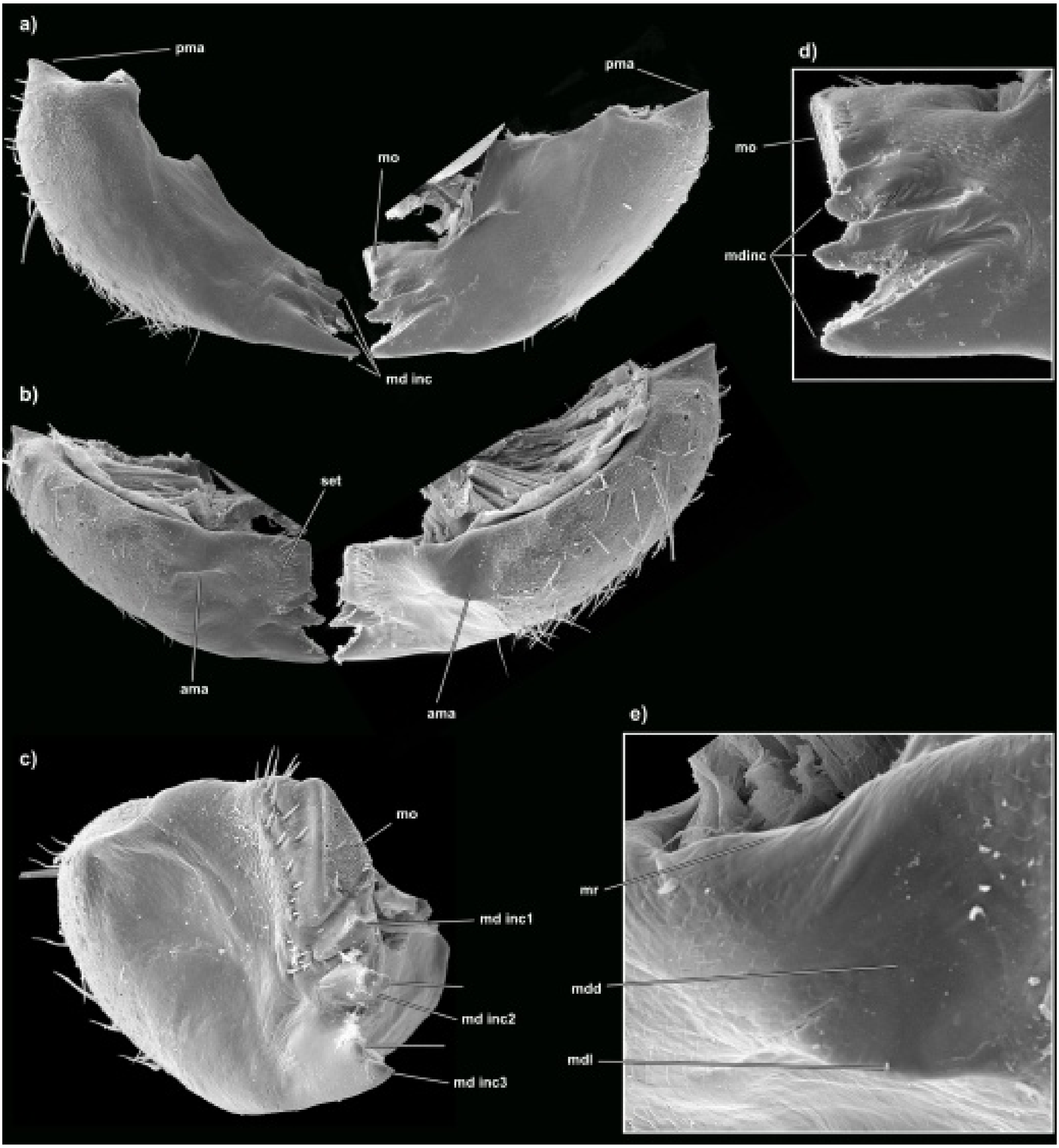

Figure 4 SEM micrographs of the mandibles of *Tricholepidion gertschi* a) posterior view; b) anterior view; c) mesal view; d) detail of the gnathal area of the left mandible; e) detail of the anterior mandibular articulation complex. Abbreviations: ama, anterior mandibular articulation; mdinc, mandibular incisivi; mdd, mandibular depression; mdl, mandibular lateral edge; mo, mola; mr, mandibular ridge; pma, posterior mandibular articulation; set, setae. Scale bar = 1 mm.

fronto-laterad. The membranous antennal bases are half as long as the scapus and entirely devoid of hairs (Figure 3a). The scapus is approximately one third longer and wider as the pedicellus. The first antennomere of flagellum is nearly as wide as the pedicellus but twice as long. All following antennormeres are shorter than the first one and become gradually thinner. The last one is approximately half as thick as the first one (Figure 2e).

Mandibles

The mandibles (Figure 4) are formed like an elongated bowl in dorsal view with an oval dorso-mesal oriented opening for attachment for various muscles inside the mandible lumen (see below). The mandibles are overall heavily sclerotised with the greatest wall thickness at the gnathal region (incisivi and mola) and the posterior and anterior mandibular articulation regions. Proximally, the mandibles are tapered forming an edge which harbours dorsally the mola and ventrally three incisivi. The gnathal edges are almost symmetrical on both mandibles.

The distalmost part of the mandibles bears the posterior mandibular articulation which is continuous with the overall form of the mandible, so that no distinct knob is formed. The anterior mandibular articulation complex is situated at height of the dorsal molar part, a short distance distal to it.

The anterior mandibular articulation complex is a concave depression with its opening directed anterad at a 45° angle (Figure 4e). Dorsad to this depression the mandible border is heavily sclerotized. The clypeus forms a process which fits into the depression. On the other side of the mandible border the anterior tentorial arms from a process reaching into the lumen of the mandible directly posterad the anterior mandible border. The two processes (clypeal and tentorial) thus form a "clasp" between which the mandible border lies, so that an antero-posterad movement is prevented.

The mola is almost formed like a right-angled triangle in lateral view (Figure 4c), with the hypotenuse directed anteriorly. The anterior edge of the mola is armed with a row of setae which are oriented medially in the direction of the chewing surface of the mola. The surface of the mandibles is covered with trichoid sensillae on parts of the anterior side only. From hight of the anterior mandibular articulation towards the incisivi as well as on the whole posterior side, the mandibles are devoid of sensillae.

Maxillae

The maxillae are three times longer than wide in overall shape (Figure 5). The cardo is approximately triangular containing a medially oriented lever serving as attachment for the M. craniocardinalis (0mx1). The cardo bears some setae and is moveably connected to the stipes by a very narrow mambrane lying at the base of the cardo-stipital ridge.

The stipes is composed of a narrow basistipes and a much larger mediostipes harbouring palpus, galea and lacinia. The whole stipes is devoid of sensillae except for the part directly posterad the palpal base (the area which is externally visible in lateral view; see Figure 2e). The base of the maxillar palpus is surrounded by protuberances of the stipes forming a ring around the palpal foramen.

The palpus is five segmented and densely covered with trichoid and campaniform sensillae. The first segment is half as long as the second one. The third one is slightly longer than the second one, the fourth and fifth are as long as the second one. Each segment is slightly thinner than the preceeding one. The fifth segment distally bears six special sensillae formed by a basal cylindrical segment densely covered with very small setae and four to six bigger setae on the tip of the cylindrical structure.

The galea is sickle shaped, distally covered with setae and bears apically two (sensory?) cones which in turn harbour several smaller denticles at their apices. The lacinia is also sickle shaped, bears three apical mesally oriented incisivi, three subapical setae with comb like hairs on their apical ends (pectinate lamellae) and further posterior one row of six setae without hairs at their apices. A row of trichoid sensillae follows directly posterior the setae from half the length of the lacinia to the base of the lacinia. Dentisetae are absent.

Labium

The labium (Figure 2a) is divided into postmentum, prementum, glossae, paraglossae and palpus. All externally visible parts are covered with sensillae in the same density like the rest of the head. The postmentum is an approximately rectangular plate. The prementum is

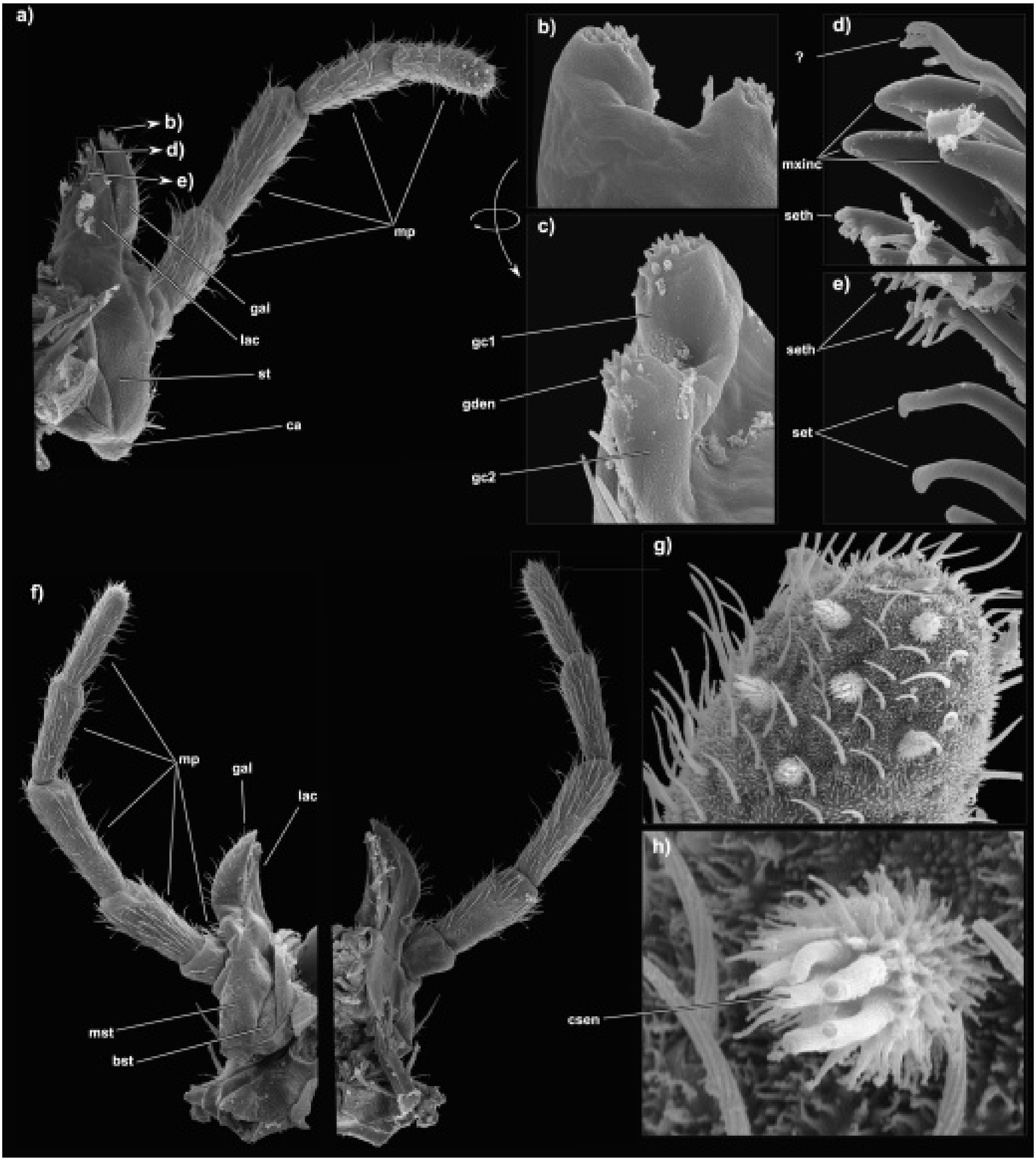

Figure 5 SEM micrographs of the maxillae of *Tricholepidion gertschi* a) posterior view; b) detail of the apical area of the galea (posterior view); c) detail of the apical area of the galea (meso-anterad view); d) detail of the apical area of the lacinia; e) detail of the subapical area of the lacinia; f) anterior view; g) detail of the apical area of the maxillar palpus; h) detail of a sensilla at the apex of the maxillary palpus. Abbreviations: ?, ?; bst, basistipes; ca, cardo; csen, conical sensillae; gal, galea; gc1, first apical cone of galea; gc2, second apical cone of galea; gden, galeal denticles; mxinc, maxillar incisivi; lac, lacinia; mp, maxillar palpus; mst, mediostipes; seth, hairy setae; st, stipes. Scale bar = 1 mm.

also rectangular in ventral view and bears a deep premental cleft. Glossae and paraglossae are short and finger like. The palpus is four segmented with a short basal segment followed by two twice as long segments.

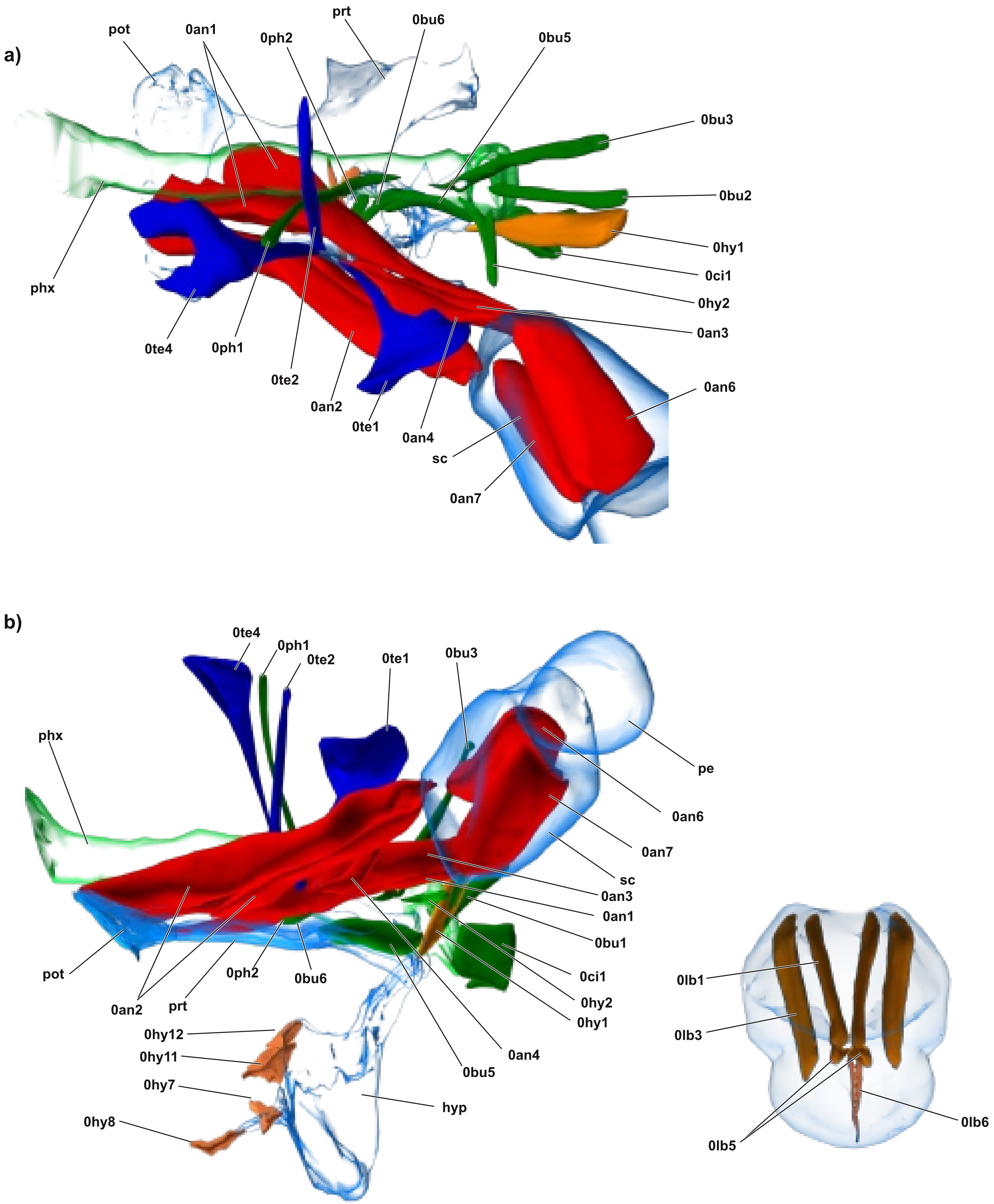

The apical segment is widened with a cleft at its anterior (or ventral) surface where it is also densely covered with

Figure 6 a) The musculature of the antenna, cephalic digestive tract, tentorium and hypopharynx of *Tricholepidion gertschi*. Three-dimensional reconstructions; cuticular structures: blue (semi-transparent); digestive tract: green (semi-transparent). Muscles are coloured according to functional groups and are not transparent: antennal muscles: red; pharyngeal muscles: green; hypopharyngeal muscles: orange; tentorial muscles: blue. Antennal muscles: XX; tentorial muscles: XX; hypopharyngeal muscles: XX; pharyngeal muscles: XX. b) musculature of the labrum; Abbreviations:. For muscle references see Data S X.

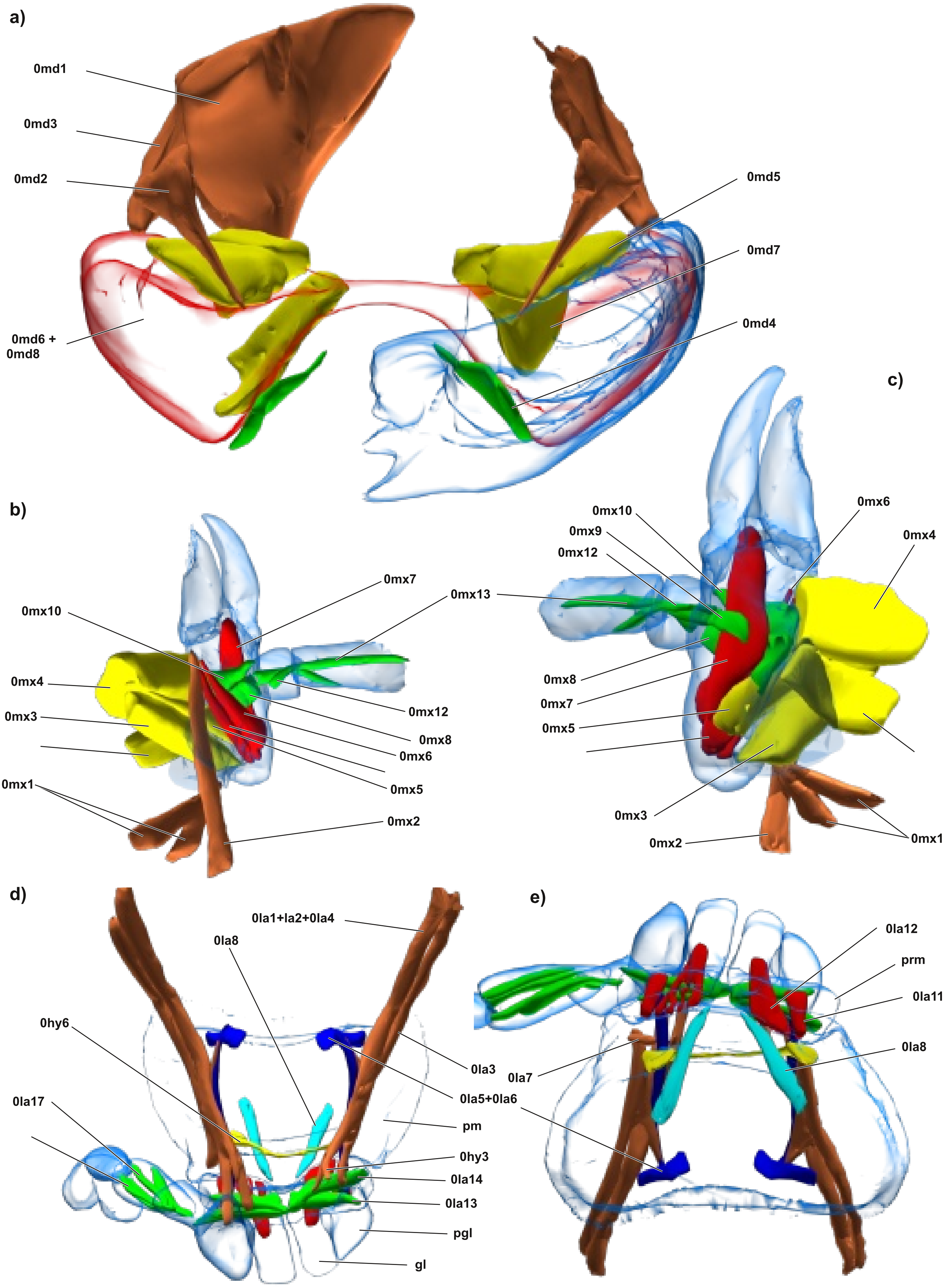
a)
0md1
0md3
0md2
0md6 +
0md8
0md5
0md7
0md4
c)
b)
0mx7
0mx13
0mx10
0mx4
0mx3
0mx1
0mx12
0mx8
0mx6
0mx5
0mx2
0mx10
0mx9
0mx12
0mx6
0mx4
0mx8
0mx7
0mx5
0mx3
0mx2
0mx1
d)
0la1+la2+0la4
0la8
0hy6
0la17
0la3
0la5+0la6
pm
0hy3
0la14
0la13
pgl
gl
e)
0la12
prm
0la11
0la7
0la8

trichoid and campanifom sensillae. Two additional sensillae types are present in this region. Towards the apical end there are three brush like fields of thin setae. More mesally follow three sensillae closely resembling those at the apical segement of the maxillar palpus but with a basal cylindrical segment apically composed of four finger like processes (Figure 2b-d).

Epipharynx

The epipharynx (= inner side of the labrum) is a concave structure and bears two fields of hairs on the inner side. The mandibles fit into the concave space of the epipharynx. When closed the right mandible is positioned a short distance in front and more ventrally of the left one.

Pharynx and oesophagus

Pharynx and oesophagus are solid and have a wide lumen. They are not clearly discernible from each other. Various muscles hold the digestive tract into position (Figure 6).

Discussion

This is the first account of the complete head anatomy of Tricholepidion covering all muscles and endoskeletal features. In contrast to Wygodzinski (Wygodzinsky, 1961) we interprete the general head orientation as orthognathous. Only the labial palps are in hypognathous position.

Staniczek (Staniczek, 2000; Staniczek, 2001) already studied the mandible and mandible musculature of *Tricholepidion* and stated the absence of the M. hypopharyngo-mandibularis (0md4). In our specimens a M. hypopharyngo-mandibularis (0md4) is clearly visible, origin, insertion, and course of this muscle are in line with the organisation in other taxa. Thus, only one cephalic argument for the paraphyly of Zygentoma remains: the ligamentous connection of muscles between the mandibles.

Although Tricholepidion possesses three ocelli, we consider this a weak argument in favour of zygentoman paraphyly, since the loss of ocelli occured several times among Dicondylia, e.g. in Xenonomia, Phasmatodea {Wipfler, 2011 #2910} and Zoraptera {Beutel, 2005 #16575}. Indeed, phylogenetic analysis of the head data results in monophyletic Zygentoma, although the mandible ligament is contained in the character matrix (69). The synapomorphies of Zygentoma presented in this study mostly concern the composition of the labium (103:3; 107:0; 108:0; 109:0; 110:0). Zygentoma possess a remarkable set of labial muscles which originate in the postoccipital region and continue dorso-ventrally through the whole head into the labium. Potential further synapomorphies are the number ommatidia (less than 80; 2:1), the wing-like processes at the ventral base of the anterior tentorial arms reaching into the lumen of the mandible (49:1) and presence of M. epistoepipharyngealis (0lb3; 22:0). In the present analysis the low number of ommatidia is not optimized as an synapomorphy of Zygentoma since Grylloblattodea also possess reduced eyes. Wing-like tentorial processess reaching into the lumen of the mandible are also present in Odonata.

The cephalic morphology of Tricholepidion is characterized by numerous potential apomorphies: absence of 0lb2 and 0hy10, presence of specialized (sensory?) sensillae on the apices of the maxillary and labial palps (with two different types on the labial palps), presence of two short (sensory?) cones on the apex of the galea, a clypeus with two distinct areas (however, without any suture or ridge) and a mandible with a distinct anterior depression for the clypeal process (in Lepisma and Thermobia the clypeus is also in contact with the mandible, but no distinct depression is formed).

Except for the loss of the mandible ligament (see above) and the loss of M. verticopharyngealis (0ph1) we found no headwise apomorphies defining the rest of Zygentoma excluding Tricholepidion.

Figure 7 The musculature of the mouthparts of *Tricholepidion gertschi*. Three-dimensional reconstructions; cuticular structures: blue (semi-transparent). Muscles are coloured variously to facilitate discrimination. a) mandibular musculature; b) maxillar musculature (anterior view); c) maxillar musculature (posterior view); d) labial musculature (anterior view); e) labial musculature (posterior view). For abbreviations please refer to the appendix.

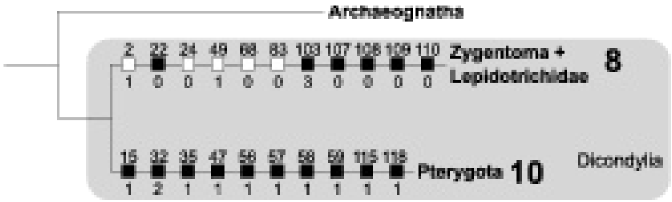

Zygentoma + Lepidotrichidae:
22) M. epistoepipharyngealis (0lb3) present
103) 4 labial palpomeres
107) M. postoccipitoglossalis medianus (0la1) present
108) M. postoccipitoglossalis lateralis (0la2) present
109) M. postoccipitoparaglossalis (0la3) present
110) M. postoccipitoprementalis (0la4) present

Pterygota:
15) Clypeus subdivided into ante- and postclypeus
32) antennal muscle 0an2 originating on dorsal tentorial arms only
35) Circumesophageal vessel ring branching off posterior to the brain
47) Anterior and posterior tentorium merged
56) M. tentoriofrontalis posterior (0te1) absent
57) M. posteriotentorialis (0te4) absent
58) M. tentoritentorialis longis (0te5) absent
59) M. tentoritentorialis brevis (0te6) absent
115) M. tentorioglandularis (0la7) absent
118) M. postmentomembranus (0la9) absent

Figure 8 Strict consensus of the two equally parsimonious trees derived from the TNT analysis of the morphological data matrix. Bremer support values are stated in bold numbers. For trait reference see Data S X

Autapomorphies of Dicondylia (Zygentoma + Pterygota) are the presence of a coronal suture, cuticular dorsal tentorial arms, the anterior mandibular joint, presence of M. labroepipharyngealis (0lb5), M. verticopharyngealis (0ph1), M. tentoriopharyngealis (0ph2) and the five segmented maxillar palpus.

Autapomorphies of Pterygota are divided clypeus (15:1), origin of the antennal muscle 0an2 at the dorsal tentorial arms (32:2), the fusion of the pre- and posttentoria (47:1) and the simultaneous loss of all tentorial muscles (56-59:1) as well as the absence of a circumesophageal vessel ring (35:1) and the loss labial musculature (0la7; 115:1 & 0la9; 118:1). Potential further autapomorphies of Pterygota are the loss of hypopharyngeal muscles 0hy6 and 0hy11. However, the character states at the stemline of Dicondylia is ambigous.

Acknowledgements

Karl Kjer helped to collect specimens of *T. gertschi*. Felix Beckmann, Fabian Wilde (both DESY), Marco Stampanoni, Peter Modregger and Rajmund Mokso (all PSI) provided excellent support at the synchcrotron facilities. Rolf G. Beutel is sincerely thanked for his support regarding content. The scanning was done under proposal no. I-20080169 which is gratefully acknowledged. The members of the ZFMK provided support in lab and field.

10 General Discussion

Methodological considerations

In this thesis the performance and limitations of the hard X-ray full-field microscope in Zernike phase contrast mode is discussed. It is shown how single body parts of micrometre sized samples can be displayed with nanometre resolution. Mosaic radiographic imaging is used for the identification of regions of interest, followed by inserting an array of phase shifting gold pillars (0.9 x 3 micron for each pillar) to generate Zernike phase contrast which improves sensitivity. The combination of this technique with the full-field microscope operated by the TOMCAT beamline of the SLS yielded a resolution of 140 nm. The workflow proposed in this thesis is especially useful due to the rapid characterisation of biological structures at the nanoscale. Higher resolutions can be achieved with electron tomography (30 nm; Frey et al. 2006), but this is only possible for very thin samples (100 micron³). In contrast, the penetration range of the 10 keV X-rays used here is in the range of several millimetres. With the applied Zernike phase contrast imaging hard X-rays are a highly efficient probe for sub-micrometric 3D imaging of relatively large biological samples. Today there is no alternative technique to hard X-ray microscopy to extract the 3D structural details at the nanoscale under these boundary conditions.

The Palaeoptera problem

For the first time a broad sampling of representatives of basal pterygote lineages was included in formal (numerical) phylogenetic analyses focussing on the “Palaeptera problem”. As the head of Odonata was clearly understudied one of the main topics of this thesis was the cephalic morphology of this highly specialised group. Additional reassessments of ephemeropteran, zygentoman, and archaeognathan head morphology showed that the seemingly well investigated cephalic character system still harbours new phylogenetic information. It could be shown that studies with up to date methods can produce more detailed or new anatomic information, or lead to well-founded reinterpretations of structures and their configurations.

The early evolution and phylogeny of winged insects (Pterygota) is a longstanding problem in systematic entomology (Klass, 2007; Kristensen, 1981). Several peculiarities impeding a reliable reconstruction of the evolutionary events apply to this region of the insect tree of life: (i) the outgroups relevant for winged insects are wingless (Archaeognatha, Zygentoma) which results in homologisation problems and problems with the assessment of character state polarity; (ii) profoundly different modes of flight have evolved. Odonates have a unique direct flight mechanism, whereas ephemeropteran and neopteran insects mainly use indirect flight muscles; (iii) available molecular data indicate that after the first occurrence of wings, speciation processess accelerated resulting in a rapid radiation in most extant lineages (Whitfield and Kjer, 2008); (iv) the common ancestors of Ephemeroptera, Odonata and Neoptera, respectively, emerged probably more than 400 mya ago (Engel and Grimaldi, 2004), so that the synapomorphies acquired during the splitting events may have been overwritten by subsequent morphological changes within the groups (Bergsten, 2005; Felsenstein, 2004; Whitfield and Kjer, 2008).

Most of these issues were treated in the present thesis. The problem of a lacking winged outgroup, problematic or impossible homologisations and polarisation of characters related to flight and sperm transfer was circumvented by choosing the head as a character system. Lacking information on the odonatan (chapter 7 & 8), ephemeropteran (chapter 4), and zygentoman (chapter 9) head morphology was supplemented, thus reducing the amount of missing data substantially. Evidence for negative effects of missing data is the clearly artifical placement of Odonata as the sistergroup of Orthoptera (Wipfler et al., 2011).

The problem of lineages whose apomorphies are overwritten by subsequent morphologic changes was partly assessed by the concerted convergence approach introduced by Holland et al. (2010), which was tested and refined in Blanke et al. (2012; 2012b [part of this thesis]). The phenomenon of concerted convergence can be considered as an ubiquitous evolutionary process (Morris, 2008). The change of one characteristic of an organism induces a tandem-shift of other features to maintain an optimal adaptation of the whole organism to its environment. This character interdependence results in a bias in phylogenetic reconstruction since interrelated characters are assigned an artificially increased weight.

All morphological analyses in the present thesis support Palaeoptera. The support increased after exclusion of characters which have likely evolved in a concerted convergent manner (chapter 5). This set of characters includes the subgenal ridge, the anterior mandibular articulation complex, and some muscles of the mandibles. It is interesting that exactly these characters were suggested as important derived conditions belonging to a hypothetical cephalic groundplan of Metapterygota (Odonata + Neoptera) (Staniczek, 2000; Staniczek, 2001). Based on our analyses of concerted convergence it seems highly advisable to exclude all but one of these characters to prevent a hidden weighing of the structural transformations associated with the evolution of the mandibular complex. Also, it is now evident that in future studies addressing this issue, attention should be paid to the evolutionary dependence of characters of the head capsule and mandibles. Character systems that seem to be less problematic are those related to the antennae, labrum, maxillae, labium, hypopharynx and pharynx. For a better understanding of character evolution related to the early pterygote splits, it will also be necessary to obtain more detailed and well documented data for the two apterygote key taxa, Zygentoma and Archaeognatha. The study presented in this thesis (chapter 9) is a first step towards this goal.

Although it has been shown in this thesis that the Palaeoptera grouping is most parsimonious and characters supporting this hypothesis are probably less prone to concerted convergence, principal problems remain: (i) the character analysis is restricted to a limited system, i.e. the head, and (ii) does not take into account the functional morphology of the mouthparts and head capsule. Although functional aspects cannot be incorporated in formal cladistic approaches, knowledge about the the function of structures in conjunction with other structures will be an important future aspect in systematic entomology. If, for example, only mandible characters are used to reconstruct the evolution of a given taxon sampling, the result will likely be a tree reflecting the food uptake relationships - but not necessarily the phylogenetic relationships. Exclusion of such candidate characters from tree inference is the only choice (Friedemann et al., 2012; Wipfler et al., 2011; Wipfler et al., 2012), although reasoning such exclusions is difficult without knowledge about character interdependence gained by functional studies.

For the first problem there simply exists no solution since the principal problems of homologisation and polarisation of wings and sperm transfer between Pterygota and the wingless Zygentoma will remain. Also the morphological peculiarities in the genitalic system of Odonata are likely autapomorphic. Therefore, it is futile to focus on these character systems without access to fossils unambiguously placed near the stemgroup of Zygentoma + Pterygota. This would possibly facilitate the polarisation of the above mentioned character systems. However, the availability of suitable material in the near future remains an extremely vague chance.

The second problematic issue – the insufficient understanding of functional morphology can be solved and is important for a better understanding of the characters used for phylogenetic analysis. Basically, it is necessary to provide objective means for character usage. If future functional studies are able to show that character interdependence is high in a given character system, this would aid the judgement of character usage in phylogenetics.

The evolutive success of insects is significantly dependent on the large variety of mouthpart systems which resulted in the conquest of new food recources. Here, we propose that a part of the mouthpart characters used for tree reconstruction are affected by concerted convergence. However, the approach to detect interdependencies is based on an iterative calculation of mutual pairwise compatibility of character states between two given characters (pairwise excess indices). In a methodological sense it is a mathematical approach rather than a biological one, meaning that the structural interdependency of characters (i.e. the mandibular structure or the shape of the head capsule) are not taken into consideration.

To estimate character interdependencies such as the linkage of the mandible articulation with head sutures it will be necessary to test the effect of structure changes in one system (mandible) on the other (head capsule). Finite-element simulations testing the effect of mouthpart movements on the head capsule during bite situations will be the next step in the mouthpart analysis of the early dicondylian lineages. It is possible to use the already gathered SR-microCT data for this, since current FE-programs can automatically detect structures according to their grey value and build volume models from this data.

Cephalic morphology and phylogeny of Odonata

New morphological investigations of head structures, especially of *E. superstes* and selected anisopteran families, have led to new insights in the phylogeny of Odonata and helped to correct former misinterpretations, which were at least in partly due to a serious lack of data (Wipfler et al. 2011; Blanke et al. in press). The detailed knowledge of the head morphology of *E. superstes* is apparently also crucial for the reconstruction of the cephalic groundplan of Odonata. Head characters support a sistergroup relationship Anisozygoptera + Anisoptera. However, this result should still be considered as preliminary as formal analyses of a broad spectrum of characters including extensive datasets from other tagmata are not possible yet due to homologisation problems.

The monophyly of the anisopteran families within Anisoptera is generally accepted except for the morphologically very heterogenous Corduliidae. However, the interrelationships of the families are not well resolved. Especially the position of Gomphidae (clubtails), Aeshnidae + Austropetaliidae (=Aeshnomorpha), Petaluridae (petaltails) and Cordulegastridae (spiketails) are shifting in molecular studies depending on the molecular markers and analytical approach. For example, Misof et al. (2001) recovered a sistergroup relationship Gomphidae + Petaluridae. In this study, Aeshnomorpha were recovered as the sistergroup to "Libelluloidea". Carle et al. (2008), based on nuclear and mitochondrial rRNAs and EF1-α markers, proposed basal Aeshnomorpha followed by Gomphidae as sistergroup to Petaluridae + Libelluloidea. Taking secondary structure information of mtRNA gene sequences into account, Fleck et al. (2008b) suggested monophyletic Aeshnoidea (Gomphidae + Petaluridae + (Aeshnidae + Austropetaliidae)) as sistergroup to Libelluloidea. Letsch et al. (2009) analyzed sequence data of mitochondrial and nuclear genes and refined the secondary structure analysis approach by identifying local structure constraints of each sequence, thereby uncovering phylogenetic signal in folded RNA structures. Basically, this analysis pointed towards the results of Carle et al. (2008), although the position of Gomphidae and Petaluridae did not receive strong support.

Morphology based analyses of the relationships within Anisoptera also yielded incongruent results. Based on wing characters Trueman (1996) proposed Petaluridae as sistergroup of the remaining Anisoptera, and Aeshnidae + Chlorogomphidae as sister to Gomphidae + the remaining Libelluloidea. Carle (1982) using a less limited set of characters (including features of the thoracic segments and abdomen) suggested a branching pattern with Gomphidae as sistergroup of the remaining Anisoptera, and Chlorogomphidae and Cordulegastridae as first splits within Libelluloidea. Pfau (1991) placed Aeshnidae as the first split within Anisoptera based on functional morphological analyzes of the flight apparatus and genitalia. Pfau (1991) used the structure and function of the penis and the vesica spermalis to reason the plesiomorphic condition for Odonata. Using a groundplan approach and manual cladistics, Bechly (1995) postulated Petaluridae as sister to extant Anisoptera and Gomphidae as sister to Libelluloidea. Rehn (2003) proposed Petaluridae as first split followed by Gomphidae accounting characters from the whole dragonflybody but with a strong focus on the relationships of Zygoptera. Bybee et al. (2008) used the matrix of Rehn (2003) in his combined molecular and morphological analysis and extended it by several characters to cover outgroup taxa and to increase resolution within Anisoptera. In all these studies mainly characters of wing venation and articulation were used.

The results of the present thesis show that a sistergroup relationship Gomphidae + remaining Anisoptera is most parsimonious when all currently available morphological characters are taken into account. Analyses of concerted convergence reveal the presence of a single clique of characters which support an alternative but implausible tree. Tree reconstruction using the remaining character set corroborated the position of Gomphidae. Analyses of the significant *clique* showed that especially characters of the head - and to a minor extent - thoracic characters require extensive reevaluation with regards to possible interdependence. Moreover, characters of the wing venation showed an unusual distribution among the significant character clique. Results suggest that especially the venation near the wing base may harbour concerted convergent characters.

Character distribution analysis shows that characters of internal structures do not group into cliques, which suggests that interdependencies are not likely for this character group. Further studies, especially focused on the internal anatomy of thorax and abdomen may yield new characters which have a low probability of concerted convergence and are thus potentially important for our understanding of dragonfly evolution.

11 References

Allman, E. S., M. T. Holder, and J. A. Rhodes. 2009. Estimating trees from filtered data: identifiability of models for morphological phylogenetics. Journal of Theoretical Biology 263:108-119.

Ando, H. 1962. The Comparative Embryology of Odonata with Special Reference to a Relic Dragonfly, *Epiophlebia superstes*. The Japan Society for the Promotion of Science Tokyo:205 p.

Andrews, J. C., E. Almeida, M. C. van der Meulen, and J. S. Alwood. 2010. Nanoscale X-ray microscopic imaging of mammalian mineralized tissue. Microscopy and Microanalysis 16:327-336.

Andrews, J. C., S. Brennan, C. Patty, K. Luening, and P. Pianetta. 2008. A high resolution, hard X-ray bio-imaging facility at ssrl. Synchrotron Radiation News 21:17-26.

Asahina, S. 1954. A morphological study of a relic dragonfly *Epiophlebia superstes* Selys (Odonata, Anisozygoptera). The Japan Society for the Promotion of Science: 153p, Tokyo.

Ax, P. 1999. Das System der Metazoa II - Ein Lehrbuch der phylogentischen Systematik. Akademie der Wissenschaften und der Literatur, Mainz - Stuttgart, Jena, Lübeck, Ulm: G. Fischer (ed.).

Bäcker, H., M. Fanenbruck, and J. W. Wägele. 2008. A forgotten homology supporting the monophyly of Tracheata: The subcoxa of insects and myriapods re-visited. Zool Anz 247:185 - 207.

Ballare, E. F., and J. L. Ware. 2011. Dragons fly, biologists classify: an overview of molecular odonate studies, and our evolutionary understanding of dragonfly and damselfly (Insecta: Odonata) behavior. International Journal of Odonatology 14:137-147.

Barlet, J. 1953. Morphologie du thorax de *Lepisma saccharina* L. (Aptérygote Thysanoure). II. - Musculature. Bulletin et Annales de la Societé Entomologique de Belgique 89:214-237.

Barlet, J. 1967. Squelette et musculature thoraciques de *Lepismachlis y-signata* Kratochvil (Thysanoures). Bulletin et Annales de la Societé Entomologique de Belgique 103:110-157.

Bechly, G. 1996. Morphologische Untersuchungen am Flügelgeäder der rezenten Libellen und deren Stammgruppenvertreter (Insecta; Pterygota; Odonata) unter besonderer Berücksichtigung der phylogenetischen Systematik und des Grundplanes der Odonata. Petalura (Special Volume) 2:1-402.

Bechly, G., C. Brauckmann, W. Zessin, and E. Gröning. 2001. New results concerning the morphology of the most ancient dragonflies (Insecta: Odonatoptera) from the Namurian of Hagen-Vorhalle (Germany). Journal of Zoological Systematics and Evolutionary Research 39:209-226.

Beckmann, F., J. Herzen, A. Haibel, B. Müller, and A. Schreyer. 2008. High density resolution in synchrotron-radiation-based attenuation-contrast microtomography. Proceedings of SPIE 7078:70781D-3.

Betz, O., U. Wegst, D. Weide, M. Heethoff, L. Helfen, W.-K. Lee, and P. Cloetens. 2007. Imaging applications of synchrotron X-ray phase-contrast microtomography in biological morphology and biomaterials science. I. General aspects of the technique and its advantages in the analysis of millimetre-sized arthropod structure. Journal of Microscopy 227:51-71.

Beutel, R. G., F. Friedrich, T. Hörnschemeyer, H. Pohl, F. Hünefeld, F. Beckmann, R. Meier, B. Misof, M. F. Whiting, and L. Vilhelmsen. 2010a. Morphological and molecular evidence converge upon a robust phylogeny of the megadiverse Holometabola. Cladistics 26:1-15.

Beutel, R. G., S.-Q. Ge, and X.-K. Yang. 2008. The larval head of Raphidia (Raphidioptera, Insecta) and its phylogenetic significance. Zoology 111:89-113.

Beutel, R. G., and S. Gorb. 2006a. A revised interpretation of the evolution of attachment structures in Hexapoda with special emphasis on Mantophasmatodea. Arthropod Systematics & Phylogeny 64:3-25.

Beutel, R. G., and S. N. Gorb. 2006b. A revised interpretation of the evolution of attachment structures in Hexapoda with special emphasis on Mantophasmatodea. Arthropod Systematics & Phylogeny 64:3-25.

Beutel, R. G., D. Zimmermann, M. Krauß, S. Randolf, and B. Wipfler. 2010b. Head morphology of Osmylus fulvicephalus (Osmylidae, Neuroptera) and its phylogenetic implications. Organisms Diversity & Evolution 10:311-329.

Bitsch, C., and J. Bitsch. 2002. The endoskeletal structures in arthropods: cytology, morphology and evolution. Arthropod Structure & Developement 30:159-177.

Blanke, A., F. Beckmann, and B. Misof. 2012a. The head anatomy of *Epiophlebia superstes* (Odonata: Epiophlebiidae). Organisms Diversity & Evolution 2012 DOI 10.1007/s13127-012-0097-z.

Blanke, A., C. Greve, B. Wipfler, R. G. Beutel, and B. Misof. accepted. The identification of concerted convergence in insect heads corroborates Palaeoptera. Systematic Biology.

Blanke, A., B. Wipfler, H. Letsch, M. Koch, F. Beckmann, R. G. Beutel, and B. Misof. 2012b. Revival of Palaeoptera – head characters support a monophyletic origin of Odonata and Ephemeroptera (Insecta). Cladistics DOI: 10.1111/j.1096-0031.2012.00405.x.

Blanke, A., B. Wipfler, H. Letsch, M. Koch, R. G. Beutel, and B. Misof. in press. Revival of Palaeoptera – head characters support a monophyletic origin of Odonata and Ephemeroptera (Insecta). Cladistics 2012.

Boudreaux, B. H. 1979. Arthropod phylogeny with special emphasis to insects. John Wiley & Sons Inc, New York, Chichester, Brisbane, Toronto.

Brauckmann, C., and W. Zessin. 1989. Neue Meganeuridae aus dem Namurium von Hagen-Vorhalle (BRD) und die Phylogenie der Meganisoptera (Insecta, Odonata). Deutsche Entomologische Zeitschrift 36:177-215.

Bybee, S. M., T. H. Ogden, M. A. Branham, and M. F. Whiting. 2008. Molecules, morphology and fossils: a comprehensive approach to odonate phylogeny and the evolution of the odonate wing. Cladistics 23:1-38.

Carapelli, A., P. Lio, F. Nardi, E. van der Wath, and F. Frati. 2007. Phylogenetic analysis of mitochondrial protein coding genes confirms the reciprocal paraphyly of Hexapoda and Crustacea. BMC Evolutionary Biology 7:S8.

Carapelli, A., F. Nardi, R. Dallai, and F. Frati. 2006. A review of molecular data for the phylogeny of basal hexapods. Pedobiologia 50:191-204.

Carle, F. L. 1982. The wing vein homologies and phylogeny of the Odonata: a continuing debate. Societas Internationalis Odonatologica Rapid Communications 4:1-66.

Carle, F. L. 1995. Evolution, taxonomy, and biogeography of ancient gondwanian libelluloides, with comments on anisopteroid evolution and phylogenetic systematics (Anisoptera: Aeshnidae). Odonatologica 24:383-506.

Carle, F. L. 1996. Revision of Austropetaliidae (Anisoptera: Aeshnoidea). Odonatologica 25:231-259.

Carle, F. L., K. Kjer, and M. May. 2008. Evolution of Odonata, with special reference to Coenagrionoidea (Zygoptera). Arthropod Systematics & Phylogeny 66:37-44.

Carle, F. L., and J. A. Louton. 1994. The larva of *Neopetalia punctata* and establishment of

Austropetaliidae fam. nov. (Odonata). Proceedings of the Entomological Society of Washington 96:147-155.

Chapman, R. N. 1918. The basal connection of the tracheae of the wings of insects. Pages 27-51 in: The wings of insects (J. H. Comstock, ed.). Cornell Univ. Press, Ithaca, New York.

Chaudonneret, J. 1950. La morphologie céphalique de *Thermobia domestica* (Packard) (Insecte aptérygogte Thysanoure). Annales des Sciences naturells, Zoologie et Biologie animale 11:145-302.

Chen, Y. T., T. Y. Chen, J. Yi, Y. S. Chu, and W. K. Lee. 2011. Hard X-ray zernike microscopy reaches 30 nm resolution. Optics Letters 36:1269.

Crampton, G. C. 1924. The phylogeny and classification of insects. Journal of Entomology and Zoology 16:33-47.

Dallai, R., D. Mercati, A. Carapelli, F. Nardi, R. Machida, K. Sekiya, and F. Frati. 2011. Sperm accessory microtubules suggest the placement of Diplura as the sister-group of Insecta s.s. Arthropod Structure & Development 40:77-92.

Denis, J. R., and J. Bitsch. 1973. Morphologie de la tête des Insects. (in P.-P. Grassé, Traité de Zoologie, Vol. 8, 593pp; Masson, Paris). Masson, Paris.

Dumont, H. J., A. Vierstraete, and J. R. Vanfleteren. 2010. A molecular phylogeny of the Odonata (Insecta). Systematic Entomology 35:6-18.

DuPorte, E. M. 1946. Observations on the morphology of the face in insects. Journal of Morphology 79:371-417.

DuPorte, E. M. 1957. The Comparative Morphology of the Insect Head. Annual Review of Entomology 2:55-70.

Edmunds, G. F. J. 1988. The mayfly subimago. Annual Review of Entomology 33:509-527.

Engel, M. S., and D. A. Grimaldi. 2004. New light shed on the oldest insect. Nature 427:627-630.

Fiala, J. C. 2005. Reconstruct: a free editor for serial section microscopy. Journal of Microscopy 218:52-61.

Fleck, G. 2011. Phylogenetic affinities of Petaluridae and basal Anisoptera families (Insecta: Odonata). Stuttgarter Beiträge zur Naturkunde A 4:83-104.

Fleck, G., M. Brenk, and B. Misof. 2008a. Larval and molecular characters help to solve phylogenetic puzzles in the highly diverse dragonfly family Libellulidae (Insecta: Odonata: Anisoptera): the Tetrathemistinae are a polyphyletic group. Organisms, Diversity & Evolution 8:1-16.

Fleck, G., B. Ullrich, M. Brenk, C. Wallnisch, M. Orland, S. Bleidissel, and B. Misof. 2008b. A phylogeny of anisopterous dragonflies (Insecta, Odonata) using mtRNA genes and mixed nucleotide/doublet models. Journal of Zoological Systematics and Evolutionary Research 46:310-322.

François, J. 1996. Squelette et musculature thoraciques des protures. Annales De La Societe Entomologique De France 32:233-249.

Fraser, F. C. 1957. A Reclassification of the Order Odonata. Royal Zoological Society of New South Wales, Sydney.

Friedemann, K., B. Wipfler, S. Bradler, and R. Beutel. 2012. On the head morphology of *Phyllium* and the phylogenetic relationships of Phasmatodea (Insecta). Acta Zoologica 93:184-199.

Friedrich, F., and R. Beutel. 2010. Goodbye Halteria? The thoracic morphology of Endopterygota (Insecta) and its phylogenetic implications. Cladistics 26:1-34.

Gäde, G., P. Simek, and H. W. Fescemyer. 2011. Adipokinetic hormones provide inference for the phylogeny of Odonata. Journal of Insect Physiology 57:174-178.

Gai, Y. H., D. X. Song, H. Y. Sun, and K. Y. Zhou. 2006. Myriapod monophyly and relationships among myriapod classes based on nearly complete 28S and 18S rDNA sequences. Zool Sci 23:1101 - 1108.

Garrison, R. W., N. Von Ellenrieder, and J. a. Louton. 2006. Dragonfly genera of the New World: an illustrated and annotated key to the Anisoptera. JHU Press.

Gaunt, M. W., and M. A. Miles. 2002. An Insect Molecular Clock Dates the Origin of the Insects and Accords with Palaeontological and Biogeographic Landmarks. Molecular Biology and Evolution 19:748-761.

Giribet, G., and G. D. Edgecombe. 2012. Reevaluating the arthropod tree of life. Annual Review of Entomology 57:167-186.

Giribet, G., G. D. Edgecombe, and W. C. Wheeler. 2001. Arthropod phylogeny based on eight molecular loci and morphology. Nature 413:157-161.

Givnish, T. J., J. C. Pires, S. W. Graham, M. A. McPherson, L. M. Prince, T. B. Patterson, H. S. Rai, E. H. Roalson, T. M. Evans, W. J. Hahn, K. C. Millam, A. W. Meerow, M. Molvray, P. J. Kores, H. E. O'Brien, J. Hall, C., W. J. Kress, and K. J. Sytsma. 2006. Phylogenetic relationships of monocots based on the highly informative plastid gene *ndh*F: evidence for widespread concerted convergence. Aliso 22:28-51.

Glückstad, J., and D. Palima. 2009. Generalized Phase Contrast.

Goloboff, P. A., J. S. Farris, and K. C. Nixon. 2008. TNT, a free program for phylogenetic analysis. Cladistics 24:774-786.

Goodman, J. W. 1988. Introduction to Fourier optics.

Gorb, S. N. 1999. Evolution of the dragonfly head-arresting system. Proceedings of the Royal Society of London. Series B: Biological Sciences 266:525-535.

Grimaldi, D. 2001. Insect evolutionary history from Handlirsch to Hennig, and beyond. Journal of Paleontology 75:1152-1160.

Grimaldi, D., and M. S. Engel. 2005. Evolution of the insects. Cambridge University Press, New York.

Grimaldi, D. A. 2010. 400 million years on six legs: On the origin and early evolution of Hexapoda. Arthropod Structure & Development 39:191-203.

Haas, F., and J. Kukalová-Peck. 2001. Dermapteran hindwing structure and folding: New evidence for familial, ordinal and superordinal relationships within Neoptera (Insecta). European Journal of Entomology 98:445-509.

Hakim, Z. M. 1964. Comparative anatomy of the head capsules of adult Odonata. Annals of the Entomological Society of America 57:267-278.

Hennig, W. 1969. Die Stammesgeschichte der Insekten. Waldemar Kramer, Frankfurt a. Main.

Holland, B. R., H. G. Spencer, T. H. Worthy, and M. Kennedy. 2010. Identifying cliques of convergent characters: concerted evolution in the cormorants and shags. Systematic Biology 59:433-445.

Hovmöller, R., T. Pape, and M. Kallersjo. 2002. The Palaeoptera problem: Basal pterygote phylogeny inferred from 18S and 28S rDNA sequences. Cladistics 18:313-323.

Howells, M. R., A. P. Hitchcock, and C. J. Jacobsen. 2009. Introduction: special issue on radiation damage. Journal of Electron Spectroscopy and Related Phenomena 170:1.

Hudson, G. B. 1951. Studies on the comparative anatomy and systematic importance of the hexapod tentorium - IV. Ephemeroptera. Journal of the Entomological Society of Southern Africa 14:3-23.

Huelsenbeck, J. P., and J. P. Bollback. 2001. Empirical and hierarchical bayesian estimation of ancestral states. Systematic Biology 50:351-366.

Huelsenbeck, J. P., and F. Ronquist. 2001. MrBayes: Bayesian inference of phylogenetic trees. Bioinformatics 17:754-755.

Ishiwata, K., T. Miyata, and Z. H. Su. 2011. Phylogenetic analysis of winged insects based on several nuclear protein-coding genes. Genes & Genetic Systems 85:398-398.

Jacobs, W., and F. Seidel. 1975. Wörterbuch der Biologie, Systematische Zoologie: Insekten. Gustav Fischer Verlag, Jena.

Jefimovs, K., J. Vila-Comamala, M. Stampanoni, B. Kaulich, and C. David. 2008. Beamshaping condenser lenses for full-field transmission X-ray microscopy. Journal of Synchrotron Radiation 15:106.

Jukes, T. H., C. R. Cantor, and H. N. Munro. 1969. Evolution of protein molecules. Academic Press, New York.

Katoh, K., K. Kuma, H. Toh, and T. Miyata. 2005. MAFFT version 5: Improvement in accuracy of multiple sequence alignment. Nucleic Acids Research 33:511-518.

Katoh, K., K. Misawa, K. Kuma, and T. Miyata. 2002. MAFFT: a novel method for rapid multiple sequence alignment based on fast Fourier transform. Nucleic Acids Research 30:3059-3066.

Kjer, K. 2004. Aligned 18S and insect phylogeny. Systematic Biology 53:506-514.

Kjer, K., F. L. Carle, J. Litman, and J. Ware. 2006. A molecular phylogeny of Hexapoda. Arthropod Systematics & Phylogeny 64:35-44.

Klass, K.-D. 2007. Die Stammesgeschichte der Hexapoden: eine kritische Diskussion neuerer Daten und Hypothesen. Denisia 20:413-450.

Klass, K.-D. 2008. The female abdomen of ovipositor-bearing Odonata (Insecta: Pterygota). Arthropod Systematics & Phylogeny 66:45-142.

Klass, K.-D., and U. Eulitz. 2007. The tentorium and anterior head sulci in Dictyoptera and Mantophasmatodea (Insecta). Zoologischer Anzeiger 246:205-234.

Klass, K. D. 2009. A critical review of current data and hypotheses on hexapod phylogeny. Proceedings of the Arthropod Embryological Society of Japan 43:3-22.

Koch, M. 2003. Towards a phylogenetic system of the Zygentoma. Entomologische Abhandlungen 62:122-125.

Koditschek, d. E., R. J. Full, and M. Buehler. 2004. Mechanical aspects of legged locomotion control. Arthropod Structure & Development 33:251-272.

Kristensen, N. P. 1975. The phylogeny of hexapod “orders”. A critical review of recent accounts. Journal of Zoological Systematics and Evolutionary Research 13:1-44.

Kristensen, N. P. 1981. Phylogeny of insect orders. Annual Review of Entomology 26:135-157.

Kristensen, N. P. 1991. Phylogeny of extant hexapods. In CSIRO (ed.), The Insects of Australia, Vol.1, pp. 125-140. Cornell University Press, Ithaca, New York.

Kristensen, N. P. 1998. The groundplan and basal diversification of hexapods. In R. A. Fortey, & R. H. Thomas (Eds.), Arthropod Relationships (pp. 281–293). London: Chapman & Hall. .

Kukalova-Peck, J. 1978. Origin and evolution of insect wings and their relation to metamorphosis, as documented by the fossil record. Journal of Morphology 156:53-125.

Kukalová-Peck, J. 1983. New Homoiopteridae (Insecta: Paleodictyoptera) with wing articulation from Upper Carboniferous strata of Mazon Creek, Illinois. Canadian Journal of Zoology 61:1670-1687.

Kukalová-Peck, J. 1991. Fossil history and the evolution of hexapod structures. CSIRO, Ithaca, New York.

Kukalová-Peck, J. 1997. Arthropod phylogeny and 'basal' morphological structures. Arthropod Relationships, Systematics Association Special Volume Series 55. R.A. Fortey and R. H. Thomas (eds.). Chapman & Hall, London, pp. 249-268.

Kukalová-Peck, J. 2008. Phylogeny of higher taxa in Insecta: Finding synapomorphies in the extant fauna and separating them from homoplasies. Evolutionary Biology 35:4-51.

La Greca, M. 1980. Origin and evolution of wings and flight in insects. Bulletin of Zoology 47 (Suppl.):65-82.

Letsch, H. O., C. Greve, P. Kück, G. Fleck, R. R. Stocsits, and B. Misof. 2009. Simultaneous alignment and folding of 28S rRNA sequences uncovers phylogenetic signal in structure variation. Molecular Phylogenetics and Evolution 53:758-771.

Letsch, H. O., P. Kück, R. R. Stocsits, and B. Misof. 2010. The impact of rRNA secondary structure consideration in alignment and tree reconstruction: simulated data and a case study on the phylogeny of hexapods. Molecular Biology and Evolution 27:2507-2521.

Lewis, P. O. 2001. A likelihood approach to estimating phylogeny from discrete morphological character data. Systematic Biology 50:913-925.

Li, J.-K., A. Nel, X.-P. Zhang, G. Fleck, M.-X. Gao, L. I. N. Lin, and J. I. A. Zhou. 2012. A third species of the relict family Epiophlebiidae discovered in China (Odonata: Epiproctophora). Systematic Entomology 37:408-412.

Lin, C.-P., M.-Y. Chen, and J.-P. Huang. 2010. The complete mitochondrial genome and phylogenomics of a damselfly, *Euphaea formosa* support a basal Odonata within the Pterygota. Gene 468:20-29.

Lohmann, H. 1996. Das phylogenetische System der Anisoptera (Odonata). Entomologische Zeitschrift 106:209-266.

Mallatt, J., and G. Giribet. 2006. Further use of nearly complete 28S and 18S rRNA genes to classify Ecdysozoa: 37 more arthropods and a kinorhynch. Molecular Phylogenetics and Evolution 40:772-794.

Manton, S. M. 1977. The Arthropoda, Habits, Functional Morphology and Evolution. Clarendon, Oxford.

Marone, F., C. Hintermuller, R. Geus, and M. Stampanoni. 2008. Towards real-time tomography: fast reconstruction algorithms and gpu implementation. IEEE Nuclear Science Symposium Conference Record:555-561.

Martynow, A. V. 1924. Über zwei Grundtypen der Flügel bei den Insekten und deren Evolution. Zeitschrift für Morphologie und Ökologie 4:465-501.

Mathur, K. C. 1962. The musculature of the head capsule and mouthparts of adult *Pantala flavescens* (Fabricius) (Odonata, Anisoptera, Libellulidae, Libellulinae). Journal of Animal Morphology and Physiology 9:18-31.

Mathur, P. N., and K. C. Mathur. 1961. Studies on the cephalic musculature of adult *Ictinus angulosus* Selys (Odonata, Anisoptera, Gomphidae, Ictinae). Journal of Morphology 109:237-249.

Matsuda, R. 1965. Morphology and Evolution of the insect head. Memoirs of the American Entomological Institute, Michigan 4:1-334.

Matsuda, R. 1970. Morphology and evolution of the insect thorax. Memoirs of the Entomological Society of Canada 76:1-431.

Matsuda, R. 1981. The origin of insect wings (Arthropoda, Insecta). International Journal of Insect Morphology and Embryology 10:387-398.

Matushkina, N. A. 2008a. The ovipositor of the relic dragonfly *Epiophlebia superstes*: a morphological re-examination (Odonata: Epiophlebiidae). International Journal of Odonatology 11:71-80.

Matushkina, N. A. 2008b. Skeletomuscular development of genital segments in the dragonfly *Anax imperator* (Odonata, Aeshnidae) during metamorphosis and its implications for the evolutionary morphology of the insect ovipositor. Arthropod Structure & Development 37:321-332.

Meusemann, K., B. M. von Reumont, S. Simon, F. Roeding, S. Strauss, P. Kuck, I. Ebersberger, M. Walzl,

G. Pass, S. Breuers, V. Achter, A. von Haeseler, T. Burmester, H. Hadrys, J. W. Wagele, and B. Misof. 2010. A phylogenomic approach to resolve the arthropod tree of life. Molecular Biology and Evolution 27:2451-2464.

Misof, B., and K. Misof. 2009. A monte carlo approach successfully identifies randomness in multiple sequence alignments : a more objective means of data exclusion. Systematic Biology 58:21-34.

Misof, B., O. Niehuis, I. Bischoff, A. Rickert, D. Erpenbeck, and A. Staniczek. 2007. Towards an 18S phylogeny of hexapods: Accounting for group-specific character covariance in optimized mixed nucleotide/doublet models. Zoology 110:409-429.

Misof, B., A. M. Rickert, T. R. Buckley, G. Fleck, and K. P. Sauer. 2001. Phylogenetic signal and its decay in mitochondrial SSU and LSU rRNA gene fragments of Anisoptera. Molecular Biology and Evolution 18:27-37.

Mokso, R., P. Cloetens, E. Maire, W. Ludwig, and J. Y. Buffiere. 2007. Nanoscale zoom tomography with hard X-rays using kirkpatrick-baez optics. Applied Physics Letters 90:144104.

Needham, J. G., and M. J. Westfall. 1955. A manual of the dragonflies of North America (Anisoptera) including the Greater Antilles and the provinces of the Mexican border. University of California Press, Berkeley.

Neuhausler, U., G. Schneider, W. Ludwig, M. A. Meyer, and E. Zschech. 2003. Xray microscopy in zernike phase contrast mode at 4 kev photon energy with 60nm resolution. Journal of Physics D: Applied Physics 36:79-82.

Nixon, K. C. 2002. Winclada ver. 1.00.08 Published by the author, Ithaca, NY.

Ogden, T. H., and M. F. Whiting. 2003. The problem with "the Paleoptera problem": sense and sensitivity. Cladistics 19:432-442.

Ott, M., J. Zola, S. Aluru, and A. Stamatakis. 2007. Large-scale maximum likelihood-based phylogenetic analysis on the IBM BlueGene/L. ACM/IEEE Supercomputing conference 2007. Reno, NV, USA.

Parkinson, D. Y., G. McDermott, L. D. Etkin, M. A. Le Gros, and C. A. Larabell. 2008. Quantitative 3-D imaging of eukaryotic cells using soft X-ray tomography. Journal of Structural Biology 162:380-386.

Pass, G. 1991. Antennal circulatory organs in Onychophora, Myriapoda and Hexapoda - Functional morphology and evolutionary implications. Zoomorphology 110:145-164.

Pass, G., B.-A. Gereben-Krenn, M. Merl, J. Plant, N. U. Szucsich, and M. Tögel. 2006. Phylogenetic relationships of the orders of Hexapoda: contributions from the circulatory organs for a morphological data matrix. Arthropod Systematics & Phylogeny 64:165-203.

Pass, G. n. 2000. Accessory Pulsatile Organs: Evolutionary Innovations in Insects. Annual Review of Entomology 45:495-518.

Patterson, T. B., and T. J. Givnish. 2002. Phylogeny, concerted convergence, and phylogenetic niche conservatism in the core liliales: insights from rbcL and ndhF sequence data. Evolution 56:233-252.

Pfau, H. K. 1986. Untersuchungen zur Konstruktion, Funktion und Evolution der Libellen (Insecta, Odonata). Tijdschrift voor Entomologie 129:35-123.

Pfau, H. K. 1991. Contributions to the functional morphology to the phylogenetic systematics of Odonata. Advances in Odonatology. 5:109-141.

Pfau, H. K. 2002. Tandem grip mechanics and tandem linkage shifting in Odonata - reconstruction of evolution and phylogenetic significance. International Journal of Odonatology 5:129-179.

Pfau, H. K. 2005. Structure, function and evolution of the 'glans' of the anisopteran vesica spermalis (Odonata). International Journal of Odonatology 8:259-310.

Pfau, H. K. 2011. Functional Morphology and Evolution of the Male Secondary Copulatory Apparatus of the Anisoptera (Insecta: Odonata). E. Schweizerbartsche Verlagsbuchhandlung.

Plazzi, F., A. Ricci, and M. Passamonti. 2011. The mitochondrial genome of Bacillus stick insects (Phasmatodea) and the phylogeny of orthopteroid insects. Molecular Phylogenetics and Evolution 58:304-316.

Pohl, H. 2010. A scanning electron microscopy specimen holder for viewing different angles of a single specimen. Microscopy Research and Technique 73:1073-1076.

Regier, J. C., J. W. Shultz, and R. E. Kambic. 2005. Pancrustacean phylogeny: hexapods are terrestrial crustaceans and maxillopods are not monophyletic. Proc Biol Sci 272:395-401.

Rehn, A. C. 2003. Phylogenetic analysis of higher-level relationships of Odonata. Systematic Entomology 28:181-239.

Requena, G., P. Cloetens, and W. Altendorfer. 2009. Submicrometer synchrotron tomography using kirkpatrick-baez optics. Scripta Materialia 61:760-763.

Richter, S., G. D. Edgecombe, and G. D. F. Wilson. 2002. The lacinia mobilis and similar structures - a valuable character in arthropod phylogenetics? Zoologischer Anzeiger 241:339-361.

Rokas, A., and S. B. Carroll. 2006. Bushes in the tree of life. PLoS Biology 4:e352.

Romeis, B. 1989. Mikroskopische Technik. Urban & Schwarzenberg, München.

Ronquist, F., and J. P. Huelsenbeck. 2003. MrBayes 3: Bayesian phylogenetic inference under mixed models. Bioinformatics 19:1572-1574.

Sakdinawat, A., and D. Attwood. 2010. Nanoscale X-ray imaging. Nature Photonics 4:840-848.

Sanderson, M. J., and J. J. Doyle. 1992. Reconstruction of organismal and gene phylogenies from data on multigene families: concerted evolution, homoplasy, and confidence. Systematic Biology 41:4-17.

Schönmann, H. 1981. Zur Kopfmorphologie der Ephemeridenlarven *Siphlonurus aestivalis* Rsyon und *Lepeorus goyi goyi* Peters. Zoologica 131:1-51.

Schulz, H. N., T. Brinkhoff, T. G. Ferdelman, M. Hernandez, and A. Teske. 1999. Dense population of a giant sulfur bacterium in namibian shelf sediments. Science 284:493.

Seifert, G. 1995. Entomologisches Praktikum. Georg Thieme Verlag, Stuttgart

Short, J. R. T. 1955. The morphology of the head of *Aeshna cyanea* (Müller) (Odonata, Anisoptera). Transactions of the Royal Entomological Society London 106:197-211.

Simm, K. 1914. Die larvalen Mundwerkzeuge bei *Oligoneuria rhenana* und ihre Verkümmerung bei Imago. Bulletin de l'académie des sciences de Cracovie 4:387-396.

Simon, S., B. Schierwater, and H. Hadrys. 2010. On the value of Elongation factor-1[alpha] for reconstructing pterygote insect phylogeny. Molecular Phylogenetics and Evolution 54:651-656.

Simon, S., S. Strauss, A. von Haeseler, and H. Hadrys. 2009. A phylogenomic approach to resolve the basal pterygote divergence. Molecular Biology and Evolution 26:2719-2730.

Snodgrass, R. E. 1935. Principles of insect morphology. McGraw-Hill Publications in the Zoological Sciences.

Snodgrass, R. E. 1947. The insect cranium and the “epicranial suture”. Smithsonian Miscellaneos Collections 107:1-52.

Soldán, T. 1997. The Ephemeroptera: Whose sistergroup are they? in: Ephemeroptera & Plecoptera: Biology-Ecology-Systematics, P.Landholt & M. Sartori (Eds.):514-

519.

Soldán, T. 2003. Ephemeroptera phylogeny and higher classification: present status and conflicting hypotheses. Entomologische Anhandlungen 61:125-126.

Stamatakis, A. 2006. RAxML-VI-HPC: maximum likelihood-based phylogenetic analyses with thousands of taxa and mixed models. Bioinformatics 22:2688-2690.

Stamatakis, A., P. Hoover, and J. Rougemont. 2008. A rapid bootstrap algorithm for the RAxML web servers. Systematic Biology 57:758-771.

Stamatakis, A., T. Ludwig, and H. Meier. 2005. RAxML-III: a fast program for maximum likelihood-based inference of large phylogenetic trees. Bioinformatics 21:456-463.

Stampanoni, M., F. Marone, P. Modregger, B. Pinzer, T. Thuring, J. Vila-Comamala, C. David, and R. Mokso. 2010a. Tomographic Hard X-ray Phase Contrast Micro- and Nano-imaging at TOMCAT. 6TH INTERNATIONAL CONFERENCE ON MEDICAL APPLICATIONS OF SYNCHROTRON RADIATION 1266.

Stampanoni, M., F. Marone, P. Modregger, B. Pinzer, T. Thuring, J. Vila-Comamala, C. David, and R. Mokso. 2010b. Tomographic Hard X-ray Phase Contrast Micro- and Nano-imaging at TOMCAT. AIP Conf. Proc.:CP1266.

Stampanoni, M., R. Mokso, F. Marone, J. Vila-Comamala, and S. Gorelick. 2010c. Phase-contrast tomography at the nanoscale using hard X-rays. Physical Review B 81:140105.

Staniczek, A. H. 2000. The mandible of silverfish (Insecta: Zygentoma) and mayflies (Ephemeroptera): Its morphology and phylogenetic significance. Zoologischer Anzeiger 239:147-178.

Staniczek, A. H. 2001. Der Larvenkopf von *Oniscigaster wakefieldi* McLachlan, 1873 (Insecta: Ephemeroptera: Oniscigastridae). Ein Beitrag zur vergleichenden Anatomie und Phylogenie der Eintagsfliegen. PhD thesis, Eberhard-Karls-Universität Tübingen. 160p.

Strenger, A. 1952. Die funktionelle und morphologische Bedeutung der Nähte am Insektenkopf. Zoologische Jahrbücher 72:468-521.

Strenger, A. 1954. Zur Kopfmorphologie der Ephemeridenlarven. Erster Teil. Ecdyonurus und Rhithrogena. Österreichische Zoologische Zeitschrift 4:191-228.

Strenger, A. 1970. Zur Kopfmorphologie der Ephemeridenlarven *Palingenia longicauda*. Zoologica 117:1-26.

Strenger, A. 1975. Zur Kopfmorphologie der Ephemeridenlarven *Ephemera danica*. Zoologica 123:2-22.

Strenger, A. 1977. Zur Kopfmorphologie der Ephemeridenlarven *Proboscidiplocia skorai*. Zoologica 127:1-18.

Takeuchi, A., Y. Suzuki, and K. Uesugi. 2011. Present status of the nanotomography system at BL47XU at SPring-8. AIP Conference Proceedings 1365:301-304.

Terry, M. D., and M. F. Whiting. 2005. Mantophasmatodea and phylogeny of the lower neopterous insects. Cladistics 21:240-258.

Teschke, M., and S. Sinzinger. 2009. Phase contrast imaging: a generalized perspective. JOSA A 24:1015-1021.

Tiegs, O. W. 1947. The Development and Affinities of the Pauropoda, based on a Study of *Pauropus silvaticus*. Quarterly Journal of Microscopical Science 88:275-336.

Tillyard, R. J. 1917. The biology of dragonflies (Odonata or Paraneuroptera). University Press, Cambridge.

Tillyard, R. J. 1921. On an anisozygopterous larva from the Himalayas (Order Odonata). Records of the Indian Museum 22:93-107.

Tillyard, R. J. 1928. The larva of *Hemiphlebia mirabilis* Selys (Odonata). Proceedings of the Linnean Society of

New South Wales 53:193-206.

Torre-Bueno, J. R. d. l., S. Nichols, W., G. S. Tulloch, and R. T. Schuh. 1989. The Torre-Bueno glossary of entomology. New York Entomological Society in cooperation with the American Museum of Natural History, New York.

Trautwein, M. D., B. M. Wiegmann, R. Beutel, K. M. Kjer, and D. K. Yeates. 2012. Advances in insect phylogeny at the dawn of the postgenomic era. Annual Review of Entomology 57:449-468.

Trueman, J. W. H. 1996. A prelimnary cladistic analysis of odonate wing venation. Odonatologica 25:59-72.

von Ellenrieder, N. 2002. A phylogenetic analysis of the extant Aeshnidae (Odonata: Anisoptera). Systematic Entomology 27:437-467.

von Kéler, S. 1963. Entomologisches Wörterbuch. Akademieverlag Berlin, Berlin.

von Reumont, B. M., K. Meusemann, N. U. Szucsich, E. Dell'Ampio, V. Gowri-Shankar, D. Bartel, S. Simon, H. O. Letsch, R. R. Stocsits, Y. xia Luan, J. W. Waegele, G. Pass, H. Hadrys, and B. Misof. 2009. Can comprehensive background knowledge be incorporated into substitution models to improve phylogenetic analyses? A case study on major arthropod relationships. BMC Evolutionary Biology 9:119.

Wägele, J., and C. Mayer. 2007. Visualizing differences in phylogenetic information content of alignments and distinction of three classes of long-branch effects. BMC Evolutionary Biology 7:147.

Wedmann, S., S. Bradler, and J. Rust. 2007. The first fossil leaf insect: 47 million years of specialized cryptic morphology and behavior. Proceedings of the National Academy of Sciences of the United States of America 104:2024-2024.

Whedon, A. D. 1918. The comparative morphology and possible adaptations of the abdomen in the Odonata. Transactions of the American Entomological Society 73:373-446.

Wheeler, W. C., M. Whiting, Q. D. Wheeler, and J. M. Carpenter. 2001. The phylogeny of the extant hexapod orders. Cladistics 17:113-169.

Whitfield, J. B., and K. M. Kjer. 2008. Ancient rapid radiations of insects: challenges for phylogenetic analysis. Annual Review of Entomology 53:449-472.

Whitfield, J. B., and P. J. Lockhart. 2007. Deciphering ancient rapid radiations. Trends in Ecology and Evolution 22:258-265.

Willkommen, J. 2009. The tergal and pleural wing base sclerites - homologous within the basal branches of Pterygota? Aquatic Insects 31:443-457.

Willkommen, J., and T. Hörnschemeyer. 2007. The homology of wing base sclerites and flight muscles in Ephemeroptera and Neoptera and the morphology of the pterothorax of Habroleptoides confusa (Insecta: Ephemeroptera: Leptophlebiidae). Arthropod Structure & Development 36:253-269.

Wipfler, B., R. Machida, B. Müller, and R. G. Beutel. 2011. On the head morphology of Grylloblattodea (Insecta) and the systematic position of the order, with a new nomenclature for the head muscles of Dicondylia. Systematic Entomology 36:241-266.

Wipfler, B., F. Wieland, F. DeCarlo, and T. Hörnschemeyer. 2012. Cephalic morphology of Hymenopus coronatus (Insecta: Mantodea) and its phylogenetic implications. Arthropod Structure & Development 41:87-100.

Witte, H., and D. Doring. 1999. Canalized pathways of change and constraints in the evolution of reproductive modes of microarthropods. Experimental and Applied Acarology 23:181-216.

Wootton, R. J. 1992. Functional morphology of insect wings. Annual Review of Entomology 37:113-140.

Wootton, R. J., and J. Kukalová-Peck. 2000. Flight adaptations in Palaeozoic Palaeoptera (Insecta). Biological Reviews 75:129-167.

Worthy, T. H., and M. S. Y. Lee. 2008. Affinities of Miocene waterfowl (Anatidae: Manuherikia, Dunstanetta and Miotadorna) from the St. Bathans Fauna, New Zealand. Palaeontology 5!:677-708.

Yang, Z. 1994. Maximum likelihood phylogenetic estimation from DNA sequences with variable rates over sites: approximate methods. Journal of Molecular Evolution 39:306-314.

Yoshizawa, K., and K. P. Johnson. 2011. How stable is the "Polyphyly of Lice" hypothesis (Insecta: Psocodea)? A comparison of phylogenetic signal in multiple genes. Molecular Phylogenetics and Evolution 55:939.

Zernike, F. 1934. Inflection theory of the cutting method and its improved form, the phase contrast method. Physica 1:689.

Zhang, J., C. Zhou, Y. Gai, D. Song, and K. Zhou. 2008. The complete mitochondrial genome of *Parafronurus youi* (Insecta: Ephemeroptera) and phylogenetic position of the Ephemeroptera. Gene 424:18-24.

Zhang, Y.-y., W.-j. Xuan, J.-l. Zhao, C.-d. Zhu, and G.-f. Jiang. 2010. The complete mitochondrial genome of the cockroach *Eupolyphaga sinensis* (Blattaria: Polyphagidae) and the phylogenetic relationships within the Dictyoptera. Molecular Biology Reports 37:3509-3516.

12 Appendix

Muscle name	Abbrev.	Kéler 1963	Matsuda 1965	Pass et al. 2006	**Machilis germanica (this study)**	**Lepisma saccharina (this study)**	**Zygentoma:** Chaudonneret 1950	**Zygentoma:** Woo 1950	**Ephemera danica (this study)**	**Heptagenia sulphurea (this study)**	**Siphlonurus lacustris (this study)**	Staniczek 2000	**Ephemeroptera:** Staniczek 2001	**Ephemeroptera:** Strenger 1970	**Lestes virens (this study)**	**Gomphus pulchellus (this study)**	**Epiophlebia superstes (this study)**	**Odonata:** Short 1955	**Odonata:** Mathur & Mathur 1961	**Epiophlebia superstes (Asahina 1954)**	**Davidius nanus (Asahina 1954)**	**Mnais strigata (Asahina 1954)**	**Perla marginata (this study)**	**Plecoptera:** Moulins 1968	**Plecoptera:** Chisholm 1962	**Grylloblattodea:** Wipfler et al. 2011	**Grylloblattodea:** Walker 1931	**Grylloblattodea:** Nagashima 1982	**Mantophasmatodea:** Baum et al 2006
M. tentorioscapalis anterior	**0an1**	1	52	/	+	+	pas+pps	47a	+	+	+	/	M1	5	+	+	+	4	28	+	+	+	+	3sc1+lsc2	A.D. M.	+	13	52	1
M. tentorioscapalis posterior	**0an2**	2	54	/	+	+	ras+mvs+ms+rps	48a	+	+	+	/	M3	4	+	+	+	5	27	+	+	+	+	dsc	A.E. M	+	12	54	2
M. tentorioscapalis lateralis	**0an3**	3	51	/	+	+	mvs	47b?	+	-	-	/	-	-	-	-	-	-	-	-	-	-	+	lsc	-	+	14	53	3
M. tentorioscapalis medialis	**0an4**	4	53	/	+	+	mds	48b?	-	-	+	/	M2?	-	-	-	-	-	-	-	-	-	+	-	-	-	-	-	-
M. frontopedicellaris	**0an5**	-	-	/	-	-	-	-	-	-	-	/	-	-	-	-	-	-	-	-	-	-	-	-	-	-	-	-	-
M. scapopedicellaris lateralis	**0an6**	5	+	/	+	+	+	49	-	-	-	/	-	/	+	+	+	6	29	/	/	/	+	fpd1+fpd2	-	+	15	+	5
M. scapopedicellaris medialis	**0an7**	6	+	/	+	+	+	50	-	-	-	/	M4?	/	+	+	+	7	30	/	/	/	+	epd1+epd2	-	+	16	+	6
M. intraflagellaris	**0an8**	-	-	-	?	-	-	51	-	-	-	-	-	-	-	-	-	-	-	/	/	/	-	-	-	-	-	-	-
M. interampullaris	**0ah1**	/	/	7	-	-	/	/	-	-	-	/	/	/	-	-	-	/	/	-	-	-	-	/	/	-	/	/	/
M. ampulloaortica	**0ah2**	/	/	8	-	-	/	/	-	-	-	/	/	/	-	-	-	/	/	-	-	-	-	/	/	-	/	/	/
M. ampullopharyngealis	**0ah3**	/	/	6	-	-	/	/	-	-	-	/	/	/	-	-	-	/	/	-	-	-	-	/	/	-	/	/	/
M. ampulloantennalis	**0ah4**	/	/	9	-	-	/	/	-	-	-	/	/	/	-	-	-	/	/	-	-	-	-	/	/	-	/	/	/
M. frontofrontalis	**0ah5**	/	/	5	-	-	/	/	-	-	-	/	/	/	-	-	-	/	/	-	-	-	-	/	/	-	/	/	/
M. frontolabralis	**0lb1**	8	62	/	+	+	mLa	4?	+	+	+	/	M5	1	+	+	+	2	1	+	+	+	+	mlra	LR. EL.	+	1	62	8
M. frontoepipharyngalis	**0lb2**	9	61	/	+	+	mLp	3b	+	+	+	/	M6	2	+	+	+	3	2	+	+	+	+	mlrp	LR. DEP	+	2	61	9

Appendix 1 Homologization of the cephalic musculature in the studied taxa of chapter 3

Appendix 1 continued

Muscle name	Abbrev.	Kéler 1963	Matsuda 1965	Pass et all. 2006	**Machilis germanica (this study)**	**Lepisma saccharina (this study)**	**Zygentoma:** Chaudonneret 1950	**Zygentoma:** Woo 1950	**Ephemera danica (this study)**	**Heptagenia sulphurea (this study)**	**Siphlonurus lacustris (this study)**	Staniczek 2000	**Ephemeroptera:** Staniczek 2001	**Ephemeroptera:** Strenger 1970	**Lestes virens (this study)**	**Gomphus pulchellus (this study)**	**Ephiophlebia superstes (this study)**	**Odonata:** Short 1955	**Odonata:** Mathur & Mathur 1961	**Epiophlebia superstes (Asahina 1954)**	**Davidius nanus (Asahina 1954)**	**Mnais strigata (Asahina 1954)**	**Perla marginata (this study)**	**Plecoptera:** Moulins 1968	**Plecoptera:** Chisholm 1962	**Grylloblattodea:** Wipfler et al. 2011	**Grylloblattodea:** Walker 1931	**Grylloblattodea:** Nagashima 1982	**Mantophasmatodea:** Baum et all 2006
M. epistomalabralis	**0lb3**	10		/	-	+	SCL.	3a	-	-	-	/	-	-	-	-	-	-	-	-	-	-	-	-	-	-	-	-	-
M. labralis transversalis	**0lb4**	-	-	/	mfr e	-	-	-	-	-	-	/	-	-	-	-	-	-	-	-	-	-	-	-	-	+	-	-	-
M. labroepipharyngalis	**0lb5**	7	63	/	-	+	cpL.	1	+	+	+	/	M7	33'	+	+	+	1	3	+	+	+	+	cplr	CIB. DIL.	-	-	63	7
M. labrolabralis	**0lb6**	-	-	/	-	+	rdL.	27	+	-	-	/	M8	33	-	-	-	-	-	-	-	-	-	-	-	-	-	-	-
M. craniomandibularis internus	**0md1**	11	21+24	/	+	+	adc m+a bcm d	42	+	+	+	M.1	M25	M.A	+	+	+	9	6	+	+	+	+	adm d	M.A D.M .	+	18	21	11
M. craniomandibularis externus anterior	**0md2**	-	22	/	+	+	adcl	44	+	+	+	M. 2	M26	-	-	-	-	-	-	-	-	-	-	-	-	-	-	-	-
M. craniomandibularis externus	**0md3**	12	23	/	+	+	abca	46	+	+	+	M.3	M27	25	+	+	+	8	5	+	+	+	+	abm d	M.A B.M .	+	17	23	12
M. hypopharyngo mandibularis	**0md4**	13	26	/	+	+	adh	14	+	+	+	M.8	M32	29	+	+	+	adm dh	7	?	?	?	-	-	-	+	20	26	+
M. tentoriomandibularis lateralis superior	**0md5**	-	25a	/	+	+	abl	45	+	+	+	M.4	M28	25'	+	+	+	-	-	+	+	+	-	-	-	-	-	-	-
M. zygomaticus mandibulae	**0md6**	14	25b	/	+	+	adr	43?	+	+	+	M.5	M29	26	+	+	+	adm di	-	+	+	+	+	imd v	-	+	19	25	13
M. tentoriomandibularis medialis superior	**0md7**	-	25a	/	+	+	abip	43?	+	+	+	M.6	M30	26'	+	+	-	-	9	?	?	?	-	imd d	-	-	-	-	-
M. zygomaticus mandibulae	**0md8**	14?	25b	/	+	+	adt	43?	+	+	+	M.7	M31	-	+	+	+	adm di	8	-	+	-	-	-	-	+	19?	-	im

Muscle name	Abbrev.	Kéler 1963	Matsuda 1965	Pass et all. 2006	**Machilis germanica (this study)**	**Lepisma saccharina (this study)**	**Zygentoma:** Chaudonneret 1950	**Zygentoma:** Woo 1950	**Ephemera danica (this study)**	**Heptagenia sulphurea (this study)**	**Siphlonurus lacustris (this study)**	Staniczek 2000	**Ephemeroptera:** Staniczek 2001	**Ephemeroptera:** Strenger 1970	**Lestes virens (this study)**	**Gomphus pulchellus (this study)**	**Ephiophlebia superstes (this study)**	**Odonata:** Short 1955	**Odonata:** Mathur & Mathur 1961	**Epiophlebia superstes (Asahina 1954)**	**Davidius nanus (Asahina 1954)**	**Mnais strigata (Asahina 1954)**	**Perla marginata (this study)**	**Plecoptera:** Moulins 1968	**Plecoptera:** Chisholm 1962	**Grylloblattodea:** Wipfler et al. 2011	**Grylloblattodea:** Walker 1931	**Grylloblattodea:** Nagashima 1982	**Mantophasmatodea:** Baum et all 2006
M. craniocardinalis externus+internus	0mx1	15+16	1	/	+	+	rl + rm	33	+	+	+	/	M34	6	+	+	+	10	10	+	+	+	+	rcc	PR. CA R.	+	21	1	15
M. craniolacinialis	0mx2	19	5	/	+	+	fcl	34	+	+	+	/	M35	9	+	+	+	14	13	+	+	+	+	fcl	CR. F.L.	+	24	5	19
M. tentoriocardinalis	0mx3	17	3	/	+	+	prc	35	+	+	+	/	M33	7	+	+	+	11a +b	11+ 12	+	+	+	+	acl+ acm	CA R.A D.M .	+	22	3	17
M. tentoriostipitalis	0mx4	18	4	/	+	+	ata2-3, stp1-2	36	+	+	+	/	M37-M38	8	+	+	+	12+ 13	14-16	+	+	+	+	aam	ST. AD. M.	+	23	4	18
M. tentoriostipitalis	0mx5	18	4	/	+	+	sts1	?	+	+	+	/	M36	8	+	+	+	13	14	+	+	+	+	asl	ST. AD. M.	+	22	4?	18?
M. stipitolacinialis	0mx6	20	6	/	+	+	fsl, fsl'	38	+	+	+	/	M39	10	+	+	+	15	19	+	+	+	+	ml1 +ml2	ST.F .L	+	25+26	6	20
M. stipitogalealis	0mx7	21	7	/	+	+	fg	37	-	-	-	/	-	-	-	-	-	-	-	-	-	-	+	rsg	+	+	27	7	21
M. stipitopalpalis externus	0mx8	22	10	/	+	+	lr	39	+	+	+	/	M40	12	+	+	+	18	18	+	+	+	+	abp	L.M X.P.	+	28	10	22
M. stipitopalpalis medianus	0mx9		11	/	+	-	dsa	-	-	-	-	/	-	-	-	-	-	-	-	-	-	-	-	fs	-	-	-	-	-
M. stipitopalpalis internus	0mx10	23	9	/	+	+	dsm	40	+	+	+	/	M41	13	+	+	+	17	17	+	+	+	+	adp	D.M X.P	+	29	9	23

Appendix 1 continued

Muscle name	Abbrev.	Kéler 1963	Matsuda 1965	Pass et al. 2006	**Machilis germanica (this study)**	**Lepisma saccharina (this study)**	**Zygentoma:** Chaudonneret 1950	**Zygentoma:** Woo 1950	**Ephemera danica (this study)**	**Heptagenia sulphurea (this study)**	**Siphlonurus lacustris (this study)**	Staniczek 2000	**Ephemeroptera:** Staniczek 2001	**Ephemeroptera:** Strenger 1970	**Lestes virens (this study)**	**Gomphus pulchellus (this study)**	**Epiophlebia superstes (this study)**	**Odonata:** Short 1955	**Odonata:** Mathur & Mathur 1961	**Epiophlebia superstes (Asahina 1954)**	**Davidius nanus (Asahina 1954)**	**Mnais strigata (Asahina 1954)**	**Perla marginata (this study)**	**Plecoptera:** Moulins 1968	**Plecoptera:** Chisholm 1962	**Grylloblattodea:** Wipfler et al. 2011	**Grylloblattodea:** Walker 1931	**Grylloblattodea:** Nagashima 1982	**Mantophasmatodea:** Baum et al l 2006
M. stipitotransversalis	**0mx11**	-	12	/	-	-	dsp	-	-	-	-	/	p	-	-	-	-	-	-	-	-	-	-	-	-	+	-	-	-
M. palpopalpalis maxillae primus	**0mx12**	24	+	/	+	+	rf+pf	41a	+	+	+	/	M42 +M43	27+ 28	-	-	-	-	-	-	-	-	-	-	-	+	30	ex.1	24
M. palpopalpalis secundus	**0mx13**	25	+	/	+	+	eta + fta	41b	-	-	-	/	-	-	-	-	-	-	-	-	-	-	+	fit	-	+	31	lv.1	25
M. palpopalpalis tertius	**0mx14**	26	+	/	+	+	eti +fti	41c	-	-	-	/	-	-	-	-	-	-	-	-	-	-	+	lit	-	+	32	fl.1	26
M. palpopalpalis quartus	**0mx15**	27	+	/	+	+	-	41d	-	-	-	/	-	-	-	-	-	-	-	-	-	-	+	dip	-	+	33	fl.2	-
M. postoccipitoglossalis medianus	**0la1**	-	31	/	-	+	lb	20?	-	-	-	/	-	-	-	-	-	-	-	-	-	-	-	-	-	-	-	-	-
M. postoccipitoglossalis lateralis	**0la2**	-	32	/	-	+	ablc	-	-	-	-	/	-	-	-	-	-	-	-	-	-	-	-	-	D.R. L.?	-	-	-	-
M. postoccipitoparaglossalis	**0la3**	-	33	/	-	+	llc	21?	-	-	-	/	-	-	-	-	-	-	-	-	-	-	-	-	-	-	-	-	-
M. postoccipitopraementalis	**0la4**	-	34	/	-	+	cprm	-	-	-	-	/	-	-	-	-	-	-	-	-	-	-	-	-	-	-	-	-	-
M. tentoriopraementalis inferior	**0la5**	29	35	/	+	+	rpm	25	+	+	+	/	M46	14?	-	-	-	-	-	-	-	-	+	adpr	PR. R.L.	+	34	35	29
M. tentoriopraementalis superior	**0la6**	30	36	/	+	+	able	-	-	+	+	/	M47	17	-	-	-	-	-	-	-	-	+	aspr	D.R. L.?	-	-	-	-
M. tentorioglandularis	**0la7**	-	37	/	+	+	tg	-	-	-	-	/	-	-	-	-	-	-	-	-	-	-	-	-	-	-	-	-	-
M. submentopraementalis	**0la8**	28	38	/	+	+	rpm	22	+	+	+	/	(M48)	20a	+	+	+	af	24 +21	+	+	+	+	rpmt	M.R .M.	+	35	38	28

Appendix 1 continued

Muscle name	**Abbrev.**	Kéler 1963	Matsuda 1965	Pass et all. 2006	**Machilis germanica (this study)**	**Lepisma saccharina (this study)**	**Zygentoma:** Chaudonneret 1950	**Zygentoma:** Woo 1950	**Ephemera danica (this study)**	**Heptagenia sulphurea (this study)**	**Siphlonurus lacustris (this study)**	Staniczek 2000	**Ephemeroptera:** Staniczek 2001	**Ephemeroptera:** Strenger 1970	**Lestes virens (this study)**	**Gomphus pulchellus (this study)**	**Ephiophlebia superstes (this study)**	**Odonata:** Short 1955	**Odonata:** Mathur & Mathur 1961	**Epiophlebia superstes (Asahina 1954)**	**Davidius nanus (Asahina 1954)**	**Mnais strigata (Asahina 1954)**	**Perla marginata (this study)**	**Plecoptera:** Moulins 1968	**Plecoptera:** Chisholm 1962	**Grylloblattodea:** Wipfler et al. 2011	**Grylloblattodea:** Walker 1931	**Grylloblattodea:** Nagashima 1982	**Mantophasmatodea:** Baum et all 2006
M. postmentomembranus	**0la9**	-	40	/	+	+	dlp	-	-	-	-	/	-	-	-	-	-	-	-	-	-	-	-	-	-	-	-	-	-
M. submentomentalis	**0la10**	-	41	/	+	-	-	-	-	-	-	/	-	-	-	-	-	-	-	-	-	-	+	rml	-	-	-	-	-
M. praementoparaglossalis	**0la11**	31	43	/	+	+	rdpr rs	29	+	+	+	/	M56	19	-	-	-	-	-	-	-	-	+	fpgl	P.F. M.	+	39	43	31
M. praementoglossalis	**0la12**	32	42	/	+	+	abll	28	+	+	+	/	M55	20	-	-	-	-	-	-	-	-	+	fgl	-	+	40	42	32
M. praementopalpalis internus	**0la13**	33	44	/	+	+	dlr	23	+	+	+	/	M50	18	+	+	+	29	20	+	+	+	+	-	-	+	42	44	33
M. praementopalpalis externus	**0la14**	34	45	/	+	+	lvlr	24	-	-	-	/	-	-	-	-	-	-	-	-	-	-	+	dplb	-	+	41	45	34
M. praementomembranus	**0la15**	-	-	/	-	?	dla	-	-	-	-	/	-	-	+	+	+	-	-	+	+	+	-	-	-	-	-	-	-
M. palpopalpalis labii primus	**0la16**	35	+	/	+	+	/	26a- c	+	+	+	/	M51 +M5 2+M 53	23	-	-	-	-	-	-	-	-	+	lplb	-	+	43	ex.1	35
M. palpopalpalis labii secundus	**0la17**	36	+	/	+	+	/	26d- e	+	-	+	/	M54	21+ 22	-	-	-	-	-	-	-	-	+	dp3a +lp3 a	-	+	44	fl.1	36
M. frontohypopharyngalis	**0hy1**	41	74	4	+	+	mo	10	+	+	+	/	M18	3	-	+	+	38	-	/	/	/	+	mo	E.M. A.	+	4	74	41
M. frontobuccalis lateralis	**0hy2**	47	75	/	+	+	slb	31	+	+	?	/	M19	-	-	-	-	-	-	/	/	/	+	dlb	-	+	5	75	47
M. tentoriohypopharyngalis	**0hy3**	42	37	/	+	+	lg	-	+	+	+	/	M45 ?	15	-	-	-	rplb(32)	25	-	-	-	+	rhy	HY P.R ET.	-	-	-	30
M. postoccipitalohypopharyngealis	**0hy4**		78		-	+	cf	-	-	-	-		-	-	+	+	+	-	-	?	?	?	-	-	-	-	-	-	-

Appendix 1 continued

Muscle name	Abbrev.	Kéler 1963	Matsuda 1965	Pass et all. 2006	**Machilis germanica (this study)**	**Lepisma saccharina (this study)**	**Zygentoma:** Chaudonneret 1950	**Zygentoma:** Woo 1950	**Ephemera danica (this study)**	**Heptagenia sulphurea (this study)**	**Siphlonurus lacustris (this study)**	Staniczek 2000	**Ephemeroptera:** Staniczek 2001	**Ephemeroptera:** Strenger 1970	**Lestes virens (this study)**	**Gomphus pulchellus (this study)**	**Ephiophlebia superstes (this study)**	**Odonata:** Short 1955	**Odonata:** Mathur & Mathur 1961	**Epiophlebia superstes (Asahina 1954)**	**Davidius nanus (Asahina 1954)**	**Mnais strigata (Asahina 1954)**	**Perla marginata (this study)**	**Plecoptera:** Moulins 1968	**Plecoptera:** Chisholm 1962	**Grylloblattodea:** Wipfler et al. 2011	**Grylloblattodea:** Walker 1931	**Grylloblattodea:** Nagashima 1982	**Mantophasmatodea:** Baum et all 2006
M. tentoriobuccalis anterior	**0hy5**	48?	60	/	+	+	dvc	30	-	-	-	/	-	-	+	-	-	-	-	/	/	/	+	dvc	HY P.D BP.	+	-	-	42
M. postmentoloralis	**0hy6**	-	72	/	+	+	lpm	19	-	-	-	/	-	-	-	-	-	-	-	-	-	-	-	-	-	-	-	-	-
M. praementosalivarialis anterior	**0hy7**	38	76+46+(39?)	/	?	+	ldr	27?	+	+	+	/	M49 ?	-	+	+	+	f?	23?	+	+	+	+	dvas	-	+	38	76	38
M. praementosalivarialis posterior	**0hy8**	39	77+47+(39?)	/	+	+	dvas	-	+	+	+	/	M49 ?	-	-	-	-	ae?	26?	-	-	-	+	dvps	-	+	37	77	39
M. transversalis buccae	**0hy9**	67	-	/	+	+	M. semi circu laire	-	+	+	+	/	M.s uspe nsor es	+	+	+	-	-	-	-	-	-	+	m. semi annu laire s	-	+	-	-	67
M. loroloralis	**0hy10**	-	73	/	+	+	ht	-	-	-	-	/	M24	-	-	-	-	-	-	-	-	-	I	-	-	+	-	-	-
M. lorosalivarialis	**0hy11**	-	-	/	?	+	dl	-	-	-	-	/	-	-	-	-	-	-	-	-	-	-	-	-	-	-	-	-	-
M. hypopharyngosalivarialis	**0hy12**	37	71+79	/	+	+	ddos	-	-	-	-	/	-	-	+	+	+	ls?	-	-	-	-	+	dds	H.C OM	+	36	71	37
M. anularis salivarii	**0hy13**	40	-	/	?	+	sph	-	-	-	-	/	-	-	-	-	-	-	-	-	-	-	-	-	-	?	-	-	-
M. tentoriofrontalis posterior	**0te1**	-	-	/	+	+	spt	17	-	-	-	/	-	-	-	-	-	-	-	-	-	-	-	-	-	-	-	-	-
M. tentoriofrontalis anterior	**0te2**	-	-	/	+	+	spat	18	-	-	-	/	-	-	-	-	-	-	-	-	-	-	+	SCT	-	+	-	-	+
M. tentoriofrontalis dorsalis	**0te3**	-	-	/	sdT A	(ST) ?	-	-	-	-	-	/	-	-	-	-	-	-	-	-	-	-	-	SST	-	-	-	-	-
M. posteriotentorialis	**0te4**	-	-	/	+	+	stp	-	-	-	-	/	-	-	-	-	-	-	-	-	-	-	-	-	-	-	-	-	-
M. tentoriotentorialis longis	**0te5**	-	-	/	+	+	tt	-	-	-	-	/	-	-	-	-	-	-	-	-	-	-	-	-	-	-	-	-	-

Appendix 1 continued

Muscle name	Abbrev.	Kéler 1963	Matsuda 1965	Pass et al. 2006	**Machilis germanica (this study)**	**Lepisma saccharina (this study)**	**Zygentoma:** Chaudonneret 1950	**Zygentoma:** Woo 1950	**Ephemera danica (this study)**	**Heptagenia sulphurea (this study)**	**Siphlonurus lacustris (this study)**	Staniczek 2000	**Ephemeroptera:** Staniczek 2001	**Ephemeroptera:** Strenger 1970	**Lestes virens (this study)**	**Gomphus pulchellus (this study)**	**Ephiophlebia superstes (this study)**	**Odonata:** Short 1955	**Odonata:** Mathur & Mathur 1961	**Epiophlebia superstes (Asahina 1954)**	**Davidius nanus (Asahina 1954)**	**Mnais strigata (Asahina 1954)**	**Perla marginata (this study)**	**Plecoptera:** Moulins 1968	**Plecoptera:** Chisholm 1962	**Grylloblattodea:** Wipfler et al. 2011	**Grylloblattodea:** Walker 1931	**Grylloblattodea:** Nagashima 1982	**Mantophasmatodea:** Baum et al 2006
M. tentoriotentorialis brevis	**0te6**	-	-	/	+	+	tc	-	-	-	-	/	-	-	-	-	-	-	-	-	-	-	-	-	-	-	-	-	-
M. clypeopalatalis	**0cl1**	43	81	/	+	+	dc	5-7	+	+	+	/	M11- M14 ?	32	-	-	-	-	-	-	-	-	+	ddc1 +ddc 2	A.O ES. DIL.	+	3	-	43
M. clypeobuccalis	**0bu1**	44	82	/	+	+	db	-	+	+	+	/	M14 ?	-	+	+	+	33+ 34	4	+	+	+	+	ddb	-	-	-	82	44?
M. frontobuccalis anterior	**0bu2**	45	83	/	+	+	ddph 1	9	+	+	+	/	M15	PhM ?	+	+	+	35.3 6.39	-	+	+	+	+	ddp1	P.O ES. DIL. ?	+	6	83	45
M. frontobuccalis posterior	**0bu3**	46	84	/	+	+	ddph 2	11	+	+	+	/	M16	PhM ?	-	-	-	-	-	-	-	-	+	ddp2	P.O ES. DIL. ?	+	7	84	46
M. tentoriobuccalis lateralis	**0bu4**	49	85	/	-	-	-		+	-	+	/	M20	PhM ?	-	-	-	-	-	-	-	-	-	-	-	+	9	85	+
M. tentoriobuccalis anterior	**0bu5**	48	87	/	+	+	dvp1	15	+	+	+	/	M21	-	-	-	-	42?	-	-	-	-	+	dvpa 1+d vpa2	-	+	-	87	48
M. tentoriobuccalis posterior	**0bu6**	50	88	/	+	+	dvp2	16	+	+	+	/	M21	-	+	+	?	43'?	-	/	/	/	+	dvp m1- 4	-	+	10	88	50
M. verticopharyngalis	**0ph1**	51	86	/	-	-	-	8	+	+	+	/	M17	-	+	+	+	37	+	/	/	/	+	ddp3	-	+	8	86	51
M. tentoriopharyngalis	**0ph2**	52	89+90	/	-	+	dvp2 ?	32	-	-	+	/	M21 ?	-	?	+	?	44	-	/	/	/	+	dvpp 1-4	-	+	11	90	52

Appendix 1 continued

Appendix 1 continued

Muscle name	Abbrev.	Kéler 1963	Matsuda 1965	Pass et all. 2006	**Machilis germanica (this study)**	**Lepisma saccharina (this study)**	**Zygentoma:** Chaudonneret 1950	**Zygentoma:** Woo 1950	**Ephemera danica (this study)**	**Heptagenia sulphurea (this study)**	**Siphlonurus lacustris (this study)**	Staniczek 2000	**Ephemeroptera:** Staniczek 2001	**Ephemeroptera:** Strenger 1970	**Lestes virens (this study)**	**Gomphus pulchellus (this study)**	**Epiophlebia superstes (this study)**	**Odonata:** Short 1955	**Odonata:** Mathur & Mathur 1961	**Epiophlebia superstes (Asahina 1954)**	**Davidius nanus (Asahina 1954)**	**Mnais strigata (Asahina 1954)**	**Perla marginata (this study)**	**Plecoptera:** Moulins 1968	**Plecoptera:** Chisholm 1962	**Grylloblattodea:** Wipfler et al. 2011	**Grylloblattodea:** Walker 1931	**Grylloblattodea:** Nagashima 1982	**Mantophasmatodea:** Baum et all 2006
M. postoccipitopharyngealis	**0ph3**	-	-	/	-	-	-	-	-	-	-	-	-	-	+	-	-	-	-	-	-	-	+	dpop1+dpop2	-	+		-	-
M. anularis stomodaei	**0st1**	68	93	/	+	+	+	12+13?	+	+	+	/	M10	-	+	+	+	-	+	+	+	+	+	M.annulaires	-	+	-	-	68
M. longitudinalis stomodaei	**0st2**	69	91+92	/	+	+	+	-	+	+	+	/	M9	-	+	+	+	-	-	+	+	+	+	M.longitudinale	-	+	-	-	69

Appendix 1 continued

Abbrev.	**Mantophasmatodea:** Wipfler et al. 2011	**Blattodea:** Wipfler et al. 2011	**Blattodea:** Dorsey 1943	**Blattodea:** Snodgrass 1943, 1944	**Isoptera:** Vishnoi 1956, 1962	**Mantodea:** Hymenopus	**Mantodea:** Leverault 1938	**Mantodea:** Carbonaro 1949	**Orthoptera:** Zolessi 1968	**Orthoptera:** Strenger 1942	**Orthoptera:** Blackith & Blackith 1967	**Orthoptera:** Albrecht 1953	**Dermaptera:** Strenger 1942	**Dermaptera:** Kadam 1961	**Dermaptera:** Dorsey 1943	**Embioptera:** Rähle 1970	**Phasmatodea:** Wipfler et al. 2011	**Phasmatodea:** Marquardt 1940	**Phasmatodea:** Maki 1935	**Zoraptera:** Beutel & Weide 2005	**Psocoptera:** Badonnel 1934	**Hymenoptera:** Beutel & Vilhelmsen 2007	**Neuroptera:** Beutel 2010
0an1	+	+	/	-	3	1	5	35	5	5	5	5	4?	dp.a	/	1	+	-	5a+b	1	X	1	1
0an2	+	+	/	-	4	2	4	36	4	4	4	4	5?	lvs	/	3	+	-	4b	2	Y	2	2
0an3	+	+	/	-	-	3	6	37	-	-	-	-	-	-	/	-	-	-	4a?	-	Z	3	-
0an4	-	-	/	-	3	-	-	-	-	-	-	-	-	-	/	2	+	-	4a?	4	-	4	4
0an5	-	-	/	-	-	-	-	-	-	-	-	-	-	-	/	-	-	-	-	-	-	-	-
0an6	+	+	/	-	5	5	7	38+39	6	-	6	6	-	lv.fl	/	4+6	+	-	7	5	1-3	5	5
0an7	+	+	/	-	6	6	8	40	7	-	7	7	-	dp.fl	/	5+7	+	-	6	6	4-6	6	6
0an8	-	-	-	-	-	-	-	-	-	-	-	-	-	-	-	-	-	-	-	-	-	-	-
0ah1	-	+	/	/	/	-	/	/	/	/	/	/	/	/	/	/	+	/	/	Msy?	/	/	/
0ah2	-	+	/	/	/	-	/	/	/	/	/	/	/	/	/	/	+	/	/	/	/	/	/
0ah3	-	-	/	/	/	-	/	/	/	/	/	/	/	/	/	/	-	/	/	/	/	/	/
0ah4	-	-	/	/	/	-	/	/	/	/	/	/	/	/	/	/	-	/	/	/	/	/	/
0ah6	-	-	/	/	/	-	/	/	/	/	/	/	/	/	/	/	-	/	/	/	/	/	/
0lb1	+	+	4	3	1	8	2	1	2	1	2	2	1	d.lr	4	45	+	-	2	8	b	-	8
0lb2	+	+	3	4	2	9	3	2	3	2	3	3	2	v.lr	3	46	+	-	3	9	a	9	9

Appendix 1 continued

Abbrev.	0lb3	0lb4	0lb5	0lb6	0md1	0md2	0md3	0md4	0md5	0md6	0md7	0md8
Mantophasmatodea: Wipfler et al. 2011	-	-	+	-	+	-	+	+	-	+	-	+
Blattodea: Wipfler et al. 2011	-	+	+	-	+	-	+	+	-	+	-	+
Blattodea: Dorsey 1943	-	2	1	-	/	/	/	14	/	/	/	/
Blattodea: Snodgrass 1943, 1944	-	-	+	-	28	-	27	29	-	30	-	-
Isoptera: Vishnoi 1956, 1962	-	-	-	-	8	-	7	9	-	10	-	-
Mantodea: Hymenopus	-	?	?	-	11	-	12	13	-	14a	-	14b
Mantodea: Leverault 1938	-	-	1	-	19	-	20	22	-	21	-	-
Mantodea: Carbonaro 1949	-	-	3	-	4	-	5	6	-	7	-	-
Orthoptera: Zolessi 1968	-	-	1	-	9	-	8	-	-	-	-	-
Orthoptera: Strenger 1942	-	-	-	-	MA+MB	-	25	-	-	26	-	-
Orthoptera: Blackith & Blackith 1967	-	-	1	-	9	-	8	-	-	-	-	-
Orthoptera: Albrecht 1953	-	-	1	-	9	-	8	-	-	-	-	-
Dermaptera: Strenger 1942	-	-	-	-	MA+MB	-	25	-	-	26	-	-
Dermaptera: Kadam 1961	-	-	com.lr	-	add.md	-	abd.md	-	-	-	-	-
Dermaptera: Dorsey 1943	-	?	1	-	/	/	/	?	/	/	/	/
Embioptera: Rähle 1970	-	-	47	-	8	-	9	13	-	10+12	-	11
Phasmatodea: Wipfler et al. 2011	-	-	+	-	+	-	+	+	-	+	-	+
Phasmatodea: Marquardt 1940	-	-	-	-	L2 gr-md	-	L1 gr-md	L md-ao	-	L ta.md	-	-
Phasmatodea: Maki 1935	-	-	1	-	9	-	8	12	-	10+11	-	-
Zoraptera: Beutel & Weide 2005	-	-	7	-	11	-	12	-	-	13	-	-
Psocoptera: Badonnel 1934	-	-	L	-	M	-	N	O	-	Q	-	P
Hymenoptera: Beutel & Vilhelmsen 2007	-	-	7	-	11	-	12	-	-	13	-	-
Neuroptera: Beutel 2010	-	-	-	-	11	-	12	-	-	14	-	14?

Abbrev.	0mx1	0mx2	0mx3	0mx4	0mx5	0mx6	0mx7	0mx8	0mx9	0mx10
Mantophasmatodea: Wipfler et al. 2011	+	+	+	+	-	+	+/?	+	-	+
Blattodea: Wipfler et al. 2011	+	+	+	+	+	+	+	+	-	+
Blattodea: Dorsey 1943	/	/	/	/	/	/	/	/	/	/
Blattodea: Snodgrass 1943, 1944	31	32	33	34	33?	41	42	-	-	-
Isoptera: Vishnoi 1956, 1962	11	14	12	13a-c	13d	15	16	18	-	17
Mantodea: Hymenopus	15	19	17	18	18	20	21	22a	22b	23
Mantodea: Levereault 1938	23	26c	24+25	27+28	25	26a,b	37	30	31	29
Mantodea: Carbonaro 1949	8	12	9 + 10	11	7	13	14	16	16	15
Orthoptera: Zolessi 1968	10	14	11	12+13	-	15	16	17		18
Orthoptera: Strenger 1942	6	9	7	8	-	10	11	12	-	13
Orthoptera: Blackith & Blackith 1967	10	14	11	12-14	-	15	16	18	-	17
Orthoptera: Albrecht 1953	10	14	11	12+13	-	15a+b	16	18	-	17
Dermaptera: Strenger 1942	6	9	7	8	-	10	11	12	-	13
Dermaptera: Kadam 1961	fl.car	-	add.car	add.st	-	fl.lc	Fl.gs	3v.plp	-	dp.plp
Dermaptera: Dorsey 1943	/	/	/	/	/	/	/	/	/	/
Embioptera: Rähle 1970	14	15	16	18	17	21+22	20	24	25	23
Phasmatodea: Wipfler et al. 2011	+	+	+	+	+	+	+	+	+	+
Phasmatodea: Marquardt 1940	L.ge-cd	L.ge-lc	L.tt-cd	L.tt-sti	-	P.sti-lc	P1,2 sti-gs	P2 sti-tr	-	P1 sti-tr
Phasmatodea: Maki 1935	13	17	14	15+16	-	18a+b	19	20	21	22
Zoraptera: Beutel & Weide 2005	15	19	17	18	-	20	21	22	-	23
Psocoptera: Badonnel 1934	-	80	-	R	-	Lp1-Lp3	-	m1	-	m27
Hymenoptera: Beutel & Vilhelmsen 2007	15	19	17	18	-	20	21	22	-	23
Neuroptera: Beutel 2010	15	19	17	18	-	20	21	22	-	23

Appendix 1 continued

Abbrev.	**Mantophasmatodea:** Wipfler et al. 2011	**Blattodea:** Wipfler et al. 2011	**Blattodea:** Dorsey 1943	**Blattodea:** Snodgrass 1943, 1944	**Isoptera:** Vishnoi 1956, 1962	**Mantodea:** Hymenopus	**Mantodea:** Leverault 1938	**Mantodea:** Carbonaro 1949	**Orthoptera:** Zolessi 1968	**Orthoptera:** Strenger 1942	**Orthoptera:** Blackith & Blackith 1967	**Orthoptera:** Albrecht 1953	**Dermaptera:** Strenger 1942	**Dermaptera:** Kadam 1961	**Dermaptera:** Dorsey 1943	**Embioptera:** Rähle 1970	**Phasmatodea:** Wipfler et al. 2011	**Phasmatodea:** Marquardt 1940	**Phasmatodea:** Maki 1935	**Zoraptera:** Beutel & Weide 2005	**Psocoptera:** Badonnel 1934	**Hymenoptera:** Beutel & Vilhelmsen 2007	**Neuroptera:** Beutel 2010
0mc11	+	+	/	-	-	+	-	-	-	-	-	-	-	-	/	-	-	-	-	-	-	-	-
0mc12	+	+	/	-	19	24	32+33	17	19	-	19	19	/	82	/	26	+	P tr-p2	23	24	m3?	24	24
0mc13	+	+	/	-	20	25	34	18	20	-	20	20	/	83	/	27	+	P tr-p3	24	25	-	25	25
0mc14	+	+	/	-	21	26	35	19	21	-	21	21	/	84	/	28	+	P p3-p4	25+26	26	-	26	26
0mc15	+	+	/	-	22	27	36	20	22	-	22	22	/	85	/	29+30	+	P p4-p5	27+28	27	-	27	27
0la1	-	-	-	-	-	-	-	-	-	-	-	-	-	-	-	-	-	-	-	-	-	-	-
0la2	-	-	-	-	-	-	-	-	-	-	-	-	-	-	-	-	-	-	-	-	-	-	-
0la3	-	-	-	-	-	-	-	-	-	-	-	-	-	-	-	-	-	-	-	-	-	-	-
0la4	-	-	-	-	-	-	-	-	-	-	-	-	-	-	-	-	-	-	-	-	-	-	-
0la5	+	+	21	44	23	29	39	23	23	15	23	23	15	add.prm	21	31	+	L.tp-prm ?	29	29	o	29	29
0la6	-	+	20	43	-	30	38	22	24	14	24	24	14	l.re.prm	20	34	+	-	33	30?	-	30	?
0la7	-	-	-	-	-	-	-	-	-	-	-	-	-	-	-	-	-	-	-	-	-	-	-
0la8	+	+	22	45	24	28	44	21	-	16	+	-	16	m.re.prm	22	32	+	L.sm-prm	30	28	p	28	28

Appendix 1 continued

Abbrev.	**Mantophasmatodea:** Wipfler et al. 2011	**Blattodea:** Wipfler et al. 2011	**Blattodea:** Dorsey 1943	**Blattodea:** Snodgrass 1943, 1944	**Isoptera:** Vishnoi 1956, 1962	**Mantodea:** Hymenopus	**Mantodea:** Leverault 1938	**Mantodea:** Carbonaro 1949	**Orthoptera:** Zolessi 1968	**Orthoptera:** Strenger 1942	**Orthoptera:** Blackith & Blackith 1967	**Orthoptera:** Albrecht 1953	**Dermaptera:** Strenger 1942	**Dermaptera:** Kadam 1961	**Dermaptera:** Dorsey 1943	**Embioptera:** Rähle 1970	**Phasmatodea:** Wipfler et al. 2011	**Phasmatodea:** Marquardt 1940	**Phasmatodea:** Maki 1935	**Zoraptera:** Beutel & Weide 2005	**Psocoptera:** Badonnel 1934	**Hymenoptera:** Beutel & Vilhelmsen 2007	**Neuroptera:** Beutel 2010
0la9	-	-	-	-	-	-	-	-	-	-	-	-	-	-	-	-	-	-	-	-	-	-	-
0la10	-	-	-	-	-	-	-	-	-	-	-	-	-	-	-	-	-	-	-	-	-	-	-
0la11	+	+	29	+	26	31	49	28	25	19	25	25	20	fl.li	29	33	+	P prm-pgl	32	31	j?	?	-
0la12	+	+	28	+	25	32	50	29	-	20	-	-	-	-	-	-	+	P prm-gl	31	32	i	32	-
0la13	+	+	23	+	28	33	46	30	29	18	29	29	18	dp.plp	-	35	+	P1 prm-tr	37	33	g	-	33
0la14	+	+	24	+	27	34	45	31	28	17	28	28	17	lv.plp	24	36+37	+	P2 prm-tr	36	34	l	34	34
0la15	-	-	-	-	-	-	-	-	-	-	-	-	-	-	-	-	-	-	-	-	-	-	-
0la16	+	+	25	+	29	35	47	32	30	-	30	30	/	fl2	?	38	+	P tr-p2	38+39	35	-	35	35
0la17	+	+	26+27	+	30	36	48	33+34	31	-	31	31	/	fl.t.plp	?	39+40	+	P tr-p3	40+41	36	-	36	36
0hy1	+	+	10	13	45	41	11	45	38	3	38	38	/	s.dl.ph?	10	52b	+	-	49	41	C1	41	41a
0hy2	+	+	31	14	46	47	12	47	-	/	39?	39?	/	-	?	52a	-	-	52	47	C2?	lm?	41b
0hy3	+	+	19	16	31	42	43	24	32	/	32	32	/	pr.hyph	19	42	+	-	42	42+mx.z ?	r	-	42?
0hy4	-	-	-	-	-	-	-	-	-	-	-	-	-	-	-	-	-	-	-	-	-	-	-

Appendix 1 continued

Abbrev.	**Mantophasmatodea:** Wipfler et al. 2011	**Blattodea:** Wipfler et al. 2011	**Blattodea:** Dorsey 1943	**Blattodea:** Snodgrass 1943, 1944	**Isoptera:** Vishnoi 1956, 1962	**Mantodea:** Hymenopus	**Mantodea:** Leverault 1938	**Mantodea:** Carbonaro 1949	**Orthoptera:** Zolessi 1968	**Orthoptera:** Strenger 1942	**Orthoptera:** Blackith & Blackith 1967	**Orthoptera:** Albrecht 1953	**Dermaptera:** Strenger 1942	**Dermaptera:** Kadam 1961	**Dermaptera:** Dorsey 1943	**Embioptera:** Rähle 1970	**Phasmatodea:** Wipfler et al. 2011	**Phasmatodea:** Marquardt 1940	**Phasmatodea:** Maki 1935	**Zoraptera:** Beutel & Weide 2005	**Psocoptera:** Badonnel 1934	**Hymenoptera:** Beutel & Vilhelmsen 2007	**Neuroptera:** Beutel 2010
0hy5	+	+	-	+	-	M c.	15?	49	-	/	41?	41?	/	-	-	53	+	-	-	-	z	-	42?
0hy6	-	-	-	-	-	-	-	-	-	/	-	-	/	-	-	-	-	-	-	-	-	-	-
0hy7	+	+	17	19	34	38	41	26	27	/	27	27	/	v.dl.sl+	17	43	+	P1 pera-sa	35	38	k?	38	-
0hy8	+	+	18	20	35	39	40	25	26	/	26	26	/	-	18	44	+	P2 pera-sa	34	39	h	39	39
0hy9	+	+	12+13?	-	40	67	-	-	-	/	-	-	/	-	12+13?	51	+	-	-	67	+	ms?	67
0hy10	?	-	-	-	-	M b.	-	-	-	/	-	-	/	-	-	50	+	-	-	-	-	-	-
0hy11	-	-	-	-	-	-	-	-	-	/	-	-	/	-	-	-	-	-	-	-	-	-	-
0hy12	+	+	15+16	17+18	32-33	37	42	27	-	/	-	-	/	d.dl.sl+	16	41	+	V sa-hy	43	37	-	37	37
0hy13	-	-	-	-	-	?			-	/	-	-	/	-	-	-	-	-	-	40?	-	-	-
0oc1	-	-	-	-	-	-	-	-	/	/	-	-	/	-	-	-	-	-	-	-	-	-	-
0oc2	+	+	-	-	-	-	-	-	/	/	-	-	/	-	-	67	+	-	-	-	-	-	-
0oc3	-	-	-	-	-	-	-	-	/	/	-	-	/	-	-	-	-	-	-	-	-	-	-
0oc4	-	-	-	-	-	-	-	-	/	/	-	-	/	-	-	-	-	-	-	-	-	-	-
0oc5	-	-	-	-	-	-	-	-	/	/	-	-	/	-	-	-	-	-	-	-	-	-	-

Appendix 1 continued

Abbrev.	**Mantophasmatodea:** Wipfler et al. 2011	**Blattodea:** Wipfler et al. 2011	**Blattodea:** Dorsey 1943	**Blattodea:** Snodgrass 1943, 1944	**Isoptera:** Vishnoi 1956, 1962	**Mantodea:** Hymenopus	**Mantodea:** Leverault 1938	**Mantodea:** Carbonaro 1949	**Orthoptera:** Zolessi 1968	**Orthoptera:** Strenger 1942	**Orthoptera:** Blackith & Blackith 1967	**Orthoptera:** Albrecht 1953	**Dermaptera:** Strenger 1942	**Dermaptera:** Kadam 1961	**Dermaptera:** Dorsey 1943	**Embioptera:** Rähle 1970	**Phasmatodea:** Wipfler et al. 2011	**Phasmatodea:** Marquardt 1940	**Phasmatodea:** Maki 1935	**Zoraptera:** Beutel & Weide 2005	**Psocoptera:** Badonnel 1934	**Hymenoptera:** Beutel & Vilhelmsen 2007	**Neuroptera:** Beutel 2010
0cu6	-	-	-	-	-	-	-	-	/	/	-	-	/	-	-	-	-	-	-	-	-	-	-
0ci1	+	+	5-8	5a	36-37	43	9	42+43	/	/	33	33	/	d1.cb	5-7	48+49	+	-	44	43	A+A´	43a+b	43
0bu1	-	+	-	5b?	41	-	-	-	/	/	34?	34?	/	-	-	54	-	-	45	?	B	44	44
0bu2	+	+	9	6	42	45	10	44	/	/	35	35	/	dl.b	9	55	+	-	46+47	45	E1+E2	45	45
0bu3	+	+	11	7	43	46	13	46	/	/	36+40?	36+40?	/	-	11	56+57	+	-	-	46	F	46	46
0bu4	+	-	-	-	-	-	-	-	/	/	40+45	40+45	/	-	-	64	+	-	50	-	-	-	-
0bu5	+	+	30	+	38	48	16	50	/	/	42	42	/	-	30	59	+	-	51	+	x	42?	48
0bu6	+	+	-	+	48+49	50	17	51	/	/	43	43	/	-	-	60	+	-	53	50	y	-	50
0ph1	+	+	-	8	44+47	51	14	48	/	/	37	37	/	d.dl.ph	-	58	+	-	48	51	H	51	51
0ph2	+	+	-	+	50-51	52a	18	52	/	/	44	44	/	v.dl.ph	-	61+62	+	-	54+55	52	u+v	52	52

Appendix 1 continued

Appendix 1 continued

Abbrev.	**Mantophasmatodea:** Wipfler et al. 2011	**Blattodea:** Wipfler et al. 2011	**Blattodea:** Dorsey 1943	**Blattodea:** Snodgrass 1943, 1944	**Isoptera:** Vishnoi 1956, 1962	**Mantodea:** Hymenopus	**Mantodea:** Leverault 1938	**Mantodea:** Carbonaro 1949	**Orthoptera:** Zolessi 1968	**Orthoptera:** Strenger 1942	**Orthoptera:** Blackith & Blackith 1967	**Orthoptera:** Albrecht 1953	**Dermaptera:** Strenger 1942	**Dermaptera:** Kadam 1961	**Dermaptera:** Dorsey 1943	**Embioptera:** Rähle 1970	**Phasmatodea:** Wipfler et al. 2011	**Phasmatodea:** Marquardt 1940	**Phasmatodea:** Maki 1935	**Zoraptera:** Beutel & Weide 2005	**Psocoptera:** Badonnel 1934	**Hymenoptera:** Beutel & Vilhelmsen 2007	**Neuroptera:** Beutel 2010
0ph3	+	+	-	11	-	52b	-	-	/	/	-	-	/	-	-	63	+	-	-	-	-	-	-
0st1	+	+	12+13	-	-	68	-	41	/	/	-	-	/	-	12+13	-	+	-	-	68	+	68	-
0st2	+	+	-	-	-	69	-	-	/	/	-	-	/	-	-	-	+	-	-	69	+	69	-

Character no.	*Machilis*	*Thermobia*	*Oniscigaster wakefieldi* (Staniczek 2001)	*Ephemera danica* (this study)	*Heptagenia sulphurea* (this study)	*Siphlonurus lacustris* (this study)	*Onychogomphus forcipatus* (this study)	*Lestes virens* (this study)	*Epiophlebia superstes* (this study)	*Perla marginata* (this study)	*Nemoura cinerea* (Moulins 1968)	*Galloisiana yuasai*	*Grylloblatta campodeiformis* (Walker 1931)	*Austrophasma spec.*	*Karoophasma spec.* (Baum et al. 2007)	*Timema*	*Agathemera*	*Phyllium*	*Sipyloidea*	*Megacrania sp.* (Musculature Maki 1935)	*Hymenopus coronatus* (Wipfler et al. XXX)	*Periplaneta americana*	*Embia ramburi* (Rähle 1970)	*Labidura riparia* (Kadam 1961)	*Locusta migratoria* (Albrecht 1953)	*Zorotypus hubbardi* (Beutel & Weide 2005)	*Stenopsocus stigmaticus* (Badonnel 1934)	*Macroxyela sp.* (Beutel & Vilhelmsen 2007)
0	0	0	0	0	1	0	0	0	0	1	1	1	1	0	0	1	1	1	1	1	0	2	1	1	0	0	0	0
1	2	0	2	2	2	2	2	2	2	2	2	0	0	0	0	0	0	0	0	0	2	1	0	0	2	2	2	2
2	0	1	0	0	0	0	0	0	0	0	0	1	1	0	0	0	0	0	0	0	0	0	0	0	0	0	0	0
3	3	1	0	1	0	0	0	1	0	1	1	1	1	1	1	1	1	1	1	1	1	0	1	1	0	?	1	1
4	0	0	0	0	0	0	1	0	1	0	0	0	0	0	0	0	0	0	0	0	?	0	0	0	0	0	0	0
5	1	0	0	0	0	0	0	0	0	0	0	0	0	0	0	0	0	0	0	0	0	0	0	0	0	1	0	1
6	0	0	0	0	0	0	0	0	0	0	0	0	0	0	0	0	0	0	0	0	1	0	0	0	0	0	0	0
7	?	0	0	0	0	0	0	0	0	0	0	0	0	0	0	0	0	0	0	0	0	0	0	0	0	1	0	0
8	0	0	0	0	0	0	1	1	1	1	1	1	1	1	1	1	1	1	1	1	1	1	1	1	1	0	1	0
9	-	-	-	-	-	-	0	0	0	0	0	0	0	0	0	0	0	0	0	0	1	0	0	0	0	-	0	-
10	0	0	0	0	0	1	1	1	1	0	0	0	0	0	0	0	0	0	0	0	1	0	0	0	0	0	0	0
11	0	0	0	0	0	0	1	0	1	0	0	0	0	0	0	0	0	0	0	0	0	0	0	0	0	0	0	0
12	0	0	0	0	0	0	0	0	0	0	0	0	0	0	0	1	1	1	1	1	0	0	0	0	0	0	0	0
13	0	0	0	0	0	0	0	0	0	0	0	0	0	0	0	0	0	0	0	0	1	0	0	0	0	0	0	0
14	0	0	0	0	0	0	0	0	0	0	0	0	0	1	1	0	0	0	0	0	0	0	0	0	0	0	0	0
15	0	0	0	1	0	0	1	1	1	0	1	1	1	1	1	1	1	1	1	1	1	1	1	1	1	1	1	0
16	-	-	0	0	-	0	0	0	0	-	0	0	0	0	0	0	0	0	0	0	0	0	0	0	0	0	1	-
17	-	-	-	1	-	-	1	1	1	-	0	0	0	0	0	0	0	0	0	0	0	0	0	0	0	0	0	-
18	0	0	1	1	1	1	0	0	0	0	0	0	0	0	0	0	0	0	0	0	0	0	0	0	0	0	0	0
19	0	0	0	0	0	0	0	0	0	0	0	0	0	1	1	0	0	0	0	0	0	0	0	0	0	0	0	0
20	0	1	0	0	0	?	0	0	0	0	0	0	0	0	0	0	0	0	0	0	0	0	0	0	0	0	0	0
21	?	-	0	0	0	?	0	0	0	1	1	0	0	0	0	1	1	1	1	1	0	0	1	?	0	1	?	?
22	0	0	1	1	1	1	1	1	1	1	1	1	1	1	1	?	1	1	1	1	1	1	1	1	1	1	1	1
23	1	0	0	0	0	0	0	0	0	0	0	1	1	0	0	?	0	0	0	0	0	0	0	0	0	0	0	0
24	1	0	?	0	1	1	1	1	1	1	1	1	1	1	1	?	1	1	1	1	1	1	1	1	1	1	1	1
25	-	0	1	1	1	1	1	1	1	0	0	0	0	1	1	0	0	0	0	0	1	1	0	0	1	?	1	1
26	0	1	1	1	1	1	1	1	1	0	0	0	0	0	0	0	1	1	1	1	0	0	0	0	0	?	1	1
27	1	1	0	0	0	0	0	0	0	1	1	1	1	2	2	1	1	1	1	1	1	1	1	1	2	1	2	1
28	0	0	0	0	0	0	0	0	0	0	0	0	0	1	1	0	0	0	0	0	0	0	0	0	0	0	0	0
29	0	0	0	0	0	0	0	0	0	0	0	0	0	0	0	0	0	1	0	0	0	0	0	0	0	0	0	1
30	0	0	0	0	0	0	0	0	0	0	0	0	0	0	0	0	0	1	0	0	0	0	0	0	0	0	0	0
31	1	1	2	2	2	2	2	2	2	2	2	4	4	4	0	?	4	0	?	4	0	0	2	0	4	4	0	0
32	4	1	3	2	2	2	2	2	2	2	2	2	2	5	0	?	5	5	5	?	0	0	2	2	5	2	5	5
33	0	0	1	0	1	1	1	1	1	0	0	0	0	0	0	?	1	1	1	1	0	0	1	1	1	1	0	0
34	0	0	?	1	1	0	1	1	1	0	1	1	1	1	1	?	0	0	0	0	1	1	0	1	1	0	1	0
35	0	0	1	1	1	?	1	1	1	1	1	1	1	1	1	1	1	1	1	1	1	1	1	1	1	1	1	1
36	?	0	0	0	0	?	0	0	0	1	1	1	1	0	0	1	1	1	1	1	1	1	1	1	1	0	0	0
37	?	-	-	-	-	?	-	-	-	1	1	0	0	-	-	0	0	0	0	0	0	0	1	0	0	-	-	-
38	0	0	1	1	1	1	1	1	1	0	0	0	0	0	0	0	0	0	0	0	0	0	0	0	0	?	?	0
39	0	0	-	-	-	-	-	-	-	0	0	0	0	1	1	1	1	1	1	1	1	1	0	0	0	?	?	0
40	0	0	-	-	-	-	-	-	-	0	0	0	0	0	0	1	1	1	1	1	1	1	1	1	1	?	?	0
41	-	-	-	-	-	-	-	-	-	-	-	-	-	-	-	?	1	1	1	1	1	1	0	0	1	?	?	-
42	-	-	-	-	-	-	-	-	-	-	-	-	-	-	-	?	1	0	0	1	1	1	0	0	1	?	?	-
43	-	-	-	-	-	-	-	-	-	1	1	-	-	-	-	?	0	0	0	0	0	0	0	0	1	?	?	-
44	-	-	-	-	-	-	-	-	-	-	-	-	-	-	-	?	0	0	0	0	0	0	1	0	0	?	?	-
45	0	0	-	-	-	-	-	-	-	1	1	1	1	1	1	0	0	0	0	0	0	0	0	1	0	?	?	0
46	-	-	-	-	-	-	-	-	-	0	0	1	1	1	1	-	-	-	-	-	-	-	-	0	-	?	?	-
47	0	0	1	1	1	1	1	1	1	1	1	1	1	1	1	0	1	1	1	1	1	1	1	1	1	1	1	1
48	0	1	1	1	1	1	1	1	1	1	1	1	1	1	1	1	1	1	1	1	1	1	1	1	1	1	1	1
49	0	1	-	0	0	0	1	1	1	0	0	0	0	0	0	0	0	0	0	0	0	0	0	0	0	0	0	0

Appendix 2 Character matrix used for phylogenetic analysis in chapter 3

50	-	-	0	0	0	0	0	0	0	1	1	1	1	0	0	0	0	0	0	0	0	0	0	1	0	0	0	0
51	-	-	0	0	0	0	0	0	0	0	0	0	0	0	0	0	0	0	1	1	0	0	0	0	0	0	0	0
52	-	-	0	0	0	0	0	0	0	0	0	0	0	0	0	0	0	0	0	0	1	1	0	0	0	0	0	0
53	0	0	0	0	0	0	0	0	0	0	0	0	0	0	0	0	0	0	0	0	1	0	0	0	0	0	0	0
54	0	1	1	1	1	1	1	1	1	1	1	1	1	1	1	1	1	1	1	1	1	1	1	1	1	1	1	1
55	0	0	0	0	0	0	0	0	0	0	0	0	0	0	0	0	0	0	0	0	1	0	1	1	1	1	1	1
56	0	0	1	1	1	1	1	1	1	1	1	1	1	1	1	?	1	1	1	1	1	1	1	1	1	1	1	1
57	0	0	1	1	1	1	1	1	1	1	1	1	1	1	1	?	1	1	1	1	1	1	1	1	1	1	1	1
58	0	0	1	1	1	1	1	1	1	1	1	1	1	1	1	?	1	1	1	1	1	1	1	1	1	1	1	1
59	0	0	1	1	1	1	1	1	1	1	1	1	1	1	1	?	1	1	1	1	1	1	1	1	1	1	1	1
60	5	1	0	0	0	0	1	1	1	2	2	0	0	4	4	1	1	3	3	3	1	1	1	1	1	2	?	?
61	2	1	0	0	0	0	1	1	1	3	3	1	0	5	5	1	1	4	4	4	1	1	0	1	?	3	?	2
62	-	-	-	-	-	-	-	-	-	-	-	-	-	-	-	-	-	1	0	2	-	-	-	-	-	-	-	-
63	-	-	-	-	-	-	-	-	-	-	-	-	-	-	-	0	0	1	0	1	-	-	-	-	-	-	-	-
64	0	0	0	0	0	0	0	0	0	0	0	0	0	0	0	0	0	0	0	0	1	1	0	0	0	0	0	0
65	0	1	1	1	1	1	1	1	1	1	1	1	1	1	1	1	1	1	1	1	1	1	1	1	1	1	1	1
66	-	0	1	1	1	1	2	2	2	2	2	2	2	2	2	2	2	2	2	2	2	2	2	2	2	2	2	2
67	-	0	0	0	0	0	1	1	1	1	1	1	1	1	1	1	1	1	1	1	1	1	1	1	1	1	1	1
68	1	0	0	0	0	0	1	1	1	1	1	1	1	1	1	1	1	1	1	1	1	1	1	1	1	1	1	1
69	0	0	0	0	0	0	1	1	1	1	1	1	1	1	1	?	1	1	1	1	1	1	1	1	1	1	1	1
70	0	0	0	0	0	0	0	0	0	1	1	0	0	0	0	?	0	0	0	0	0	0	0	?	?	1	0	1
71	0	0	0	0	0	0	0	0	0	1	1	1	1	1	1	?	1	1	1	1	1	1	1	1	1	1	1	1
72	0	0	0	0	0	0	0	0	1	1	1	1	1	1	1	?	1	1	1	1	1	1	1	1	1	1	1	1
73	0	0	0	0	0	0	0	0	0	0	0	0	0	0	0	0	0	0	0	0	0	0	0	0	0	0	1	0
74	0	0	0	0	0	0	0	0	0	0	0	0	0	0	0	0	0	0	0	0	0	0	0	0	0	1	1	1
75	0	0	0	0	0	0	1	1	1	0	0	0	0	0	0	0	0	0	0	0	0	0	0	0	0	0	0	0
76	?	?	-	-	-	-	-	-	-	?	?	0	?	0	0	0	0	2	1	?	0	0	?	?	0	0	?	?
77	0	0	1	1	1	1	-	-	-	0	0	0	0	0	0	0	0	0	0	0	0	0	0	0	0	0	0	0
78	3	0	0	0	1	0	0	0	0	0	0	0	0	0	0	0	0	0	0	0	0	0	0	0	0	0	1	2
79	0	0	0	0	0	0	0	0	0	0	0	0	0	0	0	0	0	0	0	0	0	0	0	0	0	1	1	1
80	0	0	-	-	-	-	-	-	-	0	0	0	0	0	0	0	0	0	0	0	1	1	0	0	0	?	0	0
81	0	0	0	0	0	0	0	0	0	0	0	0	0	0	0	0	0	0	0	0	0	0	0	0	0	0	1	1
82	1	0	2	2	2	2	1	1	1	1	1	0	1	1	1	1	0	3	0	1	1	1	1	?	0	1	-	-
83	1	1	0	0	0	0	0	0	0	1	1	1	1	1	1	1	1	1	1	1	1	1	1	1	1	1	1	1
84	0	0	0	0	0	0	0	0	0	0	0	1	1	0	0	0	0	0	0	0	0	0	0	0	0	0	0	0
85	0	0	0	0	0	0	-	-	-	0	0	0	0	0	0	0	1	1	1	1	0	0	0	0	0	0	0	0
86	5	4	3	3	3	3	2	2	2	0	0	0	0	0	0	0	0	0	0	0	0	0	0	0	0	0	1	0
87	1	1	0	1	0	0	1	1	1	1	1	1	?	1	1	0	0	1	1	1	1	1	0	0	0	1	0	1
88	0	0	1	1	1	1	-	-	-	0	0	0	0	0	0	0	0	0	0	0	0	0	0	0	0	0	1	0
89	0	0	0	0	0	0	1	1	1	1	1	0	0	0	0	?	0	0	0	0	0	0	0	0	0	0	?	0
90	0	0	0	0	0	0	0	0	0	1	1	1	1	1	1	1	1	1	1	1	0	1	1	1	1	0	0	0
91	-	-	-	-	-	-	-	-	-	0	0	1	?	1	1	0	0	0	0	0	-	0	0	0	0	-	-	-
92	-	-	-	-	-	-	-	-	-	0	0	1	1	0	0	0	0	0	0	0	-	0	-	0	0	-	-	-
93	0	0	0	0	0	0	0	0	0	0	0	0	0	0	0	0	0	0	0	0	0	0	0	0	0	0	1	0
94	0	0	0	0	0	0	0	0	0	0	0	1	1	1	1	0	0	0	0	0	1	1	0	1	0	0	0	0
95	0	0	0	0	0	0	1	1	0	0	0	0	0	0	0	0	0	0	0	0	0	0	0	-	0	0	0	-
96	0	0	0	0	0	0	0	0	0	0	0	0	0	0	0	0	0	0	0	0	0	0	0	1	0	0	0	1
97	0	1	1	1	1	1	-	-	1	1	1	1	1	1	1	1	1	1	1	1	1	1	1	-	1	1	1	-
98	0	1	1	1	1	1	-	-	1	1	1	1	1	1	1	1	1	1	1	1	1	1	1	1	1	1	1	1
99	0	0	0	0	1	0	-	-	-	0	0	0	0	0	0	1	1	1	1	1	0	0	1	1	1	0	1	2
100	0	0	0	0	0	0	0	0	0	1	0	0	0	0	0	1	1	1	1	1	0	0	1	-	1	0	0	-
101	0	0	0	0	0	0	0	0	0	0	0	1	1	1	1	0	0	0	0	0	0	0	0	0	0	0	0	0
102	0	3	0	0	2	0	1	1	1	0	0	0	0	0	0	0	0	0	0	0	0	0	0	0	0	0	1	0
103	0	0	0	0	0	0	1	1	1	0	0	0	0	0	0	0	0	1	0	0	0	0	0	0	0	0	0	0
104	0	0	0	0	0	0	1	1	1	0	1	0	0	0	0	0	0	0	0	1	0	0	0	0	0	0	0	0
105	0	0	0	0	0	0	1	1	1	0	0	0	0	0	0	0	0	0	0	0	0	0	0	0	0	0	0	0
106	1	0	1	1	1	1	1	1	1	1	1	1	1	1	1	?	1	1	1	1	1	1	1	1	1	1	1	1
107	1	0	1	1	1	1	1	1	1	1	1	1	1	1	1	?	1	1	1	1	1	1	1	1	1	1	1	1
108	1	0	1	1	1	1	1	1	1	1	1	1	1	1	1	?	1	1	1	1	1	1	1	1	1	1	1	1
109	1	0	1	1	1	1	1	1	1	1	1	1	1	1	1	?	1	1	1	1	1	1	1	1	1	1	1	1
110	0	0	0	0	0	0	1	1	1	0	0	0	0	0	0	?	0	0	0	0	0	0	0	0	0	0	0	0
111	1	1	1	1	1	1	-	-	-	0	0	0	0	1	1	?	0	0	0	0	1	0	1	1	1	1	1	1
112	0	0	0	1	0	0	1	1	1	0	0	1	1	1	1	?	0	0	0	0	0	0	0	0	0	?	1	0
113	0	0	?	-	0	0	-	-	-	0	0	0	0	0	0	?	1	1	1	1	0	0	1	0	0	0	0	0
114	0	0	1	1	1	1	1	1	1	1	1	1	1	1	1	?	1	1	1	1	1	1	1	1	1	1	1	1
115	0	0	0	0	0	0	0	0	0	0	0	0	0	0	0	?	0	0	0	0	0	0	0	0	1	0	0	0

Appendix 2 continued

116	0	0	0	0	-	0	0	0	0	0	0	0	0	0	0	?	0	0	0	0	0	0	0	0	-	1	0	0
117	0	0	1	1	1	1	1	1	1	1	1	1	1	1	1	?	1	1	1	1	1	1	1	1	1	1	1	1
118	1	0	0	0	0	0	0	0	0	1	1	0	0	0	0	?	0	0	0	0	0	0	0	0	0	0	0	0
119	?	?	0	0	0	0	1	1	1	0	0	0	0	0	0	?	0	0	0	0	0	0	0	0	0	0	0	?
120	0	0	0	0	0	0	1	1	1	0	0	0	0	0	0	?	0	0	0	0	0	0	1	1	1	0	0	0
121	0	0	0	0	0	0	0	0	0	0	1	0	0	0	0	?	0	0	0	0	0	0	0	0	0	0	0	1
122	0	0	1	1	1	1	1	1	1	0	0	0	0	0	0	?	0	0	0	0	0	0	0	0	0	0	0	0
123	0	0	0	0	0	0	0	0	0	0	0	1	?	0	0	0	0	0	0	0	0	0	0	0	0	0	0	0
124	0	0	0	0	0	0	0	0	0	0	0	1	1	1	1	0	0	0	0	0	0	0	0	0	0	?	0	-
125	0	1	0	0	0	0	1	1	1	1	1	1	1	1	1	1	1	1	1	1	1	1	1	?	1	1	1	1
126	0	0	1	1	1	1	0	0	0	0	0	0	0	0	0	0	0	0	0	0	0	0	0	0	0	0	0	0
127	0	0	-	-	-	-	0	0	0	0	?	0	?	0	0	0	1	1	1	1	0	0	0	?	0	?	?	?
128	0	0	0	0	0	?	1	1	1	0	0	0	0	0	0	?	0	0	0	0	0	0	1	0	0	0	0	1
129	0	0	?	1	1	1	1	1	1	0	0	1	1	0	0	?	0	0	0	0	0	0	0	0	0	0	0	1
130	0	0	1	1	1	1	1	1	1	1	1	1	1	1	1	?	1	1	1	1	1	1	1	1	1	1	1	1
131	?	1	?	1	1	1	0	0	0	1	1	1	1	1	1	?	1	1	1	1	1	1	1	0	1	1	1	1
132	?	0	1	1	1	1	1	1	1	1	1	1	1	1	1	?	1	1	1	1	1	1	1	1	1	1	1	1
133	1	0	1	1	1	1	0	0	0	0	0	0	0	0	0	0	0	0	0	0	0	0	0	0	1	0	1	0
134	0	0	0	0	0	0	1	1	1	0	0	0	0	0	0	?	0	1	1	1	0	0	0	0	0	0	0	0
135	1	0	1	1	0	1	0	0	0	0	0	1	1	1	1	?	1	1	1	1	0	0	1	0	1	0	0	0
136	0	0	0	0	0	0	1	1	1	0	0	0	0	0	0	?	0	0	0	0	0	0	0	1	0	0	0	?
137	0	0	0	0	0	0	0	0	0	0	0	0	0	0	0	?	0	0	0	0	0	0	0	0	0	0	1	1
138	1	1	?	0	0	0	0	0	0	0	0	0	0	0	0	?	1	1	1	1	0	0	0	0	0	0	-	-

Appendix 2 continued

Appendix 3: List of phylogenetically relevant characters used in chapter 3: The following list comprises 139 characters of the head capsule, its appendages and musculature.

Head capsule:

0. **Orientation of head: (0) orthognathous; (1) prognathous or slightly inclined (2) hypognathous** (character 0 of Wipfler *et al.* 2011). The headcapsule of *Periplaneta* [Blattodea] is hypognathous, while it is distinctly prognathous in *Galloisiana* [Grylloblattodea] (Wipfler *et al.* 2011), *Grylloblatta* [Grylloblattodea] (Walker 1931), *Labidura* [Dermaptera] (Kadam 1961), *Embia* [Embioptera] (Rähle 1970), Phasmatodea (Friedemann *et al.* in press) and the nymphs of *Nemoura* [Plecoptera] (Moulins 1968) and *Perla* [Plecoptera]. It is orthognathous in *Machilis* [Archaeognatha], *Thermobia [*Zygentoma] and all examined species of Odonata, Ephemeroptera (Staniczek 2001), Mantophasmatodea (Baum *et al*. 2007), *Hymenopus* [Mantodea] (Wipfler *et al*. submitted), *Stenopsocus* [Psocoptera] (Badonnel 1934), *Macroxyela* [Hymenoptera] (Beutel & Vilhelmsen 2007), *Locusta* [Orthoptera] (Albrecht 1953), *Ictinus* [Odonata] (Mathur & Mathur 1961) and *Zorotypus* [Zoraptera] (Beutel & Weide 2005).

1. **Number of ocelli (0) 0; (1) 2; (2) 3**: Three are present in most groups of Pterygota (e.g., Yuasa, 1920) and in *Machilis*. Ocelli are absent in *Thermobia* and *Ctenolepisma* (Chaudonneret, 1950; Woo, 1950) and different degrees of reductions occur in other groups. Pipa (Pipa et al. 1964) describes a median frontal organ which shows a structural resemblance to photoreceptors, but its homology with the ocelli of pterygotes is unclear. Ocelli are also missing in *Galloisiana* (Wipfler *et al.* 2011) and *Grylloblatta* (Walker, 1931), in both studied species of Mantophasmatodea (Baum *et al*., 2007), in *Embia* (Rähle, 1970), in *Labidura* (Kadam, 1961), and in the studied phasmatodeans (Friedemann *et al.* in press). In *Periplaneta* - as in all roaches and termites (Klass & Eulitz, 2007) - the median ocellus is missing, a potential autapomorphy of Blattodea s.l. (i.e. incl. Isoptera). All extant dermapterans lack ocelli, but they are present in fossil species (Grimaldi & Engel, 2005). This might possibly also apply to Grylloblattodea (Storozhenko, 1997) and Mantophasmatodea (Engel & Grimaldi, 2004). It is very likely that the presence of three ocelli is ancestral for Pterygota (and probably even Insecta), and that reduction has taken place many times.

2. **Compound eyes: (0) more than 80 ommatidia; (1) less than 80 ommatidia** (character 1 of Wipfler *et al.* 2011) Compound eyes with more than 80 ommatidia are commonly found in ectognathous insects. Only around 60 are present in *Galloisiana* (Wipfler *et al.* 2011) and *Grylloblatta* (Walker 1931). Only 12 ommatidia are present in *Thermobia* and *Ctenolepisma* (Chaudonneret 1950; Woo 1950).

3. **Distance between compound eyes: (0) less than their own width; (1) greater than their own width; (2) eyes fused at single point; (3) eyes broadly fused along an eye seam.** In *Machilis* the compound eyes are broadly fused along an eye seam. In the ephemeropterans *Oniscigaster* (Staniczek 2001), *Ephemera*, *Heptagenia* and the odonatans *Onychogomphus* and *Epiophlebia* the distance between the eyes is smaller than the diameter of one eye. In all other examined species it is greater than one ocular diameter.

4. **Shape of vertex: (0) flat, not developed into large protuberance; (1) conical, or developed into a large transverse ridge.** A conical vertex is present in *Onychogomphus* and *Epiophlebia* and states a potential apomorphy for Epiprocta.

5. **Epicranial or coronal suture: (0) present; (1) absent** (character 3 of Wipfler *et al.* 2011)**.** A coronal or epicranial suture is absent in *Machilis*, *Macroxyela* (Beutel & Vilhelmsen 2007) and *Zorotypus* (Beutel & Weide 2005), but present in all other species examined. A coronal suture is reported for embryonic stages of Archaeognatha, but vanishes in the postembryonic ones. Mathur & Mathur (1961) report its absence in the odonatan *Ictinus angulosus* but since it is present in all studied odonatans and also in *Davidinius nanus* and *Mnais strigata* (both Asahina 1954) its presence can be considered a groundplan character of Odonata.

6. **Parietal ridge: (0) absent; (1) present** (character 2 of Wipfler *et al.* 2011). The parietal ridge is only present in Mantodea (Levereault 1936; Beier 1964, 1968; Wipfler *et al.* submitted). It runs from the posterior articulation of the mandible around the posterior (prognathous) or dorsal (orthognathous) head capsule and joins the coronal sulcus. A small transverse ridge connects the parietal ridge with the occipital foramen. Beier (1964, 1968) discussed this structure as a possible remnant of the occipital ridge.

7. **Postoccipital ridge: (0) present; (1) absent** (character 4 of Wipfler *et al.* 2011). A postoccipital ridge is present in all species examined with the exception of *Zorotypus* (Beutel & Weide 2005). The situation in *Machilis* is unclear (coded with ?). Mathur & Mathur (1961) describe an incomplete ridge in the odonatan *Ictinus angulosus* while it is fully developed in all other studied species (also see Asahina 1954). The absence is most likely an autapomorphy of Zoraptera.

8. **Subgenal ridge: (0) absent; (1) present** (character 5 of Wipfler *et al.* 2011). A subgenal ridge (=hypostomal + pleurostomal ridge) is present in all studied odonatans and all neopteran representatives examined with the exception of *Zorotypus* (Beutel & Weide 2005) and *Macroxyela* (Beutel & Vilhelmsen 2007). Chaudonneret (1950) considered a subgenal ridge as to be present in *Thermobia domestica*, but we could not detect this ridge in our analysis by µCT and accordingly score it as absent in this species. Absence of the subgenal ridge in Zygentoma and Ephemeroptera has already been corroborated by Staniczek (2000, 2001).

9. **Pleurostomal ridge and circumoccular ridge: (0) not in contact; (1) partly in contact** (character 7 of Wipfler *et al.* 2011). Partly in contact in *Hymenopus* (Wipfler *et al*. subm.b) and also in *Eremiaphila*, *Sphodromantis* and *Mantoida* (Klass & Eulitz 2007). The descending posterior part of the pleurostomal ridge is missing in *Mantoida*. Not applicable to species without a subgenal ridge (see character 9).

10. **Interantennal ridge: (0) absent; (1) present** (character 8 of Wipfler *et al.* 2011). Present in all studied odonatans and the mantodeans *Hymenopus* (Wipfler *et al*. submitted), *Mantoida*, *Eremiaphila* and *Sphodromantis* (Klass & Eulitz 2007). This might be a potential autapomorphy of Mantodea (Wipfler *et al*. submitted) and Odonata, respectively. Klass & Eulitz (2007) discussed the possibility that the epistomal ridge in *Thermobia domestica* may rather represent the interantennal ridge. We consider the origin of muscles 0ci1 and 0bu1 at this ridge in *Thermobia* as sufficient evidence in support of its interpretation as epistomal ridge (see also origins of muscle "db" and "dc" in Chaudonneret (1950) Fig. 7).

11. **Shape of frons: (0) flat when seen from lateral; (1) outwardly bulged when seen from lateral.** A grossly enlarged frons is present in the studied odonatans Onychogomphus and Epiophlebia. It is present in all Anisoptera (Rehn 2003) and Epiophlebioptera and is a potential autapomorphy for Epiprocta.

12. **Distinct convexity ventrad the antennal bases: (0) absent; (1) present** (character 104 of Friedemann *et al.* in press). A distinct convexity ventrad the antennal bases is a potential autapomorphy of Phasmatodea (Bradler 2009). A similar condition does not occur in potentially related groups including Embioptera and Orthoptera (e.g. Rähle 1970; Albrecht 1953).

13. **Scutellum: (0) absent; (1) present** (character 10 of Wipfler *et al.* 2011). A frontal shield or scutellum as defined by Klass & Eulitz (2007) is present in *Hymenopus* (Wipfler et al. subm) and in other mantids (Levereault 1936; Beier 1968; Lombardo 1984; Ehrmann 2002; Klass & Eulitz 2007). This is a potential autapomorphy of Mantodea (Wipfler et al. subm).

14. **X-shaped median apodeme on the frontal region: (0) absent; (1) present** (character 11 of Wipfler *et al.* 2011). An x-shaped apodeme is present on the frontal region of *Karoophasma* (Baum *et al*. 2007) and *Austrophasma*. This is an autapomorphy of Mantophasmatodea (Baum *et al*.

2007, Wipfler *et al.* 2011).

15. **Clypeus: (0) not subdivided; (1) subdivided into ante- and postclypeus** (character 12 of Wipfler *et al.* 2011)**. The clypeus is subdivided in a harder post- and a softer anteclypeus** in most pterygote insects, but this is not the case in *Heptagenia, Oniscigaster*, *Siphlonurus, Perla* and *Macroxyela* (Beutel & Vilhelmsen 2007. It is neither subdivided in *Machilis*, *Thermobia* and *Ctenolepisma* (Woo 1950).

16. **Postclypeus: (0) not outwardly bulged; (1) outwardly bulged** (character 13 of Wipfler *et al.* 2011)**.** An enlarged postclypeus as it is present in *Stenopsocus* (Badonnel 1934) is likely an autapomorphy of Acercaria (Willmann 2003). This condition is correletated with a distinctly enlarged M. clypeopalatalis (0ci1) and a strongly developed cibarial pumping apparatus. This condition must not be mixed up with the condition in many other pterygotes where the postclypeus is wider the the anteclypeus when seen from frontal, but condition of 0ci1 and the cibarial pumping apparatus are not as stated above.

17. **Anteclypeus: (0) membranous; (1) chitinous. The anteclypeus that can be separated by the postclypeus by being softer is membranous** in all neopterans possessing this structure. In *Ephemera* and all studied Odonata it is sclerotized but distinctively softer than the postclypeus

18. **Adult mouthparts: (0) with function; (1) without function.** Adult mouthparts without function are a potential autapomorphy of Ephemeroptera. All other examined species posses fully functional mouthparts in their adult livestage.

Labrum:

19. **Oval sclerotisation of labral base: (0) absent; (1) present** (character 14 of Wipfler *et al.* 2011)**.** An oval median sclerotisation of the labral base is probably an autapomorphy of Mantophasmatodea (Baum *et al*. 2007, Wipfler *et al.* 2011). It is absent in all other species examined.

20. **Tormae: (0) present; (1) absent** (character 34 of Wipfler *et al.* 2011). Not present in *Thermobia* (Chaudonneret 1950) but mentioned explicitly by Woo (1950) (*Ctenolepisma*).

21. **Mesal extension of tormae: (0) present; (1) absent** (character 35 of Wipfler *et al.* 2011). Present in Ephemeroptera, Odonata, *Galloisiana* (Wipfler *et al.* 2011), *Grylloblatta* (Walker 1931), *Mantophasmatodea*, *Hymenopus* (Wipfler et al. subm), *Periplaneta* (Wipfler *et al.* 2011) and *Locusta* (Albrecht 1953). There is no information for *Machilis, Siphlonurus*, *Labidura* (Kadam 1961), *Stenopsocus* (Badonnel 1934) and *Macroxyela* (Beutel & Vilhelmsen 2007) (coded as ?). This character is not applicable to *Thermobia* (Chaudonneret 1950). Absent in all examined Phasmids (Friedemann *et al.* in press), Embioptera (Rähle 1970) and Zoraptera (Beutel & Weide 2005).

22. **M. epistoepipharyngealis (0lb3): (0) present; (1) absent** (character 74 of Wipfler *et al.* 2011). Only present in *Thermobia* (Chaudonneret 1950) and *Machlis* (Bitsch 1963).

23. **M. labroepipharyngalis (0lb5): (0) present; (1) absent** (character 75 of Wipfler *et al.* 2011). Present in all taxa under consideration with the exception of *Machilis* (Bitsch 1963), *Galloisiana* (Wipfler *et al.* subm.a) and *Grylloblatta* (Walker 1931).

24. **M. labrolabralis (0lb6): (0) present; (1) absent** (character 76 of Wipfler *et al.* 2011)**.** Present in *Thermobia* (Chaudonneret 1950). The situation in *Oniscigaster* (Staniczek 2001) is unclear (coded as ?).

Antenna:

25. **Insertion of antennae: (0) close to the anterior mandibular articulation with the pleurostomal and circumantennal ridges in contact (where applicable); (1) distinctly separated from the anterior mandibular articulation, pleurostomal and circumantennal ridges not in contact.** (character 9 of Wipfler *et al.* 2011)**.** The antennal socket of *Nemoura* (Moulins 1968), *Perla* (Chisholm 1962), all examined Phasmatodea, Grylloblattodea (Walker 1931, Wipfler *et al.* 2011), *Embia* (Rähle 1970), and various dermapterans (Kadam 1961;

Giles 1963) is adjacent to the anterior mandibular articulation.

26. **Antennifer: (0) present; (1) reduced** (character 108 of Friedemann *et al.* in press)**.** Generally missing in Euphasmatodea (Bradler 2009). Distinctly developed in *Timema* (Tilgner 1999), *Embia* (Rähle 1970) and Mantophasmatodea (Baum et al. 2007). Reduced in Orthoptera according to Tilgner (2002) but present in *Locusta migratoria* (Albrecht 1953: fig. 15). The antennifer is also reduced in *Thermobia*, Ephemeroptera (Staniczek 2001), Odonata, *Stenospocus* (Badonnel 1934) and *Macroxyela* (Beutel & Vilhelmsen 2007). Data is missing for *Zorotypus* (Beutel & Weide 2005).

27. **Length of pedicel and scapus: (0) pedicel longer than scapus; (1) scapus longer than pedicel; (2) scapus and pedicel equal in length.** In Ephemeroptera and Odonata the pedicellus is longer than the scape while in Mantophasmatodea (Baum *et al.* 2007, Wipfler *et al.* 2011), *Locusta* (Albrecht 1953) and *Stenopsocus* (Badonnel 1934) they are of equal length.

28. **Oval sclerite in membrane connecting scapus and pedicellus: (0) absent; (1) present** (character 15 of Wipfler *et al.* 2011)**.** A small oval sclerite in the articulatory membrane between the scapus and pedicellus is present in *Austrophasma* (Wipfler *et al.* 2011) and *Karoophasma* (Baum *et al*. 2007), but not known for any other group of insects. This is very likely an autapomorphy of Mantophasmatodea.

29. **Size of first flagellomere: (0) not enlarged; (1) first flagellomere more than twice as long as second one** (character 109 of Friedemann *et al.* in press)**.** The first flagellomere is more than twice as long as second one in *Phyllium*. A similar condition is present in *Pseudodatames* (Bradler 2009). The first flagellomere of *Macroxyela* (Beutel & Vilhelmsen 2007) is enlarged as well.

30. **Antennal stridulatory organ: (0) absent; (1) present** (character 110 of Friedemann *et al.* in press)**.** The stridulatory file and ridge are present in *Phyllium*. The presence on the enlarged first flagellomere of adult females and juvenile males is very likely an autapomorphy of Phylliinae (Bradler 2009). The organ produces a defensive stridulatory sound (Bedford 1978).

31. **Areas of origin of antennal muscle 0an1: (0) anterior tentorial arms only; (1) anterior tentorial arms and tentorial bridge; (2) on dorsal tentorial arms only; (3) anterior and dorsal tentorial arm.** The M. tentorioscapalis anterior (0an1) originates on the anterior tentorial arms in *Karoophasma* (Baum *et al*. 2007), *Hymenopus* (Wipfler et al. subm), *Periplaneta* (Wipfler *et al.* 2011), *Phyllium* (Friedemann et al. in press), *Labidura* (Kadam 1961), *Stenopsocus* (Badonnel 1934) and *Macoxyela* (Beutel & Vilhelmsen 2007). In *Machilis* and *Thermobia* it originates on the anterior tentorial arms and the tentorial bridge, in all ephemeropterans, odonates and plecopterans as well as *Embia* (Rähle 1970) it originates on the dorsal tentorial arms only. The muscle originates on the anterior and dorsal tentorial arms in Grylloblattodea, *Austrophasma* (Wipfler *et al.* 2011), *Agathemera* (Wipfler *et al.* 2011), *Megacrania* (Maki 1934), *Locusta* (Albrecht 1953) and *Zorotypus* (Beutel & Weide 2005).

32. **Areas of origin of antennal muscle 0an2: (0) anterior tentorial arms only; (1) anterior tentorial arms and tentorial bridge; (2) on dorsal tentorial arms only; (3) on dorsal arms and tentorial bridge; (4) tentorial bridge only; (5) dorsal and anterior tentorial arms.** The M. tentorioscapalis posterior (0an2) originates on the anterior tentorial arms in *Karoophasma* (Baum et al. 2007), *Hymenopus* (Wipfler et al. subm)*, Periplaneta* (Wipfler *et al.* 2011)*, Locusta* Albrecht 1953)*, Stenopsocus* (Badonnel 1934) *and Macroxyela* (Beutel & Vilhelmsen 2007). In *Thermobia* it originates on the anterior tentorial arms and tentorial bridge, in Odonata, Ephemeroptera (except *Oniscigaster*), Plecoptera, Grylloblattodea, *Embia* (Rähle 1970), *Labidura* (Kadam 1961) and *Zorotypus* (Beutel & Weide 2005) on the dorsal tentorial arms only. In *Oniscigaster* (Staniczek 2000) the muscle originates on the dorsal arms and

tentorial bridge, while it originates on the tentorial bridge only in *Machilis*. In all remaining taxa the muscle originates on the dorsal and anterior tentorial arms.

33. **M. tentorioscapalis lateralis (0an3): (0) present; (1) absent** (character 70 of Wipfler *et al.* 2011)**:** Present in *Thermobia* (Chaudonneret 1950), *Ephemera*, *Nemoura* (Moulins 1968), *Perla*, *Galloisiana*, *Grylloblatta* (Walker 1931), *Austrophasma*, *Karoophasma* (Baum *et al*. 2007), *Hymenopus* (Wipfler et al. subm.b), *Periplaneta*, *Stenopsocus* (Badonnel 1934) and *Macroxyela* (Beutel & Vilhelmsen 2007). The situation in *Timema* is unknown (coded with ?).

34. **M. tentorioscapalis medialis (0an4): (0) present; (1) absent** (character 71 of Wipfler *et al.* 2011). Present in *Machlis*, *Thermobia* (Chaudonneret 1950), *Siphlonurus*, *Perla, Agathemera*, *Phyllium, Sipyloidea, Megacrania* (Maki 1934), *Embia* (Rähle 1970), *Zorotypus* (Beutel & Weide 2005) and *Macroxyela* (Beutel & Vilhelmsen 2007). The situation in *Oniscigaster* (Staniczek 2001) and *Timema* (Tilgner et al. 1999) is unclear (coded as ?).

Circulatory system:

35. **Circumesophageal vessel ring branching off the dorsal aorta posterior to the brain: (0) absent; (1) present** (character 16 of Wipfler *et al.* 2011)**.** A circular circumoesophageal vessel is present in Diplura, Collembola, Archaeognatha and Zygentoma (Pass 1991; Hertel & Pass 2002; Pass *et al*. 2006). Its presence is likely a groundplan feature of Hexapoda and is lost in the groundplan of Pterygota.

36. **Ostia of dorsal vessel: (0) lips always present; (1) ostia with and without lips (excurrent ostia)** (character 17 of Wipfler *et al.* 2011)**.** A dorsal vessel containing excurrent ostia without lips is present in Plecoptera, Grylloblattodea, Phasmatodea, Mantodea, Blattodea, Embioptera, Dermaptera, and Orthoptera (Pass 1991; Pass *et al*. 2006).

37. **Position and number of excurrent ostia within a segment: (0) one ventrolateral pair; (1) ventromedian** (character 18 of Wipfler *et al.* 2011)**.** Only Plecoptera and Embioptera possess excurrent ostia which are unpaired and located ventromedially (Pass 1991; Pass *et al*. 2006). The position is ventrolateral on both sides of the vessel in all other taxa with excurrent ostia (see char. 37).

38. **Antennal circulatory organs in adults: (0) present; (1) absent** (character 19 of Wipfler *et al.* 2011). Antennal circulatory organs in adults are present in all taxa under consideration with the exception of Ephemeroptera and Odonata (Pass *et al*. 2006). The situation in Zoraptera and Psocoptera is unknown (coded as ?). Beutel & Weide (2005) described a muscle connecting both sides of the vertex in *Zorotypus* (Mxy). Considering its position and course between the brain and M. frontobuccalis posterior it is very likely that this is the ampullo-ampullary dilator. But further investigation is necessary.

39. **Antennal vessel wall: (0) uniform; (1) bipartite** (character 20 of Wipfler *et al.* 2011)**.** Bipartite antennal vessel walls are present in Mantophasmatodea, Phasmatodea, Mantodea and Blattodea (Pass *et al*. 2006). The vessel is absent in Ephemeroptera and Odonata (coded as inapplicable) and the situation in Zoraptera and Psocoptera is unknown (coded as ?).

40. **Contractibility of antennal ampulla: (0) absent (non-pulsatile); (1) present (pulsatile)** (character 21 of Wipfler *et al.* 2011)**.** Pulsatile antennal ampullae are associated with contracting muscles. They are present in Phasmatodea, Mantodea, Blattodea, Embioptera, Dermaptera, Orthoptera, Neuroptera and in some species of Plecoptera (Pass *et al*. 2006). The character is coded as inapplicable for Ephemeroptera and Odonata (ampullae absent) and the situation in Zoraptera and Psocoptera is unknown (coded as ?).

41. **M. interampullaris (0ah1): (0) absent; (1) present** (character 22 of Wipfler *et al.* 2011)**.** The ampullo-ampullary dilator is present in Euphasmatodea, Mantodea, Blattodea and Orthoptera (Pass *et al*. 2006). The situation in Zoraptera, *Timema* and Psocoptera is unknown

(coded as ?) and coded as inapplicable for taxa without ampullae (*Machilis*, *Termobia*, Ephemeroptera, Odonata, Grylloblattodea, Mantophasmatodea, Hymenoptera).

42. **M. ampulloaortica (0ah2): (0) absent; (1) present** (character 23 of Wipfler *et al.* 2011)**.** Present in Phasmatodea (unknown for *Timema*, coded as ?), Mantodea, Blattodea and Orthoptera (Pass *et al*. 2006). Other taxa see previous characters.

43. **M. ampullopharyngealis (0ah3): (0) absent; (1) present** (character 24 of Wipfler *et al.* 2011)**.** Present in Plecoptera and Orthoptera (Pass *et al*. 2006). Other taxa see previous characters.

44. **M. ampullo-frontalis (0ah4): (0) absent; (1) present** (character 25 of Wipfler *et al.* 2011)**.** Only present in Embioptera (Pass *et al*. 2006) and probably autapomorphic. Other taxa see previous characters.

45. **Connection of antennal ampulla to supraoesophageal ganglion: (0) absent; (1) present** (character 26 of Wipfler *et al.* 2011)**.** Antennal ampullae with a connection to the supraoesophageal ganglion are present in Grylloblattodea, Plecoptera, Dermaptera (Pass 1991) and Mantophasmatodea.

46. **Oval nuclei in tissue connecting the antennal ampulla and supraoesophageal ganglion: (0) absent; (1) present** (character 27 of Wipfler *et al.* 2011)**.** In Dermaptera and Plecoptera a broad band of connective tissue connects the lateral wall of the antennal ampullae with the supraoesophageal ganglion (Pass 1991). No nuclei are reported for Plecoptera and Dermaptera. In Grylloblattodea (Pass 1991) and Mantophasmatodea small bands are present and contain small nuclei.

Cephalic endoskeleton:

47. **Anterior and posterior tentorium: (0) separated; (1) merged** (character 28 of Wipfler *et al.* 2011)**.** The anterior tentorial complex is not connected to the posterior elements in *Machilis* (Bitsch 1963) and *Thermobia* (Chaudonneret 1950). In all pterygote insects the anterior and posterior tentorial parts are merged, a condition interpreted as a pterygote autapomorphy by Staniczek (2000, 2001).

48. **Transverse mandibular tendon: (0) present; (1) absent.** A transverse mandibular tendon is only present in *Machilis* (Bitsch 1963). Its loss is likely an autapomorphy of dicondylic insects.

49. **Processes of the anterior tentorial apodemes extending into the lumen of the mandibular base: (0) absent; (1) present.** In Zygentoma and Odonata wing-like cuticular processes protrude into the mandibular lumen. They serve as attachment structures for 0md5+6+7 in *Thermobia* and for 0md6+8 in Odonata.

50. **Corpotentorium: (1) elongated; (0) short** (character 29 of Wipfler *et al.* 2011)**.** An elongated corpotentorium with short anterior arms is present in *Galloisiana* (Wipfler *et al.* 2011) and *Grylloblatta* (Walker 1931), Dermaptera (Strenger 1950; Kadam 1961; Giles 1963) and some representatives of Plecoptera (Hoke 1924; Moulins 1968). It is described as “distinctly extended bridge (corpotentorium)” in Karoophasma (Baum *et al*. 2007), but distinctly shorter than in the above mentioned taxa (coded as 0). The situation is completely different in Dictyoptera even though the anterior tentorial arms appear short. Their posterior parts have merged and form the secondary anterior tentorial bridge which is not part of the corpotentorium. Character not applicable for Zygentoma and Archaeognatha.

51. **Apophyses on the anterior surface of the corpotentorium: (0) absent; (1) present** (character 107 of Friedemann *et al.* in press)**.** Wing-shaped processes are present on the anterior surface of the corpotentorium of *Megacrania* and *Sipyloidea* only (Friedemann *et al.* in press).

52. **Secondary anterior tentorial bridge (“perforation of the corpotentorium”): (0) absent; (1) present** (character 31 of Wipfler *et al.* 2011)**.** The tentorium is not perforated in dictyopterans, but the anterior tentorial arms have merged thus forming a secondary anterior tentorial bridge. This is likely an autapomorphy of Dictyoptera (Hudson

1945; Deitz *et al*. 2003; Willmann 2003).

53. **Lateral lobes on the anterior tentorial arms: (0) absent; (1) present** (character 32 of Wipfler *et al.* 2011)**.** Only occuring in Mantodea (*Hymenopus*: Wipfler et al. subm; *Stagmomantis*: Levereault 1936; *Mantoida*: Klass & Eulitz 2007) and likely autapomorphic for the order (Wipfler et al. subm).

54. **Cuticular dorsal tentorial arms: (0) absent; (1) present.** Dorsal tentorial arms are present in all dicondylic insects.

55. **Trabeculae tentorii of posterior tentorial arms (0) present; (1) absent** (character 33 of Wipfler *et al.* 2011)**.** Trabeculae tentorii are apodemes on the ventral side of the posterior tentorial arms. They serve as muscular attachment areas and are present in all studied species with the exception of *Hymenopus* (Wipfler *et al.* sub.), *Embia* (Rähle 1970), *Labidura* (Kadam 1961), *Locusta* (Albrecht 1953), *Zorotypus* (Beutel & Weide 2005), *Stenopsocus* (Badonnel 1934) and *Macroxyela* (Beutel & Vilhelmsen 2007).

56. **M. tentoriofrontalis posterior (0te1): (0) present; (1) absent** (character 99 of Wipfler *et al.* 2011)**.** Only present in *Machlis and Thermobia.*

57. **M. posteriotentorialis (0te4): (0) present; (1) absent** (character 100 of Wipfler *et al.* 2011). Only present in *Machilis* and *Thermobia*.

58. **M. tentoritentorialis longis (0te5): (0) present; (1) absent** (character 101 of Wipfler *et al.* 2011). Only present in *Machilis* and *Thermobia*.

59. **M. tentoritentorialis brevis (0te6): (0) present; (1) absent** (character 102 of Wipfler *et al.* 2011). Only present in *Machilis* and *Thermobia*.

Mandible:

60. **Numbers of incisivi on the left mandible: (0) 2; (1) 3; (2) 5; (3) 0; (4) 1** (character 36 of Wipfler *et al.* 2011). Incisivi are almost generally present but are usually missing in Phasmatodea (present in *Timema* Tilgner *et al*. 1999 and *Agathemera*). Four are present in *Machilis,* two in Ephemeroptera (Staniczek 2001) and Grylloblattodea (Walker 1931; Wipfler *et al.* 2011), three in *Thermobia,* Odonata, *Hymenopus* (Wipfler et al. subm), *Periplaneta* (Wipfler *et al.* 2011), *Embia* (Rähle 1970), *Labidura* (Kadam 1961) and *Locusta* (Albrecht 1953), and five in *Nemoura* (Moulins 1968) and *Zorotypus* (Beutel & Weide 2005). In Mantophasmatodea (Baum *et al*. 2007) only one incisivus is present, the other protuberances belong to the mesal cutting edge. The situation in *Stenopsocus* and *Macroxyela* is unclear (coded as ?).

61. **Numbers of incisivi on the right mandible: (0) 2; (1) 3; (2) 4; (3) 5; (4) 0; 5 (1)** (character 37 of Wipfler *et al.* 2011)**.** Two are present in Ephemeroptera (Staniczek 2001), *Embia* (Rähle 1970) and *Grylloblatta* (Walker 1931), three in *Thermobia,* Odonata, *Galloisiana* (Wipfler *et al.* 2011), *Hymenopus* (Wipfler et al. subm.b), *Periplaneta*, and *Labidura* (Kadam 1961), four in *Machilis, Macroxyela* (Beutel & Vilhelmsen 2007), and five in *Perla*, *Nemoura* (Moulins 1968) and *Zorotypus* (Beutel & Weide 2005). Only one is present in Mantophasmatodea (Baum *et al*. 2007). They are absent in the studied representatives of Phasmatodea (Friedemann *et al.* in press), except for *Agathemera* and *Timema* (3 teeth, respectively).

62. **Armament on the mesal side of the left mandible: (0) without teeth or ridges; (1) one tooth; (2) three ridges** (character 111 of Friedemann *et al.* in press)**.** A conical protuberance or tooth is present on the mesal side of the left mandible of *Phyllium* (Friedemann *et al.* in press). The mesal side is smooth in *Sipyloidea* and *Carausius* (Marquardt 1940). Three elongate and strongly sclerotised ridges are present in *Megacrania* (pers. obs.). This character is not applicable for the outgroup taxa as the protuberance is missing.

63. **Dorsal cutting edge of the left mandible: (0) notched; (1) smooth** (character 112 of Friedemann *et al.* in press)**.** The dorsal cutting edge is notched in *Timema* (Tilgner 2002), *Agathemera* and *Sipyloidea* (Friedemann *et al.* in press), whereas it is completely smooth in *Phyllium* (Friedemann *et al.* in press), *Megacrania* (Friedemann *et al.* in press) and *Phryganistria* (Strenger 1932). The character is

inapplicable for the outgroup taxa as the cutting edge is missing.

64. **Mandibular postmola: (0) absent; (1) present** (character 39 of Wipfler *et al.* 2011). A membranous extension is present at the mediomesal part of the mandible in Mantodea and Blattodea (s.l., incl. Isoptera). This is probably an autapomorphy of Dictyoptera (Weidner 1970).

65. **Anterior mandibular joint: (0) absent; (1) present.** An anterior mandibular joint is present in dicondylic insects.

66. **Anterior mandibular joint: (0) cuticular hardening on the mandibular depression; (1) channel-joint (2) ball-and-socket joint** (character 40 of Wipfler *et al.* 2011)**.** The mandibular element of the anterior (secondary) mandibular joint is formed by a field of strengthened cuticle in Zygentoma, whereas nymphs of Ephemeroptera possess a channel-like articulation (Staniczek 2000, 2001). A ball-and-socket joint is present in Odonata and neopterans with normally developed mandibles. This character is not applicable to *Machilis* (coded with "–").

67. **Anterolateral part of the anterior mandibular articulation (paratentorial joint): (0) present; (1) absent** (character 41 of Wipfler *et al.* 2011)**.** A paratentorial mandibular joint is present in nymphs of Ephemeroptera and in Zygentoma (Strenger 1970; Staniczek 2000, 2001). It is absent in all other studied species. This character is not applicable to *Machilis* (coded with "–").

68. **Posterior mandibular joint: (0) cylinder-shaped (1) ball-and-socket joint** (character 42 of Wipfler *et al.* 2011)**.** In Zygentoma and nymphs of Ephemeroptera the posterior mandibular joint is cylinder-shaped, whereas it is a ball-and-socket joint in all other taxa under consideration.

69. **M. craniomandibularis externus anterior (0md2): (0) present; (1) absent** (character 77 of Wipfler *et al.* 2011). Present in *Machilis*, *Thermobia* (Chaudonneret 1950) and Ephemeroptera, absent in all other studied species.

70. **M. hypopharyngomandibularis (0md4): (0) present; (1) absent** (character 78 of Wipfler *et al.* 2011). Present in all taxa under consideration except for *Perla*, *Nemoura* (Moulins 1968), *Labidura* (Kadam 1961), *Locusta* (Albrecht 1953), *Zorotypus* (Beutel & Weide 2005) and *Macroxyela* (Beutel & Vilhelmsen 2007). It is not recorded for the dermapteran *Labidura* (Kadam 1961) but described for *Anisolabis* (Dorsey 1943). It is also present in the orthopteran *Troglophilus* (pers. obs. Wipfler). It was possibly overlooked in *Labidura* and *Locusta* (coded with ?). Since it is absent in *Nemoura* (Moulins 1968) and *Perla* (Strenger 1952; Chisholm 1962) it seems to be absent in Plecoptera.

71. **M. tentorio-mandibularis lateralis superior (0md5): (0) present; (1) absent** (character 79 of Wipfler *et al.* 2011)**.** Present in *Machilis*, *Thermobia*, Ephemeroptera and all studied odonatans.

72. **M. tentorio-mandibularis medialis superior (0md7): (0) present; (1) absent** (character 80 of Wipfler *et al.* 2011)**.** Present in *Machilis*, *Thermobia*, Ephemeroptera, *Lestes* and *Onychogomphus*.

Maxilla:

73. **Cardo: (0) present; (1) absent** (character 43 of Wipfler *et al.* 2011)**.** The cardo is reduced in *Stenopsocus* (Badonnel 1934). This is a potential autapomorphy of Psocoptera (Matsuda 1965; Willmann 2003).

74. **Division of stipes into bastistipes and mediastipes: (0) present; (1) absent** (character 44 of Wipfler *et al.* 2011)**.** The internal stipital ridge separating the basistipes from the mediostipes serves as attachment for musculature. It is absent in *Stenopsocus* (Badonnel 1934), Zorotypus (Beutel & Weide 2005) and *Macroxyela* (Beutel & Vilhelmsen 2007).

75. **Galea: (0) present; (1) absent** (character 45 of Wipfler *et al.* 2011). The homology of the inner lobe of the odonatan maxilla is ambiguous, whereas the musculature clearly identifies the outer lobe as the palp. The inner lobe contains the lacinia since two lacinial muscles (0mx2 + 0mx6) are present. The authors follow Asahina (1954), Short (1955) and

Staniczek (2001) in assuming that the galea has been reduced.

76. **Distal field of trichomes on the galea: (0) undivided; (1) divided; (2) just a U-shaped seam** (character 116 of Friedemann *et al.* in press). A field densely covered with microtrichia is present on the apex of the galea of most examined species. This field is undivided in *Galloisiana* (Wipfler *et al.* 2011), Mantophasmatodea (Baum et al. 2007), *Hymenopus* (Wipfler et al. subm), *Periplaneta* (Wipfler *et al.* 2011), *Locusta* (Albrecht 1953), Zoraptera (Beutel & Weide 2005) and *Agathemera* and *Timema* (Bradler 2009). It is distinctly divided into two areas in *Sipyloidea* and *Carausius* (Friedemann *et al.* in press). In *Phyllium* it forms a thin U-shaped seam enclosing the apex of the galea *Carausius* (Friedemann *et al.* in press). The trichomes are short and bristle-shaped in *Phyllium* but long and lobate in *Sipyloidea*. Data regarding the shape of the field of trichomes are missing for all the other examined species (coded as „?“).

77. **Connection of lacinia and galea: (0) separated; (1) fused** (character 46 of Wipfler *et al.* 2011). Fused in Ephemeroptera. The two lobes are connected by a membrane but still discernable in *Oniscigaster* (Staniczek 2001), whereas they are completely fused in other members of the group examined (see also Strenger 1970, 1975, 1977).

78. **Shape of lacinia: (0) sickle-shaped; (1) chisel-shaped; (2) truncate; (3) short claw** (character 47 of Wipfler *et al.* 2011). A sickle-shaped lacinia with its apical part bent inwards is present in all studied species with the exception of *Heptagenia*, *Stenopsocus* (Badonnel 1934) and *Macroxyela* (Beutel & Vilhelmsen 2007). In *Stenopsocus* genus it is chisel-shaped and located in an epipharyngeal pouch. This modification is typical for psocopterans (Matsuda 1965) and is most likely an autapomorphy of this group. In *Macroxyela* it is distally widened, truncate apically and covered with setae (Beutel & Vilhelmsen 2007). The lacinia of Heptagenia is chisel-shaped but not located in an epipharyngeal pouch. The lacinia of *Machilis* is a short claw.

79. **Mesally directed setae on lacinia: (0) present; (1) absent** (character 48 of Wipfler *et al.* 2011). Mesally directed setae are present in all studied species with the exception of *Zorotypus* (Beutel & Weide 2005), *Stenopsocus* (Badonnel 1934) and *Macroxyela* (Beutel & Vilhelmsen 2007). Moulins (1968) makes no statement about them in *Nemoura*, but Hoke (1924) reports their presence in a wide array of different plecopterans including *Nemoura*.

80. **Lacinia: (0) free; (1) in galeal cavity** (character 49 of Wipfler *et al.* 2011). The lacinia is located in a cavity of the galea in *Periplaneta*, *Hymenopus* (Wipfler et al. subm) and other dictyopterans (Crampton 1923). It is a potential autapomorphy of this group.

81. **Lacinial incisivi: (0) present; (1) absent** (character 50 of Wipfler *et al.* 2011). Present in most taxa under consideration, but absent in *Stenopsocus* (Badonnel 1934) and *Macroxyela* (Beutel & Vilhelmsen 2007).

82. **Number of incisivi on lacinia: (0) 3; (1) 2; (2) 1; (3) more than 3** (character 51 of Wipfler *et al.* 2011). Three in *Thermobia* (Chaudonneret 1950), *Galloisiana*, *Agathamera, Sipyloidea* and *Locusta* (Albrecht 1953), two in Machilis, *Perla*, *Nemoura* (Moulins 1968), Grylloblatta (Walker 1931), Mantophasmatodea (Baum *et al*. 2007), *Timema, Megacrania, Hymenopus* (Wipfler et al. subm.b), *Periplaneta*, *Embia* (Rähle 1970) and *Zorotypus* (Beutel & Weide 2005), and only one in *Ephemeroptera* and *Odonata*. Euphasmatodea generally have three incisici on the lacinia, but *Megacrania* just like *Timema* has two, whereas *Phyllium* has five to six (Friedemann *et al.* in press). This character is not applicable to *Stenopsocus* (Badonnel 1934) and *Macroxyela* (Beutel & Vilhelmsen 2007).

83. **Dentisetae on lacinia: (0) present; (1) absent** (character 52 of Wipfler *et al.* 2011). Dentisetae are extremely enlarged bristles beneath the apex of the lacinia. They are present in Ephemeroptera (Staniczek 2001) and Odonata.

84. **Proximal apodeme on the lacinia: (0) absent; (1) present** (character 53 of Wipfler *et al.* 2011). A

proxomedian apodeme on the lacinia is present in *Galloisiana* (Wipfler *et al.* 2011) and *Grylloblatta* (Walker 1931). This is a potential autapomorphy of Grylloblattodea (Walker 1933).

85. **Galeolobulus: (0) absent; (1) present** (character 54 of Wipfler *et al.* 2011). A laterobasal apodeme of the galea is present in all examined phasmatodeans except *Timema* (Bradler 2009; Friedemann et al in press). A potential autapomorphy of Euphasmatodea.

86. **Maxillary palp: (0) 5-segmented; (1) 4-segmented; (2) 1-segmented; (3) 3-segmented; (4) 6-segmented; (5) 7-segmented** (character 55 of Wipfler *et al.* 2011). A five segmented palpus is present in all studied neopterans with the exception of *Stenopsocus* (4 segments: Badonnel 1934). Three segments are present in Ephemeroptera (Staniczek 2001), one in odonatans (e.g. Short 1955), six in *Thermobia* (Chaudonneret 1950; Matsuda 1965) and seven in *Machilis*.

87. **Orientation of maxillary palps: (0) ventrally oriented; (1) anteriorly or dorsally directed** (character 114 of Friedemann *et al.* in press)**.** The maxillary palps of *Timema* (Tilgner et al. 1999) and *Agathemera* are ventrally directed, whereas an anterior or even dorsal orientation is found in all other examined phasmids (Friedemann *et al.* in press). They are strongly curved upwards in *Phyllium*, thus covering the anterior side of the mandibles, and a similar condition is found in *Extatosoma tieratum* (Seiler et al. 2003). The maxillary palps of *Machilis*, *Thermobia*, Ephemeroptera, Plecoptera, *Galloisiana* (Wipfler *et al.* 2011), *Zorotypus* (Beutel & Weide 2005) and *Macroxyela* (Beutel & Vilhelmsen 2007) are oriented dorsally or anteriorly whereas they are oriented ventrally in the other examined species.

88. **M. stipitogalealis (0mx7): (0) present; (1) absent.** Present in all studied species with the exception of Ephemeroptera and Stenopsocus (Badonnel 1934). This character is not applicable to odonatans since they lack the galea (coded as “-“).

89. **M. palpopalpalis maxillae primus (0mx12): (0) present; (1) absent** (character 82 of Wipfler *et al.* 2011)**.** Absent in Odonata and Plecoptera but present in all other taxa under consideration.

Labium

90. **Postmentum: (0) not subdivided; (1) subdivided into submentum and mentum** (character 56 of Wipfler *et al.* 2011)**.** Not subdivided in *Machilis*, *Thermobia*, Ephemeroptera, Odonata, *Hymenopus* (Wipfler et al. subm), *Zorotypus* (Beutel & Weide 2005), *Stenopsocus* (Badonnel 1934) and *Macroxyela* (Beutel & Vilhelmsen 2007). The postmentum is subdivided into the posterior submentum and the mentum in all other taxa under consideration.

91. **Angle between submentum and mentum: (0) less than 60° or absent; (1) more than 60°** (character 57 of Wipfler *et al.* 2011)**.** The submentum and mentum are attached to each other at an angle of nearly 90% in Grylloblattodea (Walker 1931; Wipfler *et al.* 2011) and Mantophasmatodea (Baum *et al*. 2007). This is condition was not observed in the other taxa under consideration.

92. **Curvature of submentum: (0) absent; (1) curved in lateral view** (character 58 of Wipfler *et al.* 2011). In all studied species with the exception of Grylloblattodea (Walker 1931, Wipfler *et al.* 2011) the submentum is a nearly even plate. It forms a semicircle in lateral view in Grylloblattodea. Inapplicable where a separate submentum is absent.

93. **Median longitudinal tunnel of labium: (0) absent; (1) present** (character 59 of Wipfler *et al.* 2011). A median longitudinal tunnel continuous with the salivarium is present in Psocoptera (Matsuda 1965).

94. **Median cleft of prementum: (0) absent; (1) present** (character 60 of Wipfler *et al.* 2011)**.** A median premental cleft i.e. an incision reaching beyond the base of the glossae, is present in Grylloblattodea (Walker 1931; Wipfler *et al.* 2011), Mantophasmatodea (Baum *et al*. 2007), Mantodea (Levereault 1936; Beier 1964, 1968), Blattodea (Yuasa 1920) and Dermaptera (Kadam 1961; Giles

1963).

95. **Labium: (0) paraglossa and glossa seperated; (1) paraglossa and glossae completely completely fused.** The inner labial lobes (paraglossa+glossa) are separated in all considered taxa except Odonata. The authors follow Asahina (1954) in the interpretation that the distal median lobe of Odonata is a fusion product of glossae and paraglossa. In *Epiophlebia* it still shows a separation while in all other odonatans they are completely fused (see discussion).

96. **Glossa: (0) present; (1) reduced** (character 61 of Wipfler *et al.* 2011)**.** Present in all taxa under consideration with the exception of Dermaptera (Kadam 1961; Giles 1963) and *Macroxyela* (Beutel & Vilhelmsen 2007). The authors consider the odonatan labium to posses fused glossae and paraglossae (character 97). Therefore the glossa is coded as present for Odonata.

97. **Number of glossae in the labium: (0) 4; (1) 2.** *Machilis* and all other archaeognathans (Sturm & Machida 2001) posses a total of four glossae in the labium while all other studied species posses only two. This character is not applicable to *Labidura* and *Macroxyela* since they posses no glossae (see character 98; coded as "-")**.** In *Lestes* and *Onychogomphus* the number of glossae is uncertain, since they are fused with the paraglossae (character 97) (coded as "-").

98. **Number of paraglossae: (0) 2; (1) 1; (2) 0.** *Machilis* and all other archaeognathans (Sturm & Machida 2001) posses a total of four paraglossae in the labium while all other studied species posses only two. In *Lestes* and *Onychogomphus* the number of paraglossae is uncertain, since they are fused with the glossae (character 97) (coded as "-").

99. **Shape of paraglossa: (0) cylindrical, as wide as thick; (1) flat, wider than thick; (2) palp-like;** (character 62 of Wipfler *et al.* 2011)**.** Flat in all examined Phasmatodea (Friedemann *et al.* in press), *Embia* (Rähle 1970), *Labidura* (Kadam 1961), *Locusta* (Albrecht 1953), *Stenopsocus* (Badonnel 1934) and *Heptagenia*, and palp-like in *Macroxyela* (Beutel & Vilhelmsen 2007). Cylindrical in all other taxa under consideration. This character is not applicable to Odonata since glossa and paraglossa are completely or in *Epiophlebia* partly fused (se character 97).

100. **Relative length of paraglossae and glossae: (0) about equally long; (1) paraglossae twice as long or longer** (character 63 of Wipfler *et al.* 2011). Approximately equally long in all taxa under consideration with the exception of the phasmatodean terminals (Friedemann *et al.* in press), *Embia* (Rähle 1970), *Perla* and *Locusta* (Albrecht 1953). Inapplicable in *Labidura* (Kadam 1961), *Macroxyela* (Beutel & Vilhelmsen 2007). The median lobe in Odonata is considered a fusion of glossa and paraglossa (remnants still visible in Epiophlebia, see character 97). Therefore they are also considered of equal length.

101. **Orientation of labial palpi: (0) anteriorly or laterally; (1) ventrally or posteriorly** (character 64 of Wipfler *et al.* 2011). Anteriorly or laterally oriented in most taxa under consideration, but ventrally or posteriorly in Grylloblattodea (Walker 1931; Wipfler *et al.* 2011) and Mantophasmatodea (Baum *et al*. 2007; Wipfler *et al.* 2011).

102. **Number of labial palpomeres: (0) 3; (1) 1; (2) 2** (character 65 of Wipfler *et al.* 2011). Four segmented in *Thermobia* (Chaudonneret 1950), three-segmented in almost all taxa under consideration, but one-segmented in *odonatans* and *Stenopsocus* (Badonnel 1934) and two-segmented in *Heptagenia*.

103. **Shape of labial palps: (0) approximately round in cross section; (1) dorsoventrally flattened** (character 119 of Friedemann *et al.* in press)**.** Strongly flattened in *Phyllium* (Friedemann *et al.* in press) and Odonata.

104. **Length of labial palps: (0) longer than glossae; (1) about as long as the glossae** (character 118 of Friedemann *et al.* in press)**.** Short in Odonata, *Megacrania* (Bradler 2009) and *Nemoura* (Moulins 1968). Distintcly reaching beyond the glossae in all other examined taxa.

105. **Moveable hooks of labial palpi: (0) absent; (1) present** (character 66 of Wipfler *et al.* 2011). Present in the studied Odonata, although they are lacking in Macromiidae, Libellulidae, and Corduliidae (Rehn 2003). Moveable hooks are a potential groundplan feature of Odonata.

106. **M. postoccipitoglossalis medianus (0la1): (0) present; (1) absent** (character 83 of Wipfler *et al.* 2011)**.** Only present in *Thermobia* (Chaudonneret 1948, 1950). Situation in *Timema* unknown (coded with “?”).

107. **M. postoccipitoglossalis lateralis (0la2): (0) present; (1) absent** (character 84 of Wipfler *et al.* 2011)**.** Only present in *Thermobia* (Chaudonneret 1948, 1950). Situation in *Timema* unknown (coded with “?”).

108. **M. postoccipitoparaglossalis (0la3): (0) present; (1) absent** (character 85 of Wipfler *et al.* 2011). Only present in *Thermobia* (Chaudonneret 1948, 1950). Situation in *Timema* unknown (coded with “?”).

109. **M. postoccipitoprementalis (0la4): (0) present; (1) absent** (character 86 of Wipfler *et al.* 2011). Only present in *Thermobia* (Chaudonneret 1948, 1950). Situation in *Timema* unknown (coded with “?”).

110. **M. tentoriopraementalis (0la5): (0) present; (1) absent.** Present in all studied species with the exception of Odonata. Situation in *Timema* unknown (coded with “?”).

111. **Origin of M. tentoriopraementalis inferior 0la5: (0) ventral apodeme; (1) posterior tentorial arms** (character 121 of Wipfler *et al.* 2011)**.** Originates on the trabeculae tentorii or ventral apodemes of the posterior tentorial arms in *Agathemera, Phyllium* (Friedemann *et al.* in press), *Sipyloidea* (Friedemann *et al.* in press), *Megacrania* (Maki 1935), *Phryganistria* (Strenger 1932), Grylloblattodea (Walker 1931, Wipfler *et al.* 2011) and Plecoptera. On the surface of the posterior tentorial arms in all other examined species. Situation in *Timema* unknown (coded with “?”).

112. **M. tentorioparaglossalis (0la6): (0) present; (1) absent** (character 87 of Wipfler *et al.* 2011)**.** Present in all taxa under consideration with the exception of *Ephemera*, all studied odonatans, *Grylloblattodea* (Walker 1931, Wipfler *et al.* subm.a), Mantophasmatodea (Wipfler *et al.* subm), and *Stenopsocus* (Badonnel 1934). The situation in *Timema* is uncertain (coded as "?"). The authors follow (Rähle 1970) in assuming that the superior paraglossal muscle of Embioptera and Phasmatodea is M. tentorioparaglossalis.

113. **Origin of M. tentorioparaglossalis (0la6): (0): tentorium; (1) basal edge of prementum** (character 88 of Wipfler *et al.* 2011)**.** Originates on the tentorium in all examined species with the exception of *Embia* (Rähle 1970) and all examined Euphasmatodea. It has been considered a potential apomorphy of a clade comprising Phasmatodea and Embioptera (Gorb & Beutel 2001; Bradler 2009). Data for *Oniscigaster* (Staniczek 2001) and *Timema* (Tilgner et al. 1999) is missing (coded as ?).

114. **M. tentorioglandularis (0la7): (0) present; (1) absent** (character 89 of Wipfler *et al.* 2011)**.** M. tentorioglandularis is only present in *Machilis* and *Thermobia* (Chaudonneret 1948, 1950). Situation in *Timema* unknown (coded with “?”).

115. **M. submentopraementalis (0la8): (0) present; (1) absent** (character 90 of Wipfler *et al.* 2011)**.** Present in all taxa under consideration with the exception of *Locusta* (Albrecht 1953). Absent in *Acrida*, *Pseudonura*, *Gastrimargus*, *Dissosteira* (Blackith & Blackith 1967) and *Anacrydicum* (Strenger 1942), but present in Eumastacoidea (Blackith & Blackith 1967; Zolessi 1968), *Decticus* and *Gryllotalpa* (Strenger 1942). Further studies of orthopteran representatives are needed to clarify whether it was reduced once or several times. Situation in *Timema* unknown (coded with “?”).

116. **M. submentopraementalis (0la8): (0) one component; (1) two components** (character 91 of Wipfler *et al.* 2011)**.** Composed of only one component in all taxa under consideration with the exception of *Zorotypus*, where it is bipartite (Beutel & Weide 2005). This condition is a potential

autapomorphy of Zoraptera. Situation in *Timema* unknown (coded with “?”).

117. **M. postmentomembranus (0la9): (0) present; (1) absent** (character 92 of Wipfler *et al.* 2011)**.** Only present in *Machilis* and *Thermobia* (Chaudonneret 1948, 1950). Situation in *Timema* unknown (coded with “?”).

118. **M. submentomentalis (0la10): (0) absent; (1) present** (character 93 of Wipfler *et al.* 2011)**.** Present in *Machilis,* nymphs and adults of *Nemoura* (Moulins 1968) and *Perla,* and also in some holometabolous larvae (Matsuda 1965). Situation in *Timema* unknown (coded with “?”).

119. **M. praementoparaglossalis (0la11): (0) present; (1) absent.** Absent in all studied odonatans. Situation in *Timema* and in *Macroxyela* (Beutel & Vilhelmsen 2007) unclear (coded with “?”).

120. **M. praementoglossalis (0la12): (0) present; (1) absent** (character 94 of Wipfler *et al.* 2011)**.** Present in all taxa under consideration with the exception of Odonata, *Embia* (Rähle 1970), the dermapterans (Dorsey 1943; Strenger 1950; Kadam 1961) and *Locusta* (Albrecht 1953). Situation in *Timema* unknown (coded with “?”).

121. **M. praementopalpalis internus (0la13): (0) present; (1) absent.** Present in all studied species with the exception of *Nemoura* (Moulins 1968) and *Macroxyela* (Beutel & Vilhelmsen 2007). Situation in *Timema* unknown (coded with “?”).

122. **M. praementopalpalis externus 0la14: (0) present; (1) absent.** Present in Machilis, Thermobia and all neopterans. Absent in Ephemeroptera and Odonata. Situation in *Timema* unknown (coded with “?”).

123. **Hypopharynx overlapping paraglossae and glossae 0) absent; 1) present** (character 67 of Wipfler *et al.* 2011). The hypopharynx overlaps the glossae and paraglossae in *Galloisiana* (Wipfler et al. 2011). The situation in *Grylloblatta* (Walker 1931) is not completely clear (coded as ?). Situation in *Timema* unknown (coded with “?”).

124. **Shape of hypopharynx: (0) slope like; (1) distinctly flattened** (character 68 of Wipfler *et al.* 2011)**.** Slope like in all studied species with the exception of Grylloblattodea and Mantophasmatodea. In these two taxa it is distinctively flattened and the suspensorium is located far ventrally of the anatomical mouth opening.

125. **Superlinguae: (0) present; (1) absent.** Superlinguae are present in *Machilis* and all studied ephemeropterans. Dermapterns also posses lateral lobes on the hypopharynx but their homology is unclear. (coded with “?”)

126. **Salivary glands and ductus: (0) present; (1) absent** (character 69 of Wipfler *et al.* 2011)**.** Absent in *Oniscigaster* (Staniczek 2001) and all other studied ephemeropterans. This is a potential apomorphy of this group.

127. **Connection of salivary ducts: (0) connected before opening, Y-shaped; (1) open separately** (character 120 of Friedemann *et al.* in press)**.** In Euphasmatodea both salivary ducts always open separately (Tilgner 2002). They are connected in *Machilis*, *Thermobia,* Odonata, *Timema* (Bradler 1999), *Locusta* (Albrecht 1953), *Embia* (Rähle 1970), Mantophasmatodea (Baum et al. 2007), *Galloisiana* (Wipfler et al. 2011), *Periplaneta* (Wipfler *et al.* 2011) and Mantodea (Wipfler et al. subm.). For the other examined species data is missing (coded as “?”). The character is inapplicable for Ephemeroptera because they lack salivary ducts- or glands (see character 128).

128. **M. frontobuccalis lateralis (0hy2): (0) present; (1) absent** (character 123 of Friedemann *et al.* in press)**.** Absent in Odonata, *Embia* (Rähle 1970) and *Macroxyela* (Beutel & Vilhelmsen 2007). It is unclear whether it is present in *Timema* (Tilgner 1999) and *Siphlonurus* (coded as „?“). Present in all other examined species.

129. **M. craniohypopharyngealis (0hy3): (0) present; (1) absent** (character 95 of Wipfler *et al.* 2011)**.** Present in all taxa under consideration with the exception of Ephemeroptera, Odonata, *Grylloblattodea* (Walker 1931) and *Macroxyela*

(Beutel & Vilhelmsen 2007). The situation in *Oniscigaster* (Staniczek 2001) and *Timema* is unclear (coded as ?).

130.**M. postmentoloralis (0hy6): (0) present; (1) absent** (character 96 of Wipfler *et al.* 2011)**.** Only present in *Machilis* and *Thermobia*. Situation in *Timema* unknown (coded with "?").

131.**M. praementosalivaris posterior (0hy8): (0) absent; (1) present** (character 97 of Wipfler *et al.* 2011)**.** Present in all taxa under consideration with the exception of *Labidura* and Odonata (Staniczek 2001). Kadam (1961) does not report it for *Labidura* but Dorsey (1943) found it in *Anisolabis*. Situation in *Timema* unknown (coded with "?").

132.**M. lorosalivarialis (0hy11): (0) present; (1) absent** (character 98 of Wipfler *et al.* 2011). Only present in *Thermobia* (Chaudonneret 1950). Situation in *Machilis* and *Timema* unclear (coded with "?").

133.**M. hypopharyngosalivaris (0hy12): (0) present; (1) absent.** Present in all studied species with the exception of Ephemeroptera, *Locusta* (Albrecht 1953) and *Stenopsocus* (Badonnel 1934). Situation in *Timema* unknown (coded with "?").

134.**M. frontobuccalis posterior (0bu3): (0) present; (1) absent** (character 122 of Friedemann *et al.* in press)**.** Absent in all studied Odonata, *Sipyloidea*, *Phyllium* and *Megacrania* (Maki 1935). Data is missing for *Timema* (Tilgner 1999), *Carausius* (coded as „?").

135.**M. tentoriobuccalis lateralis (0bu4): (0) absent; (1) present** (character 103 of Wipfler *et al.* 2011)**.** M. tentoriobuccalis lateralis is present in *Oniscigaster* (Staniczek 2001), Ephemera, Siphlonurus, *Galloisiana (*Wipfler *et al.* 2011), *Grylloblatta* (Walker 1931), *Austrophasma (*Wipfler *et al.* 2011), *Karoophasma* (Wipfler *et al.* 2011), *Agathemera* (Wipfler *et al.* 2011), *Phyllium* (Friedemann *et al.* in press), *Sipyloidea* Friedemann *et al.* in press), *Carausius* (Marquardt 1940), *Megacrania* (Maki 1934), *Embia* (Rähle 1970) and *Locusta* (Albrecht 1953). Data is missing for *Timema* (Tilgner et al. 1999).

136.**M. tentoriobuccalis anterior (0bu5): (0) present; (1) absent.** Present in all studied species except Odonata and *Labidura* (Kadam 1961). Unclear situation in *Timema* and *Macroxyela* (Beutel & Vilhelmsen 2007).

137.**M. tentoriobuccalis posterior (0bu6): (0) present; (1) absent.** Present in all studied species with the exception of *Macroxyela* (Beutel & Vilhelmsen 2007). Situation in *Timema* unclear (coded with "?").

138.**Origin of M. tentoriobuccalis posterior (0bu6): (0) corpotentorium, (1) anterior tentorial arms** (character 124 of Friedemann *et al.* in press)**.** This muscle arises on the anterior tentorial arms in all examined Phasmatodeans (Friedemann *et al.* in press). Data is missing for *Timema* (Tilgner 1999) and *Oniscigaster* (Staniczek 2001) (coded as „?"). It could be a potential autapomophy for Phasmatodea. The character is not applicable for *Stenopsocus* and *Macroxylea* (Beutel & Vilhemsen 2007) because in these species this muscle is missing.

References (not cited in the main body of the text)

Albrecht F.O. 1953. The anatomy of the migratory locust. London: The Athlone Press.

Badonnel A. 1934. Recherches sur l'anatomie des Psoque. Bulletin Biologique de France et de Belgique, Paris, Supplement 18:1-241.

Baum E., Dressler C., Beutel R.G. 2007. Head structures of *Karoophasma* sp. (Hexapoda, Mantophasmatodea) with phylogenetic implications. Journal of Zoological Systematics & Evolutionary Research 45:104.

Beier M. 1968. Mantodea (Fangschrecken). Handbuch der Zoologie 4:1-47.

Beier M. 1964. Blattopteroidea-Mantodea. In: Beier M., editor. Dr. H. G. Bronns Klassen und Ordnungen des Tierreichs. Leipzig: Akademische Verlagsgesellschaft Geest & Portig K.-G. p. 849-970.

Beutel R.G., Vilhelmsen L. 2007. Head anatomy of Xyelidae (Hexapoda: Hymenoptera) and phylogenetic implications. Organisms Diversity & Evolution 7:207-230.

Beutel R.G., Weide D. 2005. Cephalic anatomy of Zorotypus hubbardi (Hexapoda: Zoraptera): new evidence for a relationship with Acercaria. Zoomorphology 124:121-136.

Blackith R.E., Blackith R.M. 1967. The anatomy and physiology of the morabine grasshoppers III. Muscles, Nerves, Tracheae, and Genitalia. Australian Journal of Zoology 15:961-998.

Bradler S. 2009. Die Phylogenie der Stab- und Gespenstschrecken (Insecta: Phasmatodea). Species, Phylogeny and Evolution 2:3-139.

Chaudonneret J. 1948. Le labium des Thysanoures (Insectes Apterygotes). Annales des Sciences Naturelles - Zoologie et Biology animale 11:1-27.

Chaudonneret J. 1950. La morphologie cephalique de *Thermobia domestica* (Packard) (Insecte Apterygote Thysannoure). Ann.Sci.Nat.(Zool) 12:145-302.

Chisholm P.J. 1962. The anatomy in relation to the feeding habits of *Perla cephalotes* Curtis (Plecoptera, Perlidae) and other Plecoptera. Transactions of the Society for British Entomology 15:56-101.

Crampton G.C. 1923. A phylogenetic comparison of the maxillae throughout the orders of insects. Journal of the New York Entomological Society 31:77-106.

Deitz L.L., Nalepa C., Klass K.D. 2003. Phylogeny of the Dictyoptera re-examined (Insecta). Entmologische Abhandlungen 61:69-91.

Dorsey G.K. 1943. The musclature of the labrum, labium and pharyngeal region of adult and immature Coleoptera. Smithsonian miscellaneos collections 103:1-40.

Ehrmann R. 2002. Mantodea - Gottesanbeterinnen der Welt. Münster: Natur und Tier Verlag.

Engel M.S., Grimaldi D.A. 2004. A new rock crawler in Baltic amber, with comments on the order (Mantophasmatodea: Mantophasmatidae). American Museum Novitates 3431:1-11.

Friedemann K., Wipfler B., Bradler S., Beutel R.G. in press. On the head morphology of *Phyllium* and the phylogenetic relationships of Phasmatodea (Insecta). Acta Zoologica.

Giles E.T. 1963. The comparative external morphology and affinities of the Dermaptera. Transactions of the Royal Entomological Society of London 115:95-164.

Hertel W., Pass G. 2002. An evolutionary treatment of the morphology and physiology of circulatory organs in insects. Comparative Biochemistry and Physiology A-Molecular and Integrative Physiology 133:555-575.

Hoke G. 1924. The anatomy of the head and mouthparts of Plecoptera. Journal of Morphology 38:347-385.

Hudson G.S. 1945. A study of the tentorium in some orthopteroid Hexapoda. Journal of the Entomological Society of Southern Africa 8:71-90.

Kadam K. 1961. Studies on the Morphology of an Indian Earwig, *Labidura riparia*, Pall., var. ineris, Brunner. Journal of the Zoological Society of India 13:34-49.

Klass K.D., Eulitz U. 2007. The tentorium and anterior head sulci in Dictyoptera and Mantophasmatodea (Insecta). Zoologischer Anzeiger - A Journal of Comparative Zoology 246:205-234.

Levereault P. 1936. The morphology of the Carolina Mantis. The University of Kansas Science Bulletin 24:205-259.

Lombardo F. 1984. Morfologia del capo di *Geomantis larvoides* Pantel 1886 (Insecta, Mantodea). I: il dermascheletro. Animalia 11:67-83.

Maki T. 1935. A study of the musculature of the phasmid *Megacrania tsudai* Shiraki. Memoirs of the Faculty of Science and Agriculture Taihoku Imperial University 12:181-279.

Marquardt F. 1940. Beiträge zur Anatomie der

Muskulatur und der peripheren Nerven von *Carausius* (*Dixippus*) *morosus* BR. Zoologische Jahrbücher / Abteilung für Anatomie und Ontogenie der Tiere 66:63-128.

Matsuda R. 1965. Morphology and evolution of the insect head. Memoirs of the American Entomological Institute 4:1-334.

Strenger A. 1942. Funktionelle Analyse des Orthopterenkopfes. Zoologische Jahrbücher / Abteilung für Systematik, Ökologie und Geographie der Tiere 75:1-72.

Pipa, R.L., Nishioka R.S., Bern H.A. 1964. Thysanuran median frontal organ: its

structural resemblance to photoreceptors. Science 145: 829-831

Storozhenko S.Y. 1997. Classification of order Grylloblattida (Insecta), with description of

new taxa. Far Eastern Entomologist 42:1-20.

Tilgner E.H. 2002. Systematics of Phasmida. PhD Thesis, University of Georgia.

Tilgner E.H.,Kiselyova T.G., McHugh J.V. 1999. A morphological study of *Timema cristinae* Vickery with implications for the phylogenetics of Phasmida. Deutsche Entomologische Zeitschrift 46:149-162.

Walker E.M. 1931. On the anatomy of *Grylloblatta campodeiformis* Walker 1. Exoskeleton and musculature of the head. Annals of the Entomological Society of America 24:519-536.

Weidner H. 1970. Isoptera (Termiten). In: Helmcke J. G., Starck D., Wermuth H., editors. Handbuch der Zoologie. Berlin: Walter de Gryter. p.1-147.

Willmann R. 2003. Phylogenese und System der Insekten. Pages 1-65 In: Dathe H.H., editor Lehrbuch der speziellen Zoologie, Band I: 5. Teil: Insecta. Heidelberg, Berlin: Spektrum Akademischer Verlag. P. 1-65.

Woo W. 1950. Skeleto-muscular studies on the head and feeding apparatus of *Ctenolepisma urbana* Slabaugh (Thysanura: Lepismatidae). Peking Natural History Bulletin 18:171-188.

Yuasa H. 1920. The anatomy of the head and mouthparts of Orthoptera and Euplexoptera. Journal of Morphology 33:251-307.

Zolessi L.C. 1968. Morphologie, endosquelette et musculature d'un acridien aptère (Orthoptera: Proscopiidae). Transactions of the Royal Entomological Society of London 120:55-113.

Zwick P. 2009. The Plecoptera - who are they? The problematic placement of stoneflies in the phylogenetic system of insects. Aquatic Insects: International Journal of Freshwater Entomology 31:181-194.

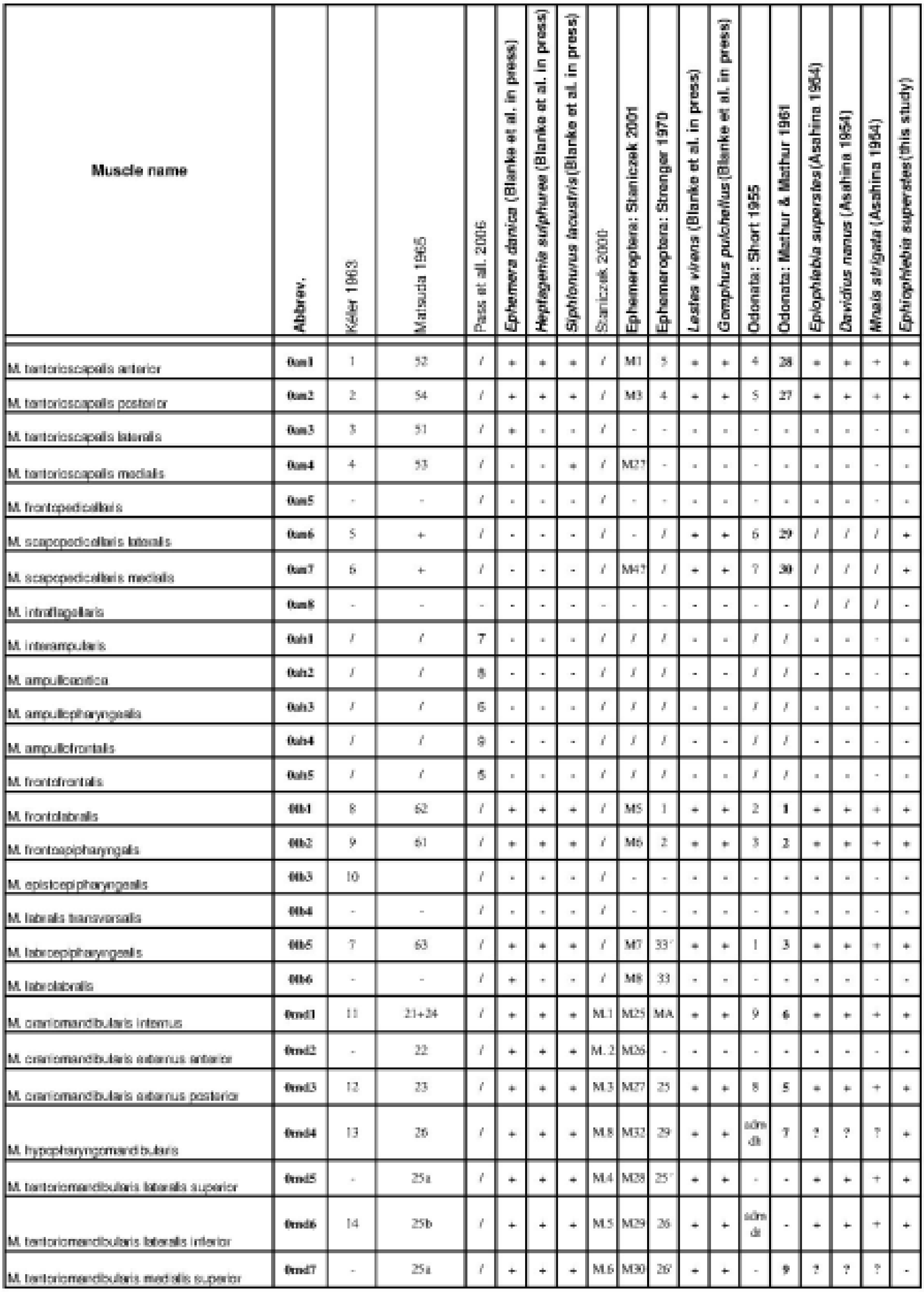

Muscle name	Abbrev.	Kéler 1963	Matsuda 1965	Pass et al. 2006	*Ephemera danica* (Blanke et al. in press)	*Heptagenia sulphurea* (Blanke et al. in press)	*Siphlonurus lacustris*(Blanke et al. in press)	Staniczek 2000	Ephemeroptera: Staniczek 2001	Ephemeroptera: Strenger 1970	*Lestes virens* (Blanke et al. in press)	*Gomphus pulchellus*(Blanke et al. in press)	Odonata: Short 1955	Odonata: Mathur & Mathur 1961	*Epiophlebia superstes*(Asahina 1954)	*Davidius nanus* (Asahina 1954)	*Mnais strigata* (Asahina 1954)	*Epiophlebia superstes*(this study)
M. tentorioscapalis anterior	**0an1**	1	52	/	+	+	+	/	M1	5	+	+	4	28	+	+	+	+
M. tentorioscapalis posterior	**0an2**	2	54	/	+	+	+	/	M3	4	+	+	5	27	+	+	+	+
M. tentorioscapalis lateralis	**0an3**	3	51	/	+	-	-	/	-	-	-	-	-	-	-	-	-	-
M. tentorioscapalis medialis	**0an4**	4	53	/	-	-	+	/	M2?	-	-	-	-	-	-	-	-	-
M. frontopedicellaris	**0an5**	-	-	/	-	-	-	/	-	-	-	-	-	-	-	-	-	-
M. scapopedicellaris lateralis	**0an6**	5	+	/	-	-	-	/	-	/	+	+	6	29	/	/	/	+
M. scapopedicellaris medialis	**0an7**	6	+	/	-	-	-	/	M4?	/	+	+	?	30	/	/	/	+
M. intraflagellaris	**0an8**	-	-	-	-	-	-	-	-	-	-	-	-	-	/	/	/	-
M. interampullaris	**0ah1**	/	/	7	-	-	-	/	/	/	-	-	/	/	-	-	-	-
M. ampulloaortica	**0ah2**	/	/	8	-	-	-	/	/	/	-	-	/	/	-	-	-	-
M. ampullopharyngealis	**0ah3**	/	/	6	-	-	-	/	/	/	-	-	/	/	-	-	-	-
M. ampullofrontalis	**0ah4**	/	/	9	-	-	-	/	/	/	-	-	/	/	-	-	-	-
M. frontofrontalis	**0ah5**	/	/	5	-	-	-	/	/	/	-	-	/	/	-	-	-	-
M. frontolabralis	**0lb1**	8	62	/	+	+	+	/	M5	1	+	+	2	1	+	+	+	+
M. frontoepipharyngalis	**0lb2**	9	61	/	+	+	+	/	M6	2	+	+	3	2	+	+	+	+
M. epistoepipharyngealis	**0lb3**	10		/	-	-	-	/	-	-	-	-	-	-	-	-	-	-
M. labralis transversalis	**0lb4**	-	-	/	-	-	-	/	-	-	-	-	-	-	-	-	-	-
M. labroepipharyngealis	**0lb5**	7	63	/	+	+	+	/	M7	33'	+	+	1	3	+	+	+	+
M. labrolabralis	**0lb6**	-	-	/	+	-	-	/	M8	33	-	-	-	-	-	-	-	-
M. craniomandibularis internus	**0md1**	11	21+24	/	+	+	+	M.1	M25	MA	+	+	9	6	+	+	+	+
M. craniomandibularis externus anterior	**0md2**	-	22	/	+	+	+	M. 2	M26	-	-	-	-	-	-	-	-	-
M. craniomandibularis externus posterior	**0md3**	12	23	/	+	+	+	M.3	M27	25	+	+	8	5	+	+	+	+
M. hypopharyngomandibularis	**0md4**	13	26	/	+	+	+	M.8	M32	29'	+	+	adm dt	?	?	?	?	+
M. tentoriomandibularis lateralis superior	**0md5**	-	25a	/	+	+	+	M.4	M28	25'	+	+	-	-	+	+	+	+
M. tentoriomandibularis lateralis inferior	**0md6**	14	25b	/	+	+	+	M.5	M29	26	+	+	adm dt	-	+	+	+	+
M. tentoriomandibularis medialis superior	**0md7**	-	25a	/	+	+	+	M.6	M30	26'	+	+	-	9	?	?	?	-

Appendix 4: Homologization of the cephalic musculature between the taxa analyzed in chapter 7

Muscle name	Abbrev.	Kéler 1963	Matsuda 1965	Pass et al. 2006	*Ephemera danica* (Blanke et al. in press)	*Heptagenia sulphurea* (Blanke et al. in press)	*Siphlonurus lacustris* (Blanke et al. in press)	Staniczek 2000	Ephemeroptera: Staniczek 2001	Ephemeroptera: Strenger 1970	*Lestes virens* (Blanke et al. in press)	*Gomphus pulchellus* (Blanke et al. in press)	Odonata: Short 1955	Odonata: Mathur & Mathur 1961	*Epiophlebia superstes* (Asahina 1954)	*Davidius nanus* (Asahina 1954)	*Mnais strigata* (Asahina 1954)	*Epiophlebia superstes* (this study)
M. tentoriomandibularis medialis inferior	**0md8**	14?	25b	/	+	+	+	M.7	M31	-	+	+	adm dt	**8**	-	+	-	+
M. craniocardinalis	**0mx1**	15+16	1	/	+	+	+	/	M34	6	+	+	10	**10**	+	+	+	+
M. craniolacinialis	**0mx2**	19	5	/	+	+	+	/	M35	9	+	+	14	**13**	+	+	+	+
M. tentoriocardinalis	**0mx3**	17	3	/	+	+	+	/	M33	7	+	+	11a +b	**11+ 12**	+	+	+	+
M. tentoriostipitalis anterior	**0mx4**	18	4	/	+	+	+	/	M37 M38	8	+	+	12+ 13	**14- 16**	+	+	+	+
M. tentoriostipitalis posterior	**0mx5**	18	4	/	+	+	+	/	M36	8	+	+	13	**14**	+	+	+	+
M. stipitolacinialis	**0mx6**	20	6	/	+	+	+	/	M39	10	+	+	15	**19**	+	+	+	+
M. stipitogalealis	**0mx7**	21	7	/	-	-	-	/	-	-	-	-	-	-	-	-	-	-
M. stipitopalpalis externus	**0mx8**	22	10	/	+	+	+	/	M40	12	+	+	18	**18**	+	+	+	+
M. stipitopalpalis medialis	**0mx9**		11	/	-	-	-	/	-	-	-	-	-	-	-	-	-	-
M. stipitopalpalis internus	**0mx10**	23	9	/	+	+	+	/	M41	13	+	+	17	**17**	+	+	+	+
M. stipitalis transversalis	**0mx11**	-	12	/	-	-	-	/	p	-	-	-	-	-	-	-	-	-
M. palpopalpalis maxillae primus	**0mx12**	24	+	/	+	+	+	/	M42 +M43	27+ 28	-	-	-	-	-	-	-	-
M. palpopalpalis maxillae secundus	**0mx13**	25	+	/	-	-	-	/	-	-	-	-	-	-	-	-	-	-
M. palpopalpalis maxillae tertius	**0mx14**	26	+	/	-	-	-	/	-	-	-	-	-	-	-	-	-	-
M. palpopalpalis maxillae quartus	**0mx15**	27	+	/	-	-	-	/	-	-	-	-	-	-	-	-	-	-
M. postoccipitoglossalis medialis	**0la1**	-	31	/	-	-	-	/	-	-	-	-	-	-	-	-	-	-
M. postoccipitoglossalis lateralis	**0la2**	-	32	/	-	-	-	/	-	-	-	-	-	-	-	-	-	-
M. postoccipitoparaglossalis	**0la3**	-	33	/	-	-	-	/	-	-	-	-	-	-	-	-	-	-
M. postoccipitopraementalis	**0la4**	-	34	/	-	-	-	/	-	-	-	-	-	-	-	-	-	-
M. tentoriopraementalis	**0la5**	29	35	/	+	+	+	/	M46	14?	-	-	-	-	-	-	-	-
M. tentorioparaglossalis	**0la6**	30	36	/	-	+	+	/	M47	17	-	-	-	-	-	-	-	-

Appendix 4: continued

Muscle name	Abbrev.	Kéler 1963	Matsuda 1965	Pass et al. 2006	*Ephemera danica* (Blanke et al. in press)	*Heptagenia sulphurea* (Blanke et al. in press)	*Siphlonurus lacustris* (Blanke et al. in press)	Staniczek 2000	Ephemeroptera: Staniczek 2001	Ephemeroptera: Strenger 1970	*Lestes virens* (Blanke et al. in press)	*Gomphus pulchellus* (Blanke et al. in press)	Odonata: Short 1955	Odonata: Mathur & Mathur 1961	*Epiophlebia superstes* (Asahina 1954)	*Davidius nanus* (Asahina 1954)	*Mnais strigata* (Asahina 1954)	*Epiophlebia superstes* (this study)
M. tentorioglandularis	0la7	-	37	/	-	-	-	/	-	-	-	-	-	-	-	-	-	-
M. submentopraementalis	0la8	28	38	/	+	+	+	/	(M48)	20a	+	+	sf	24+21	+	+	+	+
M. postmentomembranus	0la9	-	40	/	-	-	-	/	-	-	-	-	-	-	-	-	-	-
M. submentomentalis	0la10	-	41	/	-	-	-	/	-	-	-	-	-	-	-	-	-	-
M. praementoparaglossalis	0la11	31	43	/	+	+	+	/	M56	19	-	-	-	-	-	-	-	-
M. praementoglossalis	0la12	32	42	/	+	+	+	/	M55	20	-	-	-	-	-	-	-	-
M. praementopalpalis internus	0la13	33	44	/	+	+	+	/	M50	18	+	+	29	20	+	+	+	+
M. praementopalpalis externus	0la14	34	45	/	-	-	-	/	-	-	-	-	-	-	-	-	-	-
M. praementomembranus	0la15	-	-	/	-	-	-	/	-	-	+	+	-	-	+	+	+	+
M. palpopalpalis labii primus	0la16	35	+	/	+	+	+	/	M51+M52+M53	23	-	-	-	-	-	-	-	-
M. palpopalpalis labii secundus	0la17	36	+	/	+	-	+	/	M54	21+22	-	-	-	-	-	-	-	-
M. frontooralis	0hy1	41	74	4	+	+	+	/	M18	3	-	+	38	-	/	/	/	-
M. tentoriooralis	0hy2	47	75	/	+	+	?	/	M19	-	-	-	-	-	/	/	/	-
M. craniohypopharyngealis	0hy3	42	37	/	+	+	+	/	M45?	15	-	-	rplh(32)	25	-	-	-	-
M. postoccipitalohypopharyngealis	0hy4		78		-	-	-		-	-	+	+	-	-	?	?	?	+
M. tentoriosuspensorialis	0hy5	48?	80	/	-	-	-	/	-	-	+	-	-	-	/	/	/	+
M. postmentoloralis	0hy6	-	72	/	-	-	-	/	-	-	-	-	-	-	-	-	-	-
M. praementosalivaris anterior	0hy7	38	76+46+(39?)	/	+	+	+	/	M49?	-	+	+	f?	23?	+	+	+	+
M. praementosalivaris posterior	0hy8	39	77+47+(39?)	/	+	+	+	/	M49?	-	-	-	ae?	26?	-	-	-	-
M. oralis transversalis	0hy9	67	-	/	+	+	+	/	M.suspensores	-	+	+	-	-	-	-	-	+
M. loroloralis	0hy10	-	73	/	-	-	-	/	M24	-	-	-	-	-	-	-	-	-
M. lorosalivarialis	0hy11	-	-	/	-	-	-	/	-	-	-	-	-	-	-	-	-	-

Appendix 4: continued

Muscle name	Abbrev.	Kéler 1963	Matsuda 1965	Pass et al. 2006	*Ephemera danica* (Blanke et al. in press)	*Heptagenia sulphurea* (Blanke et al. in press)	*Siphlonurus lacustris* (Blanke et al. in press)	Staniczek 2000	Ephemeroptera: Staniczek 2001	Ephemeroptera: Strenger 1970	*Lestes virens* (Blanke et al. in press)	*Gomphus pulchellus* (Blanke et al. in press)	Odonata: Short 1955	Odonata: Mathur & Mathur 1961	*Epiophlebia superstes* (Asahina 1954)	*Davidius nanus* (Asahina 1954)	*Mnais strigata* (Asahina 1954)	*Epiophlebia superstes* (this study)
M. hypopharyngosalivaris	**0hy12**	37	71+79	/	-	-	-	/	-	-	+	+	1s7	-	-	-	-	+
M. anularis salivarii	**0hy13**	40	-	/	-	-	-	/	-	-	-	-	-	-	-	-	-	-
M. tentoriofrontalis posterior	**0te1**	-	-	/	-	-	-	/	-	-	-	-	-	-	-	-	-	-
M. tentoriofrontalis anterior	**0te2**	-	-	/	-	-	-	/	-	-	-	-	-	-	-	-	-	-
M. tentoriofrontalis dorsalis	**0te3**	-	-	/	-	-	-	/	-	-	-	-	-	-	-	-	-	-
M. posterotentorialis	**0te4**	-	-	/	-	-	-	/	-	-	-	-	-	-	-	-	-	-
M. tentoriotentorialis longis	**0te5**	-	-	/	-	-	-	/	-	-	-	-	-	-	-	-	-	-
M. tentoriotentorialis brevis	**0te6**	-	-	/	-	-	-	/	-	-	-	-	-	-	-	-	-	-
M. clypeopalatalis	**0ci1**	43	81	/	+	+	+	/	M11 M14 ?	32	-	-	-	-	-	-	-	-
M. clypeobuccalis	**0bu1**	44	82	/	+	+	+	/	M14 ?	-	+	+	33+ 34	4	+	+	+	+
M. frontobuccalis anterior	**0bu2**	45	83	/	+	+	+	/	M15	PhM ?	+	+	35.3 6.39	-	+	+	+	+
M. frontobuccalis posterior	**0bu3**	46	84	/	+	+	+	/	M16	PhM ?	-	-	-	-	-	-	-	+
M. tentoriobuccalis lateralis	**0bu4**	49	85	/	+	-	+	/	M20	PhM ?	-	-	-	-	-	-	-	-
M. tentoriobuccalis anterior	**0bu5**	48	87	/	+	+	+	/	M21	-	+	+	42?	-	-	-	-	+
M. tentoriobuccalis posterior	**0bu6**	50	88	/	+	+	+	/	M21	-	-	-	43'?	-	/	/	/	-
M. verticopharyngealis	**0ph1**	51	86	/	+	+	+	/	M17	-	+	+	37	+	/	/	/	+
M. tentoriopharyngealis	**0ph2**	52	89+90	/	-	-	+	/	M21 ?	-	-	-	44	-	/	/	/	-
M. postoccipitopharyngealis	**0ph3**	-	-	/	-	-	-	-	-	-	+	+	-	-	-	-	-	+
M. anularis stomodaei	**0st1**	68	93	/	+	+	+	/	M10	-	+	+	-	+	+	+	+	+
M. longitudinalis stomodaei	**0st2**	69	91+92	/	+	+	+	/	M9	-	+	+	-	-	+	+	+	+

Appendix 4: continued

Abbrev.	*Platycnemis pennipes* (this study)	*Platycnemis latipes* (this study)	*Pyrrosoma nymphula* (this study)	*Coenagrion puella* (this study)	*Calopteryx virgo* (this study)	*Cordulegaster bidentata* (this study)	*Uropetala chiltoni* (this study)	*Sympetrum sanguineum* (this study)	*Libellula depressa* (this study)	*Cordulia aenea* (this study)	*Aeshna mixta* (this study)	*Anax imperator* (this study)	*Onychogomphus forcipatus* (this study)	*Neopetalia punctata* (this study)	*Phyllopetalia apicalis* (this study)	*Macromia taeniolata* (this study)	*Orthretum cancellatum* (this study)
0an1	+	+	+	+	+	+	+	+	+	+	+	+	+	+	+	+	+
0an2	+	+	+	+	+	+	+	+	+	+	+	+	+	+	+	+	+
0an3	-	-	-	-	-	-	?	?	+	+	+	+	-	-	-	-	-
0an4	-	-	-	-	-	-	-	-	-	-	-	-	-	-	-	-	-
0an5	-	-	-	-	-	-	-	-	-	-	-	-	-	-	-	-	-
0an6	+	+	+	+	+	+	+	+	+	+	+	+	+	+	+	+	+
0an7	+	+	+	+	+	+	+	+	+	+	+	+	+	+	+	+	+
0an8	-	-	-	-	-	-	-	-	-	-	-	-	-	-	-	-	-
0ah1	-	-	-	-	-	-	-	-	-	-	-	-	-	-	-	-	-
0ah2	-	-	-	-	-	-	-	-	-	-	-	-	-	-	-	-	-
0ah3	-	-	-	-	-	-	-	-	-	-	-	-	-	-	-	-	-
0ah4	-	-	-	-	-	-	-	-	-	-	-	-	-	-	-	-	-
0ah5	-	-	-	-	-	-	-	-	-	-	-	-	-	-	-	-	-
0b1	+	+	+	+	+	+	+	+	+	+	+	+	+	+	+	+	+
0b2	+	+	+	+	+	+	+	+	+	+	+	+	+	+	+	+	+
0b3	-	-	-	-	-	-	-	-	-	-	-	-	-	-	-	-	-
0b4	-	-	-	-	-	-	-	-	-	-	-	-	-	-	-	-	-
0b5	+	+	+	+	+	+	+	+	+	+	+	+	+	+	+	+	+
0b6	-	-	-	-	-	-	-	-	-	-	-	-	-	-	-	-	-
0md 1	+	+	+	+	+	+	+	+	+	+	+	+	+	+	+	+	+
0md 2	-	-	-	-	-	-	-	-	-	-	-	-	-	-	-	-	-
0md 3	+	+	+	+	+	+	+	+	+	+	+	+	+	+	+	+	+
0md 4	+	+	+	+	+	+	+	+	+	+	+	+	+	+	+	+	+
0md 5	+	+	+	+	+	+	+	+	+	+	+	+	+	+	+	+	+
0md 6	+	+	+	+	+	+	+	+	+	+	+	+	+	+	+	+	+
0md 7	+	+	+	+	-	+	+	-	-	-	-	-	+	+	+	+	+

Appendix 4: continued

Abbrev.	0md8	0mx1	0mx2	0mx3	0mx4	0mx5	0mx6	0mx7	0mx8	0mx9	0mx10	0mx11	0mx12	0mx13	0mx14	0mx15	0la1	0la2	0la3	0la4	0la5	0la6
Platycnemis pennipes (this study)	+	+	+	+	+	+	+	-	+	-	+	-	-	-	-	-	-	-	-	-	-	-
Platycnemis latipes (this study)	+	+	+	+	+	+	+	-	+	-	+	-	-	-	-	-	-	-	-	-	-	-
Pyrrosoma nymphula (this study)	+	+	+	+	+	+	+	-	+	-	+	-	-	-	-	-	-	-	-	-	-	-
Coenagrion puella (this study)	+	+	+	+	+	+	+	-	+	-	+	-	-	-	-	-	-	-	-	-	-	-
Calopteryx virgo (this study)	+	+	+	+	+	+	+	-	+	-	+	-	-	-	-	-	-	-	-	-	-	-
Cordulegaster bidentata (this study)	+	+	+	+	+	+	+	-	+	-	+	-	-	-	-	-	-	-	-	-	-	-
Uropetala chiltoni (this study)	+	+	+	+	+	+	+	-	+	-	+	-	-	-	-	-	-	-	-	-	-	-
Sympetrum sanguineum (this study)	+	+	+	+	+	+	+	-	+	-	+	-	-	-	-	-	-	-	-	-	-	-
Libellula depressa (this study)	+	+	+	+	+	+	+	-	+	-	+	-	-	-	-	-	-	-	-	-	-	-
Cordulia aenea (this study)	+	+	+	+	+	+	+	-	+	-	+	-	-	-	-	-	-	-	-	-	-	-
Aeshna mixta (this study)	+	+	+	+	+	+	+	-	+	-	+	-	-	-	-	-	-	-	-	-	-	-
Anax imperator (this study)	+	+	+	+	+	+	+	-	+	-	+	-	-	-	-	-	-	-	-	-	-	-
Onychogomphus forcipatus (this study)	+	+	+	+	+	+	+	-	+	-	+	-	-	-	-	-	-	-	-	-	-	-
Neopetalia punctata (this study)	+	+	+	+	+	+	+	-	+	-	+	-	-	-	-	-	-	-	-	-	-	-
Phyllopetalia apicalis (this study)	+	+	+	+	+	+	+	-	+	-	+	-	-	-	-	-	-	-	-	-	-	-
Macromia taeniolata (this study)	+	+	+	+	+	+	+	-	+	-	+	-	-	-	-	-	-	-	-	-	-	-
Orthretum cancellatum (this study)	+	+	+	+	+	+	+	-	+	-	+	-	-	-	-	-	-	-	-	-	-	-

Appendix 4: continued

Abbrev.	*Platycnemis pennipes* (this study)	*Platycnemis latipes* (this study)	*Pyrrosoma nymphula* (this study)	*Coenagrion puella* (this study)	*Calopteryx virgo* (this study)	*Cordulegaster bidentata* (this study)	*Uropetala chiltoni* (this study)	*Sympetrum sanguineum* (this study)	*Libellula depressa* (this study)	*Cordulia aenea* (this study)	*Aeshna mixta* (this study)	*Anax imperator* (this study)	*Onychogomphus forcipatus* (this study)	*Neopetalia punctata* (this study)	*Phyllopetalia apicalis* (this study)	*Macromia taeniolata* (this study)	*Orthretum cancellatum* (this study)
θla7	-	-	-	-	-	-	-	-	-	-	-	-	-	-	-	-	-
θla8	+	+	+	+	+	+	+	+	+	+	+	+	+	+	+	+	+
θla9	-	-	-	-	-	-	-	-	-	-	-	-	-	-	-	-	-
θla10	-	-	-	-	-	-	-	-	-	-	-	-	-	-	-	-	-
θla11	-	-	-	-	-	-	-	-	-	-	-	-	-	-	-	-	-
θla12	-	-	-	-	-	-	-	-	-	-	-	-	-	-	-	-	-
θla13	+	+	+	+	+	+	+	+	+	+	+	+	+	+	+	+	+
θla14	-	-	-	-	-	-	-	-	-	-	-	-	-	-	-	-	-
θla15	+	+	+	+	+	+	+	+	+	+	+	+	+	+	+	+	+
θla16	-	-	-	-	-	-	-	-	-	-	-	-	-	-	-	-	-
θla17	-	-	-	-	-	-	-	-	-	-	-	-	-	-	-	-	-
θhy1	-	-	-	-	-	-	-	-	-	-	-	-	-	-	-	-	-
θhy2	-	-	-	-	-	-	-	-	-	-	-	-	-	-	-	-	-
θhy3	-	-	-	-	-	-	-	-	-	-	-	-	-	-	-	-	-
θhy4	+	+	+	+	+	+	+	+	+	?	+	?	+	+	+	+	+
θhy5	+	+	+	+	+	+	?	+	+	+	+	+	+	+	+	+	+
θhy6	-	-	-	-	-	-	-	-	-	-	-	-	-	-	-	-	-
θhy7	+	+	+	+	+	+	+	+	+	+	+	+	+	+	+	+	+
θhy8	-	-	-	-	-	-	-	-	-	-	-	-	-	-	-	-	-
θhy9	+	+	+	+	+	+	+	+	+	+	+	+	+	+	+	+	+
θhy10	-	-	-	-	-	-	-	-	-	-	-	-	-	-	-	-	-
θhy11	-	-	-	-	-	-	-	-	-	-	-	-	-	-	-	-	-

Appendix 4: continued

Abbrev.	0hy1 2	0hy1 3	0tc1	0tc2	0tc3	0tc4	0tc5	0tc6	0ci1	0bu 1	0bu 2	0bu 3	0bu 4	0bu 5	0bu 6	0ph 1	0ph 2	0ph 3	0st1	0st2
Platycnemis pennipes (this study)	+	-	-	-	-	-	-	-	-	+	+	+	+	?	+	+	+	+	+	+
Platycnemis latipes (this study)	+	-	-	-	-	-	-	-	-	+	+	+	-	?	+	+	+	+	+	+
Pyrrosoma nymphula (this study)	+	-	-	-	-	-	-	-	-	+	+	+	-	?	+	+	+	+	+	+
Coenagrion puella (this study)	+	-	-	-	-	-	-	-	-	+	+	+	+	?	+	+	+	+	+	+
Calopteryx virgo (this study)	+	-	-	-	-	-	-	-	-	+	+	+	-	+	+	+	+	+	+	+
Cordulegaster bidentata (this study)	+	-	-	-	-	-	-	-	-	+	+	+	-	-	+	+	+	+	+	+
Uropetala chiltoni (this study)	+	-	-	-	-	-	-	-	-	+	+	+	-	-	+	+	+	?	+	+
Sympetrum sanguineum (this study)	+	-	-	-	-	-	-	-	-	+	+	+	-	+	+	+	+	+	+	+
Libellula depressa (this study)	+	-	-	-	-	-	-	-	-	+	+	+	-	?	+	+	+	+	+	+
Cordulia aenea (this study)	+	-	-	-	-	-	-	-	-	+	+	+	-	+	+	+	+	+	+	+
Aeshna mixta (this study)	+	-	-	-	-	-	-	-	-	+	+	+	-	+	+	+	?	+	+	+
Anax imperator (this study)	+	-	-	-	-	-	-	-	-	+	+	+	+	+	+	+	+	+	+	+
Onychogomphus forcipatus (this study)	+	-	-	-	-	-	-	-	-	+	+	+	-	-	+	+	+	+	+	+
Neopetalia punctata (this study)	+	-	-	-	-	-	-	-	-	+	+	+	-	-	+	+	+	+	+	+
Phyllopetalia apicalis (this study)	+	-	-	-	-	-	-	-	-	+	+	+	-	-	+	+	+	+	+	+
Macromia taeniolata (this study)	+	-	-	-	-	-	-	-	-	+	+	+	-	-	+	+	+	+	+	+
Orthretum cancellatum (this study)	+	-	-	-	-	-	-	-	-	+	+	+	-	-	+	+	+	+	+	+

Appendix 4: continued

Character no.	Character description	Ephemeroptera	Zygoptera	Anisozygoptera	Anisoptera
1	Composition of mandibular abductor: (0) undivided (0md3); (1) divided into two bundles (0md2 & 0md3).	1	0	0	0
2	M. frontobuccalis lateralis: (0) absent; (1) present.	1	0	0	0
3	M. tentoriohypopharyngalis (0hy3): (0) absent; (1) present.	1	0	0	0
4	M. praementosalivarialis posterior (0hy8): (0) absent; (1) present.	1	0	0	0
5	M. tentoriopraementalis inferior (0la5): (0) absent; (1) present.	1	0	0	0
6	M. praementoglossalis (0la11): (0) absent; (1) present.	1	0	0	0
7	Galea: (0) absent; (1) present.	1	0	0	0
8	Salivary system: (0) absent; (1) present.	0	1	1	1
9	Head: (0) transversely elongate; (1) globular.	1	0	1	1
10	M. tentoriomandibularis medialis superior (0md7): (0) absent; (1) present.	1	1	0	0
11	Eyes: (0) seperated by less than their own width; (1) separated by more than their own width.	1	1	0	0
12	Anteclypeus and postclypeus: (0) not facing anteriorly; (1) facing anteriorly.	1	1	0	0
13	Labrum transversely enlarged: (0) absent; (1) present.	0	0	1	0
14	Vertex: (0) flat; (1) grossly enlarged.	0	0	1	1
15	Pedicellus: (0) flattened with a lateral vestiture of long setae; (1) not as above.	1	1	0	1
16	M. frontobuccalis posterior (0bu3): (0) absent; (1) present.	1	0	1	0
17	Internal part of the interantennal ridge (interantennal apodeme): (0) absent; (1) present.	0	0	0	1
18	Internal part of the epistomal ridge (epistomal apodeme): (0) absent; (1) present.	0	0	0	1

Appendix 5: Character matrix used for analysis in chapter 7.

		Data source (morphology)				Data source (molecular)						
Family	Species	DESY	PSI	SI	other source	12S	16S	COII	18S	28S	H3	Species
Coenagrionidae	*Coenagrion puella*	-	10 / 1.25 / 5.9	-	collection ZFMK	EU055031	EU055128	EU055417	EU055221	EU055319	EU055514	*Argia nahuana*
	Pyrrhosoma nymphula	-	10 / 1.25 / 5.9	-	collection ZFMK							
	Platycnemis pennipes	-	10 / 1.25 / 5.9	-	collection ZFMK							
Calopterygidae	*Calopteryx virgo*	8 / 2.7 / 5.0	-	-	collection ZFMK	EU054990	EU055086	EU055378	EU055181	EU055279	EU055472	*Matrona basilaris*
Lestidae	*Lestes virens*	8 / 3.4 / 4.7	-	-	collection ZFMK	EU054938	AY749828	EU055330	AY338721	AY338677	EU055423	*Lestes sp.*
Epiophlebiidae	*Epiophlebia superstes*	8 / 1.9 / 9.5	10 / 2 / 3.7	-	collection ZFMK	EU477631	EU055132	EU055421	EU055226	EU055324	EU055518	*Epiophlebia superstes*
Aeshnidae	*Aeshna mixta*	8 / 3.7 / 3.7	-	-	collection ZFMK	EU054953	EU055053	EU055343	EU055147	EU055242	EU055438	*Aeshna multicolor*
	Anaciaeschna isoceles	-	10 / 2 / 3.7	-	collection ZFMK	EU477649	EU477649	–	DQ008199	FJ596528	–	
	Anax imperator	-	-	20.5 / 4 / 7.9	collection ZFMK	AY749694	AY749829	EU055328	AY749808	AY750038	AY748748	*Anax junius*
	Austrogynacantha	-	-	-	Theischinger & Hawking 2006	EU054971	–	–	EU055162	EU055260	EU055453	*Austrogynacantha heterogena*
	Brachytron pratense	-	-	-	collection ZFMK	EU477641	EU055106	–	EU055199	EU055297	EU055492	*Brachytron pratense*
	Caliaeschna	-	-	-	collection ZFMK							
	Gomphaeschna	-	-	-	collection ZFMK							
	Gynacantha	-	-	-	Needham & Westfall (1955)							
	Hemianax	-	-	-	collection ZFMK							
	Oligoaeschna pryeri	-	10 / 2 / 3.7	-	collection ZFMK							
	Staurophlebia	-	-	-	collection ZFMK							
Austropetaliidae	*Austropetalia*	-	-	-	collection ZFMK							
	Phyllopetalia apicalis	-	10 / 2 / 3.7	-	collection ZFMK	EU055033	EU055130	EU055419	EU055224	EU055322	EU055516	*Phyllopetalia apollo*
	Hypopetalia pestilens	-	10 / 2 / 3.7	-	collection ZFMK							
Chlorogomphidae	*Chlorogomphus*	-	-	-	Subramanian 2005	EU054995	EU055091	EU055383	EU055186	EU055284	EU055477	*Chlorogomphus brunneus*
Cordulegastridae	*Cordulegaster bidentata*	-	10 / 2 / 3.7	20.5 / 4 / 7.9	collection ZFMK	EU054988	EU055084	EU055376	EU055179	EU055277	EU055470	*Cordulegaster dorsalis*
	Sonjagaster	-	-	-	collection ZFMK							
	Anotogaster sieboldii	-	10 / 2 / 3.7	-	collection ZFMK							
Gomphidae	*Antipodogomphus*	-	-	-	Theischinger & Hawking 2006	EU054972	EU055068	EU055360	EU055163	EU055261	EU055454	*Antipodogomphus acolythus*
	Armagomphus	-	-	-	Theischinger & Hawking 2006	EU054961	EU055059	EU055350	EU055153	EU055250	EU055444	*Armagomphus armiger*
	Austrogomphus	-	-	-	collection ZFMK	EU054978	EU055074	EU055366	EU055169	EU055267	EU055460	*Austrogomphus amphiclitus*
	Cyclogomphus	-	-	-	DeFonseka 2000	EU054996	EU055092	EU055384	EU055187	EU055285	EU055478	*Cyclogomphus heterostylus*
	Davidioides	-	-	-	Subramanian 2005	EU054997	EU055093	EU055385	EU055188	EU055286	EU055479	*Davidioides martini*
	Gomphus vulgatissimus	8 / 2.7 / 5.0	-	-	collection ZFMK	EU054949	EU055048	EU055338	EU055142	EU055237	EU055433	*Gomphus sp.*
	Onychogomphus forcipatus	8 / 1.9 / 9.5	-	-	collection ZFMK							
	Hagenius brevistylus	-	10 / 2 / 3.7	-	Needham & Westfall (1955)	EU054943	EU055043	EU055334	EU055137	EU055232	EU055428	*Hagenius sp.*
	Hemigomphus	-	-	-	Theischinger & Hawking 2006	EU054939	EU055039	EU055331	EU055133	EU055228	EU055424	*Hemigomphus magela*
	Ictinogomphus	-	-	-	collection ZFMK	EU054969	EU055066	EU055358	EU055160	EU055258	EU055451	*Ictinogomphus australis*
	Stylurus plagiatus	-	8.5 / 2 / 3.7	-	collection ZFMK							
	Dromogomphus	-	-	-	Needham & Westfall (1955)	EU054982	EU055078	EU055370	EU055173	EU055271	EU055464	*Progomphus borealis*
	Zonophora batesi	-	10 / 2 / 3.7	-	collection ZFMK	–	–	–	–	–	–	
Petaluridae	*Petalura*	-	-	-	Theischinger & Hawking 2006	EU054963	EU055061	EU055352	EU055155	EU055252	EU055446	*Petalura gigantea*
	Phenes raptor	-	10 / 2 / 3.7	-	collection ZFMK	EU054937	EU055038	EU055329	AY338720	EU055227	EU055422	*Phenes raptor*
	Tanypteryx pryeri	-	10 / 2 / 3.7	-	Needham & Westfall (1955)	EU054979	EU055075	EU055367	EU055170	EU055268	EU055461	*Tanypteryx hageni*
	Tachopteryx thoreyi	-	10 / 2 / 3.7	-	collection ZFMK							
	Uropetala chiltoni	-	-	20.5 / 4 / 7.9	collection ZFMK	EU477633	EU477633	–	–	FJ596525	–	*Uropetala carovei*
Neopetaliidae	*Neopetalia punctata*	-	8.5 / 2 / 3.7	-	collection ZFMK	EU477684	EU477684	–	FJ010021	FJ596535	–	*Neopetalia punctata*
Libellulidae	*Brachydiplax*	-	-	-	collection ZFMK	EU054976	EU055072	EU055364	EU055167	EU055265	EU055458	*Brachydiplax denticauda*
	Erythrodiplax	-	-	-	collection ZFMK	EU054950	EU055050	EU055340	EU055144	EU055239	EU055435	*Erythrodiplax minuscula*
	Libellula depressa	8 / 3.7 / 4.1	-	-	collection ZFMK	EU054935	EF640401	EU055326	AY338717	AY338674	AY338637	*Libellula saturata*
	Macrodiplax	-	-	-	Needham & Westfall (1955)	EU054940	EU055040	EU055332	EU055134	EU055229	EU055425	*Macrodiplax balteata*
	Nannophlebia	-	-	-	Theischinger & Hawking 2006	EU054944	EU055044	–	EU055138	EU055233	EU055429	*Nannophlebia sp.*
	Pantala flavescens	-	-	-	collection ZFMK	EU054947	EU055047	EU055337	EU055141	EU055236	EU055432	*Perithemis intensa*
	Perithemis	-	-	-	Needham & Westfall (1955)	EU054941	EU055041	–	EU055136	EU055230	EU055426	*Sympetrum corruptum*

Appendix 6: List of taxa analyzed in chapter 8

Muscle name	Muscle name acc. Wipfler 2011	Muscle name acc. Kéler 1963	Muscle name acc. Matsuda 1965	Muscle name acc. Pass et al. 2006	Muscle name acc. Blanke et al. (2012) for Ephemera danica	Muscle name acc. Blanke et al. (2012) for Heptagenia sulphurea	Muscle name acc. Blanke et al. (2012) for Siphlonurus lacustris	Muscle name acc. Staniczek 2000	Muscle name acc. Staniczek (2001) for Ephemeroptera	Muscle name acc. Strenger (1970) for Ephemeroptera:	Epiophlebia superstes (this study)	Platycnemis pennipes (this study)	Platycnemis latipes (this study)	Pyrrhosoma nymphula (this study)	Coenagrion puella (this study)	Lestes virens (this study)	Calopteryx virgo (this study)	Gomphus pulchellus (this study)	Cordulegaster bidentata (this study)	Uropetala (this study)	Sympetrum sanguineum (this study)	Libellula depressa (this study)	Cordulia aenea (this study)	Aeshna mixta (this study)	Anax imperator (this study)	Muscle name acc. Blanke et al. (2012) for Onychogomphus forcipatus	Muscle name acc. Short (1955) for Odonata	Muscle name acc. Mathur & Mathur (1961) for Odonata	Muscle name acc. Asahina (1954) for Epiophlebia superstes	Muscle name acc. Asahina (1954) for Davidius nanus	Muscle name acc. Asahina (1954) for Mnais strigata	Muscle name acc. Blanke et al. (2012) for Perla marginata	Muscle name acc. Moulins (1968) for Plecoptera	Muscle name acc. Chisholm (1962) for Plecoptera
M. tentorioscapalis anterior	0an1	1	52	/	+	+	+	/	M1	5	+	+	+	+	+	+	+	+	+	+	+	+	+	+	+	+	4	28	+	+	+	+	lsc1+lsc2	A.D.M.
M. tentorioscapalis posterior	0an2	2	54	/	+	+	+	/	M3	4	+	+	+	+	+	+	+	+	+	+	+	+	+	+	+	+	5	27	+	+	+	+	dsc	A.E.M
M. tentorioscapalis lateralis	0an3	3	51	/	+	-	-	/	-	-	-	-	-	-	-	-	-	-	-	?	?	+	+	+	+	-	-	-	-	-	-	+	fsc	-
M. tentorioscapalis medialis	0an4	4	53	/	-	-	+	/	M2?	-	-	-	-	-	-	-	-	-	-	-	-	-	-	-	-	-	-	-	-	-	-	+	-	-
M. tentoriopedicellaris																										+								
M. frontopedicellaris	0an5	-	-	/	-	-	-	/	-	-	-	-	-	-	-	-	-	-	-	-	-	-	-	-	-	-	-	-	-	-	-	-	-	-
M. scapopedicellaris lateralis	0an6	5	+	/	-	-	-	/	-	/	+	+	+	+	+	+	+	+	+	+	+	+	+	+	+	+	6	29	/	/	/	+	fpd1+fpd2	-
M. scapopedicellaris medialis	0an7	6	+	/	-	-	-	/	M4?	/	+	+	+	+	+	+	+	+	+	+	+	+	+	+	+	+	7	30	/	/	/	+	epd1+epd2	-
M. intraflagellaris	0an8	-	-	-	-	-	-	-	-	-	-	-	-	-	-	-	-	-	-	-	-	-	-	-	-	-	-	-	/	/	/	-	-	-
M. interampullaris	0ah1	/	/	7	-	-	-	/	/	/	-	-	-	-	-	-	-	-	-	-	-	-	-	-	-	-	/	/	-	-	-	-	/	/
M. ampulloaortica	0ah2	/	/	8	-	-	-	/	/	/	-	-	-	-	-	-	-	-	-	-	-	-	-	-	-	-	/	/	-	-	-	-	/	/
M. ampullopharyngealis	0ah3	/	/	6	-	-	-	/	/	/	-	-	-	-	-	-	-	-	-	-	-	-	-	-	-	-	/	/	-	-	-	-	/	/
M. ampullofrontalis	0ah4	/	/	9	-	-	-	/	/	/	-	-	-	-	-	-	-	-	-	-	-	-	-	-	-	-	/	/	-	-	-	-	/	/
M. frontofrontalis	0ah5	/	/	5	-	-	-	/	/	/	-	-	-	-	-	-	-	-	-	-	-	-	-	-	-	-	/	/	-	-	-	-	/	/
M. frontolabralis	0lb1	8	62	/	+	+	+	/	M5	1	+	+	+	+	+	+	+	+	+	+	+	+	+	+	+	+	2	1	+	+	+	+	mlra	LR.EL..
M. frontoepipharyngalis	0lb2	9	61	/	+	+	+	/	M6	2	+	+	+	+	+	+	+	+	+	+	+	+	+	+	+	+	3	2	+	+	+	+	mlrp	LR.DEP
M. epistoepipharyngealis	0lb3	10		/	-	-	-	/	-	-	-	-	-	-	-	-	-	-	-	-	-	-	-	-	-	-	-	-	-	-	-	-	-	-

Appendix 7: Homologized cephalic musculature of the taxa analyzed in chapter 8

Muscle name	Muscle name acc. Wipfler 2011	Muscle name acc. Kéler 1963	Muscle name acc. Matsuda 1965	Muscle name acc. Plass et al. 2006	Muscle name acc. Blanke et al. (2012) for Ephemera danica	Muscle name acc. Blanke et al. (2012) for Heptagenia sulphurea	Muscle name acc. Blanke et al. (2012) for Siphlonurus lacustris	Muscle name acc. Staniczek 2000	Muscle name acc. Staniczek (2001) for Ephemeroptera	Muscle name acc. Strenger (1970) for Ephemeroptera:	Epiophlebia superstes (this study)	Platycnemis pennipes (this study)	Platycnemis latipes (this study)	Pyrrhosoma nymphula (this study)	Coenagrion puella (this study)	Lestes virens (this study)	Calopteryx virgo (this study)	Gomphus pulchellus (this study)	Cordulegaster bidentata (this study)	Uropetala (this study)	Sympetrum sanguineum (this study)	Libellula depressa (this study)	Cordulia aenea (this study)	Aeshna mixta (this study)	Anax imperator (this study)	Muscle name acc. Blanke et al. (2012) for Onychogomphus forcipatus	Muscle name acc. Short (1955) for Odonata	Muscle name acc. Mathur & Mathur (1961) for Odonata	Muscle name acc. Asahina (1954) for Epiophlebia superstes	Muscle name acc. Asahina (1954) for Davidius nanus	Muscle name acc. Asahina (1954) for Mnais strigata	Muscle name acc. Blanke et al. (2012) for Perla marginata	Muscle name acc. Moulins (1968) for Plecoptera	Muscle name acc. Chisholm (1952) for Plecoptera
M. labralis transversalis	0lb4	-	-	/	-	-	-	/	-	-	-	-	-	-	-	-	-	-	-	-	-	-	-	-	-	-	-	-	-	-	-	-	-	-
M. labroepipharyngealis	0lb5	7	63	/	+	+	+	/	M7	33'	+	+	+	+	+	+	+	+	+	+	+	+	+	+	+	+	1	3	+	+	+	+	cgir	CIB.DI L.
M. labrolabralis	0lb6	-	-	/	+	-	-	/	M8	33	-	-	-	-	-	-	-	-	-	-	-	-	-	-	-	-	-	-	-	-	-	+	-	-
M. craniomandibularis internus	0md1	11	21+24	/	+	+	+	M.1	M25	MA	+	+	+	+	+	+	+	+	+	+	+	+	+	+	+	+	5	6	+	+	+	+	admd	M.AD. M.
M. craniomandibularis externus anterior	0md2	-	22	/	-	-	+	M. 2	M26	-	-	-	-	-	-	-	-	-	-	-	-	-	-	-	-	-	-	-	-	-	-	-	-	-
M. craniomandibularis externus posterior	0md3	12	23	/	+	+	+	M.3	M27	28	+	+	+	+	+	+	+	+	+	+	+	+	+	+	+	+	8	8	+	+	+	+	abmd	M.AB. M.
M. hypopharyngomandibularis	0md4	13	26	/	+	+	+	M.8	M32	29	+	+	+	+	+	+	+	+	+	+	+	+	+	+	+	+	admd h	7	-	-	-	-	-	-
M. tentoriomandibularis lateralis superior	0md5	-	25a	/	+	-	+	M.4	M28	25'	+	+	+	+	+	+	+	+	+	+	+	+	+	+	+	+	-	-	+	+	+	-	-	-
M. tentoriomandibularis lateralis inferior	0md6	14	25b	/	+	+	+	M.5	M29	26	+	+	+	+	+	+	+	+	+	+	+	+	+	+	+	+	admd t	-	+	+	+	-	tmdv	-
M. tentoriomandibularis medialis superior	0md7	-	25a	/	+	+	+	M.6	M30	26'	-	+	+	+	+	+	-	+	+	+	-	-	-	-	-	+	-	9	-	-	-	+	tmdd	-
M. tentoriomandibularis medialis inferior	0md8	14?	25b	/	+	+	+	M.7	M31	-	+	+	+	+	+	+	+	+	+	+	+	+	+	+	+	+	admd t	8	-	+	-	+	-	-
M. craniocardinalis	0mx1	15+16	1	/	+	+	+	/	M34	6	+	+	+	+	+	+	+	+	+	+	+	+	+	+	+	+	10	10	+	+	+	+	rcc	PR.CA R.
M. craniolacinialis	0mx2	19	5	/	+	+	+	/	M35	9	+	+	+	+	+	+	+	+	+	+	+	+	+	+	+	+	14	13	+	+	+	+	fcl	CR.F.L.
M. tentoriocardinalis	0mx3	17	3	/	+	+	+	/	M33	7	+	+	+	+	+	+	+	+	+	+	+	+	+	+	+	+	11a+b	11+12	+	+	+	+	acl+acm	CAR.AD.M.
M. tentoriostipitalis anterior	0mx4	18	4	/	+	+	+	/	M37-M38	8	+	+	+	+	+	+	+	+	+	+	+	+	+	+	+	+	12+13	14-16	+	+	+	+	ssm	ST.AD. M.
M. tentoriostipitalis posterior	0mx5	18	4	/	+	+	+	/	M36	8	+	+	+	+	+	+	+	+	+	+	+	+	+	+	+	+	13	14	+	+	+	+	asl	ST.AD. M.
M. stipitolacinialis	0mx6	20	6	/	+	+	+	/	M39	10	+	+	+	+	+	+	+	+	+	+	+	+	+	+	+	+	16	19	+	+	+	+	rsl1+rsl2	ST.F.L.

Appendix 7: continued

Muscle name	Muscle name acc. Wipfler 2011	Muscle name acc. Kéler 1963	Muscle name acc. Matsuda 1965	Muscle name acc. Plass et al. 2005	Muscle name acc. Blanke et al. (2012) for Ephemera danica	Muscle name acc. Blanke et al. (2012) for Heptagenia sulphurea	Muscle name acc. Blanke et al. (2012) for Siphlonurus lacustris	Muscle name acc. Staniczek 2000	Muscle name acc. Staniczek (2001) for Ephemeroptera	Muscle name acc. Strenger (1970) for Ephemeroptera:	Epiophlebia superstes (this study)	Platycnemis pennipes (this study)	Platycnemis latipes (this study)	Pyrrhosoma nymphula (this study)	Coenagrion puella (this study)	Lestes virens (this study)	Calopteryx virgo (this study)	Gomphus pulchellus (this study)	Cordulegaster bidentata (this study)	Uropetala (this study)	Sympetrum sanguineum (this study)	Libellula depressa (this study)	Cordulia aenea (this study)	Aeshna mixta (this study)	Anax imperator (this study)	Muscle name acc. Blanke et al. (2012) for Onychogomphus forcipatus	Muscle name acc. Short (1955) for Odonata	Muscle name acc. Mathur & Mathur (1961) for Odonata	Muscle name acc. Asahina (1954) for Epiophlebia superstes	Muscle name acc. Asahina (1954) for Davidius nanus	Muscle name acc. Asahina (1954) for Mnais strigata	Muscle name acc. Blanke et al. (2012) for Perla marginata	Muscle name acc. Moulins (1968) for Plecoptera	Muscle name acc. Chisholm (1962) for Plecoptera
M. stipitogalealis	0mx7	21	7	/	-	-	-	/	-	-	-	-	-	-	-	-	-	-	-	-	-	-	-	-	-	-	-	-	-	-	-	+	rsg	+
M. stipitopalpalis externus	0mx8	22	10	/	+	+	+	/	M40	12	+	+	+	+	+	+	+	+	+	+	+	+	+	+	+	+	19	18	+	+	+	+	abp	L.MX.P. -
M. stipitopalpalis medialis	0mx9		11	/	-	-	-	/	-	-	-	-	-	-	-	-	-	-	-	-	-	-	-	-	-	-	-	-	-	-	-	suche n	bi	-
M. stipitopalpalis internus	0mx10	23	9	/	+	+	+	/	M41	13	+	+	+	+	+	+	+	+	+	+	+	+	+	+	+	+	17	17	+	+	+	+	adp	D.MX. P
M. stipitalis transversalis	0mx11	-	12	/	-	-	-	/	p	-	-	-	-	-	-	-	-	-	-	-	-	-	-	-	-	-	-	-	-	-	-	-	-	-
M. palpopalpalis maxillae primus	0mx12	24	+	/	+	+	+	/	M42+M4 3	27+2 8	-	-	-	-	-	-	-	-	-	-	-	-	-	-	-	-	-	-	-	-	-	-	-	-
M. palpopalpalis maxillae secundus	0mx13	25	+	/	-	-	-	/	-	-	-	-	-	-	-	-	-	-	-	-	-	-	-	-	-	-	-	-	-	-	-	+	ftt	-
M. palpopalpalis maxillae tertius	0mx14	26	+	/	-	-	-	/	-	-	-	-	-	-	-	-	-	-	-	-	-	-	-	-	-	-	-	-	-	-	-	+	ltt	-
M. palpopalpalis maxillae quartus	0mx15	27	+	/	-	-	-	/	-	-	-	-	-	-	-	-	-	-	-	-	-	-	-	-	-	-	-	-	-	-	-	+	dtp	-
M. postoccipitoglossalis medialis	0la1	-	31	/	-	-	-	/	-	-	-	-	-	-	-	-	-	-	-	-	-	-	-	-	-	-	-	-	-	-	-	-	-	-
M. postoccipitoglossalis lateralis	0la2	-	32	/	-	-	-	/	-	-	-	-	-	-	-	-	-	-	-	-	-	-	-	-	-	-	-	-	-	-	-	-	-	D.R.L. ?
M. postoccipitoparaglossalis	0la3	-	33	/	-	-	-	/	-	-	-	-	-	-	-	-	-	-	-	-	-	-	-	-	-	-	-	-	-	-	-	-	-	-
M. postoccipitopraementalis	0la4	-	34	/	-	-	-	/	-	-	-	-	-	-	-	-	-	-	-	-	-	-	-	-	-	-	-	-	-	-	-	-	-	-
M. tentoriopraementalis	0la5	29	35	/	+	+	+	/	M46	14?	-	-	-	-	-	-	-	-	-	-	-	-	-	-	-	-	-	-	-	-	-	+	adpr	PR.R.L. -
M. tentorioparaglossalis	0la6	30	36	/	-	+	+	/	M47	17	-	-	-	-	-	-	-	-	-	-	-	-	-	-	-	-	-	-	-	-	-	+	aspr	D.R.L. ?
M. tentorioglandularis	0la7	-	37	/	-	-	-	/	-	-	-	-	-	-	-	-	-	-	-	-	-	-	-	-	-	-	-	-	-	-	-	-	-	-
M. submentopraementalis	0la8	28	38	/	+	+	+	/	(M48)	20a	+	+	+	+	+	+	+	+	+	+	+	+	+	+	+	+	sf	24 +21	+	+	+	+	rpmt	M.R.M.

Appendix 7: continued

Muscle name	Muscle name acc. Wipfler 2011	Muscle name acc. Kéler 1963	Muscle name acc. Matsuda 1965	Muscle name acc. Plass et al. 2005	Muscle name acc. Blanke et al. (2012) for Ephemera danica	Muscle name acc. Blanke et al. (2012) for Heptagenia sulphurea	Muscle name acc. Blanke et al. (2012) for Siphlonurus lacustris	Muscle name acc. Staniczek 2000	Muscle name acc. Staniczek (2001) for Ephemeroptera	Muscle name acc. Strenger (1970) for Ephemeroptera:	Epiophlebia superstes (this study)	Platycnemis pennipes (this study)	Platycnemis latipes (this study)	Pyrrhosoma nymphula (this study)	Coenagrion puella (this study)	Lestes virens (this study)	Calopteryx virgo (this study)	Gomphus pulchellus (this study)	Cordulegaster bidentata (this study)	Uropetala (this study)	Sympetrum sanguineum (this study)	Libellula depressa (this study)	Cordulia aenea (this study)	Aeshna mixta (this study)	Anax imperator (this study)	Muscle name acc. Blanke et al. (2012) for Onychogomphus forcipatus	Muscle name acc. Short (1955) for Odonata	Muscle name acc. Mathur & Mathur (1961) for Odonata	Muscle name acc. Asahina (1954) for Epiophlebia superstes	Muscle name acc. Asahina (1954) for Davidius nanus	Muscle name acc. Asahina (1954) for Mnais strigata	Muscle name acc. Blanke et al. (2012) for Perla marginata	Muscle name acc. Moulins (1968) for Plecoptera	Muscle name acc. Chisholm (1962) for Plecoptera
M. tentorioscapalis anterior	Oan1	1	52	/	+	+	+	/	M1	5	+	+	+	+	+	+	+	+	+	+	+	+	+	+	+	+	4	28	+	+	+	+	lsc1+lsc2	A.D.M.
M. tentorioscapalis posterior	Oan2	2	54	/	+	+	+	/	M3	4	+	+	+	+	+	+	+	+	+	+	+	+	+	+	+	+	5	27	+	+	+	+	dsc	A.E.M
M. tentorioscapalis lateralis	Oan3	3	51	/	+	-	-	/	-	-	-	-	-	-	-	-	-	-	-	?	?	+	+	+	+	-	-	-	-	-	-	+	lsc	-
M. tentorioscapalis medialis	Oan4	4	53	/	-	-	+	/	M2?	-	-	-	-	-	-	-	-	-	-	-	-	-	-	-	-	-	-	-	-	-	-	+	-	-
M. tentoriopedicellaris																										+								
M. frontopedicellaris	Oan5	-	-	/	-	-	-	/	-	-	-	-	-	-	-	-	-	-	-	-	-	-	-	-	-	-	-	-	-	-	-	-	-	-
M. scapopedicellaris lateralis	Oan6	5	+	/	-	-	-	/	-	/	+	+	+	+	+	+	+	+	+	+	+	+	+	+	+	+	6	29	/	/	/	+	fpd1+fpd2	-
M. scapopedicellaris medialis	Oan7	6	+	/	-	-	-	/	M4?	/	+	+	+	+	+	+	+	+	+	+	+	+	+	+	+	+	7	30	/	/	/	+	epd1+epd2	-
M. intraflagellaris	Oan8	-	-	-	-	-	-	-	-	-	-	-	-	-	-	-	-	-	-	-	-	-	-	-	-	-	-	-	/	/	/	-	-	-
M. interampullaris	Oah1	/	/	7	-	-	-	/	/	/	-	-	-	-	-	-	-	-	-	-	-	-	-	-	-	-	/	/	-	-	-	-	/	/
M. ampulloaortica	Oah2	/	/	8	-	-	-	/	/	/	-	-	-	-	-	-	-	-	-	-	-	-	-	-	-	-	/	/	-	-	-	-	/	/
M. ampullopharyngealis	Oah3	/	/	6	-	-	-	/	/	/	-	-	-	-	-	-	-	-	-	-	-	-	-	-	-	-	/	/	-	-	-	-	/	/
M. ampullofrontalis	Oah4	/	/	9	-	-	-	/	/	/	-	-	-	-	-	-	-	-	-	-	-	-	-	-	-	-	/	/	-	-	-	-	/	/
M. frontofrontalis	Oah5	/	/	5	-	-	-	/	/	/	-	-	-	-	-	-	-	-	-	-	-	-	-	-	-	-	/	/	-	-	-	-	/	/
M. frontolabralis	Olb1	8	62	/	+	+	+	/	M5	1	+	+	+	+	+	+	+	+	+	+	+	+	+	+	+	+	2	1	+	+	+	+	mlra	LR.EL.
M. frontoepipharyngealis	Olb2	9	61	/	+	+	+	/	M6	2	+	+	+	+	+	+	+	+	+	+	+	+	+	+	+	+	3	2	+	+	+	+	mlrp	LR.DEP
M. epistoepipharyngealis	Olb3	10		/	-	-	-	/	-	-	-	-	-	-	-	-	-	-	-	-	-	-	-	-	-	-	-	-	-	-	-	-	-	-

Appendix 7: continued

Muscle name	Muscle name acc. Wipfler 2011	Muscle name acc. Kéler 1963	Muscle name acc. Matsuda 1965	Muscle name acc. Pass et al. 2006	Muscle name acc. Blanke et al. (2012) for Ephemera danica	Muscle name acc. Blanke et al. (2012) for Heptagenia sulphurea	Muscle name acc. Blanke et al. (2012) for Siphlonurus lacustris	Muscle name acc. Staniczek 2000	Muscle name acc. Staniczek (2001) for Ephemeroptera	Muscle name acc. Strenger (1970) for Ephemeroptera:	Epiophlebia superstes (this study)	Platycnemis pennipes (this study)	Platycnemis latipes (this study)	Pyrrhosoma nymphula (this study)	Coenagrion puella (this study)	Lestes virens (this study)	Calopteryx virgo (this study)	Gomphus pulchellus (this study)	Cordulegaster bidentata (this study)	Uropetala (this study)	Sympetrum sanguineum (this study)	Libellula depressa (this study)	Cordulia aenea (this study)	Aeshna mixta (this study)	Anax imperator (this study)	Muscle name acc. Blanke et al. (2012) for Onychogomphus forcipatus	Muscle name acc. Short (1955) for Odonata	Muscle name acc. Mathur & Mathur (1961) for Odonata	Muscle name acc. Asahina (1954) for Epiophlebia superstes	Muscle name acc. Asahina (1954) for Davidius nanus	Muscle name acc. Asahina (1954) for Mnais strigata	Muscle name acc. Blanke et al. (2012) for Perla marginata	Muscle name acc. Moulins (1968) for Plecoptera	Muscle name acc. Chisholm (1962) for Plecoptera
M. tentorioscapalis anterior	0an1	1	52	/	+	+	+	/	M1	5	+	+	+	+	+	+	+	+	+	+	+	+	+	+	+	+	4	28	+	+	+	+	tsc1+tsc2	A.D.M.
M. tentorioscapalis posterior	0an2	2	54	/	+	+	+	/	M3	4	+	+	+	+	+	+	+	+	+	+	+	+	+	+	+	+	5	27	+	+	+	+	dsc	A.E.M.
M. tentorioscapalis lateralis	0an3	3	51	/	+	-	-	/	-	-	-	-	-	-	-	-	-	-	-	?	?	+	+	+	+	-	-	-	-	-	-	+	fsc	-
M. tentorioscapalis medialis	0an4	4	53	/	-	-	+	/	M2?	-	-	-	-	-	-	-	-	-	-	-	-	-	-	-	-	-	-	-	-	-	-	+	-	-
M. tentoriopedicellarus																										+								
M. frontopedicellaris	0an5	-	-	/	-	-	-	/	-	-	-	-	-	-	-	-	-	-	-	-	-	-	-	-	-	-	-	-	-	-	-	-	-	-
M. scapopedicellaris lateralis	0an6	5	+	/	-	-	-	/	-	/	+	+	+	+	+	+	+	+	+	+	+	+	+	+	+	+	6	29	/	/	/	+	fpd1+fpd2	-
M. scapopedicellaris medialis	0an7	6	+	/	-	-	-	/	M4?	/	+	+	+	+	+	+	+	+	+	+	+	+	+	+	+	+	7	30	/	/	/	+	epd1+epd2	-
M. intraflagellaris	0an8	-	-	-	-	-	-	-	-	-	-	-	-	-	-	-	-	-	-	-	-	-	-	-	-	-	-	-	/	/	/	-	-	-
M. interampullaris	0ah1	/	/	7	-	-	-	/	/	/	-	-	-	-	-	-	-	-	-	-	-	-	-	-	-	-	/	/	-	-	-	-	/	/
M. ampulloaortica	0ah2	/	/	8	-	-	-	/	/	/	-	-	-	-	-	-	-	-	-	-	-	-	-	-	-	-	/	/	-	-	-	-	/	/
M. ampullopharyngealis	0ah3	/	/	6	-	-	-	/	/	/	-	-	-	-	-	-	-	-	-	-	-	-	-	-	-	-	/	/	-	-	-	-	/	/
M. ampullofrontalis	0ah4	/	/	9	-	-	-	/	/	/	-	-	-	-	-	-	-	-	-	-	-	-	-	-	-	-	/	/	-	-	-	-	/	/
M. frontofrontalis	0ah5	/	/	5	-	-	-	/	/	/	-	-	-	-	-	-	-	-	-	-	-	-	-	-	-	-	/	/	-	-	-	-	/	/
M. frontolabralis	0lb1	8	62	/	+	+	+	/	M5	1	+	+	+	+	+	+	+	+	+	+	+	+	+	+	+	+	2	1	+	+	+	+	mlra	LR.EL.
M. frontoepipharyngalis	0lb2	9	61	/	+	+	+	/	M6	2	+	+	+	+	+	+	+	+	+	+	+	+	+	+	+	+	3	2	+	+	+	+	mlrp	LR.DEP.
M. epistoepipharyngealis	0lb3	10		/	-	-	-	/	-	-	-	-	-	-	-	-	-	-	-	-	-	-	-	-	-	-	-	-	-	-	-	-	-	-

Appendix 7: continued

Muscle name	Muscle name acc. Wipfler 2011	Muscle name acc. Kéler 1963	Muscle name acc. Matsuda 1965	Muscle name acc. Pass et al. 2005	Muscle name acc. Blanke et al. (2012) for Ephemera danica	Muscle name acc. Blanke et al. (2012) for Heptagenia sulphurea	Muscle name acc. Blanke et al. (2012) for Siphlonurus lacustris	Muscle name acc. Staniczek 2000	Muscle name acc. Staniczek (2001) for Ephemeroptera	Muscle name acc. Strenger (1970) for Ephemeroptera:	Epiophlebia superstes (this study)	Platycnemis pennipes (this study)	Platycnemis latipes (this study)	Pyrrhosoma nymphula (this study)	Coenagrion puella (this study)	Lestes virens (this study)	Calopteryx virgo (this study)	Gomphus pulchellus (this study)	Cordulegaster bidentata (this study)	Uropetala (this study)	Sympetrum sanguineum (this study)	Libellula depressa (this study)	Cordulia aenea (this study)	Aeshna mixta (this study)	Anax imperator (this study)	Muscle name acc. Blanke et al. (2012) for Onychogomphus forcipatus	Muscle name acc. Short (1955) for Odonata	Muscle name acc. Mathur & Mathur (1961) for Odonata	Muscle name acc. Asahina (1954) for Epiophlebia superstes	Muscle name acc. Asahina (1954) for Davidius nanus	Muscle name acc. Asahina (1954) for Mnais strigata	Muscle name acc. Blanke et al. (2012) for Perla marginata	Muscle name acc. Moulins (1968) for Plecoptera	Muscle name acc. Chisholm (1962) for Plecoptera
M. tentoriobuccalis posterior	0bu6	50	88	/	+	+	+	/	M21	-	+	+	+	+	+	+	+	+	+	+	+	+	+	+	+	+	43'?	-	/	/	/	+	dvpm1-4	-
M. verticopharyngealis	0ph1	51	86	/	+			/	M17	-	+	+	+	+	+	+	+	+	+	+	+	+	+	+	+	+	37	+	/	/	/	+	ddp3	-
M. tentoriopharyngealis	0ph2	52	89+90	/	-			/	M21?	-	+	+	+	+	+	+	+	+	+	+	+	+	+	?	+	+	44	-	/	/	/	+	dvpp1-4	-
M. postoccipitopharyngealis	0ph3	-	-	/	-			-	-	-	+	+	+	+	+	+	+	+	+	?	+	+	+	+	+	+	-	-	-	-	-	+	dpop1+dpop2	-
M. anularis stomodaei	0st1	68	93	/	+	+	+	/	M10	-	+	+	+	+	+	+	+	+	+	+	+	+	+	+	+	+	-	+	+	+	+	+	M.annularis	-
M. longitudinalis stomodaei	0st2	69	91+92	/	+	+	+	/	M9	-	+	+	+	+	+	+	+	+	+	+	+	+	+	+	+	+	-	-	+	+	+	+	M.longitudinalis	-

Appendix 7: continued

Appendix 8: Complete list of morphological characters used in chapter 8

Head characters

0. Shape of clypeus (character 1 of Rehn, 2003): (0) rectangular, with anteclypeus and postclypeus forming distinct anterior and dorsal faces, respectively; (1) vertical, with anteclypeus and postclypeus facing anteriorly.

1. Shape of labial palp (character 2 of Rehn, 2003): (0) widest at base, tapering to tip; (1) parallel-sided; (2) external edge greatly expanded; (3) square shaped; (4) triangular.

2. Premental cleft (character 3 of Rehn, 2003): (0) well developed, at least one-quarter the length of entire prementum; (1) poorly developed, no more than one-quarter the length of entire prementum; (2) absent.

3. Shape of frons (character 4 of Rehn, 2003): (0) smoothly rounded in profile; (1) grossly enlarged, forming most of the head anterior to the eyes.

4. Ecdysial cleavage line (character 6 of Rehn, 2003): (0) present; (1) absent.

5. Occipital (postfrontal) suture: (0) vestigial or absent; (1) partially developed; (2) well developed.

6. Inner dorsal margins of eyes (character 8 of Rehn, 2003): (0) bent at a sharp angle so that a single point marks the narrowest space between them; (1) straight, so that no narrowest point exists between them.

7. Median lobe of labium (character 9 of Rehn, 2003): (0) bilobed; (1) not bilobed.

8. Moveable hooks of labial palpi (character 10 of Rehn, 2003): (0) present; (1) absent.

9. Shape of head (character 11 of Rehn, 2003): (0) globular; (1) transversely elongate and cylindrical.

10. Distance between eyes (character 12 of Rehn, 2003): (0) less than their own width; (1) greater than their own width; (2) eyes fused at single point; (3) eyes broadly fused along an eye seam.

11. Posterior margin of eye: (0) not sinuate; (1) sinuate.

12. Shape of vertex and location of ocelli (modified character 13 of Rehn, 2003): (0) transverse protuberance with lateral ocelli located at the lateral border and middle ocellus anteriorly; (1) small protuberance with all ocelli located on the vertex covering it almost completely; (2) large transverse oriented plate with middle ocellus located anteriorly and lateral ocelli located at the posterior side at the base; (3) flat with all ocelli located on the vertex; (4) two protuberances or horn like structures with lateral ocelli located at distal sides and middle ocellus anteriorly; (5) conical with all ocelli located on the vertex.

Wing characters

13. Shape of BxC (character 15 of Rehn, 2003): (0) triangular, widest anteriorly and well sclerotized; (1) rectangular and partially desclerotized in its anterior half; (2) triangular, broadest posteriorly and well sclerotized throughout.

14. Anterior and posterior lobes of FxC (character 18 of Rehn, 2003): (0) subequal in size; (1) posterior lobe of FxC distinctly smaller than anterior lobe; (2) posterior lobe of FxC vestigial.

15. Antenodal crossveins (Ax) (character 23 of Rehn, 2003): (0) many (at least 5, but usually 10 or more) present in C-Sc space and Sc-R space, unaligned; (1) many present in C-Sc and Sc-R space, aligned; (2) many present in C-Sc space only; (3) only 2 in C-Sc space and Sc-R space.

16. Primary Ax (character 24 of Rehn, 2003): (0) absent; (1) present.

17. Width / venation of hind wings vs. fore wings (character 25 of Rehn, 2003): (0) hind wing slightly broader and shorter than fore wing, and with similar venation; (1) hind wing and fore wing identical in size and venation; (2) hind wing broader than fore wing and with very different venation.

18. Position of IR1 (character 26 of Rehn, 2003): (0) closer to RP1 than to RP2; (1) equidistant from RP1 and RP2; (2) closer to RP2 than to RP1.

19. RP midfork (character 28 of Rehn, 2003): (0) symmetrical; (1) RP1,2 straight with RP3,4 branching

posteriorly; (2) RP3,4 straight with RP1,2 branching anteriorly.

20. Oblique vein between RP2 and IR2 (character 29 of Rehn, 2003): (0) absent; (1) present.

21. Postnodal crossveins (character 34 of Rehn, 2003): (0) unaligned in the C-RA and RA-RP spaces; (1) aligned in the C-RA and RA-RP spaces only; (2) aligned in a transverse series to beyond IR2.

22. Stigma brace vein (character 36 of Rehn, 2003): (0) absent; (1) present.

23. MP origin (character 40 of Rehn, 2003): (0) originates basally from the M stem; (1) originates from the Cu+M stem (see discussion in Introduction), and arches forward after leaving the Cu+M stem at the Cu crossing; (2) originates from the Cu+M stem and curves posteriorly or continues straight after leaving the Cu+M stem at the Cu crossing; (3) originates from the Cu+M stem and abruptly kinks backward distal of where it leaves the Cu+M stem to form the proximal side of the anisopteran triangle.

24. Position of arculus (character 43 of Rehn, 2003): (0) distal of 2Ax, or closer to 2Ax than to 1Ax; (1) arculus between 1Ax and 2Ax, or closer to 1Ax.

25. Orientation of posterior arculus (character 45 of Rehn, 2003): (0) developed at an angle with the anterior arculus; (1) posterior arculus continuing the path of the anterior arculus.

26. RP and MA divergence (character 46 of Rehn, 2003): (0) not strongly arched forward after diverging from the anterior arculus; (1) strongly arched forward after diverging from the anterior arculus.

27. Crossveins in basal space (character 47 of Rehn, 2003): (0) present; (1) absent.

28. RA-RP space proximal to the end of ScP (character 48 of Rehn, 2003): (0) crossed; (1) not crossed.

29. Position of RP midfork (character 49 of Rehn, 2003): (0) located beyond 25% wing length; (1) located at less than 25% wing length.

30. IR2 (character 53 of Rehn, 2003): (0) apparently joined to RP' with a crossvein; (1) fused directly to RP' at an acute angle, or with a gentle forward curve.

31. Subdiscoidal crossvein (character 55 of Rehn, 2003): (0) present between MP and CuA and aligned with discoidal vein; (1) secondarily lost resulting from the fusion of the posterior-apical corner of the quadrangle with the hind margin of the wing; (2) secondarily lost in only the hind wing due to the proximity of MP and CuA.

32. Quadrangle (discoidal cell) (character 56 of Rehn, 2003): (0) not divided by a crossvein into triangle and supertriangle; (1) divided by a crossvein into triangle and supertriangle in hind wing only; (2) divided by a crossvein into triangle and supertriangle in fore wing and hind wing; (3) divided by crossvein(s) but no triangle or supertriangle is formed.

33. Crossveins in subquadrangle: (0) absent; (1) present.

34. Crossveins in subquadrangle (character 58 of Rehn, 2003): (0) present only in hind wing; (1) present in fore wing and hind wing; (2) present only in fore wing.

35. Crossveins in the RP-MA space between the arculus and the distal end of the quadrangle (character 59 of Rehn, 2003): (0) absent; (1) present.

36. Petiolation of wings (character 67 of Rehn, 2003): (0) absent; (1) present.

37. Distal angle of quadrangle (character 69 of Rehn, 2003): (0) distinctly acute in both pairs of wings; (1) square in its distal angle in both pairs of wings; (2) acute in fore wing, obtuse in hind wing; (3) obtuse in both pairs of wings.

38. Position of nodus (character 70 of Rehn, 2003): (0) located beyond the middle of the wing; (1) located at one-third to one-half wing length; (2) located at one-quarter to one-third wing length; (3) located at less than one-quarter wing length.

39. Costal nodal kink (character 71 of Rehn, 2003): (0) absent; (1) present.

40. Membranule (character 72 of Rehn, 2003): (0) absent; (1) present.

41. RP1-IR1-field (character 73 of Rehn, 2003):

(0) expanded and filled by dichotomous branching of RP1; (1) expanded and filled by intercalated veins; (2) narrow, with no RP1 branches or intercalated veins.

42. IR1-RP2 field, intercalated sectors (character 74 of Rehn, 2003): (0) absent; (1) present.

43. RP2-IR2 field, intercalated sectors (character 75 of Rehn, 2003): (0) absent; (1) present.

44. IR2-RP3 field (character 76 of Rehn, 2003): (0) expanded and filled by dichotomous branching of RP3; (1) expanded and filled by intercalated veins; (2) narrow, with no RP3 branches or intercalated veins.

45. RP3-MA-field (character 77 of Rehn, 2003): (0) expanded and filled by dichotomous branching of MA; (1) expanded and filled by intercalated veins; (2) narrow, with no MA branches or intercalated veins.

46. MA-MP field (character 78 of Rehn, 2003): (0) expanded and filled by dichotomous branching of MA; (1) expanded and filled by inter- calated veins; (2) narrow, with no MA branches or intercalated veins.

47. MP-CuA-field (character 79 of Rehn, 2003): (0) expanded and filled by dichotomous branching of CuA; (1) expanded and filled by inter- calated veins; (2) narrow, with no CuA branches or intercalated veins.

48. Width of MA-MP field immediately distal of discoidal vein (character 80 of Rehn, 2003): (0) 1 cell wide immediately distal of the discoidal vein; (1) at least 2 cells wide distal of the discoidal vein.

49. Anal loop: (0) absent; (1) present.

50. Anal loop (character 81 of Rehn, 2003): (0) simple and saclike; (1) elongated with a distinct midrib; (2) with a well developed midrib and distinctively boot-shaped.

51. Secondary 'Cup' (character 83 of Rehn, 2003): (0) absent; (1) present.

52. Position of wings at rest (character 111 of Rehn, 2003): (0) wings not held pressed together over the abdomen at rest; (1) wings held pressed together over the abdomen at rest.

53. Number of crossveins basal of Cu crossing (character 118 of Rehn, 2003): (0) several; (1) none.

54. Anal triangle in hind wing of male (character 120 of Rehn, 2003): (0) absent; (1) present.

55. Triangle in fore wing and hind wing (character 121 of Rehn, 2003): (0) of similar size, shape and proximity to arculus; (1) of different size and shape, and in hind wing half as far from the arculus as in fore wing; (2) of different size and shape, and in hind wing at or close to the arculus; (3) of similar shape and proximity to arculus, but different size.

56. Pterostigma (character 123 of Bybee, 2008): (0) short; (1) long (about 12-15% of wing length).

57. No more than one basal costal Px before first radial Px (0); more than one Px (1).

58. Median (basal) space: (0) open; (1) closed.

59. Wings with several reddish spots in the C-Sc-Ra area: (0) absent; (1) present.

Thorax characters

60. Interpleural suture (character 86 of Rehn, 2003): (0) complete; (1) broken in the middle with distinct upper and lower halves; (2) upper portion of suture absent, and only a vestigial remainder below the metathoracic spiracle.

61. Tibial keel: (0) absent; (1) present.

62. Tibial keel (character 125 of Bybee, 2008): (0) present on first tibia; (1) present on 2nd or 3rd tibiae; (2) present on all tibiae.

63. Male mesotibial spines: (0) not quadrangular; (1) quadrangular.

64. Obliquity of thorax (character 87 of Rehn, 2003): (0) not oblique; (1) oblique.

Copulatory system

65. Third segment of penis: (0) vestigal or absent; (1) present.

66. Third segment of penis (character 88 of Rehn, 2003): (0) with 2 lateral lobes only; (1) with 2 apical and 2 lateral lobes; (2) filamentous; (3) present, but with no lobes.

67. Anterior hamuli directed medially (character X of Rehn, 2003): (0) no; (1) yes.

68. Anterior hamules (character 89 of Rehn, 2003): (0) external, platelike and quadrate; (1) external, platelike and triangular; (2) internal and folded; (3) internal and hooked; (4) internal and vestigial; (5) U-shaped and external.

69. Anterior lamina with elongate medial cleft (character X of Rehn, 2003): (0) absent; (1) present.

70. Ligula (character 90 of Rehn, 2003): (0) three-segmented, modified into penis; (1) one-segmented, aids posterior hamules in sperm transfer; (2) one-segmented, forms protective shield over modified vesicle spermalis.

71. Vesicle spermalis (VS) (character 91 of Rehn, 2003): (0) unsegmented, unmodified storage vesicle only; (1) segmented and modified into the intermittent organ.

72. Posterior hamules (character X of Rehn, 2003): (0) present; (1) vestigial.

73. Posterior hamules (character 92 of Rehn, 2003): (0) simple, blunt and small, not projecting beyond rim of genital fossa; (1) large, clearly projecting beyond rim of genital fossa, and variously modified into claspers with claws, sharp tips or folds; (2) posterior hamules grossly enlarged and modified into intermittent organ.

74. Epiproct: (0) present; (1) vestigal or absent.

75. Epiproct (character 93 of Rehn, 2003): (0) very large and spatulate, not modified for grasping; (1) grasping, simple; (2) grasping, lobed; (3) bifid; (4) trifid; (5) undivided.

76. Paraprocts (character 94 of Rehn, 2003): (0) simple, unmodified lobes projecting from sternum of segment 10; (1) modified into inferior appendages for grasping females.

77. Cerci (character 133 of Bybee, 2008): (0) less than 3⁄5 length of paraprocts; (1) greater than 3/5 length of paraprocts.

Abdominal characters

78. Auricles (character 119 of Rehn, 2003): (0) absent; (1) present.

79. Abdominal lateral carinae (character 124 of Bybee, 2008): (0) absent; (1) present.

80. Abdominal terga 5-8 with ventroapical tufts of long black hairs (character X of Rehn, 2003): (0) absent; (1) present.

81. Abdomen (character 134 of Bybee, 2008): (0) not triquetral; (1) triquetral.

Nymphal characters

82. Nymph with pyramidal to spike-like horn between the eyes: (0) absent; (1) present.

83. Nymphal caudal gills (character 97 of Rehn, 2003): (0) absent; (1) present.

84. Nymphal rectal gills (character 98 of Rehn, 2003): (0) absent; (1) present.

85. Shape of nymphal labium (character 99 of Rehn, 2003): (0) flat; (1) mask-shaped and covering much of face.

86. Nymphal prementum: (0) without raptorial setae; (1) with raptorial setae.

87. Nymphal prementum (character 100 of Rehn, 2003): (0) with many long raptorial setae; (1) with only 1 weak setae on the median lobe.

88. Raptorial setae on labial palps in nymph (character 101 of Rehn, 2003): (0) absent; (1) several long raptorial palpal setae present.

89. Nymphal antennae (character 127 of Bybee, 2008): (0) six- or seven-segmented; (1) four-segmented; (2) five-segmented.

90. First flagellum of nymphal antenna: (0) thinner than pedicellus; (1) at least as thick as pedicellus.

91. Fourth antennal segment very short or vestigial in nymph: (0) absent; (1) present.

92. Nymphal mesotarsi (character 128 of Bybee, 2008): (0) three-segmented; (1) two-segmented.

93. Nymphal moveable hook (character 129 of

Bybee, 2008): (0) without dorsolateral spur (spur at the base) E; (1) with spur.

94. Spur of moveable hook (character of Fleck, 2012): (0) robust; (1) thin and setae-like.

95. Distal margin of nymphal prementum (character 131 of Bybee, 2008): (0) without cleft tooth; (1) with cleft tooth.

96. Hind legs of nymph: (0) twice or more than twice as long as abdomen; (1) shorter or as long as abdomen; (2) longer than abdomen, but not twice as long.

97. Lateral spines or lobes on segment 5-9 in nymph: (0) absent; (1) present.

98. Shape of distal margin of nymphal prementum (character of Fleck, 2012): (0) with two apical, strong teeth flanked laterally by a rectangular tooth; (1) not as in (0).

99. Nymphal molar lobes of left and right mandible (character of Fleck, 2012): (0) moveable; (1) only left molar lobe moveable (flexible area present); (2) both molar lobes fixed (no flexible area present).

100. Dorsal spines or hooks on abdominal segments of nymph: (0) absent; (1) present.

Inner anatomy characters

101. Number of dental folds in proventriculus (character of Fleck, 2012): (0) 16; (1) 8; (2) 4.

102. Ventral dental folds of proventriculus with median elongated rasp-like dentition (character of Fleck, 2012): (0) present; (1) absent.

103. Internal part of the interantennal ridge (interantennal apodeme): (0) absent; (1) present.

104. Internal part of the epistomal ridge (epistomal apodeme): (0) absent; (1) present.

105. Internal part of the interantennal ridge (interantennal apodeme): (0) short, no longer than one third the length of epistomal apodeme; (1) longer than one third of epistomal apodeme.

106. Apodeme posteriorly of the anterior tentorial arm (attachment for 0md7): (0) present; (1) absent.

107. Apodeme posteriorly of the anterior tentorial arm (attachment for 0md7): (0) proximally in contact with the base of the anterior tentorial arm; (1) seperated at the entire length.

108. M. tentorioscapalis lateralis (0an3): (0) present; (1) absent.

109. Origin of M. frontolabralis (0lb1): (0) at the interantennal ridge; (1) at the interantennal apodeme; (2) partly at the interantennal ridge, partly at the interantennal apodeme.

110. Origin of M. frontoepipharyngalis (0lb2): (0) partly on the interantennal ridge, partly on the interantennal apodeme; (1) only on the interantennal apodeme; (2) only on the interantennal ridge.

111. M. labroepipharyngalis (0lb5): (0) one muscle bundle; (1) two distinct muscle bundles.

112. M. labroepipharyngalis (0lb5): (0) originating directly ventral of the labral ridge; (1) originating centered at the labium; (2) one bundle centered in the labium, the other directly ventral the labral ridge.

113. M. craniomandibularis internus (0md1): (0) without second origin; (1) with two clearly seperated, well defined origins.

114. M. craniomandibularis externus (0md3): (0) without second origin; (1) with two clearly seperated, well defined origins.

115. Origins of M. craniomandibularis externus (0md3): (0) only ventral of M. craniomandibularis internus (0md1) and M. craniolacinialis (0mx2); (1) one origin ventral of 0md1 & 0mx2, one dorsal of 0mx2; (2) one origin ventral of 0md1, one origin dorsal of 0md1.

116. M. tentoriomandibularis medialis superior (0md7): (0) present; (1) absent.

117. Insertion of M. tentoriomandibularis medialis superior (0md7): (0) at the ventral side of the anterior tentorial arms near the base; (1) at own apodeme posterior of the anterior tentorial arms; (2) at the posterior side of the dorsal tentorial arm base.

118. M. craniocardinalis (0mx1): (0) without second

origin; (1) with two clearly seperated, well defined origins.

119. M. tentoriobuccalis anterior (0bu5): (0) present; (1) absent.

120. Location of pharynx: (0) in touch with the corpotentorium; (1) not in touch with the corpotentorium.

Characters not included in the morphological data matrix

Length of pedicel and scapus: (0) pedicel longer than scapus; (1) scapus longer than pedicel; (2) scapus and pedicel equal in length. Character 5 of Rehn (2003). This character is only variable among certain Zygoptera and was therefore excluded from the present analysis.

Shape of vertex: (0) flat, not developed into large protuberance; (1) conical, or developed into a large transverse ridge. Character 13 of Rehn (2003). This character has been recoded (see character 12 of the present matrix).

Length of costal basivenale (BxC): (0) as long, from anterior to posterior margin, as the anterior platform; (1) much shorter than the anterior platform. Character 14 of Rehn (2003). This character is only variable among fossil odonatoids.

Costal axalare (AxC): (0) separated from costal fulcalare by a sulcus or suture; (1) AxC fully fused with FxC, suture absent. Character 16 of Rehn (2003). This character is only variable among fossil odonatoids.

Large lobe on the outside edge of AxC: (0) present; (1) absent. Character 17 of Rehn (2003). This character is only variable among fossil odonatoids.

Large, proximal hornlike sclerite on posterior articular plate: (0) not developed; (1) fully developed and greatly enlarged; (2) well developed, but not greatly enlarged. Character 19 of Rehn (2003). This character is only variable among fossil odonatoids.

Posterior articular plate: (0) with a single component sclerite enlarged and distinct from the other sclerites that comprise the plate; (1) this sclerite reduced and fully fused with the other sclerites in the posterior articular plate. Character 20 of Rehn (2003). This character is only variable among fossil odonatoids.

Shape of anterior edge semidetached plate of the scutum (SDP): (0) narrow and bluntly rounded; (1) with a U-shaped invagination; (2) straight. Character 21 of Rehn (2003). This character is only relevant for the relationships between Zygoptera and Anisoptera which is not the scope of the present contribution.

Bulla on outer edge of SDP: (0) absent; (1) as large as edge of basalare and heavily sclerotized; (2) distinctly smaller than edge of basalare and not heavily sclerotized. Character 22 of Rehn (2003). This character is only relevant for the relationships between Zygoptera and Anisoptera which is not the scope of the present contribution.

CUP: (0) present; (1) absent. Character 27 of Rehn (2003). This character is only variable among fossil odonatoids.

Costal triangle: (0) incompletely formed, with ScA basally separated from costal margin by a partially sclerotized area; (1) fully formed, with ScA completely fused to costal margin. Character 30 of Rehn (2003). This character is only variable among fossil odonatoids.

Flexion line between distal edge of BxC and costal margin: (0) absent; (1) present. Character 31 of Rehn (2003). This character is only variable among fossil odonatoids.

Junction of costa and ScP: (0) acute; (1) ScP turned sharply forward to meet costa at nearly a right angle. Character 32 of Rehn (2003). This character is only variable among fossil odonatoids.

Primary and secondary braces of nodus (nodal crossvein and subnodus): (0) developed in ScP-RA and RA-RPIa2 spaces, respectively, but not aligned; (1) well developed and aligned. Character 33 of Rehn (2003). This character is only variable among fossil odonatoids.

Pterostigma (Pt): (0) present in C-RA and RA-RP spaces; (2) present in only the C-RA space; (3) secondarily lost in both sexes and replaced by a densely reticulate network of veins. Character 35 of Rehn (2003). This character is only variable among fossil odonatoids and inside Zygoptera.

MA/RP fusion: (0) MA basally connected to RP with a 'strut' crossvein; (1) MA directly fused to RP at an acute angle; (2) MA and RP kinked at point of fusion, superimposed as anterior arculus; (3) MA and RP appearing to arise directly from RA, with no common stem forming the anterior arculus. Character 37 of Rehn (2003). This character is only variable among fossil odonatoids and inside Zygoptera.

M stem: (0) complete; (1) only present at base of wing as a vestigial vein remnant; (2) completely reduced, or fused with Cu stem. Character 38 of Rehn (2003). This character is only variable among fossil odonatoids.

Anal brace (AA): (0) dichotomously branched; (1) with no secondary branches. Character 65 of Rehn (2003). This character is only variable among fossil odonatoids.

AP: (0) developed within the wing membrane; (1) fused with the hind margin of the wing, or lost. Character 66 of Rehn (2003). This character is only variable among fossil odonatoids.

Quadrangle length: (0) shorter than the basal space; (1) longer than the basal space. Character 68 of Rehn (2003). This character is only variable among certain Zygoptera.

Posterior branch of (SCA3,4): (0) oblique and developed within the wing membrane; (1) perpendicular to the wing axis, and not developed within the wing membrane. Character 82 of Rehn (2003). This character is only variable among fossil odonatoids.

Basal proximity of IR2 and RP3: (0) not positioned extremely close to one another near their origins for the length of several cells; (l) positioned extremely close to one another basally for the length of several cells. Character 84 of Rehn (2003). This character is only variable among certain Zygoptera.

Apices of RA and RP1: (0) meeting the distal wing margin anterior to the apex of the wing itself; (l) meeting the distal wing margin posterior to the wing apex. Character 85 of Rehn (2003). This character is only variable among certain Zygoptera.

Lateral abdominal gills in larva: (0) absent; (1) present on segments 2-8; (2) present on segments 2-7. Character 95 of Rehn (2003). This character is only variable among certain Zygoptera.

Larval gill tufts: (0) absent; (1) present. Character 96 of Rehn (2003). This character is only variable among certain Zygoptera.

Raptorial setae on moveable hook in larva: (0) absent; (1) present. Character 102 of Rehn (2003). This character is only variable among certain Zygoptera.

Base of larval prementum: (0) not stalked; (1) stalked. Character 103 of Rehn (2003). This character is only variable among certain Zygoptera.

Length of second antennal segment (pedicel) in larva: (0) shorter than all other segments combined; (1) longer than all other antennal segments combined. Character 104 of Rehn (2003). This character is only variable among certain Zygoptera.

Length of abdomen: (0) not greatly elongated; (1) abdomen extremely elongated (total length at least 62mm, but usually >80mm). Character 105 of Rehn (2003). This character is only variable among certain Zygoptera.

Raptorial spines on legs: (0) present; (1) vestigial, and legs extremely long. Character 106 of Rehn (2003). This character is only variable among certain Zygoptera.

Length of end hook and moveable hook of labial palp in adult: (0) distinctly less than 1.5 X the length of the base of the palp; (1) distinctly greater than 1.5 X the length of the base of the palp, and extremely sharp. Character 107 of Rehn (2003). This character is only variable among certain Zygoptera.

Ventral carina of abdominal segment 2: (0) not developed into laterally produced expansions ('pseudo-auricles'); (1) developed into conspicuous 'pseudo-auricles'. Character 108 of Rehn (2003). This character is only variable among certain Zygoptera.

Shape of seminal vesicle (SV): (0) rounded laterally, and anteriorly produced into two sclerotized tips connected by desclerotized membrane; (l) laterally produced into sharp expansions, anteriorly produced into two sclerotized tips connected by descler- otized membrane; (2) rounded laterally, anteriorly the two sclerotized tips fuse into a single tip with no membranous area. Character 109 of Rehn (2003). This character is only variable among certain Zygoptera.

Dorsum of abdominal segment 10: (0) not developed into pyramidlike carina; (1) developed into pyramidlike carina. Character 110 of Rehn (2003). This character is only variable among certain Zygoptera.

Spines projecting from ventral eye margin in larva: (0) absent; (1) present. Character 112 of Rehn (2003). This character is only variable among certain Zygoptera.

Relative length of abdomen and wings: (0) abdomen distinctly longer than wings, or extending at least to wing tips; (1) abdomen distinctly shorter than wings. Character 113 of Rehn (2003). This character is only variable among certain Zygoptera.

Posterior curve in MP distal of quadrangle: (0) absent; (1) present. Character 114 of Rehn (2003). This character is only variable among certain Zygoptera.

Relative position of RP midfork and nodus: (0) midfork not several cells distad of nodus; (1) midfork distinctly distad (by at least 3 cells) of nodus. Character 115 of Rehn (2003). This character is only variable among certain Zygoptera.

Elaborate dilation and coloration of tibiae in second and thirdpairs of legs in nudes: (0) absent; (1) present. Character 116 of Rehn (2003). This character is only variable among certain Zygoptera.

Large conical projections on larval caudal gills: (0) absent; (1) present, and gills saccoid. Character 117 of Rehn (2003). This character is only variable among certain Zygoptera.

Internal fold of ligula (penis): (0) not developed into a long filament; (1) developed into a long filament. Character 122 of Rehn (2003). This character is only variable among certain Zygoptera.

Distal margin of labial palps: (0) without deep cuts; (1) median cuts; (2) large cuts. Character 130 of Bybee et al. (2008). The definition and homologisation for this character is unclear. Therefore it was excluded from the analysis.

Lateral spines on segment 9 in larva: (0) shorter than mid-dorsal length of 9; (1) at least as long as 9. Character 132 of Bybee et al. (2008). The definition and homologisation for this character is unclear. Therefore it was excluded from the analysis.

Patella: (0) absent; (1) present. Character 135 of Bybee et al. (2008). The definition and homologisation for this character is unclear.

Superlinguae: (0) absent; (1) present; (2) interlocking. Character 136 of Bybee et al. (2008). This character is not relevant for the relationships among Anisoptera, since only Ephemeroptera and Archaeognatha possess superlinguae.

Subimago: (0) present; (1) absent. Character 137 of Bybee et al. (2008). This character is not relevant for the relationships among Anisoptera, since only Ephemeroptera run through a subimaginal stage.

Excluded because not variable within Odonata

Tracheation: (0) anterior; (1) arch. Character 138 of Bybee et al. (2008).

Direct spiracular musculature: (0) absent; (1) present. Character 139 of Bybee et al. (2008).

Tentorio-lacinial muscle: (0) present; (1) absent. Character 140 of Bybee et al. (2008).

Tentorio-mandibular muscles: (0) several bundles; (1) one. Character 141 of Bybee et al. (2008).

Loss of some pterothoracic muscles: (0) no; (1) yes. Character 142 of Bybee et al. (2008).

Sperm transfer: (0) indirect; (1) copulation; (2) indirect, using claspers. Character 143 of Bybee et al. (2008).

Male forelegs clasping: (0) absent; (1) present. Character 144 of Bybee et al. (2008).

Male styli IX: (0) not claspers; (1) claspers. Character 145 of Bybee et al. (2008).

Imaginal lifespan: (0) normal, feeding; (1) Shortened, non-feeding. Character 146 of Bybee et al. (2008).

Larval labium: (0) not prehensile; (1) prehensile. Character 147 of Bybee et al. (2008).

Lateral cervical sclerite in three pieces: (0) absent; (1) present. Character 148 of Bybee et al. (2008).

Pteropleura tilted backward with notum small: (0) absent; (1) present. Character 149 of Bybee et al. (2008).

Male accessory copulatory organs: (0) absent; (1) present. Character 150 of Bybee et al. (2008).

CuA-CuP brace ⁄ fusion: absent (0); present (1). Character 151 of Bybee et al. (2008).

CuP-kink & AA fusion: absent (0); present (1). Character 152 of Bybee et al. (2008).

Anal brace: not extending beyond CuP (0); extending beyond CuP (1). Character 153 of Bybee et al. (2008).

Curriculum vitae

Zur Person

Name: Alexander Blanke
Geburtsdatum: 27.09.1982
Nationalität: Deutsch
Personenstand: ledig
Adresse: Zoologisches Forschungsmuseum Alexander Koenig (ZFMK)
Adenauerallee 160
D-53113 Bonn, Germany
Telefon: +49 (0) 228 9122 421
Fax: +49 (0) 228 9122 295
E-mail: blanke@uni-bonn.de

Derzeitige Position: Doktorand am ZFMK, Zentrum für molekulare Biodiversität (ZMB)
Titel: Head evolution at the origin of pterygote insects

Akademischer Abschluss

Diplom am ZFMK; Rheinische-Friedrich-Wilhelms University Bonn, Germany.
Betreuer: Prof. Dr. Bernhard Misof and Prof. Dr. Karl Schuchmann
Fächer: Zoology, Botany, Physics

Universitäre Ausbildung

seit 07/2008	Doktorand am ZFMK; Thema: Head evolution at the origin of pterygote insects.
02/2007	Diplom am ZFMK; Universität Bonn, Titel: „The dragonfly assemblage of Santa Teresa – patterns of behaviour and habitat use in a tropical environment". Betreuer: Prof. Dr. Bernhard Misof and Prof. Dr. Karl Schuchmann
10/2001-02/2007	Biologiestudium an der Rheinischen-Friedrich-Wilhelms Universität Bonn. Fächer: Zoologie, Botanik, Physik.

Forschungsaktivitäten

seit 07/2008	Doktorand am ZFMK.
seit 02/2007	studentische Hilfskraft am ZFMK; Thema: Revision der Gattung Perithemis Hagen (Odonata: Anisoptera)
05/2005-11/2005	studentische Hilfskraft am Nees Institut für Biodiversität der Pflanzen, Bonn (Germany). Betreuung des Kurses: "Scanning electron microscopy (SEM) and atomic-force microscopy (AFM) of biological surfaces.
02/2004-08/2005	studentische Hilfskraft am Nees Institut für Biodiversität der Pflanzen, Bonn (Germany). Arbeitsgruppe Bionik. Arbeitsfelder: Charakterisierung biologischer Oberflächen mittels Raster-Elektronen-Mikroskopie (REM) und atomic-force microscopy (AFM) sowie anderen Visualisierungsmethoden.
06/2001-10/2001	Praktikum am Universitätsklinikum, Bonn; Sektion: Chirugische Forschung. Thema: Histologische Studien an verschiedenen Organstrukturen von Vertebraten.

Publikationen

Blanke, A., Beckmann, F., Misof, B. 2012. The head anatomy of Epiophlebia superstes (Odonata: Epiophlebiidae). Accepted for publication in Organisms Diversity and Evolution

Blanke, A., Wipfler, B., Letsch, H., Koch, M., Beutel, R., Misof, B. 2012. Revival of Palaeoptera – head characters support a monophyletic origin of Odonata and Ephemeroptera (Insecta). Accepted for publication in Cladistics.

R. Mokso, L. Quaroni, F. Marone, S. Irvine, J. Vila-Comamala, A. Blanke, M. Stampanoni. 2012 X-ray Mosaic Nanotomography of Large Microorganisms. Journal of Structural Biology 177: 233-238.

Blanke, A., Thelen, M., 2011. SR-microCT-data helps to develop a phylogenetic character matrix for head structures of lower Pterygota. HASYLAB annual report 2011.

Blanke, A., Bartel, D., Dambach, J., Thelen, M., Beckmann, F., Misof, B., 2010a. Inner morphology of "basal" Hexapoda – new character interpretation made possible by SRµCT. HASYLAB annual report 2010

Blanke, A., Meusemann, K., von Reumont, B.M., Meusemann, H., Beckmann, F., Misof, B., 2010b. Contributions to the phylogeny of Anisoptera from SRµCT-data of internal head morphology. HASYLAB annual report 2010.

Blanke, A. 2008. Four new dragonfly records for the state of Espiríto Santo, Brazil: Erythrodiplax clitella Borror, Orthemis ambinigra Calvert, Lestes forficula Rambur and Heteragrion petiense Machado (Odonata: Libellulidae, Lestidae, Megapodagrionidae). Notulae odonatologicae 7(2): 13-15.

Rödder, D., Dambach, J., Blanke, A. 2006. Anurendiversität in Santa Teresa (Mata Atlântica). Eine Bestandsaufnahme. Elaphe 14 (1): 45-54.

Publikationen (in Vorbereitung)

Blanke, A., Greve, C., Wipfler, B., Beutel, R.G., Holland, B., Misof, B. Assessing data quality and the evolution of winged insects – contradicting hypotheses tighten the Palaeoptera. Systematic Biology.

Blanke, A., Misof, B. Assessing convergence in wing venation – head characters help to develop a robust phylogeny of major anisopteran families (Hexapoda: Odonata). Systematic Entomology.

Büsse, S., Blanke, A., Misof, B., Hörnschemeyer, T. The nympheal head morphology of Epiophlebia laidlawi.

Blanke, A., Misof, B. The head anatomy of adult Ephemeroptera as inferred by microCT – phylogenetic implications.

Blanke, A., Misof, B. The head anatomy of Meinertellus cundinamarcensis (Archaeognatha: Meinertellidae).

Blanke, A., Wipfler, B., Koch, M., Misof, B. The head anatomy of Tricholepidion gertschi (Zygentoma).

Vorträge

Blanke, A, and Misof, B. How much convergence is "in the wing"? – Anisopteran phylogeny reassessed. 5th Dresden Meeting on Insect Phylogeny, Dresden, September 21 - 23, 2011.

Blanke, A. microCT - theory and application at the ZFMK. Colloquium at the ZFMK. July 2011.

Eigene workshops

High Quality 3D Reconstruction for Everyone: open-Source Solutions and their Workflow to analyse and publish MicroCT Data. Workshop at the GfBS meeting 2012

Gutachtertätigkeiten

International Journal of Odonatology

Forschungsaufenthalte

2010 & 2011 Paul-Scherrer institute (PSI), Switzerland, Villigen: synchrotron radiation micro computer tomography of arthropods, cooperation: A. Böhm (group Pass, Vienna), K. Meusemann, M. Thelen, v. Reumont, B. (all ZFMK).

2011 Paul-Scherrer institute (PSI), Switzerland, Villigen: synchrotron radiation micro computer tomography of arthropods, cooperation: K. Meusemann, M. Thelen (all ZFMK)

2009 & 2010 Deutsches Elektronen Synchrotron (DESY), Germany, Hamburg: synchrotron radiation micro computer tomography of arthropods, cooperation: D. Bartel (group Pass), K. Meusemann, M. Thelen, v. Reumont, B. (all ZFMK).

2007-2009 Besuch der zoologischen Sammlungen in Wien, Brüssel, München, Berlin

Feldaufenthalte

USA, Brasilien, Frankreich, Italien, Marokko, Rumanien, Griechenland

EDV-Kenntnisse

Sehr gute Kenntnisse des MS Office Pakets, XLStat, Adobe Creative Suite, Inkscape, GIMP, Scribus, Blender, Reconstruct, Image J, Amira, Maya, Bitplane Imaris, VG Studio Max, PreView, FeBio and PostView
Erfahrung mit verschiendenen Phylogenie Programmen

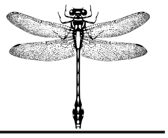

14 Erklärung

Hiermit versichere ich an Eides statt, dass die vorgelegte Arbeit, abgesehen von den ausdrücklich bezeichneten Hilfsmitteln, persönlich, selbstständig und ohne Benutzung anderer als der angegebenen Hilfsmittel angefertigt wurde. Daten und Konzepte die aus anderen Quellen direkt oder indirekt übernommen wurden sind unter Angaben von Quellen kenntlich gemacht. Diese Arbeit hat in dieser oder ähnlichen Form keiner anderen Prüfungsbehörde vorgelegen und ich habe keine früheren Promotionsversuche unternommen. Für die Erstellung der vorliegenden Arbeit wurde keine fremde Hilfe, insbesondere keine entgeltliche Hilfe von Vermittlungs- bzw. Beratungsdiensten in Anspruch genommen.

Alexander Blanke
Bonn, den 12.2.2013